Transactions

of the

ASME

Symposium on Cooling Towers:

Some Economic Factors in the Selection of Cooling Towers . . . *A. R. LaBailly* 1021

Cooling Towers for Steam-Electric Stations—Economic Applications . *Louis Elliott* 1027

Selection, Operation, and Maintenance of Industrial Cooling Equipment . . . . . *H. E. Degler* 1031

Recirculation in Cooling Towers . . . . . *Joseph Lichtenstein* 1037

Operating Experience With Cooling Towers in the Central Gulf Area . . . . . *H. G. Hiebeler* 1043

Problems Relating to Operation, Maintenance, and Chemical Control of Cooling Towers for Steam-Electric Generating Stations . . . . . *V. F. Estcourt* 1047

Deterioration of Wood in Cooling Towers . . *R. H. Baechler and C. A. Richards* 1055

The Hydrodynamic Lubrication of Sector-Shaped Pads . . . . . *R. S. Brand* 1061

The Nonsteady-State Load-Supporting Capacity of Fluid Wedge-Shaped Films . . . . . *E. K. Gatcombe* 1065

Aircraft Turbosupercharger Bearings—Their History, Design, and Application Technique . . . . . *S. R. Puffer* 1077

The Fatigue Strength of Threaded Connections . . . . . *R. C. A. Thurston* 1085

Comparative Surface-Hardening Characteristics of Commercial Pearlitic Malleable Irons . . . . . *S. H. Bush, W. P. Wood, and F. B. Rote* 1093

Dynamic Force Reactions in Double-Ported Control Valves . . . . . *C. F. King and G. F. Breckett* 1101

Metastable Flow of Saturated Water . . . . . *J. F. Bailey* 1109

Intermittent Heating for Aircraft Ice Protection With Application to Propellers and Jet Engines . . . . . *Myron Tribus* 1117

Further Remarks on Intermittent Heating for Aircraft Ice Protection . . . . . *Frederick Weiner* 1131

NOVEMBER, 1951

VOL. 73, No. 8

Transactions

of The American Society of Mechanical Engineers

Published on the tenth of every month, except March, June, September, and December

---

OFFICERS OF THE SOCIETY:

J. Calvin Brown, *President*

Joseph L. Koff, *Treasurer*
Edgar J. Kates, *Ass't Treasurer*

C. E. Davies, *Secretary*

COMMITTEE ON PUBLICATIONS:

John Haydock, *Chairman*

C. B. Campbell
George R. Rich
Paul T. Norton, Jr.
Otto de Lorenzi

D. R. Thomas
Morris Gerb
Junior Advisory Members

George A. Stetson, *Editor*
K. W. Clendenning, *Managing Editor*

REGIONAL ADVISORY BOARD OF THE PUBLICATIONS COMMITTEE:

Kerr Atkinson—I
J. de S. Coutinho—II
W. E. Reaser—III
F. C. Smith—IV
Hendley Blackmon—V
Chester R. Earls—VI
R. G. Robledo—VII
M. A. Durland—VIII

Published monthly by The American Society of Mechanical Engineers. Publication office at 20th and Northampton Streets, Easton, Pa. The editorial department is located at the headquarters of the Society, 29 West Thirty-Ninth Street, New York 18, N. Y. Cable address, "Dynamic," New York. Price $1.50 a copy, $12.00 a year for Transactions and the *Journal of Applied Mechanics* to members and affiliates, $1.00 a copy, $6.00 a year. Changes of address must be received at Society headquarters four weeks before they are to be effective on the mailing list. Please send old as well as new address. . . . By-Law: The Society shall not be responsible for statements or opinions advanced in papers or . . . printed in its publications (B13, Par. 4). . . . Entered as second-class matter March 2, 1928, at the Post Office at Easton, Pa., under the Act of August 24, 1912. . . .

Copyrighted, 1951, by The American Society of Mechanical Engineers. Reprints from this publication may be made on condition that full credit be given the Transactions of the ASME and the author, and that date of publication be stated.

Some Economic Factors in the Selection of Cooling Towers

By A. R. LeBAILLY,[1] CHICAGO, ILL.

This paper deals with performance studies of selected condenser-cooling tower combinations and their economics. Comparison is made between the cost of circulating-water supply from a river source with the cooling tower.

FOR a specified heat cycle, turbine heat balances are usually calculated for a standard vacuum condition for full and fractional loads. For ASME-AIEE units, the turbine heat rates (Btu/kwhr) are published for 110 per cent, 100 per cent, 75 per cent, 50 per cent, and 25 per cent of name-plate rating.

The turbine manufacturer supplies a vacuum correction chart for correcting the heat rate for any deviation from the standard vacuum used in the heat balance. Fig. 1 illustrates the vacuum correction chart for a 30,000 to 33,000-kw ASME-AIEE turbine, 850 psi, 900 F, 1½-in. Hg vacuum with four extraction feedwater heaters. The per cent changes in heat rate and turbine loads are used as co-ordinates with the vacuum curves shown for 1, 1½, 2, 2½, and 3 in.

The latent heat of the turbine exhaust steam is transferred to the condenser circulating water and later dissipated in the cooling tower. For a specific turbine load, the condenser and cooling towers are two heat exchangers operating under the same heat load, water flow, and circulating-water temperatures. It is their combined characteristics that determine the condenser vacuum at each turbine load.

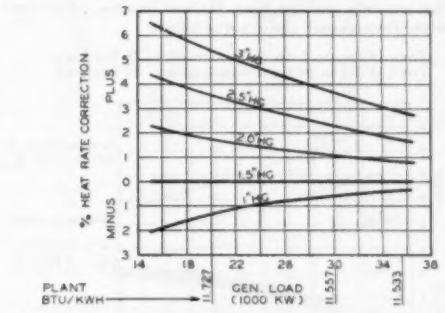

FIG. 1 VACUUM CORRECTION TO HEAT RATE CHART FOR A 30,000 TO 33,000-KW ASME-AIEE TURBINE
(850-psig, 900 F, four-stage feedwater heating.)

CONDENSER-COOLING TOWER COMBINATIONS

There is no practical and simple formula to compare directly the combined performance of different combinations of condensers and cooling towers operating under the same heat load and wet-bulb temperature. However, it is possible by making relatively few performance studies of selected "condenser-cooling tower" combinations to calculate the respective vacuums and plot them on the correction chart shown in Fig. 1.

Fig. 2 shows three vacuum performance curves of a 30,000-sq ft 2-pass condenser with three different cooling towers A, B, and C, operating under the same heat load, wet bulb, and cooling range but of different approach design: tower A, 8 deg; tower B, 10 deg; tower C, 14 deg.

The performance lines for A, B, and C show the vacuum obtained with each tower when operating at 77 deg wet bulb between 15,000 and 35,000-kw turbine loads. These lines are almost parallel and indicate for all loads the following improvements in Btu rate per kwhr:

From 14 deg to 8 deg approach design—102 Btu/kwhr
From 14 deg to 10 deg approach design— 72 Btu/kwhr

Actually, these cooling towers would operate most of the time at a wet bulb below the design wet bulb of 77 F. Fig. 3 shows three performance lines of the same towers when operated at 70

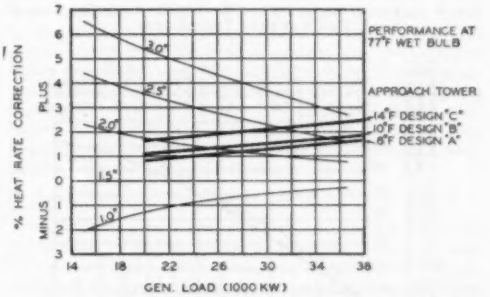

FIG. 2 VACUUM PERFORMANCE CURVES OF A 30,000-SQ FT, 2-PASS 28,000-GPM, CONDENSER WITH COOLING TOWERS A, B, AND C
(Tower, 16.5 F range; 77 deg wet bulb; 8, 10, and 14 deg approach.)

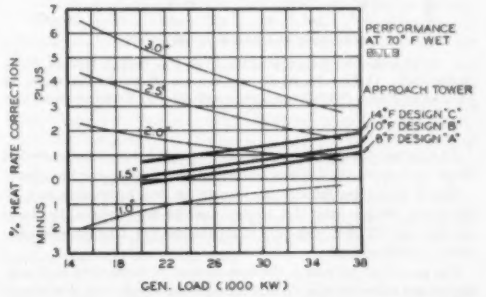

FIG. 3 PERFORMANCE CURVES OF TOWERS SHOWN IN FIG. 2, AT 70 DEG WET-BULB TEMPERATURE

[1] Partner, Sargent & Lundy. Mem. ASME.

Contributed by the Power Division and presented at the Spring Meeting, Atlanta, Ga., April 2–5, 1951, of THE AMERICAN SOCIETY OF MECHANICAL ENGINEERS.

NOTE: Statements and opinions advanced in papers are to be understood as individual expressions of their authors and not those of the Society. Manuscript received at ASME Headquarters, March 8, 1951. Paper No. 51—S-5.

deg wet bulb instead of at their design point. This temperature happens to be the yearly average at the proposed plant location and was used for comparing the respective yearly fuel consumptions. At 70 deg wet bulb the differences are as follows:

From 14 deg to 8 deg approach design—96 Btu/kwhr
From 14 deg to 10 deg approach design—68 Btu/kwhr

Fig. 4 shows the performance lines of the towers when operated at 45 deg wet bulb which would correspond to a yearly average wet-bulb condition for a Midwest location. The benefits of the low approach design are as follows:

From 14 deg to 8 deg approach design—38 Btu/kwhr
From 14 deg to 10 deg approach design—27 Btu/kwhr

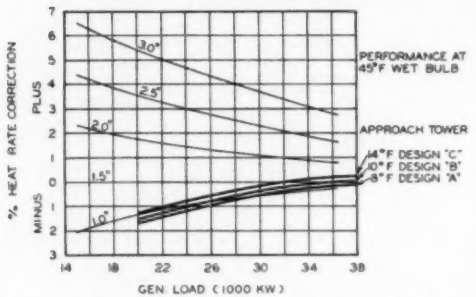

FIG. 4 PERFORMANCE CURVES OF TOWERS SHOWN IN FIG. 2, AT 45 DEG WET-BULB TEMPERATURE

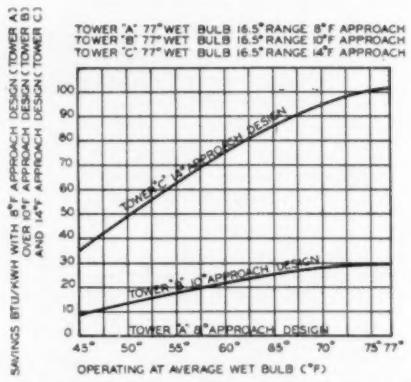

FIG. 5 BENEFIT IN BTU-KWHR OBTAINED BY 8-DEG DESIGN OVER 10-DEG AND 14-DEG DESIGNS OF COOLING TOWERS, BETWEEN 45 DEG AND 77 DEG WET-BULB TEMPERATURE FOR TOWERS SHOWN IN FIG. 2

The same comparison could be repeated for other selected range and approach designs operating under the same heat load.

Fig. 5 shows graphically the benefit in Btu/kwhr obtained by the 8-deg design over the 10-deg and 14-deg designs, between 45 deg and 77 deg wet-bulb temperature for the specific case under consideration.

For practical purposes, the comparison in respective fuel consumptions is satisfactory if the vacuum determination is made at only one point corresponding to the yearly average load and wet bulb. It will supply the fuel factor entering in the selection of the optimum arrangement giving the lowest annual cost of operation (fixed charges and operating cost considered).

The engineering factors used in preparing a cooling-tower specification are reviewed in the following.

HEAT LOAD

Turbine contracts state the guaranteed turbine capability. In ASME-AIEE units the manufacturers recognize the higher capability of the turbine with better vacuum and also with the elimination of the top feedwater heater as part of the contract. Turbine manufacturers provide a margin for contingencies, and it has been our experience that the control valves will pass more steam than required to meet the guaranteed capability. The use of higher hydrogen pressures has also permitted carrying higher loads on the generators at the system power factor.

Tests to determine the difference between the nominal and actual capability of several turbines have been made and show the following increase in capability:

One 33,000-kw turbine carried 38,000 kw
One 66,000-kw turbine carried 80,000 kw
One 62,500-kw turbine carried 72,000 kw

Boilers are frequently designed for safe circulation at 110 per cent of rated capacity, and the manufacturer provides a margin of safety in his design above this figure.

Condensers are normally designed for 85 per cent cleanliness factor, which provides an overload margin for clean condensers. The designing engineer normally provides margin in the boiler and turbine auxiliaries to match the manufacturer's allowances. These margins of safety against possible error actually provide insurance of continuous full-load operation during the life of the equipment with reasonable wear and deterioration due to age.

The problem that confronts the engineer to obtain a balanced design is to provide the same conservative margin in the cooling towers as those that exist in the other power-plant equipment.

During recent years and under the present conditions, operating companies have been forced occasionally and perhaps reluctantly to load the generating units beyond their rated capability.

Cooling towers are designed for an approach to a specified wet bulb, heat load, and cooling range without provision for contingencies matching the extra circulation design in boilers, cleanliness factor in condensers, and manufacturers' allowance on turbines.

In several instances, new cooling towers have not met their performance guarantees, probably due to insufficient margin for contingencies in the manufacturer's design. Delignification and deterioration of fill have been encountered in other cases.

It is the job of the designing engineer to provide in the specification the margin of safety which is not supplied by the manufacturer, in order to avoid designing the cooling towers below the capacity of the other equipment of the power plant. Therefore the specified heat load should be not less than the maximum flow to the condenser with the highest turbine capability. In view of our recent experience it should allow some margin above the capability limitation set forth in the turbine contract.

WET-BULB TEMPERATURE

The wet-bulb temperature is selected from the "summer weather data" at the proposed plant location. The wet-bulb temperature selected for design is very often a temperature not exceeded more than 5 per cent during a normal year between June and September. For the 5 per cent period, when the wet bulb exceeds the specified temperature, or for a longer period during an abnormal year, the predicted performance of the cooling tower will not be met. The condenser vacuum and actual turbine capability will be affected. This may become a factor of

TABLE 1 COMPARISON IN 1948 OF EIGHT CONDENSER COOLING-TOWER COMBINATIONS DESIGNED FOR HEAT LOAD OF 216,000,000 BTU PER HR, 76 F WET-BULB TEMPERATURE; APPROACH DESIGNS OF 8, 10, 12, AND 14 DEG, AND COOLING RANGE OF 14 AND 16 F

	Summary of Data and Costs							
Case	7	8	1	2	3	4	5	6
Design approach, deg F	8	8	10	10	12	12	14	14
Design range, deg F	14	16	14	16	14	16	14	16
Condenser area, sq ft	30000	27500	30000	27500	30000	27500	30000	27500
Circ. water, gpm	30800	26900	30800	26900	30800	26900	30800	26900
Tower head, ft	32	32	32	32	26	26	20	20
Cond. friction, ft	26.3	24	26.3	24	26.3	24	26.3	24
Pipe friction, ft	10	10	10	10	10	10	10	10
Pump head, ft	68.3	66	68.3	66	62.3	60	56.3	54
Pump, hp	608	513	608	513	555	467	502	420
Fan, hp	242	210	191	175	203	213	223	208
Kw (total)	693	589	651	562	619	558	595	516
Design wet bulb, deg F	76	76	76	76	76	76	76	76
Average wet bulb, deg F	45	45	45	45	45	45	45	45
Average load, kw gross	26500	26500	26500	26500	26500	26500	26500	26500
Average vacuum, in. Hg	1.03	1.17	1.18	1.37	1.20	1.33	1.28	1.46
Hours operation	8300	8300	8300	8300	8300	8300	8300	8300
Cost tower, dollars	117800	117800	95800	95800	80700	80700	82400	82400
Basin	25080	25080	20575	20595	20595	20595	23075	23075
Condenser equipment	160060	146260	160060	146260	156210	145580	158360	144895
Total cost, dollars	302940	289140	276435	262635	269505	255875	263865	252370
	Operating Costs—Year							
12 per cent fixed charges, dollars	36353	34697	33172	31516	32340	30705	31904	30844
Fan and pump power, 3 mills/kwhr	17255	14666	16610	13994	15413	13894	14816	12848
Excess steam cost at 25¢ million Btu	Base	1300	1300	3570	1625	3055	2470	4545
Total	53608	50663	51282	49080	49378	47654	49190	48237

importance when the highest wet bulb is coincidental with the peak load. We understand that with the growth of the air-conditioning load in the southwestern part of the country, this situation is occurring frequently. This can be compensated by specifying a higher wet bulb or closer approach than would be justified in the northern districts where the two peak loads are rarely coincidental.

Cooling Range and Approach

The wet bulb and heat load being set for the maximum design conditions, the initial costs of the condenser and cooling tower will be affected by the cooling range and approach of the alternate designs selected for comparison. Table 1 shows a comparison made in 1948, of eight different "condenser-cooling tower" combinations all designed for a heat load of 216,000,000 Btu per hr, 76 deg wet bulb, with respective approach designs of 8, 10, 12, and 14 deg, and cooling range of 14 and 16 F.

The cooling-tower prices were obtained from the same manufacturer to obtain a comparable basis for the different arrangements.

The fixed charges are tabulated at 12 per cent.

The power for the circulating pumps and cooling-tower fans is charged at fuel cost or 3 mills per kwhr.

The average yearly wet-bulb temperature was 45 F. The average load was 26,500 kw for 8300 hr, and the yearly difference in fuel cost, resulting from better condenser performance, was tabulated on a fuel cost of 25 cents per million Btu.

The yearly operating costs, including fixed charges and auxiliary power for the assumed average kilowatt load and wet-bulb condition, are given in Table 2 in rising order.

TABLE 2 YEARLY OPERATING COSTS, INCLUDING FIXED CHARGES AND AUXILIARY POWER

Condenser, sq ft	Cooling tower		Yearly cost
	Approach, deg F	Range, deg F	
26900	12	16	$47654
26900	14	16	48237
26900	10	16	49080
30800	14	14	49190
30800	12	14	49373
26900	8	16	50663
30800	10	14	51282
30800	8	14	53683

Based on yearly operating costs, the 26,900-sq ft condenser with 12-deg-approach 16-deg-range tower combination has a slight theoretical advantage over the other designs.

Generating Capability

Most power companies assign a value to the available kilowatt capability of the respective turbogenerators. In this particular case, it was important to provide the maximum peak plant capacity during the most adverse wet bulb. It was calculated that with the maximum steam flow, indicated by the turbine manufacturer, the turbine capability would increase more than 300 kw by changing the approach design from 12 to 8 deg. Actually, the margin provided by the turbine manufacturer will permit a higher throttle flow and the additional available kilowatt capacity will be increased in proportion. If this extra capacity was capitalized at only $100 per kw, it did cancel out the slight advantage of the 12-deg approach, and, in the final analysis, the combination of a 26,900-sq ft condenser with 8-deg-approach 16-deg-range cooling tower was selected.

Conclusions on Economic Aspects of Cooling Towers

Cooling towers are subject to performance degradation resulting from age. Chemical deterioration will slowly affect the wood fill and structures with some local waters. More recently, biological deterioration has been encountered in several locations, and investigation of the corrective measures to be applied are now in progress. The designer should allow for such degradation margin in the cooling-tower specification.

The heat load used in the design should provide a margin to permit operation at full capability of plant generating equipment.

Closer approach to the maximum normal wet-bulb temperature should be used for design, especially in locations where the peak load is coincidental with high wet-bulb temperature.

An economic study should include an evaluation of the extra turbine capacity available due to better vacuum, resulting from a closer approach design. A comparison based on the yearly operating cost and fixed charges only, without a consideration of the extra available capacity would be misleading and would not result in the optimum selection.

It is the engineer's responsibility to provide a margin in a cooling-tower design equal to the margin used in the generating equipment and insure performance at the plant at rated capacity during the expected life of the unit.

Construction Cost of Circulating-Water Supply From River as Compared With Cooling Tower

Steam plants are preferably located where abundant circulat-

ing water is available either near large bodies of water or rivers. Cooling towers are generally used in plant locations where surface water is lacking or insufficient.

Generally, the plant initial and operating costs with circulating-water supply from rivers and lakes are lower than from cooling towers. In some instances local conditions may justify the use of cooling towers in preference to an available river-water supply at the plant site.

On some rivers, extreme level variations require deep substructures for the intake and condenser pit. The condenser-pit floor and walls must be designed to withstand the maximum hydrostatic pressure exerted at high water. Owing to an increasing number of flood-protection levees on river banks, the hydrostatic design often must be based on water levels substantially above the highest flood on record. River-bank construction under such conditions may become unduly expensive especially for small and medium-sized plants.

The cost of deep substructures is affected considerably by the nature of the subsoil. Cofferdam river work has sometimes been abandoned in favor of concrete pits sunk by the dredging method. Either method is expensive. Rock excavation on a large scale may become prohibitive in cost.

In some cases the cost of pumping ground water during construction becomes a serious problem. On one job it was necessary to add river-bank protection for a distance of 1/2 mile upstream as the deterioration of the shore had caused sand accumulation in the river channel which eventually drifted into the water intake during flood. In addition, a system of jetties had to be built to maintain a deep river and intake channel.

In a recent project on the bank of the Rio Grande, consideration was given to the conventional intake and traveling screen. During floods the river contains as high as 40,000 ppm of solids. The extreme water variation on record was 51 ft, but provisions were made in the construction for a possible fluctuation of 65 ft. Previously, an intake tower for the town water supply had been constructed at the edge of the normal river bank a short distance from the proposed plant site. This intake had been surrounded progressively by silt deposit, and considerable work is required to maintain the intake channel especially during floods.

In view of this experience for the proposed new power station, some thought was given to locating the intake and traveling screen some distance away from the river bank and providing an intake tunnel to the river channel. A deep condenser pit was required to locate the condenser outlet at the proper elevation above low water. This arrangement required considerable rock excavation and was likely to be unsafe because of silt deposits and obstruction in time of flood.

After a careful study of the initial and operating costs, it was decided to locate the plant on the high plateau above the flood stage and thus avoid deep condenser-pit work. The circulating-water supply was obtained from a cooling tower, and greater reliability was secured at a lower cost.

In another plant location the minimum river flow was adequate throughout the year. The river temperature in summer reached the maximum of 90 F. A wet-bulb temperature of 77 F was not exceeded more than 200 hr. In winter the river temperature dropped considerably faster than the wet-bulb temperature which averaged yearly between 65 and 70 F. The soil conditions were normal, and the river-level variation did not exceed 28 ft.

The first step of construction consisted of one 30,000 to 33,000-kw ASME-AIEE unit to be followed within the next 5 to 10 years by another unit of the same size or larger. Preliminary estimates indicated that there would be little difference between the river-water supply and cooling tower if installed only for one unit at a time. With the possibility of the second unit being required earlier than anticipated, a comparative study was made of the construction cost of a two-unit crib house as the first step against one cooling tower installed separately with each unit. Both units were assumed to be duplicate in size and water requirements. The cooling tower was designed for 8 deg approach to a wet-bulb temperature of 77 F.

Construction costs for the single unit program were as follows:

River-water supply	$230,000
Cooling tower	254,000

If the water intake was built for two units immediately the respective costs were as follows:

River-water supply	$277,000
Cooling tower	254,000 first step
plus	244,000 second step

The investment cost at the completion of the construction of two units based on 66,000 kw capability was $4.30 per kw for river-water supply and $7.60 for cooling towers.

In view of the small increment in the cost of the intake it was decided to proceed on the basis of a two-unit intake crib with the initial installation.

At another plant site an artificial lake was available and surface cooling of the circulating water could be accomplished by dredging a discharge ditch approximately 1 1/2 miles long. A financial agreement was made with the lake owners for a nominal yearly charge, and the ditch was completed for an estimated cost of $115,000. It could be made adequate later for a total of four units of the same size as the original installation at very little extra cost.

In résumé, the circulating-water supply from rivers and lakes, with normal subsoil conditions and reasonable water-level variations, gives lower initial and operating costs. Under some special conditions, however, the use of cooling towers in preference to river or lake water supply may be found justified after an analysis of local conditions at the plant site.

Discussion

C. C. Willis.[3] Our experience with large cooling towers is very limited, having had less than one year's experience with one 47,500-gpm tower at a new plant, and some years of experience on a 15,000-gpm tower which is used during the summer months only to augment lake cooling. Both of these towers are induced-draft-fan type.

We have observed on our property and from the experience of others that cooling towers, in general, seldom come out with any margin for overload and very often are found short. This is due in most cases to the manufacturer's desire to meet competition, and in some cases to engineers' oversight and failure to provide adequate overload capacity in the tower to meet the requirements of the turbo-generator unit.

On our small tower it was necessary to add one complete cell in order to meet contract specifications. On the large tower we found on preliminary tests that it did meet the guarantee. However, we have learned that in order to obtain consistent results for comparison, the cooling tower should be tested when there is little or no wind and when wet-bulb temperatures are on contract.

In the middle Southwest, where there is a limited amount of stream flow available for extensive power-plant circulating-water supplies, cooling towers are the only answer. Also, in this area, the annual system peak loads generally occur in the dry, hot summer months and when the wet bulb limitations are seldom a factor. This condition, of course, would be different on the coast where high wet-bulb temperatures prevail.

[3] Superintendent of Generation, Oklahoma Gas and Electric Company, Oklahoma City, Okla. Mem. ASME.

The analysis in the paper gives a good comparison of the cost problems involved in determining the method of circulating-water cooling, whether from rivers, lakes, or cooling tower. Any location selected would require special study to determine the economics involved. We know of one plant located on the Arkansas River where there is adequate water supply, but the engineers decided that, owing to the variation in elevation, distance from the plant site to the river, and chemical treatment required, a cooling tower should be installed with make-up supplied from wells. Therefore the scale-forming and corrosion tendencies of cooling-water supply should also be considered.

According to Table 1 (Summary of Data and Costs) for various cooling-tower jobs, the tower with the 12-deg approach and 16-deg range seems to result in the lowest over-all operating cost per year. Our new large tower is designed with approximately these specifications. This would indicate that the benefits from the tower with the 8-deg approach could hardly be justified.

Our main problem with the large tower, which is on a base load, year-round operating plant, is the difficulty during extreme cold-weather operations. We have not yet determined the most practical and economical arrangement for deicing. The latest attempt which showed promise was the operation of the fans at rated speed and deicing at from 2 to 3-hr intervals for 15 to 20 min with the fans operating at low speed in reverse. The removal of the distributing nozzles from the outside row adjacent to louvers decreased the time required to deice when running the fans in reverse. It has been suggested further that we consider operating the fans in reverse at full speed, in order to shorten the deicing time, and further experiments will be made along this line when we go into cold weather next winter.

Another difficulty which we experienced with our large induced-draft-fan tower, and this has to do with the plant efficiency, was that during extremely cold weather, with temperatures from 0 to 15 deg above, we were unable to obtain circulating-water inlet temperature much below 60 F. The cooling-tower manufacturers tell us that we should be able to operate as low as 40 F from the tower during extremely cold weather without excessive difficulty due to icing. We know that on streams, the plant circulating-water system would obtain the benefits of water cooler than 60 F inlet, and we would be interested in knowing how other operators with cooling towers get down to 40 F water from the tower during cold weather.

Author's Closure[1]

Cooling towers operated in freezing weather are subject to ice formation at the air inlets; small amounts of water vapor are likely to freeze on the inlet louvers and the nearby wood filling. Ice starts to form on the lower section of the louvers and progresses upward; this accumulation of ice restricts the inlet area and reduces the air flow, thus increasing the temperature of the water being circulated through the tower.

The main mass of the tower circulating water is rarely cooled much below 60 F, because the approach (difference between cold water and design wet-bulb temperature) for power-plant applications is generally 10 to 15 F. If the approach (design) temperature were 5 F (at greater cost), then the tower would have sufficient cooling capacity to give cold-water temperatures approaching the 40 F mentioned by Mr. Willis.

Since the cold-water temperature is seldom below 60 F, ice formation generally occurs only on parts of the tower that are lightly wetted by fine drops which splash toward the entering air stream. To *prevent icing* during cold-weather operation, one of the following procedures is recommended for induced-draft towers: (*a*) shut down fans completely but do not shut off water; and (*b*) shut off some of the cells.

If ice should form on the louvers and filling, more of the following methods of *ice removal* could be used: (*a*) reversing (for a limited time) at full or half speed the rotation of the motor(s) that drive the fan(s) and thus blowing the warm air backwards and out through the louvers; and (*b*) shut down some fans temporarily but do not shut off the water.

In general, the overall plant economy of a steam-electric generating station is improved very little (if any) when the condenser circulating-water temperature is less than 60 F. The back pressure may decrease about 0.10 in. of Hg per 10 deg drop in water temperature below 60 F (as compared to 0.55 in. per 10 deg drop from 90 to 80 F); however, the advantage of this slight decrease in back pressure would decrease the condensate temperature and indirectly effect the performance of the turbine, condenser, and/or feedwater heating.

---

[1] At the request of the author of this paper, A. R. LeBailly, H. E. Degler has prepared the closure. Mr. Degler is the author of the paper in this issue "Selection, Operation, and Maintenance of Industrial Cooling Equipment," pages 1031–1036 of this issue.

Cooling Towers for Steam-Electric Stations—Economic Applications

By LOUIS ELLIOTT,[1] NEW YORK, N. Y.

The paper outlines a method of making economic comparison as between the use of a cooling tower and a direct-condensing arrangement for a steam station; the method is illustrated by analyzing a specific problem. Remarks on the placing of cooling towers are included, and problems requiring research are mentioned.

Economic Comparison of Cooling-Tower With Direct-Condensing Plant.

IT is frequently desirable to draw an economic comparison between direct use of river or pond water for condensing and utilization of cooling towers. Such a comparison, made not long ago for a 60/66-mw 1250-psig 950 F steam-electric generating plant, employing 10-year data on river temperatures, and records of atmospheric temperature and humidity over a longer period, is presented in this paper.

At the site studied, long intake and discharge conduits are required for river installation, and therefore a two-pass condenser is adopted for that case as well as for a cooling-tower installation. For the direct-condensing plant, the use of 120 cfs of cooling water is assumed, with a velocity of 7 fps through the tubes. For a cooling-tower installation, the same condenser is assumed, with 137 cfs of circulating water, giving a tube velocity of 8 fps. The condenser selected is a 45,000-sq ft unit with $^7/_8$-in. tubes, designed to condense 398,000 lb of steam per hr, at 66-mw gross generation, and giving 2 in. absolute back pressure with entering water at 82 F. Heat load for either case is figured at 368 million Btu per hr.

The cooling tower is specified to give an approach of 14 F to a normal maximum wet-bulb temperature of 76 F, with the 368-million-Btu heat load. That wet-bulb temperature is considered reasonable, as basis of the 14 F approach, for the climate in question. Climatic data indicate that 76 F wet bulb is exceeded 90 hr annually on the average; maximum recorded wet-bulb temperature is about 80 F.

Fig. 1 shows the monthly average water temperatures anticipated, on the basis of Weather Bureau and river-temperature records, and of cooling-tower selection. River temperature closely follows the dry-bulb air temperature, and for practical purposes is assumed equal to it. Temperature of water leaving the cooling tower, at full load, is a few degrees higher than river temperatures in the summer and roughly 30 F higher in the winter. Cooling-tower at half load is slightly lower than river temperature in summer, and about 20 F higher in winter. The greater difference during cold weather is accounted for by the greater spread between ambient wet bulb and temperature of water from the tower during cold-weather conditions.

Using water temperatures shown in Fig. 1, calculations are

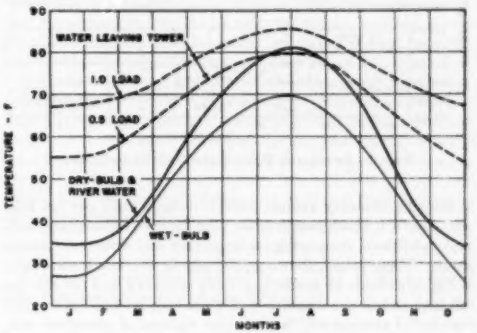

Fig. 1 Water-Temperature Data

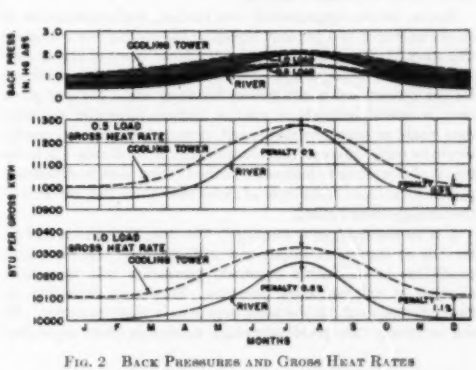

Fig. 2 Back Pressures and Gross Heat Rates

made based on design performance of turbine and condenser, assuming 85 per cent condenser cleanliness factor, to arrive at turbine back pressure and gross kilowatt-hour heat rate. The results are shown in Fig. 2. At full load, the cooling-tower penalty in gross heat rate ranges from about 0.5 to 1.5 per cent at full load and from zero to 0.5 per cent at half load. Here again the penalty is greater in the winter. The upper curves in Fig. 2 show computed differentials in condenser back pressure, for full and half load, comparing use of river and cooling tower. The spread at full load ranges from 0.2 to 0.3 in., and at half load roughly the same. It is from these values that the lower curves in Fig. 2 are calculated.

Estimates are made of auxiliary energy use at full and half load, using river water and cooling tower, respectively. The top chart in Fig. 3 shows the results, indicating a spread of something under 1000 kw or 1.5 per cent of 66,000 kw, as between river and cooling tower. This spread depends upon relative design of the two kinds of plant. The auxiliary-energy requirement is applied

---

[1] Consulting Mechanical Engineer, Ebasco Services Incorporated. Mem. ASME.

Contributed by the Power Division and presented at the Spring Meeting, Atlanta, Ga., April 2–5, 1951, of The American Society of Mechanical Engineers.

Note: Statements and opinions advanced in papers are to be understood as individual expressions of their authors and not those of the Society. Manuscript received at ASME Headquarters, February 20, 1951. Paper No. 51—S-6.

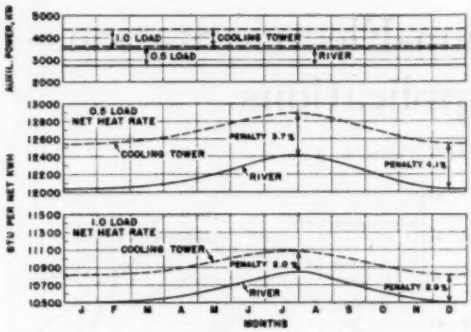

FIG. 3 AUXILIARY POWER AND NET HEAT RATES

in deriving economy values—British thermal units per net kilowatt-hour—for each month of the year, for both full-load and half-load conditions, comparing cooling-tower and direct-condensing plant. These values, shown graphically in the two lower charts in Fig. 3, indicate an economy penalty of from 2 to 3 per cent for full load and of the magnitude of 4 per cent for half load. The year-round average will depend upon regimen of operation, and, for the usual base-load plant, the year-round average will be nearer to the full-load conditions.

Hence, for the hypothetical case studied, fuel consumption is shown as from 2 to 3 per cent higher for the cooling-tower station, this spread being accounted for by combined effect of higher condensing-water temperatures and resulting higher back pressures for the former, and of the greater auxiliary use. For any given case, a careful estimate of relative temperatures and auxiliary uses would of course be made, and in some instances the results would be quite different from those shown on the charts. It is the intent of this study to indicate a method rather than to determine precise magnitude of differential as between these two methods of condensing-water cooling.

If it be assumed, as is frequently the case, that steam flow to throttle at maximum output and with standard throttle steam conditions is reasonably constant, generation will vary with changes in exhaust back pressure. Maximum capability is then affected in about the same degree as is plant economy. In the particular case previously cited, maximum plant capability of a cooling-tower plant, as compared with a direct-condensing, is penalized by from 2 to 3 per cent.

The differentials between the two types of plant, in fuel use and in capability, may be combined in any way desired. Cost of fuel is a major element of operating expenses, and loss of plant capability may be evaluated as a fixed-charge component of total energy cost.

A cooling-tower plant may be considered as carrying slightly higher depreciation and maintenance expense than a direct-condensing plant. Certain data have been developed recently as to delignification and other deterioration of wood in a cooling tower, which tend under some conditions to shorten life. However, a cooling-tower installation is frequently economical, when large expenditures for storage reservoirs, for intake structures, or for long transmission lines are avoided.

COOLING-TOWER PERFORMANCE

Cooling towers are usually guaranteed to produce a stated approach to a specific wet-bulb temperature of water temperature leaving the tower with a given heat load. The wet-bulb temperature selected is frequently near the maximum for climatic conditions to be experienced, and heat load usually corresponds to maximum plant capability.

Towers, after they are put into service, should be tested to determine whether they meet the guarantee. Because guarantee conditions cannot always be obtained during the tests, it is desirable that a set of correction curves form part of the specifications. Results of such acceptance tests, run over a period of years at a number of client-company installations, are summarized in Table 1. In about 90 per cent of the tests recorded, there is indicated a deficiency in performance. This sometimes can be corrected by alteration to fans, tower fill, or water distribution; more frequently, an addition of cells is required. In a few cases, in lieu of changes to the tower, a cash settlement is made, based in some degree on capitalized value of loss in plant efficiency and capability resulting from deficiency of tower performance.

Competition between manufacturers is keen, and it appears that sufficient margins have not been provided in the equipment. Not all towers are tested after installation, and adjustment of test results, from conditions actually obtaining to guarantee conditions, is difficult. There are likewise difficulties in determining the performance of a large tower from a factory test of a single cell. The process of cooling, itself, and the effects of nonuniform air and water distribution are complicated; accurate predictions of performance are difficult to make. Conditions after installa-

TABLE 1 COOLING-TOWER PERFORMANCE DATA

Turbine-generator, rating, mw	Tower Mfr	Tower Type	Tower Cells	Design, cfs	Heat load, million Btu	Cooling range, deg F	Max W-B, deg F	Approach, deg F	Initial test Date	Initial test Deficiency deg F	Action taken	Final result or deficiency
25/31.25	A	F-d	12	57	205	16	76	18	10/39	3.5	4 cells added	Satisfactory
25/31.25		F-d	16	76	257	15	76	14	10/43	0	None	Satisfactory
30/33		I-d	6	62	242	17.5	70	14	6/48	6.6	New fans, 2 cells added	Not tested
30/33		I-d	6	67	242	15.6	78	13	6/49	2.0	3 new fans	Pending
25/31.25, 20/25		F-d	18	93.5	293	14	78	14	6/49	5.8	Cash settlement	5.8 deg F
11.5/12.65		I-d	3	31	121	17.5	70	14	8/49	3.8	One cell added	Not tested
40/44 (2)		I-d	16	192	600	14	75	14	8/50	3.8	Pending	
30/33		I-d	6	62	242	17.5	76	14	10/50	1.5	Fans changed	Pending
25/31.25	B	F-d	3	71.1	208	13	74	16	6/39	3.8	New fans, ext tower	Satisfactory
25/31.25		I-d	8	65	278	15	76	14	7/47	2.4	Cash settlement	1.0 deg F
35/43.75		I-d	6	93.5	316	13	76	14	6/48	3.6	One cell added	Satisfactory
11.5/12.65 (2)		I-d	6	61.9	222	16	74	14	11/48	1.0	Cash settlement	0.8 deg F
25/31.25		I-d	5	73.3	214	13	78	13	10/48	1.2	Fans adjusted	Satisfactory
11.5/12.65 (2)		I-d	6	61.9	222	16	74	14	8/49	1.0	Cash settlement	0.8 deg F
60/66		I-d	9	121	460	17.5	76	14	10/49	7.5	Fans changed, cash settlement	1.0 deg F
11.5/12.65 (2)		I-d	6	59.8	225	16	76	12	8/49	0	None	Satisfactory
30/33		I-d	5	73.3	214	13	78	13	6/49	1.5	Fans adjusted	Satisfactory
30/37.5	C	I-d	16	82	277	15	76	12	8/47	1.5	2 cells added	Satisfactory
60/66 (2)		I-d	48	285	1000	15.6	76	14	5/49	5.7	8 cells added	1.5 deg F
30/33		I-d	14	84.5	293	15.4	76	14	7-49	4.3	2 cells added	1.3 deg F
40/44		I-d	18	96	335	15.6	78	13	3/50	1.5	Pending	
60/75 (2)		I-d	52	318	1190	16.6	76	14	8/50	0.1	None	Satisfactory
60/66	D	I-d	6	130	495	17.5	70	12	6/50	3.4	Pending	

tion, taking into consideration spacing between towers and other local factors, introduce further complexities.

It would appear that standards for tower design might well be adopted by the industry, which would contain a margin sufficient to assure a reasonable expectation of meeting guarantees. This margin is frequently built into other equipment. Conformity of results from turbine and boiler tests, with the guarantees, is, in general, good.

Location and Orientation of Towers

In the matter of location, spacing, and orientation of cooling towers, there still remains much to be learned—particularly for the larger installations. With the use of induced-draft-type towers, there is somewhat less tendency for recirculation of discharge air back into the tower inlet. A common practice is to locate the lengthwise axis of the tower parallel to the usual wind direction, on the theory that there will be less tendency for recirculation than if prevailing winds were to blow crosswise of the tower, causing the discharge air to be drawn back in again. The spacing between towers, if they are located end to end, is usually not great. Large towers preferably should be located 300 to 500 ft away from the plant or from main roadways or power lines to guard against nuisance from driftage of mist. The use of induced-draft fans more or less nullifies any requirement for locating the tower on top of a hill or away from obstructions that might interfere with the free access of air, so long as sufficient area is available for the air volume required by the tower to flow in freely.

Research Needed

While experience with actual installations has indicated reasonable distances for spacing between buildings and towers and between multiple towers themselves, and best orientation with respect to prevailing direction of wind, a great deal more information is necessary in order to determine the best placement of towers. A tower, once placed, cannot be moved around to determine more favorable conditions.

Research is under way by Marley and other tower manufacturers, with the co-operation of the United States Department of Agriculture, Forest Products Laboratory, with respect to deterioration of towers, including delignification and general decay of the wood in them. This deterioration has been more active along the Gulf Coast, and it is hoped preventive measures will be found effective, so that tower life will not be shortened materially under adverse conditions of this kind.

Acknowledgment

The author is greatly indebted to the work of W. F. Friend and other associates in preparing this paper.

Selection, Operation, and Maintenance of Industrial Cooling Equipment

Cooling Towers and Air-Cooled Exchangers

By H. E. DEGLER,[1] KANSAS CITY, KAN.

To avoid water shortages, conservation and re-use of water have become a necessity in many areas. Water can be purified, cooled, and re-used. Large industrial water users are power plants, manufacturers of paper, petroleum products, rayon, linens, textiles, lactose, sugar, explosives, hydrogen, rubber, steel, and so forth. Requirements are frequently in excess of 300 lb of water per lb of finished product. Water usage has doubled in the past decade—hence selection of cooling equipment becomes more important as power demands increase, industries expand, and new processes are perfected. Mechanical-draft cooling towers can cool water evaporatively to a temperature approaching the wet-bulb temperature of the ambient air. This evaporative method requires less than 1 per cent evaporation of the water circulated to dispose of the heat load economically. Air-cooled finned-tube exchangers are having increased acceptance and usage for "high-level heat removal" (for example, above 130 F referred to 100 F dry-bulb air), where water is scarce, expensive, and/or badly polluted; small space requirements and easy control are other features. The performance and life of any piece of cooling equipment is directly dependent upon its inherent qualities, type of service, severity of operation, general care and maintenance, and climatic environment.

The Water Problem

In general, water shortage has nothing to do with drought but can be attributed to overpopulation in cities and increased industrial and agricultural requirements. The requirements of the United States are 100 billion gal per day for everything from drinking and irrigation to making steel and watering the lawn, that is, 700 gal per day per person.

The unsuspecting housewife and the indifferent businessman have teamed up with the many industrial users to make water the nation's most precious natural resource. Like the automobile and radio, ample water is part of the American way of life. Most people are surprised to learn that our water supply is exhaustible and, like coal and oil, water can be taken from the ground faster than nature can replenish it. Centuries of rainfall had accumulated tremendous quantities of underground water; these are approaching depletion in some areas because of seasonal overpumping. Surface water from rivers and lakes is also approaching depletion during drought and high-temperature periods. As the frontiers of our country were extended, the clearing of lands increased the water run-off from rainfall and further decreased the underground water supplies.

Cooling-Water Requirements

The irrigation of 1 acre of oranges requires 800,000 gal of water per wetting. Producing 1 kw of electric power or 1 ton of ice takes about 4000 gal per day. Midsummer cooling of a large theater requires 80,000 gal per day. One large paper mill uses 25,000,000 gal per day, more than the total water pumped for the domestic and industrial use of a city of 200,000 population.

Many industries require huge quantities of water; Table 1 lists 17 specific examples.

TABLE 1 WATER USE IN TYPICAL INDUSTRIES

Product	Lb of water per lb of product
Ammonium sulphate	700
Butadiene	1200
Gun powder	400
Hydrogen	2500
Lactose	900
Linen	700
Milk products	20
Oil refining	500
Paper	200
Rayon	800
Rubber (synthetic GR-s)	2500
Soap	15
Soda pulp	300
Steel	350
Sugar refining	100
Textiles	350
Wool	500

Great as the total water requirements are, they are much less than the total amount of rainfall and less than the smaller amount available for use from streams and underground sources. However, the availability is continuously decreasing and the need for water conservation and regulation becomes more imminent.

In general, the quantity (and temperature) of water available are of the utmost importance, far outweighing considerations of quality. But the quality of water supply cannot be ignored because dissolved solids, gases, and other impurities can corrode or foul metal surfaces.

Cooling Methods for Water Re-Use

There is plenty of water, at a price! Since the past decade's doubled demand for water, underground sources in many areas have become dangerously depleted by overuse; but with adequate knowledge of these resources there will come effective legal control in more states.

Run-off water is that which remains on the earth's surface after the prior claims of evaporation, transpiration of plants, and absorption by the ground have been satisfied. Thus run-off water varies much more widely than rainfall. Consequently, the selection of a new plant location on the bank of a river or near an adequate fuel supply is an economic problem which today requires more careful study than ever before.

Once-through use of cooling water is wasteful. In many applications the same water can be used for additional service and/or

---

[1] Technical Director, The Marley Company, Inc. Mem. ASME.

Contributed by the Power Division and presented at the Spring Meeting, Atlanta, Ga., April 2–5, 1951, of The American Society of Mechanical Engineers.

Note: Statements and opinions advanced in papers are to be understood as individual expressions of their authors and not those of the Society. Manuscript received at ASME Headquarters, February 20, 1951. Paper No. 51—S-7.

continuous re-use. Selection of the most economical water-cooling method becomes more important as power demands increase and industries expand their water usage.

During the past 40 years the progressive improvement of methods for cooling and subsequent re-use of water have been utilized in the following sequence: (1) Rivers, lakes, wells, and cooling ponds; (2) spray ponds; (3) evaporative condensers; (4) natural-draft water-cooling towers; (5) forced-draft cooling towers; (6) induced-draft cooling towers; and (7) dry-surface coolers (air-cooled exchangers).

Prior to 1920, large water-cooling systems were used only with steam-electric generating stations, usually located on the banks of rivers, lakes, or artificial cooling ponds. In some installations it was expedient to use spray ponds. Refrigeration and ice making constituted the second largest usage, with roof-located natural-draft towers and spray ponds.

Since the year 1920, numerous new applications have arisen, others grown; and, with this shift, requirements have become increasingly varied and exacting, necessitating refinements and specialized adaptations of water-cooling equipment. The principal demand for large water-cooling systems in recent years has been from the petroleum industry, steam power plants, process industries, and chemical plants. Refrigeration, air-conditioning, and engine-jacket cooling employ a large percentage of the medium-sized and small cooling units installed today.

Progress in the cooling-equipment industry is apparent when it is realized that for a definite need, a modern cooling unit requires only 1 sq ft of ground area as compared to 50 sq ft for the spray pond and about 1000 sq ft for a natural cooling lake or pond. The continuous demand for a more compact design, better construction, lower cost, larger capacity, greater flexibility of operation, independence of atmospheric uncertainties, and improved all-round performance has resulted in the modern induced-draft water-cooling tower.

Principles of Evaporative Cooling

A water-cooling tower is an enclosed structure for the evaporative cooling of water by contact with moving air, Figs. 1 and 2. Water, when cooled by the evaporative effect in a cooling tower, transfers to the air about 1000 Btu per lb of water evaporated. In other words, 100 lb of water can be cooled 10 F by the evaporation of 1 lb of water. Air, absorbing heat from water in this manner, is capable of cooling water below the atmospheric (dry-bulb) temperature; the process is adiabatic (constant enthalpy).

Theoretically, water may be cooled by the evaporative method (as in a cooling tower) until its temperature is lowered to the air's wet-bulb temperature. In practice, however, water is cooled to a temperature approaching the wet-bulb; the closer this "approach" the larger the size of the cooling equipment required for a given duty. Generally, used wet-bulb design temperatures are 70 to 80 F, depending upon the service and geographical location of the unit.

"Cooling range" is the number of degrees F that the water is cooled with water-cooling equipment. It is the difference between the temperature of the hot water coming to the cooling tower and temperature of the cold water leaving the tower.

Water-Cooling Towers

A "conventional" induced-draft cooling tower is an enclosed structure for the evaporative cooling of water by contact with the air, consisting of one or more individual adjacent cells, each with its own induced-air-circulation fan, gear and motor drive mounted on top of the tower structure. Generally, wood filling is used (spray-filled for some applications) to provide wetted cooling surface and water break-up. In many cases, a combination of the spray-filled and wood-filled design is used, as shown in Fig. 1.

Another induced-draft tower, developed for the purpose of obtaining more compactness, better construction, lower cost, larger capacity, increased flexibility, and improved performance, is the crossflow type (also called double-flow), Fig. 2. This distinctive tower employs multiple fans (adjustable-pitch blades) centered along the top, each fan drawing air through two cells paired to the plenum chamber which is partitioned midway beneath each fan and fitted with "drift eliminators" that also turn the air upward toward the fan outlet. This tower obtains a horizontal air movement as water falls in a cascade of small drops over the wood-filling and across the air stream with low resistance to the air flow. The air travel is longer than with the conventional counterflow design as shown in Fig. 1.

Selection of Cooling Equipment

Cooling Towers. Because of the many variables in water-cooling-tower calculations and performance, it is difficult to provide simple handbook equations and tables whereby an engineer can readily select the type and size of unit for a definite water-cooling requirement.[3] Each manufacturer has a semiconfidential method of sizing a tower, based largely upon research and actual performance correlated with definite requirements. Selection of cooling equipment for any specified service must ultimately depend upon over-all considerations established from reliable design and performance data.

The performance of a cooling tower is improved by increasing the amount of filling, height, area, and/or air quantity. Increasing the tower height increases the length of time the air is in contact with the water, without seriously affecting the fan power required, but increases the pumping power. Increasing the tower area, while maintaining constant fan power, increases the air quantity somewhat and increases the time that this air is in contact with the water because of lower velocity. The surface area of water in contact with the air is increased in both cases.

Increasing the air velocity through the tower decreases the time the air is in contact with the water, but, since a greater quantity is passing through, the average differential between the water temperature and wet-bulb temperature of the air is increased, and this increases the rate of heat transfer. Increased air quantities are obtained only at the expense of increased fan power, which increases approximately as the cube of the air quantity. Air velocities through induced-draft towers vary from 250 to 450 fpm over the gross area of the structure; pumping heads vary from 12 to 30 ft, depending upon the design.

Table 2 presents the characteristics and costs of two representative sizes of water-cooling towers for the years 1925, 1932, 1941, and 1950. Careful study will indicate that improved designs have continuously reduced costs during this 25-year period, despite the recent inflationary period. Even greater reductions have been made in fan horsepower, number of fans required, and the water pumping heads required, with improved performance and flexibility. Space requirements are less, appearance is better, drift loss has been practically eliminated, and structural details have been simplified and improved, with resultant lower maintenance and greater safety. The increased costs of labor and materials for modern water-cooling towers have been offset by better engineering as reflected by continued improvement, simplification, and closer adaptation to the specific requirements of each application, and developing every opportunity for wise reductions in the cost of production and operation.

Air-Cooled Exchangers. The air-cooled exchanger is a device for cooling or condensing fluids by circulation of the fluid through

[3] Unreliable estimates are frequently based upon L/G (liquid to gas ratio), gpm per sq ft plan area, hp per 100 gpm water, weight of tower per gpm of water, cooling efficiency, etc.

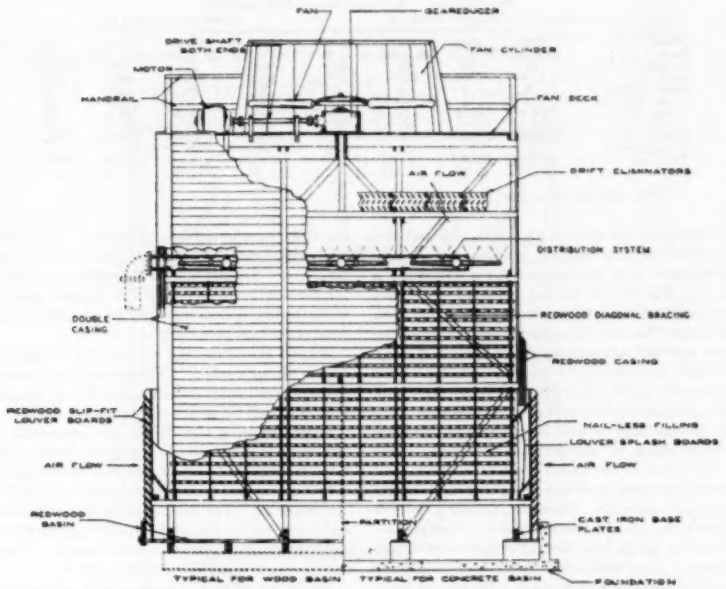

FIG. 1 SECTION THROUGH AN INDUCED-DRAFT COUNTERFLOW WATER-COOLING TOWER

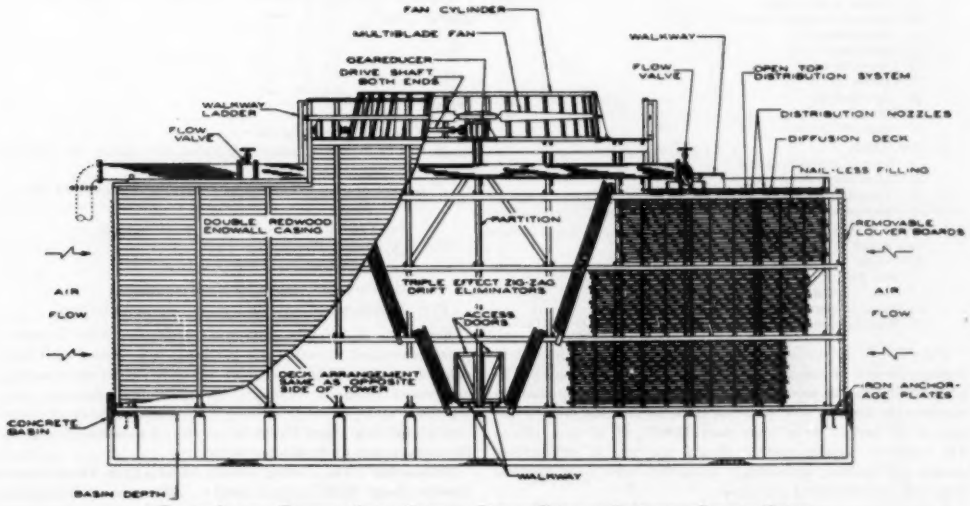

FIG. 2 SECTION THROUGH LARGE-CAPACITY DOUBLE-FLOW OR CROSSFLOW COOLING TOWER

TABLE 2 CHARACTERISTICS AND COSTS OF WATER COOLING TOWERS—1925 TO 1950

	95 F hot water—85 F cold water—75 F wet bulb							
Capacity	5000 gpm (3000 kw)				20,000 gpm (12,500 kw)			
Years	1925	1932	1941	1950	1925	1932	1941	1950
Base, ft	22 × 95	30 × 72	30 × 80	36 × 36	36 × 220	26 × 240	40 × 240	60 × 60
Height, ft	40	36	26	30	40	36	26	36
Area, sq ft	2112	2160	2400	1000	8420	8640	9600	3600
Fans, number	6	6	4	2	22	24	10	2
size, diam, ft	11	11	13	12	12	11	16	22
bhp, each	28.4	19.2	24	25	30	19.2	38.4	70
bhp, total	170.4	114.9	96	50	660	460.8	384.0	140
Weight, dry, lb	280000	260000	240000	90000	960000	940000	900000	290000
Pump head, ft	27	27	20	14	28	28	20	26
Total cost	$22000	$20000	$19000	$18500[a]	$78000	$71000	$67000	$62000[a]
Cost per kw	$7.30	$6.70	$6.30	$6.17	$6.30	$5.70	$5.40	$4.95

[a] 1943–1945 costs were 60 per cent of these amounts.

finned tubes and forcing of atmospheric air across the coil sections. This dry-surface cooler is basically a noncontact convection-type heat exchanger. One arrangement for a dry cooler is the induced-draft unit, Fig. 3, with the fan mounted on top discharging the air upward and inducing air across a horizontal bank of coils mounted below the fan. Another arrangement is the forced-draft, Fig. 4, with the fan discharging air upward across a horizontal bank of coils mounted above the fan. Small portable units are conventionally arranged with a vertical coil bank mounted to receive a horizontal stream of air across the coil.

The air-cooled exchanger may be used in preference to a water-cooling tower for applications of "high-level heat removal" where temperatures of the fluids to be cooled are above 130 F, and where water is scarce, expensive, and/or badly polluted, or where the portable features are desirable. Normally, a cooling tower is more economical, but the cost of the air-cooled exchanger decreases relatively to that of the tower as the temperature of the fluid to be cooled rises. Both units have their own applications and in some instances either type may be used. However, a careful evaluation of both methods should be made to insure that the most suitable cooling equipment is selected in each case.

The following list shows typical applications for finned-tube air-cooled units:

1 Liquid cooling:
   (*a*) Engine jacket water
   (*b*) Engine lube oil
   (*c*) Absorption oil
   (*d*) Stabilized crude
   (*e*) Vegetable oil
   (*f*) Cotton oil
   (*g*) Cocoanut oil
   (*h*) Quenching oil
   (*i*) Amine solutions
2 Gas cooling:
   (*a*) Natural-gas intercooler
   (*b*) Natural-gas aftercooler
   (*c*) Manufactured gas cooler
   (*d*) High-pressure gas (pressure-booster station)
3 Vapor cooling:
   (*a*) Gasoline
   (*b*) Steam
   (*c*) Still reflux
   (*d*) Still overhead
   (*e*) Debutanizer
   (*f*) Depropanizer

The place of dry-surface air-cooled heat-transfer equipment in industry should be one of increasing acceptance and usage. The basic reason for this prediction is that in spite of developments to conserve the use of water, to increase the availability, and to dispose of the heated water more conveniently, all of these efforts will increase cooling costs. Hence the use of dry-surface coolers will become increasingly attractive, and more applications will be considered and made.

A process industry found it necessary to provide an additional cooling of 25,000,000 Btu per hr and could have provided additional water only at great expense because of limitations of present size of water mains and pumps. Additional heat-exchange equipment also was needed, further complicating installation problems. An air-cooled exchanger was installed; because of the self-contained feature of this type of cooler, no modifications of the utility system were required beyond the electrical connection for the fan-drive motors.

A need was evidenced to handle a cooling load existing only during winter weather. The dry-surface cooler was preferred because of small space requirements, low air temperature, simple to start, and easy control of the freezing hazard.

When selecting the design air temperature for dry-surface coolers, it is generally acceptable to choose a dry-bulb temperature which will not be exceeded more than 5 per cent of the hours between noon and midnight during the months of June to September, inclusive. The temperatures that occur in excess of this design value will be of such short duration as not to have an appreciable effect on efficiency or performance. Frequently used dry-bulb design temperatures are 95 to 100 F.

Evaluation of Costs. A comparison of costs for various types of cooling equipment for a given application requires detailed study. To obtain an estimate, a complete analysis must be made; first cost, power costs, water costs, maintenance, etc., can be evaluated over the life expectancy of the equipment. The calculation may be made as follows.

Annual operating costs = maintenance + depreciation + power costs

$$A = M + \frac{C}{t} + P$$

where

A = annual operating costs
M = maintenance, insurance, taxes, etc., figure furnished by purchaser
C = cost of equipment; would include any or all of the following:
   (*a*) Cost of unit erected; by manufacturer
   (*b*) Pumps, piping, etc.; by purchaser
   (*c*) Electrical work; by purchaser
t = time in years, estimated life of equipment
P = annual power costs for fans and pump (or pumps)

Example. A 900-bhp., 300-rpm, two-cycle, solid injection, pump-scavenged, Diesel engine in Ohio is to be cooled with recirculated water. Make necessary estimates and select cooling equipment required. Prepare an evaluation showing cooling tower and air-cooled exchanger costs upon a basis of operation at full fan speed for 24 hr per day, 8 months per year for 20 years, power at $0.015 per kwhr.

Calculation. The cooling system for this type Diesel engine absorbs about 2500 Btu per bhphr. Assume a shell-and-tube exchanger (with cooling tower) designed to cool jacket water from 170 to 158 F, and that the raw-water temperatures are to be 115 and 95 F to a 72 F design wet-bulb air temperature.

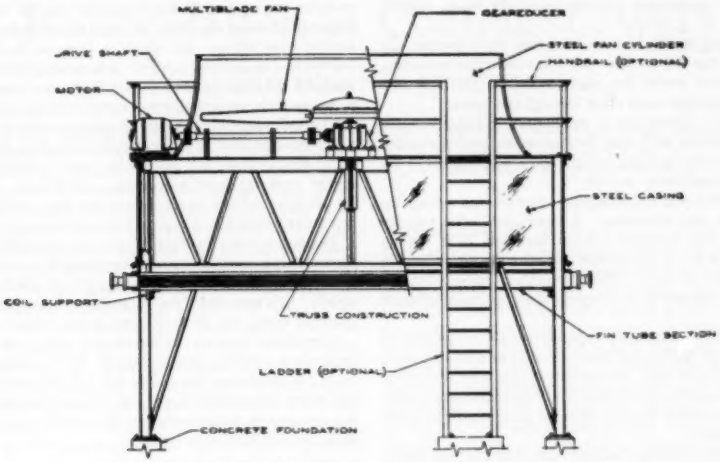

FIG. 3 INDUCED-DRAFT ARRANGEMENT FOR A DRY-SURFACE COOLING UNIT

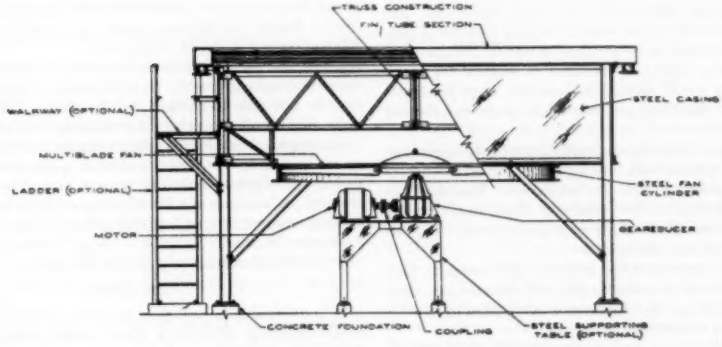

FIG. 4 FORCED-DRAFT ARRANGEMENT FOR A DRY-SURFACE COOLING UNIT

Heat to water = 900 bhp × 2500 Btu = 2,250,000 Btu per hr

$$\text{Gpm} = \frac{2{,}250{,}000}{60 \times 8.33 \times 20} = 225 \text{ gpm raw water circulated through tower}$$

$$\text{Gpm} = 225 \times \frac{115 - 95}{170 - 158} = 385 \text{ gpm soft water through engine jacket}$$

Power cost = \$0.015 × 24 × 30 × 8 = \$86.40 per kw per yr

OPERATION

Pages of recommendations could be written on the starting-up, operating, maintaining, and shutting down of cooling equipment in order to obtain maximum results under varying load requirements and changing weather conditions. The life of any piece of cooling equipment is directly dependent upon its inherent qualities, type of service, severity of operation, general care and maintenance, and climatic environment. The continued utility

TABLE 3 EVALUATION COSTS OF COOLING TOWER AND AIR-COOLED EXCHANGER FOR SAME COOLING REQUIREMENTS

900-bhp Diesel engine ..... 375-gpm soft water

	Cooling tower	Air-cooled exchanger
Cooling tower and basin	\$1800	..
Shell-and-tube heat exchanger	950	..
Pump (raw water) with motor	250	..
Air-cooled exchanger	..	\$2900
Piping and soft-water pump	400	400
Electrical work	350	300
Cost of equipment, C	\$3750	\$3600
Maintenance (5 and 3 per cent)	\$190	\$110
Water and treatment cost	350	30
Insurance at 2 per cent	75	72
Taxes at 1 per cent	38	36
Contingencies at 2 per cent	75	72
Maintenance, M	\$728	\$320
Fan horsepower, hp	5	10
Pump horsepower, hp	3	2
Kilowatts = $\frac{\text{hp} \times 0.746}{0.88 \text{ motor eff.}}$	6.8	10.2
Power costs at \$86.40 per kw-yr, P	\$587	\$880
Annual operating costs, $A = M + \frac{C}{20} + P$	\$1503	\$1380

of all mechanical equipment depends primarily upon maintenance.

For best operating results it is essential that the hot-water distribution system, the tower fill, and the cold-water collecting basin be kept clean of leaves, dirt, algae, scale, and the like; also maintain a uniform rate of water flow through the tower.

Water Treatment. Treatment of cooling-tower water includes prevention of corrosion and scale formation on heat-exchanger equipment; prevention and control of algae: and control of delignification[3] of cooling-tower lumber.

The amount of make-up water required depends upon evaporation loss, drift loss, and blowdown. Evaporation losses average 0.80 per cent of the water circulated for each 10 F cooling range. Drift loss is the water carried away by the air current in the form of droplets or mist. This loss seldom exceeds 0.1 per cent (of the water circulated) in properly designed induced-draft towers.

The amount of blowdown used depends upon the hardness of the circulating water, the type of water softener or inhibitor used, and the amount of drift loss. Blowdown is normally controlled to maintain the concentration of dissolved and scale-forming solids below the point where the formation of scale would occur or would cause corrosion.

Scale. Some scale-forming materials are found in practically all water; however, the most troublesome are normally calcium and magnesium carbonates. Scale can be reduced or prevented by softening the make-up water with lime and soda ash, zeolites, sulphuric acid, soluble phosphates, or sodium chromate. Regardless of the water-treatment method used, a systematic program of blowdown should be established to control the dissolved solids in the cooling water. The choice of method for water treatment is largely one of an economic nature: since the treatment requires close regulation and control, a competent chemist should be consulted.

Two-Speed Motors. For adapting performance to temporary or seasonal decreases in heat load, and especially for winter operation, two-speed motors are used for fan drives. The chief advantage is that at half speed fans need only about 15 per cent of their full-speed power. Particularly in multifan units, the flexibility of two-speed motors saves power.

During the winter months, when it is not cold enough to shut down the fans completely yet cold enough so that ice tends to form at full fan speed, icing may be minimized or eliminated by operating some or all of the fans at half speed.

Cold Weather. Extremely cold water normally does not increase performance to any great extent, but operating hazards are increased considerably. Cooling towers operated in freezing weather are subject to ice formation at the air inlets; small amounts of water are likely to freeze on the inlet louvers and the nearby wood filling. Ice starts to form on the lower section of louvers and progresses upward: this accumulation of ice restricts the inlet area and reduces the air flow, thus increasing the temperature of the water being circulated through the tower.

The main mass of the tower circulating water is rarely cooled to a temperature that even approaches freezing: in fact, the cold-water temperature will seldom be lower than 60 F, except with towers used for specific operating conditions. For this reason ice will form only on parts of the tower that are lightly wetted by fine drops which splash toward the entering air stream.

To prevent icing during cold-weather operation, one or more of the following procedures are recommended for induced-draft towers: (*a*) Operate motors at half speed; (*b*) shut down fans completely; this may retard ice formation; (*c*) cover upper portion of louvered area; (*d*) shut off some of the cells.

If ice should form on the louvers and filling, one of the following methods of removal could be used: (*a*) Reversing (for a limited time) the rotation of the motor driving the fan and thus blowing the warm air backward and out through the louvers; (*b*) shut down some fans temporarily but do not shut off water; (*c*) cover upper portion of louvered area.

Maintenance

Well-maintained equipment gives the best operating results and the least over-all maintenance cost. A regular schedule should be set up for the mechanical maintenance of cooling equipment. Follow instructions issued by manufacturer for proper lubrication of mechanical equipment.

Clean and paint all corrodible metals as required. Redwood does not require protection from the weather, but in some cases it may be desirable to paint it for appearance. Tighten all loose bolts, making allowance for the swelling of wood when wet.

In general, air-cooled exchangers require the same maintenance as do cooling towers, because similar mechanical equipment is employed. Certain fouling factors are used when estimating the size and performance of a finned-tube cooling unit; increased operating temperatures and greater pressure drop through a heat exchanger frequently indicate excessive fouling and the need for cleaning the tubes, internally and/or externally.

Conclusions

It is impossible to formulate any set of recommendations that would definitely establish a given cooling method as the most suitable for any particular installation. The anticipated performance of a proposed installation must be completely analyzed, and the final selection frequently becomes a matter of engineering compromise and personal preference. It is significant that as the need for water conservation increases, the manufacturers of cooling equipment have been accumulating a great reservoir of experience by continuously making more economical units and more highly specialized applications.

[3] Delignification is defined as the chemical deterioration of lumber caused by the removal of the lignin binder between the wood fibers; in cooling-tower lumber, delignification is generally caused by the combining of sodium carbonate from the water with the lignin and cellulose fibers of the wood.

Recirculation in Cooling Towers

By JOSEPH LICHTENSTEIN,[1] NEW YORK, N. Y.

After defining recirculation, the paper shows it is a characteristic of the surroundings of a cooling-tower installation and must be considered by the user in his economic calculations and by the manufacturer for the proper selection of a cooling tower to reach a specified cold-water temperature. A knowledge of recirculation factors of installations can be obtained experimentally only by co-ordinated over-all tests on actual cooling-tower installations. The paper develops the methods and equations required for such tests to find the recirculation factor. It then shows how the cold-water temperature is affected by various degrees of recirculation, and how the size of a cooling tower would have to vary, if the cold-water temperature is fixed. Finally, the variation of cold-water temperatures with varying wet-bulb temperatures is studied for a series of fixed recirculation factors, and it is shown that if the recirculation factor increases with decreasing wet-bulb temperatures, a nearly constant cold-water temperature all year round may result.

Nomenclature

The following nomenclature is used in the paper:

- h = enthalpy of atmosphere at any point inside tower, Btu per lb
- h_1 = enthalpy of ambient atmosphere, Btu per lb
- h_2 = enthalpy of atmosphere leaving tower, Btu per lb
- h_m = enthalpy of mixture of ambient and recirculated atmosphere entering tower, Btu per lb
- h' = enthalpy of saturated atmosphere at water temperature, Btu per lb
- h_T = enthalpy of circulating water at specified point, Btu per lb
- h_{T2} = enthalpy of cold water leaving tower, Btu per lb
- H_1 = specific humidity of ambient atmosphere in lb per lb of dry air
- H_2 = specific humidity of atmosphere leaving tower, lb per lb of dry air
- H_m = specific humidity of mixture of ambient and recirculated atmosphere entering tower, lb per lb of dry air
- r = recirculation factor
- r_c = critical recirculation factor
- t_1 = inlet-water temperature, deg F
- t_2 = cold outlet-water temperature, deg F
- t_m = temperature of make-up water, deg F
- t_B = water temperature in basin, deg F
- W_A = amount of ambient atmosphere entering tower, lb per hr
- W_G = total amount of atmosphere flowing through tower, lb per hr
- W_L = amount of circulating water flowing through tower, lb per hr
- W_E = amount of water evaporated in tower, lb per hr
- W_v = amount of overflow, lb per hr
- W_m = amount of make-up water, lb per hr

Introduction

Recirculation can be defined as an adulteration of the atmosphere entering the tower by a portion of the atmosphere leaving the tower, thereby increasing the enthalpy of the entering mixture above that of the ambient atmosphere. For simplicity it shall be assumed that the enthalpy of this portion is the same as the enthalpy of the exhaust atmosphere. It follows that the recirculated portion cannot participate in the heat exchange between atmosphere and water, since it passes through the tower without change. The heat exchange is entirely restricted to the ambient atmosphere flowing through the equipment. When tests are made on a cooling-tower installation, with a view of setting up thermal balances to determine the amount of cooling medium, it will be the flow of ambient atmosphere through the tower that will then be computed. The total flow, which, of course, must be handled by the fans of mechanical-draft cooling towers, can be determined only by direct measurement.

Based on the definition of recirculation, the "recirculation factor" can be introduced

$$r = \frac{W_G - W_A}{W_G} \qquad [1]$$

To determine the recirculation factor of a cooling-tower installation, therefore, requires the measurement of the total atmospheric flow through the fans and the required measurements for setting up of a thermal balance that will permit the computation of the ambient atmospheric flow through the equipment.

If such tests were made on a large variety of cooling-tower installations and the results correlated properly, typical recirculation factors for the various types of installations could be obtained. This information would permit the selection of the probable recirculation factor of a new installation so that the effect of recirculation on the performance of the new tower could be taken into account.

The essential object of a cooling-tower installation is to provide cooling water of a specified temperature. It is on this temperature that the equipment the cooling tower is serving is based. Since recirculation can affect this temperature seriously, it must be considered in the planning stage, and it must enter into the economic considerations that determine the specified cold-water temperature.

Recirculation is caused by air currents existing around the equipment, so that portions of the exhaust atmosphere tend to flow toward points of low pressure, represented by the air entrances of the equipment located in the opposite direction to the prevailing wind. Only if the mass of atmosphere surrounding the equipment were immobile would a cooling tower discharge the exhaust atmosphere of lower density straight upward where its heat would be dissipated into the ambient atmosphere. However, more or less strong winds are always present. In addition, the discharge by the tower of a hot air mass into the colder surroundings causes disturbances and air currents in the near vicinity of the equipment. A horizontal movement of air of just the right magnitude can be established that may or may not cause portions of the exhaust atmosphere to penetrate into the air

[1] Consulting Engineer, Foster-Wheeler Corporation. Mem. ASME.

Contributed by the Power Division and presented at the Spring Meeting, Atlanta, Ga., April 2–5, 1951, of The American Society of Mechanical Engineers.

Note: Statements and opinions advanced in papers are to be understood as individual expressions of their authors and not those of the Society. Manuscript received at ASME Headquarters, March 5, 1951. Paper No. 51—S-8.

entrances of the equipment located opposite to the wind direction. Whether recirculation occurs, and to what degree, will depend upon the design and size of the equipment and its location in relation to its surroundings, that is, its relation to prevailing winds, to nearby structures that can reflect the exhaust atmosphere back into the tower, and to other less definable influences.

Regarding the air entrances of the equipment that permit the penetration of exhaust gases, one might consider relocating them in such a manner that the prevailing winds are utilized to purge and prevent such penetration. Such design changes are to be expected in the development of cooling-tower designs.

At present, attempts to minimize recirculation are being made by giving careful consideration to the location of the equipment in its surroundings, and in its relation to all influences causing the difficulty. Induced-draft towers are favored against forced-draft because, in discharging the exhaust atmosphere at higher velocities, a somewhat larger degree of safety against recirculation is achieved. The higher fan power required by the induced-draft tower is the price paid for this additional safety.

However, whatever the efforts, in certain types of installations a complete suppression of recirculation is not possible. Therefore each type of installation could be characterized by its recirculation factor, which would embody the sum total of all the influences of the surroundings that contribute to recirculation. This recirculation factor should then form part of the specifications for a cooling-tower installation in the same way as the "cleanliness factor" forms part of the specifications of a condenser installation. Only then would each cooling-tower manufacturer be placed in an equal position with his competitor, and only then would he have all the information really required to meet the specified cold-water temperature.

Thermal Balance of Cooling-Tower Installation

To determine experimentally the recirculation factor of an installation, a thermal balance must be made. Fig. 1 shows a typical cooling-tower installation, indicating the data that must be measured in order to set up a complete thermal balance. The nonmeasurable data that will be determined from this balance are

W_A = the ambient flow of atmosphere through equipment

W_E = amount of water evaporated in tower

t_2 = cold-water temperature

The three simultaneous equations that will determine these three unknowns result from the following considerations:

If a boundary line is drawn around the tower installation and it is stipulated that all recirculation shall take place within the boundary, and if, for the purpose of simplification, it is further stipulated that no sources of heat or vapor be located either within or outside the boundary that could discharge heat or vapor into the ambient atmosphere or into the equipment, then under steady conditions the following statements will be true:

1 The amount of heat leaving the boundary must equal the amount of heat entering the boundary, since, under steady conditions, the temperature within the boundary remains constant.

2 The amount of vapor leaving the boundary must equal the amount of vapor entering the boundary plus the amount of water evaporated in the tower, since, under steady conditions, the total vapor content within the boundary remains constant.

3 The water temperature in the basin is the mixing temperature of the circulating water leaving the tower with the make-up water entering the basin.

In addition, it is required that during the test the level in the basin shall not change, which means that the make-up water flow shall be so adjusted that it just covers the overflow and the evaporation loss, spray losses being neglected. This is expressed by

$$W_m = W_o + W_E \quad \ldots\ldots [2]$$

The algebraic expressions of the foregoing statements lead to the following equations

1 $W_A H_2 + W_o h_{FB} + W_L h_{FB} = W_A h_1 + W_M h_{FM} + W_L h_{F1}$

2 $W_A H_2 = W_A H_1 + W_E$

3 $(W_L - W_E) t_2 + W_m t_m = (W_L + W_m - W_E) t_B$

and the solution for the three unknowns furnishes the desired data

$$W_A = \frac{W_L(t_1 - t_2)}{(h_2 - h_1) - (H_2 - H_1)h_{F2}} \quad \ldots\ldots [3]$$

$$W_E = W_A(H_2 - H_1) \quad \ldots\ldots [4]$$

$$t = \frac{(W_L + W_o)t_B - W_m t_m}{(W_L + W_o - W_m)} \quad \ldots\ldots [5]$$

If all the values on the right side of Equations [3], [4], and [5], as well as the total atmospheric flow through the fans are measured, the recirculation factor as defined by Equation [1] is determined.

The state of the mixture of ambient and recirculated atmosphere entering the equipment follows from

$$W_A h_1 + (W_G - W_A)h_2 = W_G h_m$$
$$W_A H_1 + (W_G - W_A)H_2 = W_G H_m$$

to

$$h_m = h_1 + r(h_2 - h_1) \quad \ldots\ldots [6]$$

$$H_m = H_1 + r(H_2 - H_1) \quad \ldots\ldots [7]$$

The enthalpy of the mixture as determined by Equation [6] and the specific humidity of the mixture as determined by Equation [7] of course also determine the wet-bulb temperature of the entering mixture.

Calculation of New Tower for Specified Recirculation Factor

When a new tower is required for an installation that specifies the recirculation factor, the tower manufacturer can calculate the required size with his standard methods, except, instead of figuring with the ambient atmosphere as a cooling medium, he has to figure with the entrance mixture. But the state of the exhaust atmosphere, the knowledge of which is required in Equations [6] and [7] to determine the state of the mixture, is one of the design variables in the calculation of a new tower and, therefore, not known beforehand. What is fixed is the heat load and the specified cold-water temperature. It is therefore desirable to express the state of the entrance mixture in these terms. This can be done, in accordance with Fig. 1, from the following equation

$$W_G(h_2 - h_m) = W_L(t_1 - t_2) + W_E h_{F2}$$

The enthalpy of the exhaust atmosphere in the foregoing equation can be eliminated by the use of Equation [6]. But the amount of water evaporated also depends upon the state of the exhaust atmosphere which at the start of the calculation is unknown. However, W_E is small in comparison with W_L and is proportional to the heat load

$$W_E = aW_L(t_1 - t_2) \quad \ldots\ldots [8]$$

The error will be negligible, therefore, if for a an average value is

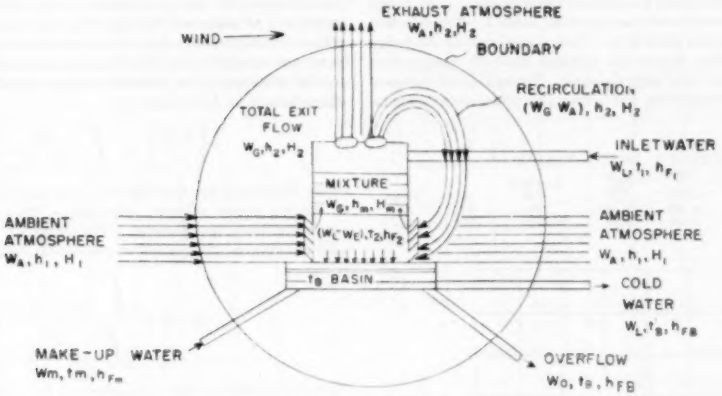

FIG. 1 TYPICAL COOLING-TOWER INSTALLATION

introduced, and found to be $a \sim 0.00085$. With the help of Equations [6] and [8], the enthalpy of the mixture is found to be

$$h_m = h_1 + \left(\frac{r}{1-r}\right)\left(\frac{W_L}{W_G}\right)(t_1 - t_2)(1 + ah_{F2}) \quad \ldots\ldots [9]$$

Similarly, the specific humidity of the mixture can be expressed in the same terms from

$$W_G(H_2 - H_m) = W_E = aW_L(t_1 - t_2)$$

and combining with Equation [7] leads to

$$H_m = H_1\left(\frac{r}{1-r}\right) a\left(\frac{W_L}{W_G}\right)(t_1 - t_2) \quad \ldots\ldots [10]$$

With Equations [9] and [10] determining the state of the entrance mixture and, therefore, also its wet-bulb temperature, the calculation of the new tower can now proceed normally using the entrance mixture as the cooling medium.

CHANGE OF COLD-WATER TEMPERATURE WITH RECIRCULATION

When a cooling-tower installation is subjected to recirculation, the cold-water temperature produced by the tower increases due to the increase of the enthalpy of the cooling medium from h_1 to h_m. A specific tower can be represented by a characteristic[2]

$$\left(\frac{KaV}{W_L}\right)$$

which determines the cooling performance in accordance with the relation

$$\left(\frac{KaV}{W_L}\right) = \int_{t_2}^{t_1} \frac{dt}{h'' - h}$$

In Fig. 2 this relation is graphically represented. The limits of the integration are the inlet and cold-water temperatures of the tower. For any water temperature between these limits, h'' is the enthalpy of a saturated air-vapor mixture at the water temperature, and h the corresponding enthalpy of the cooling medium. Term h varies with the water temperature as a straight line, called the operating line, from h_1 at the inlet to h_2 at the outlet,

[2] "Performance and Selection of Mechanical-Draft Cooling Towers," by Joseph Lichtenstein. Trans. ASME, vol. 65, 1943, pp. 779–787.

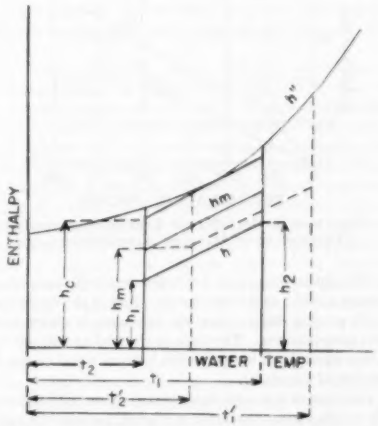

FIG. 2 GRAPHICAL METHOD FOR DETERMINING COLD-WATER TEMPERATURE AND TOWER CHARACTERISTIC RATIOS WITH RECIRCULATION

and the slope of the operating line is determined by the ratio (W_L/W_G).

When recirculation raises the enthalpy of the cooling medium to h_m, the corresponding cold-water temperature is determined by the relation

$$\left(\frac{KaV}{W_L}\right) = \int_{t_2'}^{t_1'} \frac{dt}{h'' - h}$$

where t_2' is the new cold-water temperature and $(t_1' - t_2')$ the range that, of course, has not changed.

By trial and error the foregoing integration can be accomplished graphically for varying recirculation factors, and thus the curve of cold-water temperature as a function of the recirculation factor can be obtained, starting from a specific ambient wet-bulb temperature and corresponding cold-water temperature.

In Fig. 3 the rise of the cold-water temperature with recirculation, and the corresponding rise of the wet-bulb temperature of

the mixture are shown for two typical tower designs. The design variables of the two towers are given in Table 1. The selection of the two towers was made with a view of emphasizing the design variables. For this reason the ambient wet-bulb temperature and the range have been kept the same. Tower I could represent an oil-refinery installation, and Tower II a power-plant installation.

TABLE 1 DESIGN VARIABLES

Design variable	$\frac{WL}{WQ}$	$\frac{KaV}{WL}$	Ambient WB	t_2	Range
Tower I	0.87	2.48	75	80	20
Tower II	2.39	1.04	75	95	20

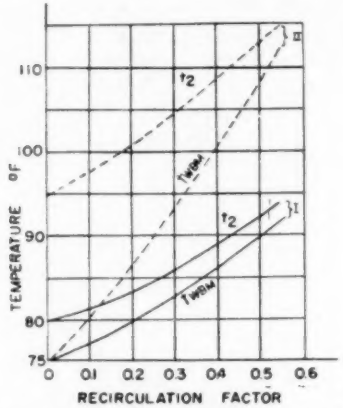

FIG. 3 VARIATION OF COLD-WATER TEMPERATURE AND WET-BULB TEMPERATURE OF MIXTURE WITH RECIRCULATION

As recirculation increases, both the wet-bulb temperature of the mixture and the cold-water temperature of the tower increase, with both getting closer, since the approach is closer at higher wet-bulb temperatures. The limit is reached at 100 per cent recirculation where both temperatures become equal to the boiling temperature of the water.

The variation of the cold-water temperature with recirculation depends at what point the curve is started, because the curvature of the saturated line h'' influences the variation and itself varies with temperature. However, with the help of Equation [9], the following general conclusions can be drawn:

The increase in enthalpy of the mixture above that of the ambient atmosphere is constant for a fixed recirculation factor. Therefore the percentage increase of the enthalpy of the mixture will be the larger the smaller the enthalpy of the ambient atmosphere is. It follows that the effect of the same degree of recirculation is magnified at low ambient wet-bulb temperatures. Recirculation affects a cooling tower more during winter than during summer operation. In addition, recirculation affects the cooling-tower performance the more the larger the cooling range and the larger the (W_L/W_G) ratio is for which the tower is designed. To minimize the effect of recirculation, the tower should be designed for a small (W_L/W_G) ratio, which of course means a more expensive tower. When $(W_L/W_G) = 0$, that is, when the atmospheric flow is infinite, the effect of a fixed recirculation is zero also.

INCREASE OF REQUIRED TOWER SIZE WITH RECIRCULATION

When, for a new cooling-tower installation, the cold-water temperature and the recirculation factor are specified, the required size of tower will be larger than for the same installation without recirculation. Since the size of a tower can be assumed to be proportional to its characteristic, and referring to Fig. 2, if recirculation raises the ambient enthalpy h_1 to h_m, the required characteristic is determined by

$$\left(\frac{KaV}{W_L}\right)_r = \int_{h_1}^{h_2} \frac{dt}{h'' - h_m}$$

under the assumption that the (W_L/W_G) ratio is selected the same as for the tower without recirculation, that is, that the two operating lines are parallel. The ratio of the recirculation characteristic to the normal characteristic follows from

$$\text{Ratio} = \frac{\int_{h_1}^{h_2} \frac{dt}{(h'' - h_m)}}{\int_{h_1}^{h_2} \frac{dt}{(h'' - h)}}$$

As recirculation increases, an operating line is established which is tangent to the saturation line, and to which an infinite characteristic belongs. This is the theoretical limit of recirculation at which the specified cold-water temperature can still be reached, and the corresponding factor is the "critical recirculation factor" r_c, and the corresponding enthalpy the "critical enthalpy" h_c of the mixture.

Evidently the sensitivity of an installation to recirculation will be the larger the smaller the critical recirculation factor is. Introducing in Equation [9] $r = r_c$ and $h_m = h_c$, and solving for r_c furnishes

$$r_c = \frac{1}{1 + \left(\frac{W_L}{W_G}\right)\left(\frac{t_1 - t_2}{h_c - h_1}\right)(1 + a \cdot h_{F2})} \quad \ldots\ldots [11]$$

From the graphical method that determines h_c and from Equation [11], the following general conclusions can be drawn.

The critical recirculation factor will be the smaller:

1 The closer the approach is for which the tower is designed. This will be particularly magnified for cooling towers that are designed for a close approach to a low ambient wet-bulb temperature.

2 The larger the range is for which the tower is designed.

3 The smaller the critical enthalpy is which results from the operating line that is tangent to the saturation line.

4 The larger the ratio (W_L/W_G) is for which the cooling tower is designed.

From the standpoint of the cooling-tower designer, Items (1) and (2) are specified values over which he has no control. But he can reduce the sensitivity of his tower to recirculation by selecting a small (W_L/W_G) ratio. This also automatically increases the critical enthalpy. It means that the tower must be designed for small loadings and for as large a total atmospheric flow as possible.

In Fig. 4 are shown the ratios of required to normal characteristics for Towers I and II used previously as examples. Since both towers are designed for the same 20 F range, the effect of range is eliminated. But the effect of approach and (W_L/W_G) ratio becomes clearly visible. Tower I is designed for a 5-deg approach but works with a (W_L/W_G) ratio of only 0.87, whereas Tower II is designed for a 20-deg approach but works with a (W_L/W_G) ratio of 2.39. The result is that both factors working in opposite directions tend to equalize the critical recirculation factor for both towers ($R_c = 0.215$ for Tower I and $R_c = 0.26$ for Tower II). Without such difference in the W_L/W_G ratios, the two critical recirculation factors would have been far apart. As a

consequence, the two curves nearly coincide. The rapid increase of the required tower characteristic with recirculation is apparent. The critical recirculation factor for towers designed for a close approach to a low ambient wet-bulb temperature is very small indeed, and this indicates the difficulties encountered in trying to

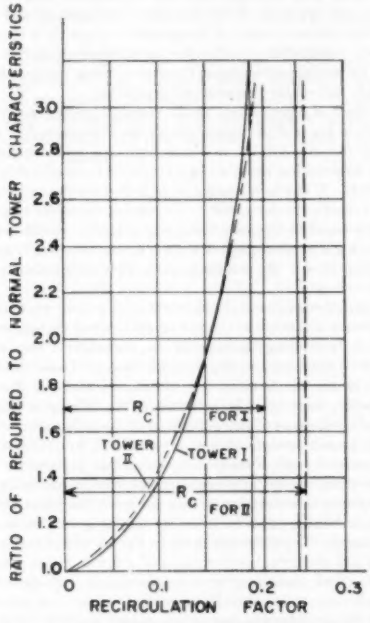

FIG. 4 VARIATION OF RATIO OF REQUIRED TO NORMAL CHARACTERISTIC WITH RECIRCULATION FACTOR

reach low cold-water temperatures with existing cooling-tower designs.

VARIATION OF COLD-WATER TEMPERATURE WITH AMBIENT WET-BULB TEMPERATURE FOR CONSTANT RECIRCULATION FACTOR

The knowledge of the (W_L/W_G) ratio and of the characteristic (KaV/W_L) of a cooling tower permits the graphic determination of the cold-water temperature for any enthalpy of the entering cooling medium, see Fig. 2. If a recirculation factor is held constant, Equation [9] will permit computation of the enthalpy of the entering mixture for any ambient enthalpy, and, consequently, the curve of cold-water temperatures as a function of the ambient wet-bulb temperature can be calculated. In Fig. 5 these curves are shown for Towers I and II for a number of constant recirculation factors.

The effect of recirculation is to raise the cold-water temperature curve which corresponds to zero recirculation. The effect of the (W_L/W_G) ratio is to flatten these curves with increasing ratios, so that the differences between summer and winter operations are reduced.

Whenever recirculation is taken into account, the emphasis is on its effect on summer operation. Accordingly, the cooling tower is placed in the correct relation to prevailing summer winds. In the winter, when prevailing winds are reversed, recirculation will

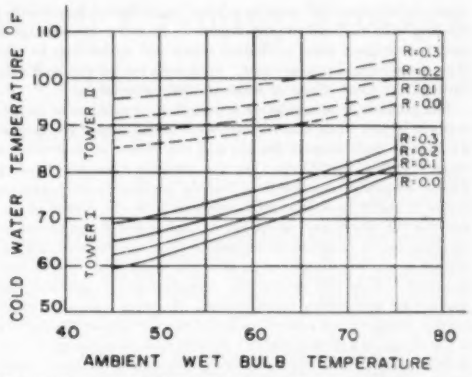

FIG. 5 VARIATION OF COLD-WATER TEMPERATURES WITH AMBIENT WET-BULB TEMPERATURE FOR VARIOUS CONSTANT RECIRCULATION FACTORS

occur. It seems that the recirculation factor of a cooling-tower installation increases with decreasing ambient wet-bulb temperatures.

Assume that Tower II works without recirculation in the summer furnishing a 95 F cold-water temperature when the ambient wet-bulb temperature is 75 F. If recirculation should increase with lowering of the ambient wet-bulb temperature in a manner determined by the intersections of a horizontal line of 95 F, with the various constant recirculation factors (see Fig. 5) the result would be a constant cold-water temperature of 95 F all year round. Cooling-tower installations serving power plants usually are designed for large (W_L/W_G) ratios, and such conditions can exist there, resulting in practically a constant cold-water temperature during the year. Where colder water temperatures, even at lower ambient wet-bulb temperatures, are of economic value, these possibilities should be taken into account when planning and designing cooling-tower installations.

SUMMARY

The essential object of a cooling-tower installation is its furnishing of a specified cold-water temperature under specified operating conditions. Recirculation affects this temperature. It must, therefore, either be suppressed by suitable design changes and careful location of the equipment in its surroundings, or, if it cannot totally be suppressed, it must be considered in the planning and dimensioning of the required equipment. Each typical installation has its characteristic recirculation factor that can be selected from tests on similar types of installations. The methods for determining these factors are developed in this paper. The recirculation factor of a new installation should form part of the specifications. Once assumed, its effect on the required size of the equipment and on the performance can be determined. Once the recirculation factor is specified, manufacturers of cooling towers will be in a better position to fulfill a need of industry for a reliable cold-water-temperature guarantee.

Discussion

J. A. BROWN.[3] The author has stressed the fact that it is the cold-water temperature which is the essential object of a cooling-

[3] Manager, Cooling Tower Division, Foster-Wheeler Corporation, New York, N. Y.

tower installation, and must be reached regardless of interferences existing that may affect performance. In order to accomplish this, the designer must have data which will enable him to take these interferences into account. Such data can be obtained only through the joint efforts of users and manufacturers.

The problem of recirculation is essentially a problem of design, and will be met when manufacturers are fully aware of the characteristics of their present designs and the effects of recirculation under varying conditions. At the present time the Cooling Tower Institute, composed of leading cooling-tower manufacturers engaged in co-operative research with the object of improving the design and operation of cooling-tower equipment, is carrying out a program to assimilate data on the recirculation factors of various designs in an effort to make more information available. This will enable the manufacturer to improve his product by minimizing recirculation. However, there are other outside interferences referred to in the paper which are also factors in the design of a cooling tower. Factors such as adjacent sources of heat and wind direction relative to the axis of the tower must also be taken into account if the user is to obtain the cold-water temperature he desires. All too often manufacturers are requested to guarantee cold-water temperatures, taking into account the effect of adjacent installations, but are given no information as to the actual change in ambient conditions in the location where the tower is to be placed. Without such information, the manufacturer is obliged to tell the user, and perfectly correctly, that he can only design and guarantee the installation based on entering-air wet-bulb temperatures. It, therefore, becomes the responsibility of the user to obtain for the manufacturer sufficient information to design his tower for the desired cold-water temperatures actually to be obtained. A practical method of providing this information could be some type of factor, as suggested in the paper, so that all designers for a particular installation will have a common basis from which to start and will be responsible for definite percentages of outside interferences.

The paper presents the problem of recirculation as faced by the user and manufacturer. As pointed out, and this cannot be emphasized too strongly, a good deal of data are still needed before the problem will be adequately met. These data must come from the combined efforts of users and manufacturers if the cooling-tower industry is to be put on a sound engineering basis. The Cooling Tower Institute's present program is a step in this direction. Cooling-tower manufacturers as a whole would be only too glad to reach the point where their guarantees, based on solid and acceptable data on recirculation and other influences, would be made solely on the basis of achieving a specified cold-water temperature.

M. W. Larinoff.[4] The behavior and adverse effects of recirculation have been well illustrated in this paper, but there still remains the problem of accurate flow and temperature measurements in the field before any specific assessments can be made. Such measurements as can be made must be done on full-scale towers, which implies permission be granted to the manufacturer by the user to make the necessary observations.

It is not possible for the purchaser to specify a recirculation factor in inquiry specifications as the author suggests. This factor is influenced by the tower surroundings and is theoretically a function of tower design, height, length, and exit-air velocity which are under the control of the manufacturer. The purchaser should inform the manufacturer of the proposed physical location of the tower in relation to its surroundings as they might influence the air approach to the tower. Similarly, he should indicate the location and size of other spray ponds, towers, or equipment discharging moisture into the atmosphere located in the vicinity. On the basis of the described surroundings and the recirculation characteristics of the proposed tower, it is the manufacturer's responsiblity to allow for the adverse effect of recirculation in his design calculations, thereby insuring the purchaser of a reliable cold-water temperature guarantee.

The effect of recirculation on the required tower characteristic, as shown in Fig. 4 of the paper, reveals the interesting fact that increasing the fill height to compensate for recirculation gives rapidly diminishing returns even for factors considerably below the critical. If the tower height were to remain the same and the W_L/W_G ratio were decreased by increasing the tower length, the ratio of normal to required tower size probably would not be as great for a given percentage of recirculation. It would have been interesting to see the comparison of this complementary approach.

The author explains that the effect of the same amount of recirculation is magnified at the low ambient wet-bulb temperature, due to the percentage increase of the enthalpy of the mixture. This is well illustrated in Fig. 5 in the case of Tower I, but it is difficult to see much difference in the operation of Tower II. Presumably, there must be a "critical" W_L/W_G ratio where the practical significance of any differences of the cold-water temperatures, as caused by recirculation, are too small to be noted.

After several years of study of tower ratings, performances, and field-test data, the writer's company has been endeavoring to develop a means of comparing cooling towers of the same manufacture theoretically, and to estimate performances from tower specifications. The difference between the calculated performance of a cell and the actual performance of a tower is that due to recirculation and possible error of measurements. From comparisons made, the correlation is surprisingly close, and the results indicate the need for due and proper consideration being given to recirculation by all the cooling-tower manufacturers in their design allowances.

Author's Closure

Mr. Larinoff points out that compensation for recirculation can also be made by increasing the tower length, thereby decreasing the W_L/W_G ratio as against increasing the tower height considered by the author. This is quite true, but will lead to large increases in air requirements until the ratio will become zero and air requirements infinite. Whether one or the other method, or a combination of both, is more economical can be determined graphically from case to case (see Fig. 2). Sooner or later a critical situation is reached.

Both Mr. Brown and Mr. Larinoff agree with the author that the essential function of a cooling-tower installation is to provide a specified cold-water temperature based on the available ambient cooling medium. Recirculation prevents reaching this cold-water temperature. The first step in the solution of the recirculation problem is its quantitative measurement. Since this can only be done on actual installations, the co-operation of owner and manufacturer is essential. But, since both have a common interest in the solution of the problem, such co-operation surely will be available.

[4] Mechanical Engineer, Ebasco Services Incorporated, New York, N. Y. Jun. ASME.

Operating Experience With Cooling Towers in the Central Gulf Area

BY H. G. HIEBELER,[1] HOUSTON, TEXAS

The author's company has had experience with both forced-draft and induced-draft cooling towers at four of its stations over a period of 12 years. He gives in some detail the experience with component parts of the systems, and indicates the direction in which improvements can be made.

Introduction

THE electric power requirements of Houston and the surrounding area are supplied from four major generating stations of the Houston Lighting & Power Company totaling about 625,000 kw in net capacity. Of this, 440,000 kw or 70 per cent operates on circulating water systems employing mechanical-draft towers for cooling. Of the other 185,000 kw, 160,000 is at Deepwater, a 1450-350 psi station on the ship channel, and the other 25,000 kw in the older 200-psi section of the uptown Gable Street plant. Gable Street also has 65,000 kw (gross) in two modern 850-psi 900 F units on towers. The largest units on towers are the two 85,000-kw machines at West Junction which with 250,000 kw (gross) on towers should rate well toward the top of the list of large central stations wholly on such systems. However, within the next 2 years it will be dwarfed when two machines of 110,000 kw gross each are added to the 140,000 kw already in service on towers at the Greens Bayou Station. This will total 360,000 kw at this site and 540,000 kw net on towers for the system.

Experience at Houston with towers goes back about 12 years to the installation of a small forced-draft tower to serve a 25,000-kw machine at Gable Street. This was followed by a 40,000-kw unit in 1943 at West Junction, also on a forced-draft tower, and by a duplicate machine there on an induced-draft tower in 1947. Two units of 70,000 kw capacity each on induced-draft towers went into service in 1949 at Greens Bayou. Another machine, 35,000 on an induced-draft tower was completed last spring at Gable Street. An 85,000-kw unit with an induced-draft tower came on last August at West Junction with a duplicate machine added at this plant in February.

The experiences which will be related refer to these installations. No criticism of any manufacturer or his product is intended. While the predicted performances were not always met initially, in every case the manufacturers, including their suppliers, gave the fullest co-operation in the correction of troubles, furnishing additional cells if required, testing, changing at their own expense here and there to effect every improvement possible.

The use of large multiple-cell mechanical-draft towers for circulating-water cooling is a development largely of the past decade during which time many of the designs were changing, evolving, and crystallizing. Much of the fundamental data on tower performance was from single-cell experimental tests and, in some cases, to say the least, the tests were not exhaustive. The effects of various groupings into multiple-cell arrangements were not known nor properly anticipated. Correct spacing and location with respect to other towers and neighboring buildings or terrain had to wait on experience. War and other conditions during part of the period were hardly conducive to study or research. With the increasing number and capacity of towers in service in industrial as well as central-station service, it should be possible to accumulate a background of information and data which will make for better design and application in the future. As a customer and operator this is what we are hoping for.

What Is Expected of Cooling Towers

The operator of a plant or of equipment of any kind is interested primarily in the reliability of that plant or equipment. He is, of course, also concerned with performance but that, if not too radically off, is usually secondary to the ability to keep going. So it is with cooling towers.

Motors. The reliability of a mechanical-draft tower is essentially the reliability of the fans and fan drives. As the motors have had the most satisfactory service record, they will be considered first. The 16 forced-draft fans on the original Gable Street towers are driven by 20-hp direct-connected 440-volt motors at 385 rpm. These have been in service 12 years. These motors, while not the conventional totally enclosed type, are enclosed in finned casings cooled by the air stream. Two weep holes at the bottom allow breathing with temperature changes and prevent accumulation of any condensation. Eighteen similar direct-connected motors, but of 25-hp size, drive the slightly larger fans on the first tower at West Junction and have seen $7\frac{1}{2}$ years of service.

There have been two motor failures at Gable Street and four at West Junction. At each plant these were divided equally between those due to ball-bearing failures, which allowed rotor to drop down and rub the stator, and actual coil failures. These six failures in approximately 327 fan years of operation or 1 in 54 fan years seem very satisfactory to the operators. Actually, some of the bearing failures might have been avoided by more frequent inspection. Because of manpower shortage and tight schedules during the war, the period between inspections of some of these fan motors went as long as 3 years. A 2-year schedule with half of the units coming out every year seems preferable. Incidentally, these ball bearings are not of the sealed type. It is possible to apply too much grease which then gets into the motor proper. With the pressure-relief design or the lifetime pregreased ball bearing, it is believed that a 5-year inspection schedule would be satisfactory.

For the second unit at West Junction an induced-draft tower was chosen. The motors are 25-hp conventional splashproof 1800 rpm design. On the 16 units in $3\frac{3}{4}$ years of service there has been one failure, a coil breakdown in the slot. This is one in 60 years' service, if this proves anything. Our electrical operating men did not recommend the application of splashproof motors here due to the general high humidity and moisture conditions. They still have not altered their opinions despite this apparently satisfactory record. These motors are on a 2-year inspection schedule.

[1] Assistant Superintendent Power, Houston Lighting & Power Company. Mem. ASME.

Contributed by the Power Division and presented at the Spring Meeting, Atlanta, Ga., April 2–5, 1951, of The American Society of Mechanical Engineers.

Note: Statements and opinions advanced in papers are to be understood as individual expressions of their authors and not those of the Society. Manuscript received at ASME Headquarters, March 12, 1951. Paper No. 51—S-9.

On the newer towers at Greens Bayou, Gable Street, and West Junction, 30-hp totally enclosed fan-cooled motors were used. All told, there are 132 of these with from 2 months to 2 years of service. No failures have occurred, but a few bearing replacements have been made. It is hoped that a 5-year schedule will work out satisfactorily here.

On experience to date, our recommendation for tower fan drives would be totally enclosed motors. In the smaller sizes the initial cost runs but 10 to 12 per cent over the splashproof type, and it appears that this extra cost will be more than offset by reduction in inspection and maintenance charges.

Forced-Draft Fans. The fans proper on the forced-draft towers also have a good record. Fifteen of the 16 fans on the original Gable Street unit are 8-bladed 11-ft-diam Dowmetal units. The other is of plastic-impregnated fabric composition which was installed to test the material. Eighteen fans, 4-bladed, of 14 ft diam on the first West Junction tower are of textolite-impregnated wood. There have been no failures at Gable Street. Two failures which occurred shortly after starting at West Junction were due to manufacturing defects. Another, which occurred during freezing weather last winter, was apparently due to the fan striking ice accumulation, but this also showed latent defect. Some "weathering" or slight roughening of surface has developed and sheet-copper protection was applied to the leading edges of blades to halt erosion.

Induced-Draft Fans. On the induced-draft towers the fan record has not been too good. On West Junction No. 2 in slightly over 3½ years, 15 blade failures have occurred. All but one of these occurred during the first year of operation and were mainly due to manufacturing defects. One occurred in February of this year, on one of the original fans which had previously had no failures. These fans have 6 blades and are of the resilient blade-mounting, unitized-pitch-adjustment type. Blades are of all-welded construction of corrosion-resistant materials of airfoil cross section. Blades contain longitudinal spars welded to strut sections around which is stretched the skin, composed of relatively heavy sheet monel or stainless steel. The inner end of the blade terminates in a spoke which is merely a transition piece changing the shape from the airfoil section to the cylindrical cuff. The cuff contains a resilient mounting in which the blade tube is mounted. The blade tube is bolted rigidly to the fabricated hub assembly. Pitch adjustment is accomplished cleverly by slight axial shifting (between screw stops) of a disk on the hub. This has holes which engage projecting yokes attached to the blade cuffs, thus allowing simultaneous pitch adjustment on all blades. A segmented air seal in the shape of a conical pan is bolted to the structural hub to form the aerodynamic hub preventing recirculation through the ineffective center of the fan assembly. This fan has somewhat higher efficiency than other types subsequently tried, but service record has not been too satisfactory.

On the two towers at Greens Bayou, five blade-tube or spoke failures have developed on the 28 fans on No. 2 tower in 2½ years' operation and none on No. 1 tower in almost 3 years. There have been two similar failures on the 16 similar fans at Gable Street in a year's running. The West Junction No. 3 tower with the same fans has been operating since last August without a failure. Another 30-fan unit there went into service early in February this year and at this writing has had no fan trouble.

The fans on these most recent towers are of four fabricated airfoil-blade construction. Each blade consists of an upper and lower sheet of stainless steel formed on presses and welded together. The upper sheet is riveted to the spoke or center support member made up of 2-in. tubing extended by a flat bar. The round section extends only about 14 in. into the airfoil section. The blades are attached to the cast-iron hub by flanges with slotted boltholes to permit pitch adjustment of individual blades. A center seal pan of relatively thin metal is bolted to the center hub and attached to the blade shafts by U-bolts. This effectively seals the hub of the fan but has proved structurally inadequate. Cracking of the seal pan at attachment points due to flexing of the blades has not yet been overcome.

The blade-tube failures at Greens Bayou and West Junction had some appearance of vibration fatigue and, as there are 132 units all told, further experience is anxiously awaited. A fan-blade failure is quite disquieting to the operator as it may result in a complete wreck of the fan and can also damage the gear. On one occasion a blade was thrown almost 100 ft from the tower. Since the time one of our operators crawled by the badly unbalanced and heavily vibrating remainder of what was once a fan to shut down a failed unit, our personnel has been instructed to cut them off in emergency by the four-unit group switches at the ground level.

Reduction Gears. However, the most serious difficulties of operation have been with the spiral-type reduction gears. Gear troubles on the first West Junction induced tower have been relatively minor. On Greens Bayou Nos. 1 and 2 towers, complete replacement of the 48 original gears was necessary after a year of service. Replacement of 16 gears at Gable Street was also made. This was done without cost to us. The severe wear was variously attributed to improper lubricating oil, wrong oil level, and poor quality of bronze in the gears. The manufacturer's lubrication recommendation had been followed throughout including two changes in grade of lubricant. After replacement, the lubricating oil was changed to an extreme-pressure type with lead napthenate added. The oil contains 7½ per cent lead-napthenate concentrates of which 20 per cent is metallic lead. Resort to this lubricant seems to indicate that high-tooth-pressure design was used.

It is planned to make an examination of some of these replacement gear units when they will have accumulated several months' operation. This has not yet been done.

As to whether or not another type of gear would prove more satisfactory we cannot say. As a result of our experience and others which have been reported, more conservatism of design or application of any gear unit seems necessary. While a fan seems to offer a uniform nonshock load, it is difficult to get and maintain good dynamic balance, particularly in the larger sizes, and most manufacturers have yet to recognize the desirability of perfect balance. Efforts are made to provide solid substantial foundations at top of a tower but they cannot compare with what may be achieved at ground level or other places where gear applications usually are made. Some effects of change of pressure on blades as they pass over cross-members in the supporting structure are noticeable.

Oil Leaks. Less serious but quite aggravating have been the numerous oil leaks from the units. As this oil drops directly into the circulating system, such leakage cannot be tolerated. The main and larger leaks are at the upper seals at the output shaft and the seals at the input shaft. Originally the latter were of the packed type which were entirely unsatisfactory. Some improvement has been made by substitution of a metallic seal here but further improvement is desirable. Leaks also developed from the oil-level standpipe connections and vent lines, from the external piping from the oil pump, and from the bottom plate which gives access for vertical adjustment of the worm wheel. On the replacement units the oil-pump piping was made internal. Oil is notably hard to hold, and the best solution is to eliminate all connections possible. These included sight oil gages which proved difficult to see anyhow, and oil pressure gages which were inaccurate and rusted badly. Except for leakage which should

be detected by the operator on his periodic rounds, the oil system should be such as to require attention only at 3 to 6 months' intervals. On present units after several months' operation the oil shows no deterioration, and it is hoped that oil changes can be set up on an annual basis.

Wood Deterioration. Mention should also be made among the operating problems of wood deterioration. To date our troubles have not been too serious, but it appears that they may increase with age of the towers. Briefly, the first Gable Street tower replacement of mist eliminators and supports due to delignification was required after about 6 years of operation. Last year evidences of brown rot and other fungi attack were found in the wet-dry zone above the trays. Replacement of inside sheathing was made in this area this year. Mist eliminators were also replaced but this was due to use of improper material for this service.

On examination last year of the West Junction No. 1 tower after 7 years of service, some spots of delignification were found on the air baffle below the fill. This baffle is installed to direct air into the center of the tower. These spots were all at points where evaporation of leakage through the baffle had built up a concentration of salts.

On No. 2 tower after 3 years of operation, several boards were replaced because of white fungi attack in the section above the distribution troughs and below the deck.

Performance of Towers

On performance, towers generally fell short on original tests of guarantees which call for a 14 F approach to a 76 F wet bulb with rated flow and heat loading. On some the deficiency was of sufficient magnitude to require that additional cells be added. On others the investment required by the company for added basin, circulating piping, electrical connections, and so forth, to accommodate manufacturers' cells was not justifiable and none or only partial correction was made and other adjustments worked out. These towers generally are low-head units with about 20 ft water fall.

West Junction No. 3 tower, on which substantial modification in design, including increase in effective height of 5 ft was made following the Greens Bayou tests, when tested alone last summer did meet predicted performances. However, these predictions were for operation with No. 4 unit in service. Such tests have not yet been run.

For future units the towers will be higher. The new towers for Greens Bayou 80/100-megawatt units will be of 35 ft effective height, 10 ft higher than the latest West Junction units, and 15 ft above the present Greens Bayou designs.

Extensive tests and observations were made on the Greens Bayou units continuing over a several months' period. These towers, as is the practice at Houston, were lined up in the direction of the prevailing breezes, which are southeast in summer. With the wind in this direction, recirculation is at a minimum, and a free flow of fresh air reaches each side of the tower. However, the leeward tower will still show 1 to 2 F poorer performance or approach to the wet bulb than the windward unit, indicating some recirculation, although it may not be apparent by observation. Individual performance also varied by as much as 2 F from day to day, probably with the wind velocity and direction, recirculation, and also with atmospheric conditions such as temperature, humidity, and the like. The exact factors or their relative effects are not known, but vapor drifts straight up on occasions with little or no recirculation and at other times whips downward in a regular ground fog. The same phenomena were observed with the vapor from 60-ft-high exhaust stacks from Maxim silencers on the atmospheric exhaust of a large turbine operated for peaking capacity a few years ago. As the velocity in this exhaust at times approached 200 fps, we would conclude that velocity of exhaust is not the controlling factor. If the induced-draft tower has any margin over the forced draft in discouraging recirculation, it is very small. The higher towers may prove better in this regard.

Location of Towers

The question is sometimes asked as to the proper spacing of towers and their location with regard to buildings and other neighboring objects. This seems to be an individual problem at each location. The answer for the 400- to 500-acre sites at Greens Bayou and West Junction is not the same as for the 12-acre site at Gable Street. Generally, locations and spacings are selected with a view of minimizing recirculation, keeping carry-over off insulators and bushings of electrical equipment and avoiding fog nuisance. The two smaller towers at West Junction are set 180 ft apart. On operation this seemed a little close as the air requirements of the inside fans required five changes per minute in the space between towers. However, photographs of other installations recently published show much closer spacings than this.

Dispersal of fog or vapor depends on atmospheric conditions, and wind velocities and direction. Under unusual conditions last winter, this ground fog was found in one instance to persist across a road over 1000 ft from the tower. Usually, the vapor will be dispersed effectively within 300 to 400 ft or less.

While individual tower tests and performances did not always measure up to expectations, the over-all performance of the condensing and tower cooling systems has been quite satisfactory. It has been possible without cleaning at Greens Bayou to maintain condenser performance at full load to within 6 F terminal difference continuously. The make-up is from plant wells, and between three and four concentrations are maintained in the tower system by overboarding or blowdown. Calgon is introduced in small dosages three times daily. The system is chlorinated with a heavy "shot" for about 2 hr daily. At West Junction after 7½ years of operation, full-load terminal difference is under 10 and can be restored by acid cleaning.

In contrast, at Deepwater, while condensers immediately after retubing maintain their guarantees for a few months, within a year, despite chlorination and hand-cleaning, terminal differences slip to between 10 and 15 F immediately after cleaning and at times exceed 20 F.

The tower-system water temperatures follow the ambient closely and rapidly. Water temperatures come up rapidly in the morning with load. With the open system there is some lag and, with any appreciable volume of water, some storage effects. If the night loads are light, some of the heat build-up of the day will be dissipated then.

Conclusion

On the whole, while there have been some operating difficulties and problems with the towers, these are not insurmountable. Possibly the biggest problem facing the tower operator will be to combat deterioration of the wood. In this connection, substitution of other materials such as transite should be investigated. As has been stated, we are proceeding confidentially with designs for two unit extensions of 80/100 megawatt each to use tower cooling.

Problems Relating to Operation, Maintenance, and Chemical Control of Cooling Towers for Steam-Electric Generating Stations

By V. F. ESTCOURT,[1] SAN FRANCISCO, CALIF.

In a generating station, cooling-tower performance must be considered not only in terms of heat dissipation but also in relation to the over-all results obtainable with a particular combination of tower, condenser, and turbine. There is an important relationship between turbine leaving losses and the optimum tower size. This approach to the subject involves not only the economic size of the tower but also certain operating problems which vitally affect the station heat rate. The problem of condenser-tube scale deposits is more likely to become critical where cooling towers are used, because of higher cooling-water temperatures. Successful results are described in the use of threshold treatment of cooling-tower water with stabilized phosphate in combination with sulphur burning for keeping condensers free of scale deposits. The problems of recirculation, fan-blade failures, and noise nuisance are also discussed.

MOST of the steam-electric generating stations on the Pacific Gas and Electric Company's system obtain their cooling-water supply from the Pacific Ocean, San Francisco Bay, or the Sacramento or San Joaquin Rivers. The exceptions to this are the Avon and Martinez Stations in Contra Costa County, and the Kern steam plant in Bakersfield.

The Avon and Martinez plants rely upon alternate cooling-water supplies obtained either from a slough in the San Joaquin River or from the Contra Costa Canal. The latter is an irrigation project of the United States Bureau of Reclamation. Since the water from either source must be purchased from a local water company, the cost of condenser cooling-water requirements made the installation of cooling towers the economic choice. It was not feasible to locate the Avon steam plant sufficiently close to the river for direct pumping to the condensers. The choice of site for both the Avon and Martinez plants was restricted by reason of the fact that it had to be located adjacent to neighboring oil refineries in order to be able to deliver process steam to the refinery.

The Kern steam plant is located just outside the city limits of the town of Bakersfield at the extreme southern end of this company's system. The only economic source of cooling water at this site was from wells, and this again dictated the use of cooling towers for condenser cooling water.

Economic Size of Tower

Figs. 1 and 2 show the general layout and cross section of the cooling towers, and Table 1 gives the essential design data. The major factors which determined the economic size of the towers at Avon and Martinez, on the one hand, and at Kern, on the other hand, were somewhat different.

The Avon and Martinez turbines are of the automatic extraction type with high and low-pressure turbine sections in tandem. Steam is extracted automatically from the exhaust of the high-pressure machine in connection with the process-steam requirements of the refinery.[2] The low-pressure turbine exhausts into a condenser which is somewhat smaller than would be used for a conventional condensing machine, due to the high percentage of extraction steam which by-passes the condenser.

It is of interest to note that approximately 50 per cent of the rated capacity of this unit can be carried with no steam going to the condenser, except that required for cooling the low-pressure turbine. Even at full load, the flow to the condenser is less than 55 per cent of the figure for condensing operation.[3] Obviously, this low heat load on the condenser affects the economic size of the cooling tower materially.

At the Kern steam plant there are two units having respective capabilities of 75,000 and 110,000 kw. The smaller unit, which was the first to be installed, was designed on the basis of an anticipated average load factor of approximately 40 per cent. Due to load growth in the area by the time the second unit was installed, the anticipated load factor more nearly approached 60 per cent. Consequently, larger cooling towers and condensers were justified in connection with the second unit. In Fig. 3 the relation between turbine-exhaust pressure and cooling-tower capacity in terms of approach temperature has been plotted. The estimated saving in fuel costs resulting from lower back pressure are also given on the basis of an assumed fuel price of 28 cents per million Btu. These figures apply to the 75,000-kw unit for the reason that it is of particular interest to show the effect of the higher load factors at which it has been necessary to operate this unit as compared with what was originally contemplated. The benefits from generously designed towers are relatively greater where turbine leaving losses are low because of the larger improvement in turbine heat rate with respect to reduced back pressure. This situation applies to both of the Kern units.

Chemical Problems in Relation to Combined Tower and Condenser Performance

Emphasis has been placed upon these special factors which influence the economic size of the cooling tower in order to bring out their importance, not only in connection with the original design of the installation but also because of their close relationship with certain operating problems which directly affect the station heat rate. In a generating station, tower performance must be considered not only in terms of heat dissipation but also in

[1] General Superintendent of Steam Generation, Pacific Gas and Electric Company. Mem. ASME.

Contributed by the Power Division and presented at the Spring Meeting, Atlanta, Ga., April 2–5, 1951, of The American Society of Mechanical Engineers.

Note: Statements and opinions advanced in papers are to be understood as individual expressions of their authors and not those of the Society. Manuscript received at ASME Headquarters, March 19, 1951. Paper No. 51—S-10.

[2] "Power and Steam Plants for Oil-Refinery Service," by C. E. Steinbeck, Trans. ASME, vol. 61, 1939, pp. 733–740.

[3] "History and Performance of Oil-Refinery Steam-Electric Generating Stations of the Pacific Gas and Electric Company," by V. F. Estcourt, Trans. ASME, vol. 72, 1950, pp. 209–216.

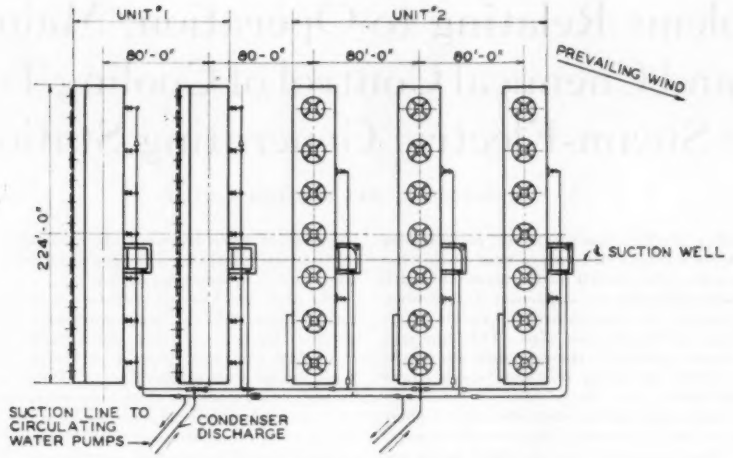

FIG. 1 COOLING-TOWER LAYOUT, KERN STEAM PLANT

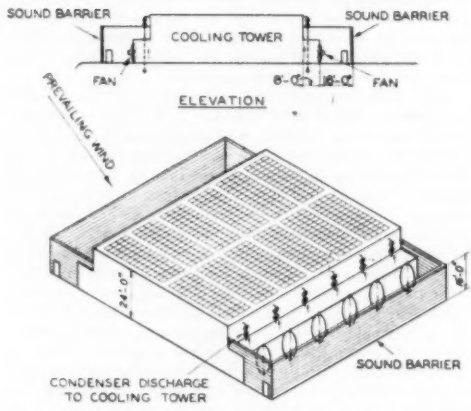

FIG. 2 MARTINEZ COOLING TOWER, SHOWING SOUND BARRIER

TABLE 1 COOLING-TOWER DESIGN DATA

Item	Kern No. 1	Kern No. 2	Avon and Martinez
Tower data:			
Type	Forced	Induced	Forced
Number of cells per battery	28	21	12
Number of batteries	2	3	1
Arrangement	14 Cells (Single rows)	7 Cells (Double inlet)	6 Cells (Back to back)
Circulating-water flow, rpm	74000	110000	37500
Pumping head, ft	23	24	20
Circulating-water inlet temperature, deg F	105	105	105
Circulating-water outlet temperature, deg F	91	90	90
Wet-bulb temperature, deg F	70	75	70
Approach, deg F	21	15	20
Air flow, M cfm	5012	7560	1800
Air/water ratio, cf per gal	67.7	68.7	48.0
Heat capacity, 10^6 Btu per hr	518	825	281
Total fan horsepower, bhp	627	924	280
Cell data:			
Air flow, M cfm	179	360	150
Fan diameter, ft	12	18.5	12
Fan speed, rpm	350	220	371
Fan brake horsepower, bhp	22.4	40	24.2
Motor horsepower, hp	25	50	25
Air outlet velocity, fpm	373	1340	312
Fan tip speed, fps	220	213	233
Internal dimensions, ft	16 × 30	32 × 32	16 × 30
Projected area, sq ft	480	1024	480
Loading, gpm per sq ft	5.5	5.1	6.5

relation to the over-all results obtainable with a particular combination of cooling tower, condenser, and turbine. As already pointed out, there is an important relationship between turbine leaving losses and optimum tower size.

The higher average cooling-water temperatures, which usually exist with cooling-tower jobs, tend to aggravate the problem of scale deposition on the condenser tubes owing to the decreasing solubility of calcium carbonate in particular with increasing temperature. This leads to a vicious cycle wherein the scale deposits on the condenser tubes lower the heat-transfer rate with resultant increase in condenser back pressure and heat load. This in turn raises the temperature of the cooling water, which further aggravates the deposition of calcium-carbonate scale on the condenser tubes.

Although this condition can be minimized by heavy blowing down of the tower basin to hold down the concentration of calcium and magnesium salts in the water to some value which will reduce scale deposits to a minimum, this single approach to the problem will not necessarily result in scale-free condenser tubes. Furthermore, such a program can be extremely wasteful in water consumption, as may be seen from the relationship between the number of concentrations and the amount of blowdown as shown in Fig. 4. It was, therefore, essential to give consideration to some form of chemical treatment of the water.

In the early days of operation of this station, reliance was placed upon sufficient blowdown of the tower basin to maintain not more than two concentrations. This was soon supplemented by the addition of a complex phosphate in threshold quantities. Due to the concentration of salts in the tower, a sufficiently low pH value could not be maintained for satisfactory control. Consequently, an organic stabilizer was added in conjunction with the phosphate. Although improved results were obtained, it was still necessary to resort to excessive blowdown of the tower basin in order to maintain the pH between 8.5 and 9.0. By the addition of sulphur burners to provide the SO_4

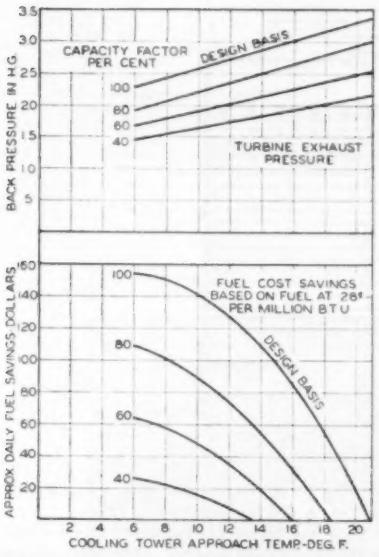

FIG. 3 COOLING-TOWER APPROACH TEMPERATURES VERSUS TURBINE-EXHAUST PRESSURE AND FUEL COSTS, KERN STEAM PLANT

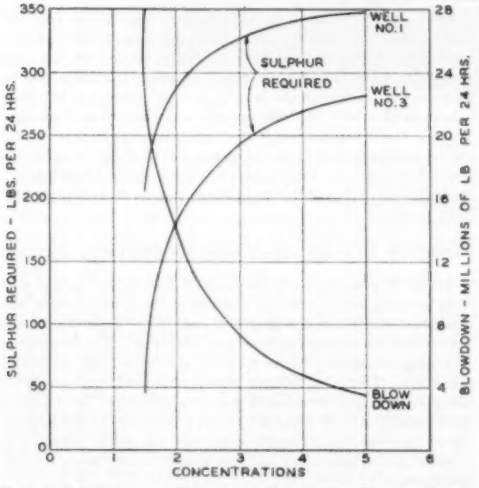

FIG. 4 SULPHUR AND BLOWDOWN QUANTITIES VERSUS TOWER BASIN CONCENTRATIONS, KERN STEAM PLANT
(Blowdown curve applies to either well, within limits of readability on chart.)

radical for the formation of sulphuric acid with the tower water, it was possible to hold the pH between 7.9 and 8.1 with greatly improved results from the phosphate threshold treatment. Actually, the control point is based on direct alkalinity determinations rather than pH for the reason that these provide more critical values as an operating guide. The control point on this basis is approximately 100 ppm in terms of calcium carbonate.

TABLE 2 TYPICAL WATER ANALYSES IN WELLS AND COOLING-TOWER BASIN, PPM

	Well No. 1	Well No. 3	Cooling-tower basin Well No. 1	Cooling-tower basin Well No. 3	Cooling-tower basin Well No. 1	Cooling-tower basin Well No. 3
Concentrations			2.0		4.0	
Carbonates, CO_3	0	0	6	6	7	7
Bicarbonates, HCO_3	101	86	80	80	76	76
Sulphates, SO_4	40	22	192	145	516	422
Chlorides, Cl	10	7	20	14	40	28
Calcium, Ca	29	21	58	42	116	84
Magnesium, Mg	4	3	8	6	16	12
Silica, SiO_2	14	15	28	30	56	60
Total solids by evaporation	177	150	354	300	708	600

NOTE: Water in tower basin does not correlate with water in wells mainly due to use of alkalinity control by sulphur burning and to normal conversion of some salts due to temperature changes.

For the well waters shown in Table 2, the burning of sulphur was selected in preference to the direct addition of sulphuric acid because of the low cost of the initial installation and also low operating costs. It should be clear from the curves in Fig. 4 that there is an optimum relationship between the number of tower concentrations and the amount of sulphur required. For the particular water under consideration, there is a sharply diminishing rate of saving in the amount of sulphur when the tower concentrations are increased above four. Because of the fact that the tower basin water is highly buffered, the amount of sulphur burned with respect to tower load is not critical, so that moderate changes in the rate of water flow for a given rate of sulphur feed result in only nominal changes in pH. Therefore it was feasible to adopt a rather primitive and extremely cheap method of burning the sulphur. The improvised type of sulphur pot which is in use at Kern is illustrated in Fig. 5. It should be noted that these pots consist of a piece of 16-in. steel pipe 36 in. long and with no bottom. These are set in a vertical position so that the sulphur comes directly in contact with the ground. This is important because the only really active attack on the metal is concentrated on the bottom. By omitting the steel bottom and allowing the sulphur to be loaded onto the ground within the steel pipe, very good life is obtained and cleaning problems are eliminated. Obviously, this further cheapens the initial cost of the installation and cuts down operating labor.

The pot is large enough to contain one 100-lb bag of sulphur. The entire bag is placed in the container and is then torn with a metal tool. The sulphur is ignited by lighting the torn paper bag and burns readily as long as air is supplied to the surface. The rate of burning is dependent on the amount of surface exposed. As soon as the sulphur is ignited, the portable cover with baffle is placed on top of the pot. The 4-in. pipe connection projects from the sulphur pot into the cell structure of the induced-draft tower. The draft produced by this type of tower draws air into the pot which is directed downward by the baffle so that it passes over the top surface of the sulphur. The sulphur-dioxide fumes liberated as a result of combustion are drawn into the tower and absorbed by the water falling over the baffles.

The gradual build-up in condenser back pressure as a result of scale formation in the condenser tubes is well illustrated in Fig. 6. Also shown is the effect of an acid-cleaning job which brought the condenser back pressure down to its original design value. The almost constant back pressure, which it has been possible to maintain subsequent to the acid-cleaning job, is the result of the chemical-treating program which has been described. It will be appreciated from a study of Figs. 4 and 6 that this not only resulted in maintaining a commercially clean condenser over extended periods of time, but also saved approximately 500,000,000 gal per year of tower blowdown.

In order to prevent algae growth in the tower, the foregoing treatment is supplemented by chlorination to maintain peak

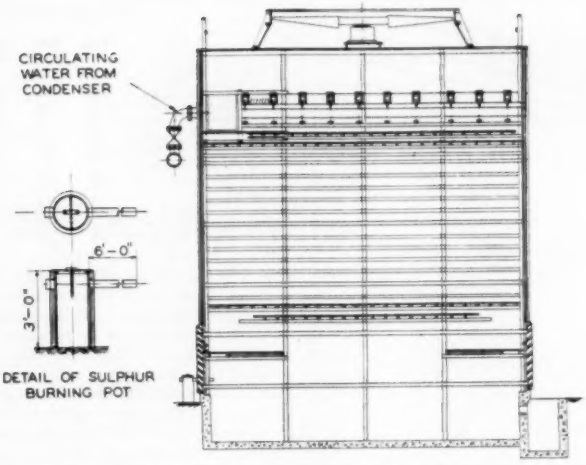

FIG. 5 CROSS SECTION OF INDUCED-DRAFT COOLING TOWER SHOWING SULPHUR-BURNING POTS, KERN STEAM PLANT

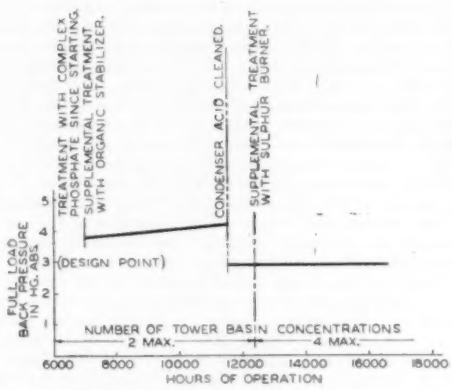

FIG. 6 TURBINE-EXHAUST PRESSURE AS AFFECTED BY COOLING-WATER TREATMENT, KERN STEAM PLANT

chlorine residuals of 0.2 to 0.5 ppm during the chlorination period. It is of course well known that not only is the tower efficiency reduced by algae growths, but the resultant slime in the condenser tubes seriously retards its heat-transfer rate.

PROBLEM OF RECIRCULATION

The problem of recirculation is subject to several variables. Generous spacing between towers and proper orientation in relation to prevailing winds are obvious factors of considerable significance. However, inherent limitations in the plant site sometimes prevent their application to best advantage. To some extent this situation existed in connection with the design of the Kern installation. Although the subject is still somewhat controversial, it is felt that the change from forced-draft towers to the induced-draft type on the second unit brought about appreciable benefits in the reduction of recirculation, particularly under certain atmospheric conditions. Due to the many variables involved, it is difficult to evaluate the effects of any reduction in recirculation, but a falling off in tower efficiency can definitely be observed to coincide with pronounced tower recirculation. This condition is reflected as an increase in turbine exhaust pressure.

Fig. 7 serves to illustrate at least in a qualitative way the better directional stability of the tower discharge in the induced-draft fans. The recirculation of tower vapors in the two forced-draft fans in the foreground of the illustration can be seen clearly. Although the heat load of the three induced-draft towers at the time the photograph was taken was somewhat less, the direct vertical rise of the vapors leaving the tower stand out by comparison with the drooping pattern of the forced-draft-tower discharge. As may be noted in Table 1, the leaving velocity in the induced-draft towers is almost 4 times that of the forced-draft towers.

FAN-BLADE FAILURES AND OTHER MAINTENANCE PROBLEMS

About 10 years ago the problem of fan-blade breakage was quite serious, and a series of changes in the type of blade was made before reaching any degree of stability. Table 3 gives the history of these changes at Avon and Martinez. The first failure of a magnesium-alloy blade occurred after about 20 months of operation. Two more failures were experienced very soon after the first one, and therefore it was concluded that the defective blades should not be replaced by others of the same construction. Apart from the cost of replacements and the risk of human life, a great deal of secondary damage usually occurs when a blade breaks off.

The magnesium-alloy blades were then replaced with so-called plastic blades which really were of laminated-wood construction. Experience was only slightly better with this type of blade. One new blade failed almost immediately and it soon became necessary to install copper shields on the leading edges due to the development of cracks in the wood at this point. No better results were obtained with the fabricated monel blades. However, very satisfactory results have been obtained with a later form of plastic blade, consisting of alternate layers of plastic and canvas. This type of blade is relatively light in weight but

TABLE 3 HISTORY OF FORCED-DRAFT FAN-BLADE FAILURES AVON AND MARTINEZ STATIONS

Material		Weight, lb			Service life—months		Failures
Blade	Hub	Blade	Hub	Total	Maximum	Minimum	per cent
Avon:							
Magnesium alloy	Magnesium alloy	136	225	361	132+	30	50
Hollow monel	Cast iron	172	425	597	72+	15	66
Plastic and fabric	Steel	100	290	390	10+	10+	0
Martinez:							
Magnesium alloy	Magnesium alloy	136	225	361	45	20	25
Laminated wood	Cast iron	112	425	537	90+	1½ (hr)	33
Hollow monel	Cast iron	172	425	597	24+	1½	50
Plastic and fabric	Steel	100	290	390	6+	6+	0

NOTE: Figures for service life followed by a plus sign indicate that blade is still in operation.

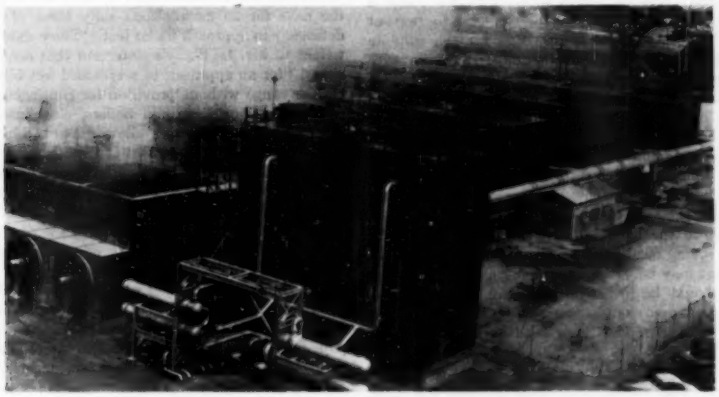

FIG. 7 FORCED AND INDUCED-DRAFT COOLING TOWERS IN ACTUAL OPERATION, KERN STEAM PLANT

of far more substantial construction than its predecessors. Although the maximum service period up to the present is only 10 months, there is every indication that these blades will last for a long time. This is deduced partly from the fact that there is complete absence of any evidence of deterioration in progress, as was the case with the earlier types of blade.

Tower efficiency can be reduced seriously by allowing distribution troughs to become obstructed or permitting them to open up and cause by-passing. These should be checked carefully to insure good intermingling of air and water. Slats and baffles may pull loose and impair air distribution, atomization, and film surface. Repairs of this nature are expensive and require protracted tower outages. Therefore, attention should be given to this construction when purchasing a new tower. The problem of delignification is being discussed currently. However, it should be stated here that difficulties from this source can be reduced by periodic washing down of the entire tower assembly with water of low concentration. This maintenance operation should be performed at least once a year.

Although better experience appears to have been obtained with fan-blade life on induced-draft towers, some of the problems with worm-gear drives have not been solved. The difficulties have to do with both lubrication and alignment tolerances. Better results appear to have been obtained with bevel-gear reductions. Consideration is being given by some operators to the application of fluid power drive for a group of fans from a common hydraulic source.

NOISE NUISANCE

When cooling towers are installed in locations close to residential areas, trouble can be experienced as a result of noise complaints. This is particularly true with forced-draft towers. At the Martinez plant it became necessary to install a sound barrier to overcome this nuisance. A sketch of this barrier is shown in Fig. 2, and it has been entirely effective in eliminating any noise complaints from surrounding neighbors. It has not resulted in any measurable reduction in tower efficiency except that, under certain atmospheric conditions, recirculation difficulties appear to have been aggravated.

TABLE 4 NOISE-LEVEL TESTS BEFORE AND AFTER INSTALLING SOUND BARRIER FORCED-DRAFT FANS—MARTINEZ STEAM PLANT

Distance from fans, ft	Noise level, decibels	
	Before installing sound barrier	After installing sound barrier
150	88	73
1000	—	70

However, the service-life data in Table 3 suggests that it has contributed somewhat to the relatively shorter life of fan blades. As an example, the maximum life of magnesium-alloy blades at Martinez was 45 months, whereas a number of blades of this composition are still in service at Avon after 132 months.

In Table 4 are given the results of noise-level tests which were conducted before and after the installation of the sound barrier. These indicate a reduction from 88 to 73 decibels at a distance of approximately 150 ft from the tower.

Discussion

D. R. Baker.[4] The discussion of water-treating practices, and especially that dealing with the use of sulphur burners, deserves careful consideration and thought. It should be pointed out that sulphur burners produce SO_2 which will convert the carbonates into sulphites rather than sulphates. There is considerable disagreement among chemists as to whether or not the sulphites in a circulating water will be oxidized over to sulphates by aeration.

The object of using sulphuric acid is not to lower the pH or alkalinity, but to convert the carbonates into the more soluble sulphates for scale prevention. Sulphites are only slightly more soluble than carbonates, so scale tendencies will not be lowered appreciably by such a conversion, although the pH and alkalinity will both be lowered. Another reason for using sulphuric acid is to convert sodium carbonate to sodium sulphate to prevent delignification. Sodium sulphite is the basis for the sulphite pulping process used in the paper industry and is a stronger pulping agent than sodium carbonate. It is therefore quite important that the sodium carbonate be converted into the sulphate if the prevention of delignification is the object.

Soon after sulphur burners became publicized, the writer's company made an investigation to determine the relative amounts of sulphites and sulphates produced. Chemical analyses showed practically no sulphites in the circulating water, but chlorine had been used as an algaecide in all of the instances investigated. Chlorine will oxidize the sulphites over to sulphates so it is possible that the saving resulting from the use of sulphur rather than sulphuric acid may be offset by a higher chlorine demand. This possibility should be investigated. Care also should be taken in the chemical analysis to determine both sulphates and sulphites rather than to report them both as sulphates as is generally done.

E. B. Powell.[5] The author very aptly stresses the close interrelation in design and proportions of cooling tower, condenser, and turbine, and the importance of the correlation of these with the expected loading of the unit. It is well to have so clear a reminder of these factors.

The currently rapid growth in power consumption and the increasing extent to which power-generating requirements are exceeding the cooling capacities of natural water sources in many parts of the country make the author's discussion of cooling-tower operation, maintenance, and chemical control of great interest. The experience cited in meeting the problems of fan maintenance and noise is immediately valuable. The simplicity of the sulphur-burning arrangements, the major element of the chemical-control equipment, is particularly impressive. The effectiveness of this element of the control equipment is shown in Fig. 6 of the paper.

The experiences reported by other users of sulphur-burning facilities in less simple form prompt questions as to whether or not there has been any evidence of unburned sublimed sulphur carried in suspension in the circulating water, accumulating in the tower or in condenser tubes; also, whether from comparison of algae, slime, and other growths in the forced and induced-type towers or in the tubes of the respective condensers at Kern steam plant there has been any indication that the oxidizing capacity of the sulphurous salts is exerting significant influence in control of such growths. If there has been any evidence of solid elemental sulphur in the circulating-water system, it would be of great interest to learn whether or not deposit of the sulphur in the tubes has been accompanied by any evidence of corrosion accelerated by the presence of the sulphur deposit.

W. L. Chadwick.[6] The Power Division is to be complimented on its most successful cooling-tower symposium. The several papers have presented both methods of analysis and operating data which it is believed have not previously been available in published form on a subject of increasing importance.

The economic factors and approaches presented by Messrs. Le Bailly and Elliott should be of especial interest to designers responsible for selecting the economic installation. The case presented by Mr. Elliott which evaluates the choice between a "straight-through" river installation and cooling towers using the river water for evaporative cooling is interesting but to the writer, the most valuable part of this paper is Table 1 presenting the data for 23 installations, only three of which showed no deficiency in approach under test. These data give quantitative weight to Mr. Le Bailly's statement that cooling towers are designed "for an approach to a specified wet bulb, heat load, and cooling range without provision for contingencies matching the extra circulation design in boilers, cleanliness factors in condensers and manufacturers' allowance in turbines."

Mr. Elliott's pointing out that there is much yet to be learned regarding the effects of location, spacing, and orientation, particularly for larger installations, is also very timely. On the effects of these factors, certainly there is no consensus. It seems to the writer that Mr. Elliott's suggestion of the need for some research into these factors could well be effectuated by a detailed, statistical study of existing installations.

Mr. Lichtenstein's paper presenting a basis for evaluating recirculation and pointing out the need to provide some recirculation factor in design is a valuable contribution. Mr. Estcourt's paper presenting the operating and water-conditioning factors involved in cooling-tower operation nicely supplements the others with valuable data and information.

Mr. Degler's statement of the economic effect of the continued increase in the use of water could hardly be more pertinent anywhere than in the Pacific Southwest. The coastal plain upon which the metropolitan area of Los Angeles is situated is the home of nearly one half the population of California, yet the same area itself possesses only about 1 per cent of that State's water resources. Fortunately for the early development of the area, this plain is formed largely of deep alluvium which over its history has been filled with water. Heavy pumping early reduced this resource, and importation of other water became necessary. Between 1907 and 1913 the Owens River aqueduct was built by the City of Los Angeles to import about 400 sec-ft, and between 1931 and 1940 the Colorado River aqueduct was built by a few far-seeing communities to import up to 1500 sec-ft. The groundwater resources and the Owens importation are now fully in use. The Colorado River source, developed for the long range, is in initial use with practically the whole coastal plain seeking rights to its use.

As industry expands, only two sources are available to serve heavy new fresh-water demands, the Colorado River aqueduct and reclamation of waste. For "once-through" condensing water, there is still some undeveloped land along the coast but its value as resort property makes plant locations there difficult because of land value and zoning restrictions.

All these factors were involved in the selection of the site for the Etiwanda Steam Station of Southern California Edison Company, plus those of accessibility to load center, transportation, and accessibility to fuel supply. Another factor of increasing

[4] Head, Engineering Service, The Marley Company, Inc., Kansas City, Kan. Mem. ASME.

[5] Consulting Engineer, Stone & Webster Engineering Corporation, Boston, Mass. Mem. ASME.

[6] Vice-President, Southern California Edison Company, Los Angeles, Calif. Mem. ASME.

importance is waste disposal. As development on the coastal plain has increased, public and political apprehension over contamination of the underground basins by industrial wastes has become acute, ending in new restrictive legislation which requires exporting all waste which would be either nonpotable or detrimental to agriculture.

After decision had been made to build the station inland rather than at tidewater, two principal sites were considered. One would have utilized water reclaimed from sewer outfalls. As this possibility was developing satisfactorily, certain situations regarding the use of Colorado River water for this purpose changed and it became possible to consider seriously that source. Accordingly, the site was shifted to the new Fontana industrial area where a site could be had astride the main distribution line of the aqueduct system, permitting cooling-tower make-up to be withdrawn directly on the site.

Hence the decision to use cooling towers was directed by other factors. The station equipment to be served by the cooling towers comprises two tandem-compound triple-flow exhaust-reheat turbine-generator sets with throttle conditions of 1800 psi 1000/1000 F with six stages of feedwater heating. The condensers, as selected after numerous comparative estimates, are of two-pass construction with 80,000 sq ft of surface requiring 65,000 gpm circulation each. The long-term average wet-bulb is 58 F. Using demand costs of $120 per kw, annual fixed costs of 12 per cent, fuel at $31^1/_4$ cents per million Btu, 85 per cent condenser-cleanliness factor, auxiliary energy at the increment fuel cost, and 7000 capacity-hr per year, the most economical cooling-tower approach was found to be 14 F.

Author's Closure

Regarding Mr. Baker's remarks on the complete conversion of the carbonates to sulphates, when burning sulphur, it should be stated that the conversion of the sulphites to sulphate is assisted not only by aeration, but also by the addition of a catalyst to the make-up water. Copper sulphate is added in the proportion of approximately one quarter part per million.

While it is recognized that the purpose of sulphuric-acid addition or the burning of sulphur is to convert the carbonates to the more soluble sulphates, the use of the corresponding reduction in pH value or alkalinity as a control medium is a realistic operating device.

Mr. Baker's comment on the pulping characteristics of sodium sulphite and sodium carbonate is also well taken. In order to avoid delignification it is desirable that the sodium carbonate be completely converted to sodium sulphate.

Increased chlorine demand on towers where sulphur is being burned is an established fact which results from oxidation of the sulphites to sulphates. To offset this, we schedule our sulphur burning so that shot-chlorination for algae control takes place once each eight-hour shift, when the sulphur burners are not in operation. Our experience indicates that the chlorine demand may be increased approximately three times, if it is introduced during the sulphur-burning operation.

In a paper intended to cover the broad aspects of the various problems of cooling-tower design and operation, we did not feel justified in going into too much elaboration of details. However, it is felt that Mr. Baker's discussion is most pertinent and has made it possible to clarify certain specific problems, thereby adding to the value of the paper.

Mr. E. B. Powell has commented upon the danger of resublimed sulphur being carried over into the circulating-water system. It would appear that the hazard would be greatest when the velocity of the combustion air is high or the sulphur-dioxide gases are being prechilled before they come in contact with the absorbing water, or perhaps if there is insufficient combustion space in the burner. The manufacturers of sulphuric acid state variable combustion space requirements from 60 to 120 cu ft per ton of sulphur per day. Our burners permit a minimum of 100 cu ft per ton per day.

We have been concerned about these potential hazards and have gone to some lengths to assure ourselves that no detrimental effects are taking place. Several condenser tubes were removed and split for inspection. There was no evidence of any corrosion or pitting. Corrosion of condenser tubing from sulphur would require that elemental sulphur adhere to the tubes thus forming local concentration cells. While this is possible, it would appear to be rather improbable unless some binder material such as slime or algae is present on the tubes.

Certainly Mr. Powell has called attention to an operating hazard which should be carefully guarded against. We do not believe that our experience, which has been very satisfactory to date, should be taken as a broad generalization that corrosion difficulties from the presence of sublimed sulphur on condenser tubes will not occur under slightly changed physical and chemical environments.

No significant indication has been noted that the sulphurous salts are exerting any influence on the decrease of algae or bacteria. However, since we are using chlorination for algae control, it would be hard to draw any reliable conclusions in this respect.

All of the discussers should be congratulated for the manner in which they have enhanced the value of the papers by their timely comments, and Mr. Chadwick specifically for the inclusion of data covering the basis of selection of the cooling towers for the Etiwanda Station.

Deterioration of Wood in Cooling Towers

By R. H. BAECHLER[1] and C. A. RICHARDS,[2] MADISON, WIS.

The premature deterioration of wood in cooling towers has received considerable attention during the past several years. Although the number of towers so affected appears to be rather small compared with the total number in use, premature deterioration nevertheless deserves serious study. The owner of a tower needing expensive repairs after only a relatively short period of use can draw small comfort from the fact that wood in most cooling towers gives satisfactory service. Furthermore, an upward trend in the percentage of towers affected must be recognized as a distinct possibility, making the need for corrective measures even greater than is indicated by past experience. The preliminary investigations described in this paper were intended to throw some light on a few of the many questions that have arisen regarding wood failure in cooling towers. A brief discussion of the nature of wood, the kinds of deterioration it may undergo, and the conditions to which it is exposed in a cooling tower are given.

Significant Properties of Redwood

REDWOOD is the species used almost exclusively in the construction of cooling towers. Its principal advantages over other species lie in its inherent resistance to decay, its relative freedom from distortion with changes in moisture content, and its availability in the clear grades needed for this purpose. It has no pronounced peculiarities of anatomical structure that would appear to have any bearing on wood deterioration. It does differ from most other species in that the heartwood is quite susceptible to penetration by liquids under pressure; this permeability may have some bearing on the rate of deterioration by chemical solutions.

As in all wood, the major constituent of redwood is cellulosic material, loosely designated as cellulose. This accounts for somewhat more than one half of the dry weight of redwood. Lignin, the other principal substance, comprises somewhat less than one third of the weight. The ratio of cellulose to lignin is normal for a coniferous wood.

The cellulosic material is fibrous in nature. It consists chiefly of a chemically stable portion called alpha cellulose but includes related compounds of lower molecular weight and greater chemical reactivity, which are known as hemicelluloses.

Lignin is a stiffening and cementing material which is present chiefly between the cells but also within the cell walls.

Cellulose, especially alpha cellulose, is quite stable chemically. It may be hydrolyzed by dilute acids into polysaccharides, which in turn break down into sugars. The action of dilute acids on cellulose, however, is very slow except at elevated temperatures. While lignin is more resistant than cellulose to dilute acids, it is attacked more readily by most other chemicals, including alkalies and oxidizing agents.

From the standpoint of chemical composition, the outstanding characteristic of redwood is its high content of material designated as extractives. These are extraneous materials that do not appear to be part of the wood structure, but may be removed by solvents such as water, alcohol, and benzol. The quantity of extractives (1)[3] varies greatly from tree to tree and even from different parts of the same tree. There is commonly from 7 to 15 per cent of hot-water-soluble extractives in the heartwood of the redwood tree, but the content of individual trees may vary considerably outside this range.

The extractives of redwood have been shown to be toxic (2) to wood-destroying fungi and, therefore, are believed to be responsible for its natural resistance to decay. The tannins, and related less-soluble phlobaphenes, which usually comprise nearly one half of the total water-soluble extracts, appear to be responsible for more of the toxic effect than do the remaining extractives. Other toxic compounds also may be present in small amounts. While considerable work has been done on the chemical nature of these extractives (1, 3), many questions concerning them remain unanswered.

Conditions Prevailing in a Cooling Tower

It should be understood that the conditions in a cooling tower apply only in a general way to any given tower. Variations are found in such factors as the design of the tower, the quality of the wood, operating practices, the treatment applied to the water, and, of course, the raw water itself.

Moisture conditions are quite different in various parts of a tower. Some parts are submerged in water, while others are dry most of the time. Some parts are subjected to constant flow of water while the tower is in operation. Wood in such locations will reach and remain at a high moisture content, so that decay presents less of a hazard than chemical attack. Nevertheless, the water is highly aerated and even these parts may decay. Other parts of a tower are bathed in a mist and, because of the favorable temperatures maintained, vulnerable wood may decay. Still other locations involve intermittent splashing or flooding, with opportunity for subsequent evaporation and concentration of any chemicals in the water.

The water in most plants is treated with various chemicals, the main objectives being: (*a*) To prevent the formation of excessive scale, especially a hard scale, in condensers, heat exchangers, boilers, and other equipment; (*b*) to minimize the corrosion of metals with which the water comes in contact; and (*c*) to prevent the fouling of equipment by algae. A pH of 8 or above is usually maintained in order to reduce corrosion; a pH of 7 or slightly below would be more favorable for wood, but protection of metallic equipment takes precedence over protection of the wood.

In some plants using a zeolite type of water softener, the pH may reach values above 11. In other plants, either sulphuric or sulphurous acid is used to convert carbonates to sulphates, which are more soluble and less prone to form scale. Imperfect control sometimes drops the pH to as low as 3.

Chlorine has been the almost universal algaecide used, although in recent years several other chemicals, such as the sodium salt of

---

[1] Chemist, Forest Products Laboratory, Forest Service, maintained at Madison, Wis., in co-operation with the University of Wisconsin.

[2] Pathologist, Division of Forest Pathology, Bureau of Plant Industry, Soils and Agricultural Engineering, U. S. Department of Agriculture; in co-operation with the Forest Products Laboratory.

Contributed by the Power Division and presented at the Spring Meeting, Atlanta, Ga., April 2-5, 1951, of The American Society of Mechanical Engineers.

Note: Statements and opinions advanced in papers are to be understood as individual expressions of their authors and not those of the Society. Manuscript received at ASME Headquarters, March 14, 1951. Paper No. 51—S-11.

[3] Numbers in parentheses refer to the Bibliography at the end of the paper.

pentachlorophenol and a proprietary quaternary compound, have been used to some extent. Most plants using chlorine attempt to keep the concentration in the neighborhood of 1 ppm, but failure of the controls may result in much higher concentrations for short periods.

In oil refineries and chemical plants, leaks in the equipment sometimes permit reactive materials, such as acids, ammonia, hydrogen sulphide, sulphur dioxide, and mercaptans, to escape into the water. The duration of the periods during which contaminated water has been passed through a tower is not always known with certainty, and so the importance of such fluctuations is difficult to estimate.

While statistics are lacking on the average amount of wood per tower required annually for the replacement of deteriorated wood, it seems to be accepted that this amount has increased in recent years. The changes in operating conditions or design of towers that have taken place are therefore of interest.

The mechanical forced-draft tower began to replace the atmospheric deck-type tower approximately 20 years ago, while the induced-draft tower has come into wide use during the past 10 years. A larger volume of water per unit time may be passed over a mechanical-draft tower; this would accelerate the leaching of extractives, the erosion of the wood, and the chemical effect of any compounds present in low concentrations. The lower drift loss in mechanical-draft towers leads to a lower requirement of make-up water. This in turn leads to a more rapid concentration of dissolved solids in the water. A further effect, of obvious significance, is that, with the lower drift loss, it has become feasible to treat the make-up water.

Operating temperatures evidently have been changed but little with the adoption of mechanical-draft towers. A generally high relative humidity of the air naturally would be found within any tower, regardless of design. Changes in wind and weather have less effect on the performance of a mechanical-draft tower than on that of an atmospheric tower, so that conditions within tend to remain more nearly constant.

In many areas, the use of enormous quantities of well water by expanding industry has led to a serious drop in ground-water levels, with the result that surface water is increasingly used. As compared with ground waters, surface waters tend to contain more suspended matter, which might increase their erosive action. They also contain more dissolved organic matter, which conceivably could stimulate the growth of wood-destroying fungi as well as fouling organisms. Surface waters are much more likely than ground waters to carry spores and fragments of mycelia of wood-destroying fungi, as well as small fragments of rotting wood. Surface waters are generally lower in content of dissolved minerals and in some areas the carbonate content is so low that caustic soda is added to compensate for the lowering of pH that accompanies the addition of chlorine.

Types of Deterioration

The premature failures of redwood in cooling towers have been attributed to one of two causes, living organisms called fungi, which are responsible for decay, and chemicals present in the water.

When wood decays it undergoes a profound chemical change. The term "chemical attack" is used in this paper, however, only to describe any deterioration caused by chemicals in the water and not influenced by the growth of fungi. The possibility that decay and chemical attack might proceed simultaneously and more or less independently has been recognized. Furthermore, it is known that chemical attack and decay are sometimes interdependent; under certain conditions, a chemical may react with toxic extractives to form nontoxic compounds and thus render the wood vulnerable to decay.

A third type of deterioration, physical erosion of the wood by the water, no doubt plays a role in the gradual reduction in cross section that occurs in members exposed to a continuous flow of water. Suspended matter in the water would be expected to intensify this eroding effect. The delignified surface fibers are frequently loosened and washed away by the water—either wearing down the wood evenly or causing deep channels in the surface. In some parts of a tower, alternate wetting and drying may result in a precipitation of dissolved chemicals whereby crystals formed within the wood may disintegrate the fibers mechanically. The solvent action of water on the toxic extractives would be expected ultimately to render the redwood susceptible to decay.

In the most common type of chemical disintegration of the wood, the surface fibers become delignified so that the surface becomes a mat of white fibers. These fibers are either loosely attached or tightly compressed on the surface, giving the wood a "painted" appearance. The interior of such pieces may appear sound, but most frequently some fungus hyphae can be found. These hyphae may be responsible for the brashness that is frequently characteristic of such pieces, but only rarely has typical decay been found.

The type of decay that has been found most frequently is a light pocket rot that commonly occurs in eliminator slats. The surface of the piece appears sound and is frequently covered with algae and fungi, but the interior is pitted, soft, and in extreme cases, fibrous. Sporophores (fruiting bodies) of the causal fungus have been found on the surface of such decayed pieces. These sporophores are crustlike forms with a pore surface varying from buff to buff pink when fresh and darkening somewhat on drying. Although the sporophores seem similar, the cultures from the rotted wood vary in appearance and growth characteristics. Since many of the sporophores have been immature, it is impossible to name them definitely, but they are either *Poria nigrescens* or closely related species.

Brown cubical rot is uncommon in the slats but has been found in the timbers. In contact with iron fastenings, this type of rot gives the wood a charred appearance. The causal fungus has not been isolated. True decay of wood in cooling towers has been established definitely in numerous instances. The question that remains is not whether redwood ever decays in a cooling tower but why it decays in one tower and not in some other in which conditions appear to be quite similar.

The possibility of attack by several chemicals commonly present in water passed through cooling towers has been recognized, but previously published studies have been confined largely to the effect of sodium carbonate. In 1941 A. R. Moberg (4) published a report on the development of a fibrous condition on the surface of cooling towers. He explained the condition as being due to a delignification caused by sodium carbonate, the concentration of which could be increased by intermittent evaporation from localized areas. Blohm and Frazier showed that when three species of wood were exposed to varied concentrations of sodium carbonate, the loss in weight was proportional to the concentration of sodium carbonate. The weight loss was independent of the pH, since the pH was practically constant in the range of concentrations used. Baker (6) pointed out a number of types of chemical attack to which wood might be exposed in towers.

Chlorine has been suspected of slowly damaging redwood even when present in very low concentrations. This theory stems from the fact that chlorine is the most reactive of the chemicals present in most water used in towers. It is known to attack all constituents of wood to some extent, lignin and hemicellulose being most susceptible. There is no evidence to show that chlorine in concentration of 1 ppm or less has any appreciable effect on the life of a tower; there are numerous examples of towers that have seemingly suffered no ill effects when such carefully controlled

amounts of chlorine are added to the water. The effect of periodic failure of the controls is likewise obscure. Blohm and Frazier (5) cite the case of a tower that was attacked rapidly by water containing 60 ppm of chlorine.

An injurious chemical effect by any of the neutral salts present in natural waters appears very improbable. Salts that occur in several hydrated forms, however, conceivably could cause mechanical damage when deposited in the fibers under conditions of alternate wetting and drying.

Iron salts are known to damage wood in two distinctly different ways. It has been shown that they may precipitate toxic extractives of a number of naturally durable species and thus render the wood vulnerable to decay. Traces of iron stimulate the growth of some fungi. Apart from this effect, there is a strictly chemical effect which can be demonstrated in the laboratory by exposing wood to solutions of iron salts under sterile conditions. Iron nails are not used in towers because of their rapid corrosion, but iron clip angles and other iron braces are used. Also, contact between wet wood and iron may occur on the members supporting the fan assembly. Redwood in contact with iron occasionally deteriorates rapidly in towers, generally if the part is not flooded with water. In most towers, however, wood and iron are compatible. Thus, while the effect of iron on redwood under the conditions found in cooling towers is of theoretical interest, it appears to be of limited practical importance.

A fairly large number of towers were inspected by the authors in the company of D. R. Baker.[4] Samples of deteriorated wood were removed from certain towers and sent to Madison for examination; chemical analyses were made of a few samples. These inspections are covered in a report distributed by Mr. Baker's company.

The work to be described concerns the nature of decay in specimens removed from cooling towers, the loss of decay resistance of thin redwood cross sections exposed to several solutions under accelerated conditions, and changes taking place in redwood during approximately seven years of service.

Experimental Work

Laboratory Leaching Studies. In these experiments, the changes that might take place in redwood in a cooling tower were accelerated by the use of thin cross sections, high temperatures, and relatively high concentrations of chemicals. Furthermore, the cross sections were only 1/4 in. thick in the direction of the grain, so that the ingress of the chemical solution and the leaching of extractives would be many times faster than would be found for lumber with side grain exposed.

The cross sections were cut from a board of dense heartwood 3 in. wide and 1 in. thick (actual dimensions). The board was selected after tests showed it to have a fairly high and reasonably uniform distribution of extractives. In starting a test, 10 cross sections were subjected to partial vacuum in a laboratory suction flask, covered with the solution to be tested, and submerged by releasing the vacuum. This cycle was repeated until all specimens were submerged. The specimens were then transferred to a 1-liter Erlenmeyer flask, and 500 ml of the boiling solution were added. The flask was then placed in a water bath, which was kept at the boiling point and maintained at constant level. A small flask was placed in an inverted position in the mouth of the flask containing the specimens in order to minimize loss by evaporation. Occasional additions of distilled water were necessary to maintain a level close to the original in the larger flask.

During the first 3 days, the solution in the flask was replaced hourly with a fresh portion; afterwards it was changed once daily. The sodium-hypochlorite solutions, however, were replaced every hour throughout, as tests showed that the drop in available chlorine was rapid enough to require this schedule. Eight 1-hr leaching cycles were completed in 1 day. At the end of each 8-hr day, the liquid was drained off and the specimens were kept overnight in the stoppered flask.

Leaching periods of 1, 3, 7, and 27 days were used with separate sets of cross sections. The following solutions were used:

A, plain distilled water.

B, 0.02 per cent sodium carbonate (200 ppm; pH = 9.95).

C, 0.2 per cent sodium carbonate (2000 ppm; pH = 10.7).

D, same as B but with a current of air passed through the solution and using a flask fitted with a water-cooled reflux condenser.

E, same as D but using 0.2 per cent sodium carbonate.

F, sodium-hypochlorite equivalent to 0.01 per cent of available chlorine.

G, sodium hypochlorite equivalent to 0.001 per cent of available chlorine.

Eight cross sections from each group of 10, were set aside after leaching, for use in decay tests. Two were used for a determination of residual water-soluble extractives. The result was compared with values obtained for unleached matched controls from the same original board. Those cross sections which had been leached for the maximum period of 27 days were also subjected to analysis for cellulose and lignin.

No strength tests were made on the cross sections after their exposure to the solutions. According to casual examination, the cross sections did not appear to be weakened, but carefully controlled strength test might have revealed some chemical deterioration. Those cross sections which had been exposed to sodium-carbonate solutions were lighter in color than those which had been exposed to water. Those which had been exposed to sodium-hypochlorite solutions were even lighter and had a slightly weathered appearance.

After leaching, eight cross sections from each group were exposed to fungus action as follows:

About 80 grams of topsoil (Miami silt loam) were placed in 8-oz French-square bottles lying on their sides. Enough water was added to bring the moisture content of the soil up to 60 per cent. Water-soaked Ponderosa pine feeder blocks 1/4 × 1 × 3 in. in size were placed on the wet soil. The bottles were closed with loosely fitting metal screw caps and then autoclaved for 30 min at 15 psi pressure. When cool, the feeder blocks were inoculated with cultures No. 4789, No. 4856, *Poria monticola* (Madison 698), or *Lenzites trabea* (Madison 617). The first two fungi had been isolated from the typical pocket rot in eliminator slats; the latter two commonly cause brown rot in a number of softwoods. After the fungi were well established, the test pieces, which had been brought to equilibrium moisture content at 30 per cent RH and 80 F, were weighed, placed on the feeder blocks and incubated for 3 months. The test blocks were again brought to equilibrium moisture content and weighed so that the weight loss due to fungus action could be calculated.

The results of analyses and decay tests are given in Table 1.

Tests on Slats Removed From Towers. Three eliminator slats were removed from each of 12 towers that had been in use for periods of from 6 to 8 years. Short sections were cut some distance from an end for the determination of residual water-soluble extractives.

Half of each slat was lightly planed to remove surface blemishes and deposits and to equalize the size of the test specimens, which were 1/4 × 1 × 2 3/4 in. in size. The specimens and sections from new unused slats were handled as those were in the first test except that *Lentinus lepideus* was used as a test fungus in addition to No. 4789, No. 4856, *Lenzites trabea*, and *Poria monticola*.

[4] Marley Company, Inc., Kansas City, Kan.

TABLE 1 TESTS ON THIN CROSS SECTIONS EXPOSED TO ACCELERATED LEACHING AND DECAY TESTS

Sample no.	Leaching conditions	Original hot-water extractive per cent	Residual extractives: Hot water, per cent	Residual extractives: Alcohol-benzene, per cent	Cellulose (Cross and Bevan), per cent	Lignin, per cent	Ratio of cellulose to lignin	Weight loss due to: No. 4856*, per cent	Weight loss due to: No. 4789*, per cent	Weight loss due to: *Poria monticola*, per cent	Weight loss due to: *Lenzites trabea*, per cent
1	1 day in water	11.4	3.40	—	—	—	——	0	3.0	39.3	21.5
2	3 days in water	11.4	1.59	—	—	—	——	0	6.8	46.8	25.7
3	9 days in water	11.2	1.38	—	—	—	——	0	8.0	47.4	22.2
4	27 days in water	11.2	1.37	0.56	53.8	36.4	1.48:1	0	7.9	50.8	—
5	1 day in 0.2 per cent Na_2CO_3	11.3	3.26	—	—	—	——	24.5	53.4	51.9	32.2
6	3 days in 0.2 per cent Na_2CO_3	11.4	3.21	—	—	—	——	25.4	54.8	51.0	47.2
7	9 days in 0.2 per cent Na_2CO_3	11.0	2.73	—	—	—	——	24.1	52.9	53.7	47.6
8	27 days in 0.2 per cent Na_2CO_3	10.9	2.66	0.41	57.8	34.8	1.66:1	24.8	41.8	54.6	—
9	1 day in 0.02 per cent Na_2CO_3	11.4	2.66	—	—	—	——	4.0	29.1	38.2	22.4
10	3 days in 0.02 per cent Na_2CO_3	11.4	1.57	—	—	—	——	9.4	38.6	45.0	33.4
11	9 days in 0.02 per cent Na_2CO_3	9.7	1.47	—	—	—	——	11.8	32.9	53.0	42.0
12	27 days in 0.02 per cent Na_2CO_3	9.7	1.47	0.26	56.0	35.1	1.59:1	13.6	33.2	52.3	—
13	1 day in 0.2 per cent Na_2CO_3 + air	11.0	3.46	—	—	—	——	20.9	43.3	51.2	31.9
14	3 days in 0.2 per cent Na_2CO_3 + air	11.2	3.53	—	—	—	——	22.2	39.9	53.7	42.4
15	9 days in 0.2 per cent Na_2CO_3 + air	10.0	3.19	—	—	—	——	20.6	46.2	54.5	34.6
16	27 days in 0.2 per cent Na_2CO_3 + air	10.0	3.17	0.24	51.4	33.7	1.52:1	20.2	68.6	53.4	—
17	1 day in 0.02 per cent Na_2CO_3 + air	11.0	3.38	—	—	—	——	3.0	16.4	37.7	20.2
18	3 days in 0.02 per cent Na_2CO_3 + air	11.3	2.13	—	—	—	——	8.8	32.4	41.0	32.0
19	9 days in 0.02 per cent Na_2CO_3 + air	10.0	1.69	—	—	—	——	12.8	40.8	49.6	36.2
20	27 days in 0.02 per cent Na_2CO_3 + air	10.0	1.60	0.11	57.2	35.0	1.63:1	10.5	47.6	54.4	—
21	1 days in 0.01 per cent Cl_2	10.8	2.82	—	—	—	——	0	9.6	39.0	25.6
22	3 days in 0.01 per cent Cl_2	9.9	2.20	—	—	—	——	0.9	15.9	41.0	27.0
23	9 days in 0.01 per cent Cl_2	10.0	1.74	—	—	—	——	2.9	20.2	49.2	21.6
24	27 days in 0.01 per cent Cl_2	9.8	1.45	0.32	56.2	35.9	1.57:1	2.2	26.0	52.8	—
25	1 day in 0.001 per cent Cl_2	10.3	3.12	—	—	—	——	0	2.0	38.0	17.4
26	3 days in 0.001 per cent Cl_2	9.7	1.54	—	—	—	——	0	8.2	45.2	23.2
27	9 days in 0.001 per cent Cl_2	10.0	1.26	—	—	—	——	0	9.6	50.9	27.3
28	27 days in 0.001 per cent Cl_2	10.0	1.05	0.37	55.5	36.9	1.54:1	0	6.2	53.0	—
29	Unleached	—	—	—	—	—	—	0	1.6	22.8	9.4

* Cultures Nos. 4856 and 4789 were isolated from decayed redwood cooling-tower slats.

The results are given in Table 2.

Discussion

The data in column 4 of Table 1 show that the effect of any of the leaching agents on the amount of water-soluble material in the thin cross sections falls off rapidly after the first day and is negligible after 9 days. While the elevated temperature contributed to this rapid leaching, it is believed that the most important factor was the small dimension of the specimens in the direction of the grain. Burr and Stamm (7) found that the true diffusion of dissolved material through sizable specimens of water-saturated wood is about 12 to 15 times as great in the fiber direction as across the fibers. In the cross sections used in the present experiments, however, a considerably higher ratio would be expected because of the stirring effect on the ends of open tracheids.

The shape and size of the specimen would likewise influence the effect of the chemicals on the wood, although not necessarily to the same degree. Both sodium carbonate and chlorine are of much smaller molecular weight and much more soluble than extractives, hence would be expected to diffuse inward much more rapidly than the extractives would diffuse outward. The chemicals might have relatively greater effect than water in lumber of conventional shape and size than in these cross sections.

At first glance, it would appear that, in so far as the removal of extractives is concerned, 1 day of exposure to the laboratory conditions described is equivalent to several years of actual service. Such an assumption may be correct, but it is a hazardous one to make, even though the results in column 4 of Table 2 seem to confirm such an assumption. The deterioration of wood, whether due to fungi, chemicals, or high temperatures, is practically always accompanied by the formation of water-soluble compounds. The hot-water-soluble material found in the slats removed from towers may include such compounds in addition to the true extractives.

This fact should also be kept in mind in a consideration of the effect of the solutions used in the laboratory experiments. The removal of the original extractives might in reality be greater than is indicated by the amount of water-soluble material found at the end of the different exposure periods. Even very dilute alkaline solutions act on lignin and hemicellulose to form water-soluble compounds of lower molecular weight. The removal of extractives by the sodium-carbonate solutions is probably masked to some extent by the formation of such water-soluble products of the decomposition of lignin and hemicellulose. The effect of chlorine may be complicated in a similar manner, although the types of reactions would be different.

The formation of water-soluble decomposition products offers an explanation for the higher extractive content of the pieces exposed to the higher concentration of both chemicals.

As compared with water, the solutions of sodium carbonate and sodium hypochlorite tended to bring about an increase in the ratio of cellulose to lignin. This is readily explained by the more rapid degradation of lignin than of cellulose by these chemicals.

Both chemicals appear to cause an increase in the total amount of cellulose plus lignin; this is a reflection of the loss of other materials, especially extractives.

The data on the controls in Table 2 show that, while there may be a general correlation, the percentage of extractives in a given piece of redwood is an unreliable indication of its resistance to decay. The composition as well as the amount of the extractive must be taken into consideration. This agrees with the results of previous work done in this laboratory and elsewhere. As was mentioned, the data on the leached cross sections, and also on the used slats, are believed to be complicated by the presence of degradation products.

Of the two fungi isolated from decayed redwood, No. 4856 caused little or no loss in weight of either new specimens or specimens exposed to leaching by water. No. 4789, on the other hand, produced some decay in specimens leached with water. Both fungi attacked most of the used slats, but No. 4789 was the more active in all the leached or used slats, while No. 4856 decayed unleached redwood slightly more.

The other two fungi, *Lenzites trabea* and *Poria monticola*, which were used in tests on the leached blocks, and *Lentinus lepideus* which was used in addition to the other four in tests on used slats, showed some ability to attack new redwood and produced profound decay in all cross sections leached in the laboratory. Their attack on used slats varied in intensity but was generally more severe than that shown by No. 4789 and No. 4856. It might be of interest to note that *Poria monticola* is closely related to *Poria sequoia*, which produces the brown cubical rot in redwood trees.

TABLE 2 EXTRACTIVE CONTENT AND DECAY RESISTANCE OF ELIMINATOR SLATS AFTER ABOUT 7 YEARS OF SERVICE

No.	Year built	Hot-water extractive, per cent	Weight loss[a] due to				
			No. 4789[b] per cent	No. 4856[b] per cent	*Lentinus lepideus*, per cent	*Lenzites trabea*, per cent	*Poria monticola*, per cent
1A	—	10.15	0.1	0.0	2.1	6.6	5.0
1B	—	11.70	0.4	1.4	6.0	3.8	6.5
1C	—	12.41	0.0	0.0	3.4	3.1	9.3
2A	1943	2.84	3.7	0.0	8.1	15.2	16.2
2B	—	2.66	2.5	0.1	3.3	14.6	12.5
2C	—	7.20	2.0	0.0	1.5	4.4	16.6
3A	1943	9.34	10.0	8.9	1.0	6.5	10.1
3B	—	7.66	13.9	9.0	1.0	2.8	2.5
3C	—	8.65	10.2	2.6	0.1	2.8	9.3
4A	1942	2.90	21.4	6.2	7.0	26.1	16.5
4B	—	3.22	3.0	0.5	12.1	13.3	19.9
4C	—	3.75	10.6	2.3	1.3	1.8	22.3
5A	1943	3.80	3.3	3.1	5.2	7.3	24.4
5B	—	2.28	5.8	0.9	13.3	26.9	8.6
5C	—	3.57	3.6	0.2	1.8	5.1	15.7
6A	1942	8.94	8.0	2.5	6.3	15.8	10.0
6B	—	6.51	18.4	4.6	9.5	19.2	25.4
6C	—	4.94	4.7	0.8	5.5	10.7	16.1
7A	1943	5.42	16.7	4.5	4.8	9.4	20.0
7B	—	3.81	30.4	10.4	8.3	11.5	24.5
7C	—	5.04	19.9	5.7	6.5	4.4	11.5
8A	1942	4.45	6.4	0.1	9.8	19.9	29.6
8B	—	5.43	4.3	1.7	7.9	12.6	17.8
8C	—	3.58	17.1	5.3	4.1	1.1	18.1
9A	1943	5.85	29.9	12.5	7.9	21.5	28.7
9B	—	4.05	49.7	11.6	15.8	36.2	43.4
9C	—	3.80	61.7	15.9	15.7	50.2	30.8
10A	1942	3.81	23.6	6.1	13.7	33.1	33.7
10B	—	5.28	4.6	1.7	1.0	6.4	6.4
10C	—	6.14	7.0	1.5	1.4	7.7	7.8
11A	1942	3.08	13.7	4.3	11.7	24.6	25.6
11B	—	3.40	20.2	3.5	8.8	31.4	32.8
11C	—	2.87	14.0	3.9	7.6	17.8	16.7
12A	1942	3.50	32.4	6.2	7.4	18.5	0.0
12B	—	4.60	27.4	7.6	6.6	31.5	18.5
12C	—	2.83	31.4	8.4	13.9	44.5	35.6
13A	1941	3.07	15.0	4.1	10.3	27.5	22.4
13B	—	3.24	23.7	3.0	11.5	15.9	28.4
13C	—	3.68	20.4	4.2	13.3	26.8	25.3
14A	—	10.75	0.6	0.5	3.8	5.1	5.6
14B	—	16.23	1.0	3.6	6.1	5.3	4.1
14C	—	8.15	0.8	0.0	9.0	11.2	13.2

[a] Each figure is the average for three replicate specimens.
[b] Cultures Nos. 4856 and 4789 were isolated from decayed redwood cooling-tower slats.

The data in Table 1 show that the weight losses produced by *Poria monticola* and *Lenzites trabea* are so high in most cases that differences between the effects of water and those of chemical solutions are obscured unless comparisons are made on cross sections leached only 1 day. When attention is directed to decay produced by the other two fungi, the difference between the effects of water and those of the sodium-carbonate solutions becomes striking. While these conditions were admittedly artificial, it is of interest to note that a pronounced reduction in decay resistance could be demonstrated before any visible signs of delignification had developed. The stronger chlorine solution also shows a decided effect, although it is less than that of the weaker sodium-carbonate solution. No appreciable difference was discernible between the effect of water and the effect of the weaker chlorine solution, which was much stronger than would normally be encountered in practice.

From the results given in Table 1 it would appear that fungus No. 4789 severely decayed wood that had been leached in 0.2 per cent sodium carbonate more than it did slats that had been in actual use except in one case. It is unfortunate that no information is available about the water used in tower No. 9.

Conclusion

The significant properties of redwood, the types of deterioration to which it is subject, and the conditions prevailing in cooling towers are reviewed. Pieces of slats removed from 12 towers after 6 to 8 years of service, and exposed to five fungi in laboratory tests, showed much greater loss in decay than pieces of unused redwood. Thin cross sections exposed to solutions of sodium carbonate and sodium hypochlorite were less resistant to decay than those exposed to water.

Acknowledgment

Acknowledgment is gratefully made to the Marley Company, Inc., for helpful advice and for financial support of this work, and also to George Englerth of the Division of Forest Pathology, and H. G. Roth of the Forest Products Laboratory, who assisted in conducting the tests.

BIBLIOGRAPHY

1 Institute of Paper Chemistry, Research Bulletin, December, 1945.

2 "Distribution of Extraction in Red Wood," by E. C. Sherrard and E. F. Kurth, *Journal of Industrial and Engineering Chemistry*, vol. 25, 1933, pp. 300–302.

3 "Sequoyite, a Cyclose From Red Wood," by E. C. Sherrard and E. F. Kurth, *Journal of the American Chemical Society*, vol. 51, 1939, pp. 3139–3141.

4 "Some Factors Influencing the Life of Wooden Cooling Towers," by A. R. Moberg, *California Oil World and Petroleum Industry*, vol. 34, 1941, pp. 8–14.

5 "Chemical Distribution of Cooling Tower Lumber," by C. L. Blohm and H. D. Frazier, *Oil and Gas Journal*, vol. 48, 1950, pp. 72–75.

6 "Wood Deterioration in Cooling Towers," by D. R. Baker, paper presented at Regional ASME Quarterly Meeting, Dallas, Texas, April 1, 1950.

7 "Diffusion in Wood," by H. K. Burr and A. J. Stamm, *Journal of Physical and Colloid Chemistry*, vol. 51, 1947, p. 240.

The Hydrodynamic Lubrication of Sector-Shaped Pads

By R. S. BRAND,[1] STORRS, CONN.

Solutions of Reynolds equation are obtained by means of relaxation methods for a sector-shaped pad. Results are given for a 45-deg "square" sector in the form of curves of operating factors plotted against a parameter of the film shape. A comparison with results based on the solutions for rectangular sliders shows that such solutions can be applied safely to sector-shaped pads in most cases.

Nomenclature

The following nomenclature is used in the paper:

x, y = Cartesian co-ordinates (Fig. 1)
R = mean radius of shoe
$x_1 = x/R$, $y_1 = y/R$ = dimensionless co-ordinates
α = angular inclination of shoe
H = film thickness at any point x, y
H_o = film thickness in Y-Z-plane
μ = viscosity
u, v, w = components of fluid velocity
ω = angular velocity of rotor
p = fluid pressure
$q = pH_o^3/R^3\beta\mu\omega$ = dimensionless pressure function
P = total load
M = friction moment on rotor
$\beta = R\alpha/H_o$ = film-shape parameter
$C_p = PH_o^3/R^4\mu\omega$ = load coefficient
$C_f = MH_o/R^4\mu\omega$ = friction-moment coefficient

Introduction

The pressure distribution in a thin film of lubricant is described by a partial differential equation due to Reynolds,[2] which has been solved for only a few simple film shapes. For the important case of a plane sector-shaped inclined shoe, such as those used in large thrust bearings, the only solutions available are those obtained by the Kingsbury electrical analogy,[3] or by other experimental means. It has been customary to predict the performance of such bearings by considering an "equivalent" rectangular slider bearing.

Christopherson[4] has shown that many lubrication problems, including that of the sector-shaped shoe, can be solved numerically by means of the relaxation methods of Southwell.[5] In this paper are presented the results of such computations for a plane 45-deg sector-shaped pad tipped about a radial axis bisecting the sector angle.

Derivation of Reynolds Equation

If it is assumed that pressure gradients across the film are negligible and that velocity gradients in the Z-direction are much greater than in the X or Y-direction, the equations of motion reduce to

$$\left.\begin{aligned} \frac{\partial p}{\partial x} &= \mu \frac{\partial^2 u}{\partial z^2} \\ \frac{\partial p}{\partial y} &= \mu \frac{\partial^2 v}{\partial z^2} \end{aligned}\right\} \quad \ldots\ldots [1]$$

Integrating these equations twice with respect to z, and making use of the boundary conditions

$$\text{when } z = 0, \quad u = -y\omega, \quad \text{and } v = x\omega$$

$$\text{when } z = H, \quad u = v = 0$$

we obtain the following expressions for the fluid velocities

$$\left.\begin{aligned} u &= \frac{1}{2}\frac{p}{\mu x}(z^2 - Hz) + y\omega\,(z/H - 1) \\ v &= \frac{2}{1}\frac{p}{\mu y}(z^2 - Hz) + x\omega\,(1 - z/H) \end{aligned}\right\} \quad \ldots\ldots [2]$$

The equation of continuity

$$\frac{\partial u}{\partial x} + \frac{\partial v}{\partial y} + \frac{\partial w}{\partial z} = 0$$

can now be integrated with respect to z, with the result

$$\frac{1}{6}\frac{\partial}{\partial x}\left(\frac{H^3}{\mu}\frac{\partial p}{\partial x}\right) + \frac{1}{6}\frac{\partial}{\partial y}\left(\frac{H^3}{\mu}\frac{\partial p}{\partial y}\right) + y\omega\frac{\partial H}{\partial x} - x\omega\frac{\partial H}{\partial y} = 0 \ldots [3]$$

Taking a plane shoe tilted about a line parallel to the y-axis, we have $\partial H/\partial x = \alpha$ and $\partial H/\partial y = 0$. Hence if μ is assumed constant

$$\frac{\partial}{\partial x}\left[H^3\frac{\partial p}{\partial x}\right] + \frac{\partial}{\partial y}\left[H^3\frac{\partial p}{\partial y}\right] + 6\mu y\omega\alpha = 0 \ldots\ldots [4]$$

This is converted to dimensionless form by the following substitutions

$$x = Rx_1 \qquad H = H_o + x\alpha = H_o(1 + \beta x_1)$$
$$y = Ry_1 \qquad p = \frac{\mu R^2\omega\beta}{H_o^3}q$$
$$\beta = R\alpha/H_o$$

---

[1] Assistant Professor of Mechanical Engineering, University of Connecticut. Jun. ASME.

[2] "On the Theory of Lubrication and Its Application to Mr. Beauchamp Tower's Experiments," by O. Reynolds, Transactions of the Royal Society of London, vol. 177 (Part I), 1886, pp. 157–234.

[3] "On Problems on the Theory of Fluid-Film Lubrication With an Experimental Method of Solution," by A. Kingsbury, Trans. ASME, vol. 53, paper No. APM-53-5, 1931.

Contributed by the Research Committee on Lubrication and the Petroleum and Machine Design Divisions, and presented at the Semi-Annual Meeting, Toronto, Can., June 11–15, 1951, of The American Society of Mechanical Engineers.

Note: Statements and opinions advanced in papers are to be understood as individual expressions of their authors and not those of the Society. Manuscript received at ASME Headquarters, March 21, 1951. Paper No. 51—SA-6.

[4] "A New Mathematical Method for the Solution of Film Lubrication Problems," by D. G. Christopherson, Proceedings of The Institution of Mechanical Engineers, vol. 146, 1941, pp. 126–135.

[5] "Relaxation Methods in Theoretical Physics," by R. V. Southwell, Oxford University Press, London, England, 1946.

The equation then reduces to

$$\frac{\partial}{\partial x_1}\left[(1+\beta x_1)^3\frac{\partial q}{\partial x_1}\right]+\frac{\partial}{\partial y_1}\left[(1+\beta x_1)^3\frac{\partial q}{\partial y_1}\right]+6y_1=0\ldots[5]$$

This is the dimensionless form of Reynolds equation applicable to our film shape and slider motion. The lubrication problem is to find a solution of Equation [5], $q = q(x_1, y_1)$, such that $q = 0$ at the boundary of the pad.

The Relaxation Solution

If q_o denotes the value of q at a point of a suitably fine network of squares, each of side a, and if q_1, q_2, q_3, q_4 are the values of q at surrounding points of the net, then a finite difference approximation for Equation [5] can be written as

$$q_1+q_2+q_3+q_4-4q_o+6\frac{y_1a^2}{(1+\beta x_1)^3}+\frac{3\beta(q_1-q_3)a}{2(1+\beta x_1)}=0\ldots\ldots[6]$$

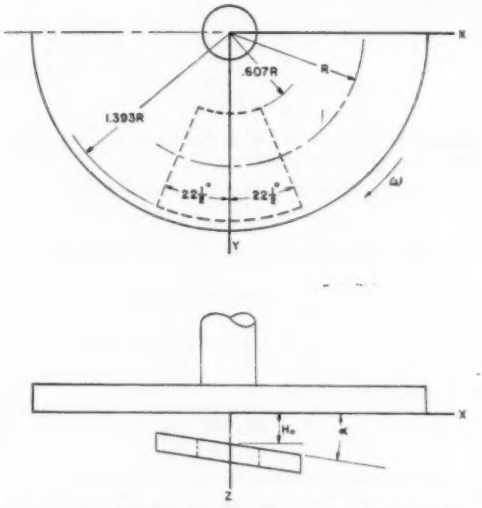

Fig. 1 Sector-Shaped Pad—Location of Co-Ordinate Axes

An equation such as Equation [6] exists for each point of the network. Southwell's relaxation method provides a means of obtaining a numerical solution for this set of many simultaneous equations. It was found that although the correct relaxation pattern for Equation [6] is as shown in Fig. 2, more rapid computation could be performed if, in the relaxing process, the last term were neglected and the relaxation pattern corresponding to the Laplacian operator, Fig. 3, were used. This accumulates a small error which is eliminated by checking the "residuals" periodically by means of Equation [6].

Computations have been completed for a sector-shaped pad for which the sector angle is 45 deg, the ratio of outside radius to inside radius is such as to make the radial dimension of the pad equal to the arc length at the mean radius (a "square" sector), and the film shape is that obtained by rotating the shoe about a radial axis in the plane of the shoe bisecting the sector angle. Various film wedge angles have been considered by taking values of β from 0.25 to 1.5. Contours of the pressure function q for $\beta = 0.75$ are shown in Fig. 4.

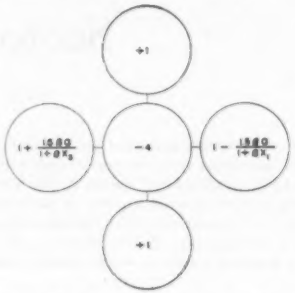

Fig. 2 Exact Relaxation Pattern for Equation [6]

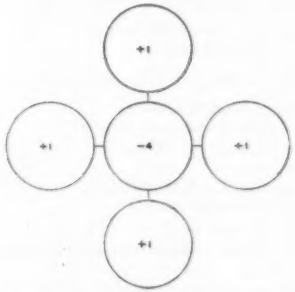

Fig. 3 Relaxation Pattern for Laplacian Operator

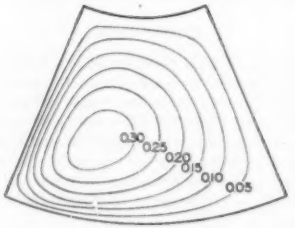

Fig. 4 Contours of Pressure Function q for $\beta = 0.75$

Operating Factors

The total load supported by the pad can be computed from the integral of the pressure function; thus

$$P=\int\int p\,dx\,dy$$

$$=\frac{\mu R^4\omega}{H_o^2}\beta\int\int q\,dx_1\,dy_1$$

$$=\frac{\mu R^4\omega}{H_o^2}C_p\ldots\ldots\ldots\ldots\ldots\ldots[7]$$

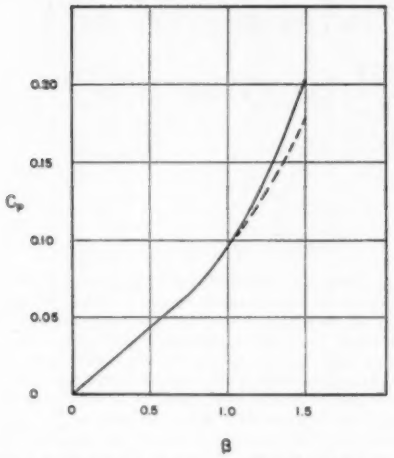

FIG. 5 LOAD COEFFICIENT C_P VERSUS FILM-SHAPE PARAMETER β

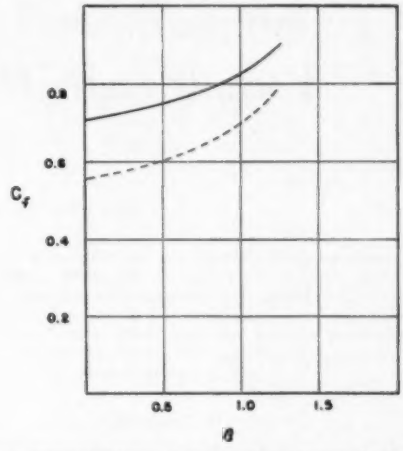

FIG. 6 FRICTION-MOMENT COEFFICIENT C_f VERSUS FILM-SHAPE PARAMETER β

For the shape just described, C_P is plotted against β as the solid line in Fig. 5.

The frictional moment on the rotor is equal to the moment about the z-axis of the shear stresses in the oil at $z = 0$. Hence

$$M = \int\int \mu \left(x \frac{\partial v}{\partial z} - y \frac{\partial u}{\partial z} \right)_{z=0} dx\, dy \quad \ldots\ldots\ldots [8]$$

Calculating the velocity gradients from Equations [2], and substituting in Equation [8]

$$M = \frac{\mu\omega R'}{H_o} \int\int \left[\frac{\beta}{2} (1 + \beta x_1) \left(y_1 \frac{\partial q}{\partial x_1} - x_1 \frac{\partial q}{\partial y_1} \right) - \frac{x_1^2 + y_1^2}{1 + \beta x_1} \right] dx_1\, dy_1$$

$$= \frac{\mu\omega R'}{H_o} C_f$$

From the values of q provided by the relaxation solutions, a numerical evaluation of the foregoing integral can be made. For the specified bearing shape, C_f is a function of β. This relation is plotted as the solid-line curve in Fig. 6.

COMPARISON WITH RESULTS FOR RECTANGULAR SLIDERS

Solutions of Reynolds equation for finite rectangular sliders are well known.[6] These results have been used to predict the performance of sector-shaped bearings. Norton[7] gives the results of these solutions in a form that easily can be converted to the notation of the present paper. C_P and C_f as computed from Norton's curves are plotted as the dash lines in Figs. 5 and 6. It is seen that the discrepancy in the load coefficient, C_P is not great except at the larger film-wedge angles. In computing C_f from Norton's data, it was assumed that the resultant friction force acts at the mean radius of the pad. This accounts for a large part of the discrepancy in the C_f curves, since the actual location of the resultant is at a considerably greater radial distance.

[6] "The Lubrication of Plane Sliders of Finite Width," by M. Muskat, F. Morgan, and M. Meres, *Journal of Applied Physics*, vol. 11, 1940, pp. 208–219.

[7] "Lubrication," by A. E. Norton, McGraw-Hill Book Company, Inc., New York, N. Y., 1942, pp. 147–168.

The Nonsteady-State Load-Supporting Capacity of Fluid Wedge-Shaped Films[1]

By ERNEST K. GATCOMBE,[2] ANNAPOLIS, MD.

PART I THEORETICAL ANALYSIS

A study is presented of the thickness and load-supporting capacity of fluid wedge-shaped films entrapped between the peripheral surfaces of rotating circular disks which are vibrated transversely, causing the wedge-shaped film to become alternately thin, then thick at moderately high frequencies. This nonsteady-state loading of the wedge is accomplished by mounting circular disks, Fig. 1, on parallel shafts with centers at *d* and *d'*, then transversely vibrating the beam which supports the complete lower-shaft assembly, consisting of bearings, bearing hangers, etc., see Fig. 4. Part 1 (see Fig. 1) is devoted to a theoretical analysis of the thickness and load-supporting capacity of these fluid wedge-shaped films under steady-state conditions, i.e., for the case where the disks are revolving at constant angular velocities and the lower disk and assembly are not vibrated. Part 2 presents the results of an experimental investigation of these thicknesses and loads under nonsteady-state conditions, i.e., when the disks are simultaneously rotated and the lower one, with its assembly, is vibrated.

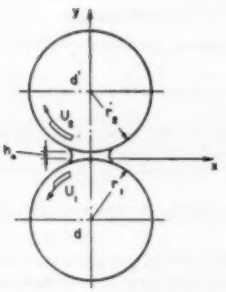

FIG. 1 DISKS POSSESSING ROTARY BUT NO APPROACH MOTION WITH ENTRAPPED FLUID WEDGE

Careful instrumentation of this very complex nonsteady-state problem has yielded solutions which have not been obtainable by theoretical studies, except for cases involving assumptions which greatly alter the true results. It is found that the normal approach vibratory motion of the surfaces bounding the film is responsible for a much greater part of its load-supporting action than is the steady-state rotational motion.

STATEMENT OF PROBLEM

THE main problem is the investigation of the thickness and the corresponding load-supporting capacity of fluid wedge-shaped films entrapped between the peripheral surfaces of circular rotating disks on parallel shafts, which have their center-to-center distance constantly changing, so as to cause the film to become alternately thin, then thick at moderately high frequencies.

METHOD OF ATTACK

An exact analytical solution to the steady-state problem is secured (see Part 1). The author had previously obtained an approximate solution.

The nonsteady-state problem was solved by experimental means; it is much too complicated to solve by analytical methods if one retains such factors as the deformation of the surfaces of the disks, surface roughness, etc. These factors occur in their natural way in the experimental solution.

DESCRIPTION OF THE EXPERIMENTAL SETUP, FIG. 4

Two parallel steel shafts, Fig. 5, were prepared and mounted with adjustable taper roller bearings in hangars, one of which was attached to the upper beam with a strongback with an adjusting screw for controlling the initial gap between disks. The other shaft was mounted in adjustable roller bearings in hangers secured to the lower beam which could be vibrated transversely by means of a Westinghouse fatigue motor. The frequency and amplitude of vibration were controlled by an oscillator and an amplifier. No lost motion was permitted in the bearings. Immediate detection of lost motion was available. Each shaft was driven by a separate air-turbine wheel mounted on the shaft. A d-c-excited coil was placed in the space provided on the lower shaft. A pickup coil was arranged in the hogged-out section of the upper shaft. These coils did not revolve with the shafts. As the lower beam vibrated a signal occurred in the pickup coil, as a result of change in reluctance. This signal was fed directly to a galvanometer-type oscillograph fitted with an automatic camera which gave permanent records of the signal generated. Oscillograms were taken for cases of the disks revolving with no oil on their surfaces; a certain height of wave form on the oscillogram resulted. Then another oscillogram was secured without changing a setting of any kind, but permitting oil to flow onto the surface of the lower disks on the oncoming side. The second oscillogram showed a much reduced amplitude of vibration of the

[1] From a portion of a research project on the study of the load-supporting action of fluid films sponsored by the Bureau of Ordnance, Washington, D. C. (Permission to publish this paper has been granted by the Bureau of Ordnance.)

[2] Associate Professor of Naval and Marine Engineering, The United States Naval Postgraduate School. Mem. ASME.

Contributed by the Research Committee on Lubrication and the Petroleum and Machine Design Divisions and presented at the Semi-Annual Meeting, Toronto, Ont., Can., June 11–15, 1951, of THE AMERICAN SOCIETY OF MECHANICAL ENGINEERS.

NOTE: Statements and opinions advanced in papers are to be understood as individual expressions of their authors and not those of the Society. Manuscript received at ASME Headquarters, March 27, 1951. Paper No. 51—SA-5.

beam. The thickness of the film and its load could be determined then by methods outlined later. Several sets of such records were taken for different settings of the amplifier.

Lead wires were rolled between the disks a sufficient number of times to insure no "springback" of the thickness of the leads with the lower beam supported by jacks to prevent bending. The thickness of these leads, determined by interferometer methods, gave the neutral gap thickness h_0. Other leads were rolled between the disks and pounded by the vibrator until the height of the scope wave form reached that which it had when the gap contained air. These lead thicknesses gave the amplitude of vibration of the lower-shaft disks for various power inputs to the vibration motor coils and the pickup excitation-coil.

The pickup apparatus showed a nearly linear response, over a limited range only, for these amplitudes of vibration (0.001 approx). The dynamic spring constant of the beam was secured. Thus there resulted a means of obtaining a continuous picture of the thickness of the film and its load-supporting capacity under these nonsteady-state conditions.

The existing experimental setup could not be used to obtain a steady-state solution of the problem, since the pickup apparatus did not respond well to a-c excitation. A relatively large neutral gap setting was chosen, which, according to existing theory, would yield but a relatively small steady-state load-supporting component. Since there is little steady-state load for the particular chosen neutral gap setting, the beam may be considered as vibrating about its neutral position.

Nomenclature

a = pole distance

α = abscissa of the bipolar co-ordinate system, pressure angle

β = ordinate of the bipolar co-ordinate system

ψ = stream function

d = distance from the origin to the center of the disk in the bipolar solution

$G = \dfrac{12\,\mu_a\,U\sqrt{2rh_0}}{h_0^3}$

h^3 = reciprocal of "stretch factor"

h_0 = neutral gap thickness between disks

p = pressure

P = load-supporting capacity of the film per unit face width, pitch point

$r = \dfrac{r_1 r_2}{r_1 + r_2}$

r_1, r_2 = radii of curvature of the disks

$S = \tan^{-1}\dfrac{x}{\sqrt{2\,rh_0}}$

T = torque

U_1, U_2 = peripheral velocities of rotating disks

$U = \dfrac{U_1 + U_2}{2}$

u, v, w = co-ordinate velocity components

x_0 = effective width of band of contact

$\nabla^2 = \dfrac{\partial^2}{\partial x^2} + \dfrac{\partial^2}{\partial y^2} + \dfrac{\partial^2}{\partial z^2}$ = Laplacian operator

μ_a = viscosity at atmospheric pressure and stated temperature

μ = viscosity

ω = angular velocity

ρ = density

$\theta = \dfrac{\partial u}{\partial x} + \dfrac{\partial v}{\partial y} + \dfrac{\partial w}{\partial z}$

$\chi = h\psi$ by definition

Introduction

For some time the author has been aware of the fact that the transient state of affairs, in many hydrodynamical problems, accounts for the relatively large load-supporting capacity of fluid films. Most practical engineering applications, involving fluid films such as the lubrication of various bearings and gear teeth, come under this category. However, these particular nonsteady-state problems are, at present, wholly unsolvable by analytical means, at least in their entirety.

It has been only recently that we at the Naval Postgraduate School have acquired accurate and delicate enough equipment to undertake the solution of such a complex problem. Part 2 of this paper presents the results of an investigation of the load-supporting capacity of two oils, namely, Navy 3100 and 2190T. The results have been limited by the capacity of the equipment, but they show clearly that relatively thin oil-film loads and thicknesses can and have been measured by these methods. Modifications are already under way which will permit the investigation of heavier film loads.

The analytical solution of the steady-state problem is obtained by employing the bipolar co-ordinate system since it provides boundaries of exactly the nature required in this investigation.

Procedure

The following general procedure is used in solving the steady-state problem:

1 Write the equations of viscous-fluid motion in the Cartesian co-ordinate system.

2 Assume that the fluid is incompressible and that constant-viscosity steady-state conditions exist.

3 Accomplish the transformation to the bipolar co-ordinate system.

4 Obtain the expressions which indicate the characteristics of the fluid film.

Equations of Motion for Steady-State Constant-Viscosity Incompressible-Fluid Conditions

Fig. 2 shows an elementary cube of the fluid with its indicated positive stresses. Texts on hydrodynamics present the following

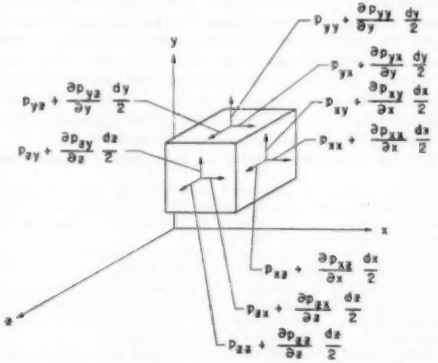
y
x
z
$p_{yy} + \frac{\partial p_{yy}}{\partial y}\frac{dy}{2}$
$p_{yx} + \frac{\partial p_{yx}}{\partial y}\frac{dy}{2}$
$p_{xy} + \frac{\partial p_{xy}}{\partial x}\frac{dx}{2}$
$p_{xx} + \frac{\partial p_{xx}}{\partial x}\frac{dx}{2}$
$p_{yz} + \frac{\partial p_{yz}}{\partial y}\frac{dy}{2}$
$p_{zy} + \frac{\partial p_{zy}}{\partial z}\frac{dz}{2}$
$p_{xz} + \frac{\partial p_{xz}}{\partial x}\frac{dx}{2}$
$p_{zx} + \frac{\partial p_{zx}}{\partial z}\frac{dz}{2}$
$p_{zz} + \frac{\partial p_{zz}}{\partial z}\frac{dz}{2}$

Fig. 2 Elementary Cube of Oil With Indicated Positive Stresses

equations for viscous-fluid motion in which the viscosity μ is considered constant

$$\left.\begin{aligned} \rho \frac{Du}{Dt} &= \rho X - \frac{\partial p}{\partial x} + \frac{1}{3}\frac{\partial \theta}{\partial x} + \mu \nabla^2 u \\ \rho \frac{Dv}{Dt} &= \rho Y - \frac{\partial p}{\partial y} + \frac{1}{3}\frac{\partial \theta}{\partial y} + \mu \nabla^2 v \\ \rho \frac{Dw}{Dt} &= \rho Z - \frac{\partial p}{\partial z} + \frac{1}{3}\frac{\partial \theta}{\partial z} + \mu \nabla^2 w \end{aligned}\right\} \quad \ldots\ldots [1]$$

If the body forces, X, Y, and Z, are neglected, the fluid assumed incompressible, and steady state exists, then Equations [1] reduce to

$$\left.\begin{aligned} \frac{\partial p}{\partial x} &= \mu \nabla^2 u \\ \frac{\partial p}{\partial y} &= \mu \nabla^2 v \\ \frac{\partial p}{\partial z} &= \mu \nabla^2 w \end{aligned}\right\} \quad \ldots\ldots [2]$$

If the Equations of [2] are differentiated with respect to x, y, and z, respectively, and added, then the following equation results

$$\nabla^2 p = 0 \quad \ldots\ldots [3]$$

We are now concerned with two-dimensional flow only, so Equation [3] may be expressed as

$$\nabla^2 p = \left(\frac{\partial^2}{\partial x^2} + \frac{\partial^2}{\partial y^2}\right) p = 0 \quad \ldots\ldots [4]$$

Equation [3] is now transformed into an equation in bipolar co-ordinates. As has been previously mentioned, these co-ordinates permit boundary conditions which are exceedingly suitable to this problem. No approximations, in regard to film thicknesses, need be made.

The equation which is used to transform from Cartesian co-ordinates to bipolar co-ordinates is

$$\alpha + i\beta = \log \frac{x + i\,(y + a)}{x + i\,(y - a)} \quad \ldots\ldots [5]$$

Fig. 3 presents the α, β plane of the bipolar co-ordinate system superimposed upon the x, y-plane of the Cartesian system. The origin for both systems is at 0. The equation of a circle which represents the circular disk of this problem is as follows

$$x^2 + (y - a \coth \alpha)^2 = a^2 \operatorname{csch}^2 \alpha \quad \ldots\ldots [6]$$

The distance d from the origin to the center of the circle is given by

$$d = a \coth \alpha \quad \ldots\ldots [7]$$

where a represents the distance from the origin to the focal point of the bipolar system. The radius (r_1) of the disk is expressed by

$$r_1 = a \operatorname{csch} \alpha \quad \ldots\ldots [8]$$

The following relationships exist

$$x = \frac{a \sin \beta}{\cos \alpha - \cos \beta}; \quad y = \frac{a \sinh \alpha}{\cosh \alpha - \cos \beta} \quad \ldots\ldots [9]$$

From the conditions of an incompressible fluid

$$\frac{\partial u}{\partial x} + \frac{\partial v}{\partial y} = 0 \quad \ldots\ldots [10]$$

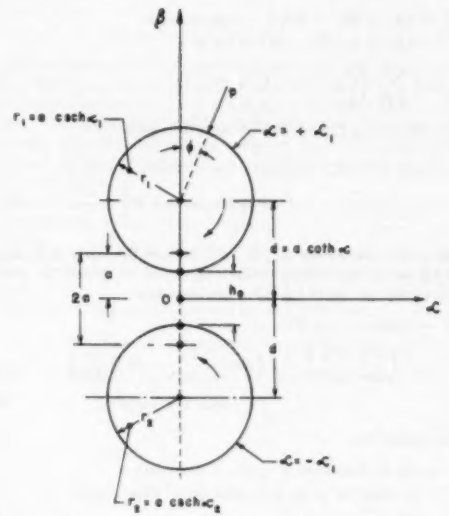

FIG. 3 CIRCULAR DISKS ASSOCIATED WITH THE BIPOLAR CO-ORDINATE SYSTEM

also

$$u = -\frac{\partial \psi}{\partial y}; \quad v = \frac{\partial \psi}{\partial x}; \quad \zeta = \frac{\partial v}{\partial x} - \frac{\partial u}{\partial y} = \nabla^2 \psi \quad \ldots\ldots [11]$$

where ψ is the stream function. In the Cartesian system

$$\zeta = \nabla^2 \psi = \frac{\partial^2 \psi}{\partial x^2} + \frac{\partial^2 \psi}{\partial y^2} \quad \ldots\ldots [12]$$

In the bipolar system Equation [12] becomes

$$\zeta = h^2 \left(\frac{\partial^2 \psi}{\partial \alpha^2} + \frac{\partial^2 \psi}{\partial \beta^2}\right) \quad \ldots\ldots [13]$$

where h^2 is the reciprocal of the "stretch factor." It is expressed symbolically by

$$\frac{1}{h^2} = \left(\frac{\partial x}{\partial \alpha}\right)^2 + \left(\frac{\partial y}{\partial \alpha}\right)^2 \quad \ldots\ldots [14]$$

or

$$h = \frac{\cosh \alpha - \cos \beta}{a} \quad \ldots\ldots [15]$$

The differential equation satisfied by $\nabla^2 \psi$ is

$$\frac{\partial^2 \zeta}{\partial \alpha^2} + \frac{\partial^2 \zeta}{\partial \beta^2} = 0 \quad \ldots\ldots [16]$$

An appropriate solution was obtained by G. B. Jeffery.[3]

[3] "Plane Stress and Plane Strain in Bipolar Co-Ordinates," by G. B. Jeffery, Philosophical Transactions of the Royal Society of London, series A, vol. 221, 1920–1921, p. 265.

$$a\zeta = 2A_0 + 2B_1 + 2D_0(1 - \cosh\alpha\cos\beta) + 2(B_0 + D_1)(\alpha - \sinh\alpha\cos\beta) + 2\sum_{n=1}^{\infty}\left\{\left[(n+1)(A_n + B_{n+1}) - (n-1)(A_{n-1} + B_n)\right]\cosh n\alpha\cos n\beta + [(n+1)(C_n + D_{n+1}) - (n-1)(C_{n-1} + D_n)]\sinh n\alpha\cos n\beta\right\} \quad [17]$$

where the coefficients A_n, B_n, C_n, D_n are arbitrary constants. If $h\psi = \chi$, the corresponding expression for χ may be determined with the aid of the differential equation

$$a\zeta = (\cosh\alpha - \cos\beta)\left(\frac{\partial^3\chi}{\partial\alpha^3} \frac{\partial^3\chi}{\partial\beta^3}\right) - 2\left(\sinh\alpha\frac{\partial\chi}{\partial\alpha} + \sin\beta\frac{\partial\chi}{\partial\beta}\right) + (\cosh\alpha + \cos\beta)\chi \quad [18]$$

It is found that

$$\chi = (A_0 + B_0\alpha)\cosh\alpha + (C_0 + D_0\alpha)\sinh\alpha + (A_1\cosh 2\alpha + B_1 + C_1\sinh 2\alpha + D_1\alpha)\cos\beta + \sum_{n=2}^{\infty}\cos n\beta\left\{A_n\cosh(n+1)\alpha + B_n\cosh(n-1)\alpha + C_n\sinh(n+1)\alpha + D_n\sinh(n-1)\alpha\right\} \quad [19]$$

Since the quantities p and $-\mu\zeta$ are conjugate function, equations of the following type are to be satisfied

$$\frac{\partial p}{\partial\beta} = \mu\frac{\partial\zeta}{\partial\alpha} \quad [20]$$

Thus an expression for p in the α, β system is

$$\frac{ap}{\mu} = C - 2D_0\sinh\alpha\sin\beta + 2(B_0 + D_1)(\beta - \cosh\alpha\sin\beta) + 2\sum_{n=1}^{\infty}\left\{\left[(n+1)(A_n + B_{n+1}) - (n-1)(A_{n-1} + B_n)\right]\sinh n\alpha\sin n\beta + [(n+1)(C_n + D_{n+1}) - (n-1)(C_{n-1} + D_n)]\cosh n\alpha\sin n\beta\right\} \quad [21]$$

Equation [21] represents the general expression for the pressure p. If the problems in which the pressure is single-valued are considered, then all terms possessing α or β alone will not be retained. The coefficient $(B_0 + D_1)$ of β may be set equal to zero.

$$B_0 + D_1 = 0 \quad [22]$$

If u_α, u_β are the velocity components in the positive α and β directions, then

$$u_\alpha = -h\frac{\partial\psi}{\partial\beta} = -\frac{\partial\chi}{\partial\beta} + \frac{\psi}{a}\sin\beta \quad [23]$$

and

$$u_\beta = -\frac{\partial\psi}{\partial\alpha} = \frac{\partial\chi}{\partial\alpha} - \frac{\psi}{a}\sinh\alpha \quad [24]$$

With the angular velocities of the cylinders represented by ω, the following equations represent the boundary conditions

For $\alpha = +\alpha_1$, $\psi = \psi_1$, and $\frac{\partial\chi}{\partial\alpha} = \frac{\psi_1}{a}\sinh\alpha_1 - a\omega\operatorname{cosech}\alpha_1$ [25]

For $\alpha = -\alpha_1$, $\psi = -\psi_1$, and $\frac{\partial\chi}{\partial\alpha} = -\frac{\psi_1}{a}\sinh(-\alpha_1) - a\omega\operatorname{cosech}(-\alpha_1)$ [26]

By symmetry for $\alpha = 0$, $\psi = 0$, and $\frac{\partial\chi^2}{\partial\alpha^2} = 0$ [27]

Thus the expression for χ of Equation [19] may be reduced, in this problem, to

$$\chi = B_0\alpha(\cosh\alpha - \cos\beta) + C_0\sin h\alpha + C_1\sinh 2\alpha\cos\beta. \quad [28]$$

where

$$B_0 = -\frac{a\omega\cosh 2\alpha_1}{2\cosh\alpha_1\sin h^2\alpha_1}$$

$$C_0 = \frac{a\omega\cosh\alpha_1}{2\sinh^2\alpha_1} \quad [29]$$

$$C_1 = -\frac{a\omega}{4\cosh\alpha_1\sinh^2\alpha_1}$$

If this simplified expression for χ, Equation [28], is substituted into Equation [18], the following expression, appropriate to this problem, may be written

$$a\zeta = 4C_1[\sinh\alpha\cos\beta - 2\sinh\alpha\cosh\alpha\cos^2\beta + \sinh\alpha\cosh\alpha] \quad [30]$$

The derivative with respect to α yields

$$a\frac{\partial\zeta}{\partial\alpha} = 4C_1[\cosh\alpha\cos\beta - 2\cos^2\beta\cosh 2\alpha + \cosh 2\alpha]. \quad [31]$$

Integrating partially with respect to β following the statement of Equation [20] gives

$$ap = C + 4\mu C_1\left[\cosh\alpha\sin\beta - \frac{1}{2}\cosh 2\alpha\sin 2\beta\right]. \quad [32]$$

Now a combination of facts, that there is symmetry, that the fluid is assumed incapable of exerting tension stresses, that we are dealing with converging and diverging spaces between the disks, require that the pressure shall pass through zero at the origin where $\beta = \pi$. This yields $C = 0$. Thus the final expression for the pressure p, in the α, β system, is

$$p = \frac{4\mu C_1}{a}(\cosh\alpha\sin\beta - \frac{1}{2}\cosh 2\alpha\sin 2\beta). \quad [33]$$

where

$$C_1 = -\frac{a\omega}{4\cosh\alpha_1\sinh^2\alpha_1} \quad [34]$$

An expression for the maximum pressure (p_{max}), along the x-axis, or $\alpha = 0$, is

$$p_{max} = \frac{3\sqrt{3}\,\mu C_1}{a} \quad [35]$$

An expression is now obtained for the load-carrying capacity

P per unit face width of the fluid wedge. From Fig. 3 an expression for this force is

$$P = \int_0^{\pi} r\, p \cos \Phi \, d\Phi \quad [36]$$

It is necessary to express p of Equation [36] in terms of ϕ remembering that α may be considered constant for any given size disk. Expressions for $\sin \alpha$ and $\sin 2\beta$ are the following

$$\sin \beta = \frac{r \sin \varphi \sinh \alpha_1}{d + r \cos \varphi} \quad [37]$$

$$\sin 2\beta = \frac{r \sin \varphi \,(d \sinh 2\alpha_1 + r \sinh 2\alpha_1 \cos \varphi - 2a \sinh^2 \alpha_1)}{(d + r \cos \varphi)^2} \quad [38]$$

An expression for P is

$$P = \frac{2\mu C_1 \sinh \alpha_1}{a} (K_1 + K_2) \quad [39]$$

where

$$K_1 = 2\left[2r_1 + d \log \frac{d - r_1}{d + r_1}\right][1 - \cosh 2\alpha_1] \cosh \alpha_1 \quad [40]$$

$$K_2 = 2a \sinh \alpha_1 \cosh 2\alpha_1 \left\{\log \frac{d + r_1}{d - r_1} - \frac{2r_1 d}{d^2 - r_1^2}\right\} \quad [41]$$

It is further observed that nearly all the load, carried by the fluid wedge, is distributed over a very small area. Let us arbitrarily define the width of the supporting band of contact x_0 as that distance from the origin, measured along the x-axis, to the point where the pressure drops off to one per cent of its maximum value. An approximate expression for x_0 is

$$x_0 = 6.3\, a \quad [42]$$

From previous work by the author[4] it was found that an approximate solution to this problem gave the following set of equations

For the pressure p

$$p = G\left[\frac{1}{24} \sin 4s + \frac{1}{12} \sin 2s\right] \quad [43]$$

where

$$G = \frac{12 \mu_0 U \sqrt{2r h_0}}{h_0^2} \quad [44]$$

U is the peripheral velocity of the disk

$$r = \frac{r_1 r_2}{r_1 + r_2}, \text{ for equal-size disks } r = \frac{r_1}{2} \quad [45]$$

$$x = \sqrt{2\, r\, h_0} \tan S \quad [46]$$

For the maximum pressure p_{max}

$$p_{max} = \frac{\sqrt{3}}{16} G \quad [47]$$

For the load-carrying capacity P

$$P = \frac{G}{6} \sqrt{2\, r\, h_0} \quad [48]$$

For the width of the band of contact

$$x_0 = \sqrt{2\, r\, h_0} \tan (80° - 58') \quad [49]$$

These equations are now applied in analyzing a given problem. Since the exact solution is obtained for the case of symmetrical flow only, disks of equal size revolving at the same speed ω are used. The disks are 3.0000 inches in diameter. Their angular velocity is (—183) rad per sec. The minimum thickness of the wedge is $h_0 = 0.00002$ inch. The viscosity of the oil $\mu = 5.5 \times 10^{-6}$ lb sec per sq in.

The following will be computed by the exact and approximate methods and the results compared:

1 The maximum pressure within the wedge.

2 The load-carrying capacity P of the wedge per inch of face width.

3 The width x_0 of the supporting band of contact.

Solution of Problem—Exact Method

Equation [35] is the expression for the maximum pressure

$$p_{max} = \frac{3\sqrt{3}\mu C_1}{a} \quad [50]$$

$$\frac{C_1}{a} = -\frac{\omega}{4 \cosh \alpha_1 \sinh^2 \alpha_1} \quad [51]$$

To find α_1 the following is used

$$d_1 = a \coth \alpha_1; \quad \rho = a \operatorname{csch} \alpha_1$$

or

$$\frac{d}{\rho} = \cosh \alpha_1$$

$$d = 1.5000 + 0.00001 = 1.50001 \text{ in.}$$

so

$$\cosh \alpha_1 = 1.000006667$$

$$\alpha_1 = 0.00365 \text{ rad}$$

and

$$a = \rho \sinh \alpha_1 = 1.5000 \times 0.00365$$

$$a = 0.00547$$

Thus

$$p_{max} = 3\sqrt{3} \times 5.5 \times 10^{-6}\left[\frac{183}{4 \times 1.000006667 \times 0.00365^3}\right] \quad [52]$$

$$p_{max} = +27{,}600 \text{ psi} \quad [53]$$

Equation [39] is the expression for the load-carrying capacity P

$$P = \frac{2\mu C_1 \sinh \alpha_1}{a} (K_1 + K_2) \quad [54]$$

$$K_1 = +0.00084$$

$$K_2 = -5.97$$

$$P = -226 \text{ lb per in. of face width} \quad [55]$$

Equation [42] is an expression for the width of the supporting band of contact

$$x = 6.3a = 6.3 \times 0.00547 = 0.0344 \text{ in.} \quad [56]$$

[4] "Lubrication Characteristics of Involute Spur Gears," by E. K. Gatcombe, Trans. ASME, vol. 67, 1945, p. 177.

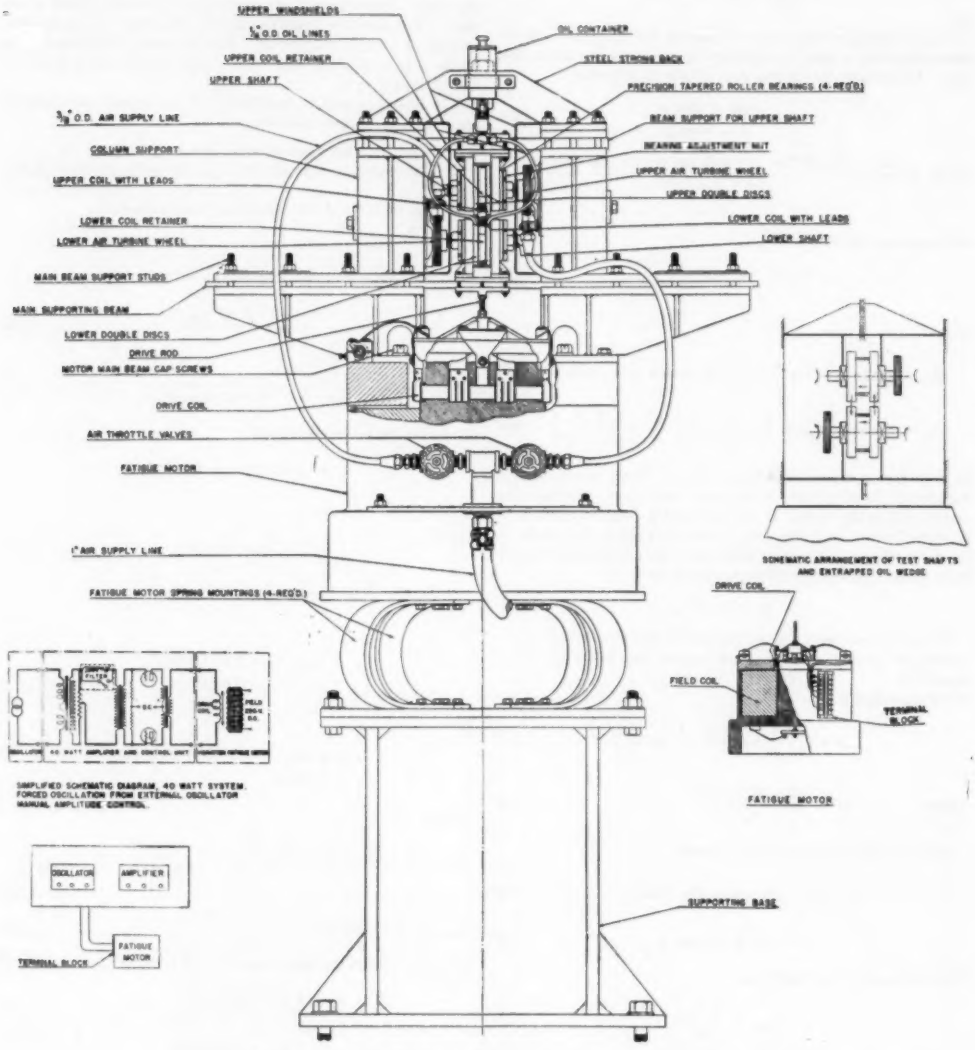

FIG. 4 ASSEMBLY VIEW OF EXPERIMENTAL TEST EQUIPMENT

Solution of Problem—Approximate Method

The maximum pressure p_{max} is given by

$$p_{max} = \frac{\sqrt{3}}{16} G = \frac{\sqrt{3}}{16} \times 247{,}000 = 26{,}700 \text{ psi}$$

The load-carrying capacity P is indicated by

$$P = \frac{G}{6} \sqrt{2 r h_0}$$

$$P = 225 \text{ lb per in. of face width}$$

The width of the band of contact is

$$x_0 = \sqrt{2 r h_0} \times \tan (80°58') = 0.034 \text{ in.}$$

Conclusion Concerning Steady-State Solution

The approximate solution derived earlier gives results which are close to the exact answers. However, at this point the author's results are of little account in the solution of the usual nonsteady-state problem except for a guide in the solution of steady-state problems. To obtain practical results for these problems in hydrodynamics, the solution of these nonsteady-state problems must be calculated through experimental analyses.

PART 2 EXPERIMENTAL ANALYSIS

Introduction

The thickness and the load-supporting capacity of oil films entrapped between the peripheral surfaces of circular rotating disks on parallel shafts were investigated by experimental methods, Fig. 4. The fluid wedge-shaped film was formed by dragging the oil between the disks which were rotated in opposite directions. The wedge was made alternately thick and thin by vibrating the main support beam with the attached lower shaft. The d-c excitation coil placed in the hogged-out section of the shaft set up magnetic lines of flux which had to pass through the neutral air gap which separated the surfaces of the two sets of double disks. The pickup coil placed in the corresponding hogged-out space in the upper shaft delivered a signal to the galvanometer oscillograph as the lower shaft was vibrated. This signal was calibrated to give the thickness and load on the films. An automatic camera was used to photograph the oscillograms. Oscillograms were taken with and without fluid wedges between the disks. The presence of oil caused the beam supporting the lower shaft to vibrate through relatively small amplitudes. Small lead wires of the order of 0.020 in. were rolled between the two sets of disks with the lower beam supported by jacks to prevent bending. The thickness of the neutral gap h_0 was measured by obtaining the thickness of the flattened lead wire. The neutral gap thickness h_0 was adjusted until the amplitude of the vibrating beam, for a power setting of the amplifier of 60, equaled the value of the gap h_0.

The constant d-c excitation current for the pickup system came from two storage batteries. The d-c and a-c and voltages to the fatigue motor were fixed for various amplifier settings. Then the values of the height of the wave form on the scope were found for various settings of the amplifier with the angular velocities of the disks at zero. These values are plotted in Fig. 6. Lead wires were then rolled between the disks, left in position with $\omega = 0$, and the vibrator pounded them until the height of the scope wave form equaled that which existed for the case of air between the disks. Leads were taken and their thickness measured for all six power settings of the amplifier, except No. 50 where the leads became too thin to handle.

Experimental Results

It is clear now that at this point information is at hand for determining the magnification factor (M.F.) of the setup. The magnification factor (M.F.) is defined as the ratio of the amplitude of the wave form on the scope to the amplitude of vibration of the main support beam. For example, we find from Fig. 6 that for an amplifier setting of 60 (without oil and $\omega = 0$) the lower disk vibrated through an amplitude of $h_0 = 0.00197$ in., while the height of the scope wave form was 1.80 in. This gives a M.F. = 914. Likewise, when the amplifier was set at 30 the leads showed that the lower shaft vibrated through $a_d = 0.00099$ in., while the scope gave $a_s = 1.44$ in. The M.F. for this setting was 1450.

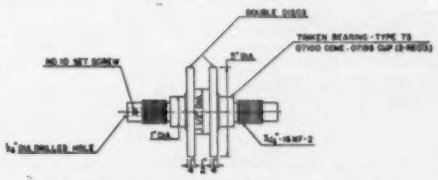

Fig. 5 Details of Circular Shafts and Disks

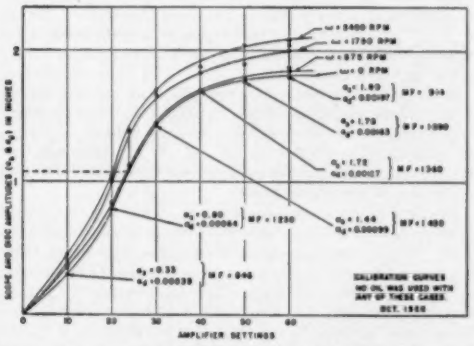

Fig. 6 Scope and Disk Amplitudes Versus Amplifier Settings

It was noticed that the a_s depended not only upon the amplitude of vibration of the disk a_d, but also upon the speed with which the disks rotated. It thus became necessary to plot the scope amplitude against the amplifier or power settings for various values of the angular velocity ω. These values are shown in Fig. 6. The magnification factor M.F. will be determined always with reference to the graph of $\omega = 0$. The increase in the amplitude of the scope wave due to the rotation of the disks is nearly nullified for the cases with and without oil, since the angular velocity was fixed.

Fig. 6 is used in the following way to determine the load carried by a certain thickness oil film wedge: From Table 1 it is found that the height of the scope wave form, corresponding to $\omega = 2400$ rpm without oil with the amplifier at 60, is 2.08 in., the amplitude of the scope wave form, corresponding to $\omega = 2400$ rpm with N3100 oil with the amplifier at 60, is 1.35 in. It is noted that 0.28 in. of the scope amplitude is due to rotational effects of the disks. Now the amplitude of vibration of the lower disk, without oil, with the amplifier at 60 and $f = 425$ cps is just sufficient to close the neutral gap setting of $h_0 = 0.00197$ in.

TABLE 1 EXPERIMENTAL DATA

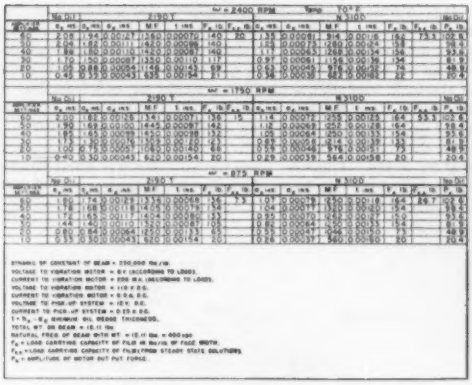

TABLE 2

Amplifier settings	Amplitude gage, in.	Amplitude gage B, in.	P_0 lb
60	1.99	2.00	102.6
50	1.90	1.91	98.4
40	1.80	1.81	93.6
30	1.58	1.59	81.9
20	0.95	0.95	48.9
10	0.35	0.40	20.4

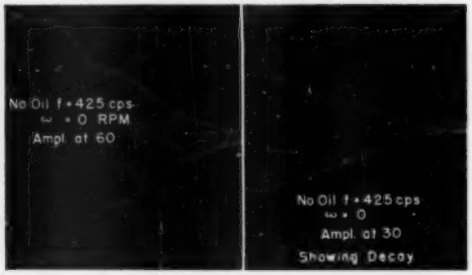

FIG. 8 WAVE FORMS INDICATING DIE-AWAY CHARACTERISTICS OF VIBRATION UNIT

Thus, for the case of no oil, with $\omega = 2400$ rpm, with $f = 425$ cps, the M.F. is found to be 1.80/0.00197 or 914. The M.F. is defined as the ratio of a_s/a_d. This value is calculated with reference to the curve $\omega = 0$. For the case of the use of N3100 oil with $\omega = 2400$ rpm, with $f = 425$ cps it is found from Table 1 that the $a_s = 1.35$ in. It is recalled that 0.28 in. of this amplitude is due to rotational effects; thus the value corrected to the $\omega = 0$ curve is 1.07 in. This gives a M.F. = 1326. This scope amplitude of 1.07 in. on the $\omega = 0$ curve corresponds to an amplifier setting of 24, and thus a disk amplitude of 0.00081 in. The amplitude of vibration of the beam was thus reduced from $h_0 = 0.00197$ in. without oil to 0.00081 in. with oil. It is known now that the minimum oil-film wedge thickness was 0.00116 in. The load on the film will be computed now.

From the mechanics of the problem the beam may be regarded as massless with an equivalent weight placed at the center of the span. There is also the weight of the lower shaft, bearings, hangers, motor drive coil, etc., which may be considered concentrated at the midsection of the beam. This total weight = 12.11 lb. Four forces act on the beam in the displaced position, namely, the beam restoring force F_k, the force of internal damping F_d, the force of the oil-film wedge F_0, and the force of the vibration motor F_m. The amplitude and the phase relationship of these forces are shown in Fig. 9. The sum of the vertical components may be written as

$$m\omega^2 y_0 + P_0 \cos \varphi - F_0 - k y_0 = 0 \quad \ldots\ldots [57]$$

The value of P_0, the amplitude of the motor output force, was found for different amplifier settings, by placing SR4 strain gages on a specially prepared drive rod. These values are given in Table 2. It was found that the amplitude of the motor output force P_0 depended upon the amplifier setting for a given frequency. Thus the motor output force was evaluated without the use of oil between the disks.

The phase angle φ is shown to be

$$\tan \varphi = \frac{2\dfrac{b}{b_{cr}} \times \dfrac{\omega}{\omega_n}}{1 - (\omega^2/\omega_n^2)} \quad \ldots\ldots [58]$$

where b is the damping constant of the system and is evaluated from the die-away wave form shown in the preceding paragraph. It was found that $b = 0.95$ lb sec per in. The value of the

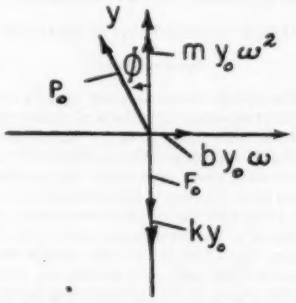

FIG. 9 FORCE COMPONENT DIAGRAM

critical damping constant $b_{cr} = \sqrt{4mk}$ was found to be $b_{cr} = 177$ lb sec per in. The weight on the beam was 12.11 lb and the dynamic spring constant was 250,000 lb per in. The undamped natural frequency of the system was $\omega_n = 2830$ rad per sec. It was found that $\varphi = 5° - 10'$.

The amplitude of load F_0 carried by the oil-film wedge may be found now from Equation 57. The disk or beam amplitude of vibrations a_d or y_0 was found to be 0.00081 in. The mass m on the beam was 0.0314 $\frac{\text{lb sec}^2}{\text{in.}}$. The frequency of vibration of the beam was 425 cps or 2670 rad per sec. The value of P_0 was 102.61 lb. Thus the oil wedge, the minimum thickness of which was 0.00116 in., carried a load of

$$F_0 = -250{,}000 \times 0.00081 + 102.6 \times 0.996 + 0.0314 \times \overline{2670}^2 \times 0.00081 \quad \ldots\ldots [59]$$

or

$$F_0 = 81 \text{ lb per half-inch face width} \quad \ldots\ldots [60]$$

$$F_0 = 162.0 \text{ lb per inch of face width} \quad \ldots\ldots [61]$$

If one used the results of Part 1 (Equation [56]) to predict the

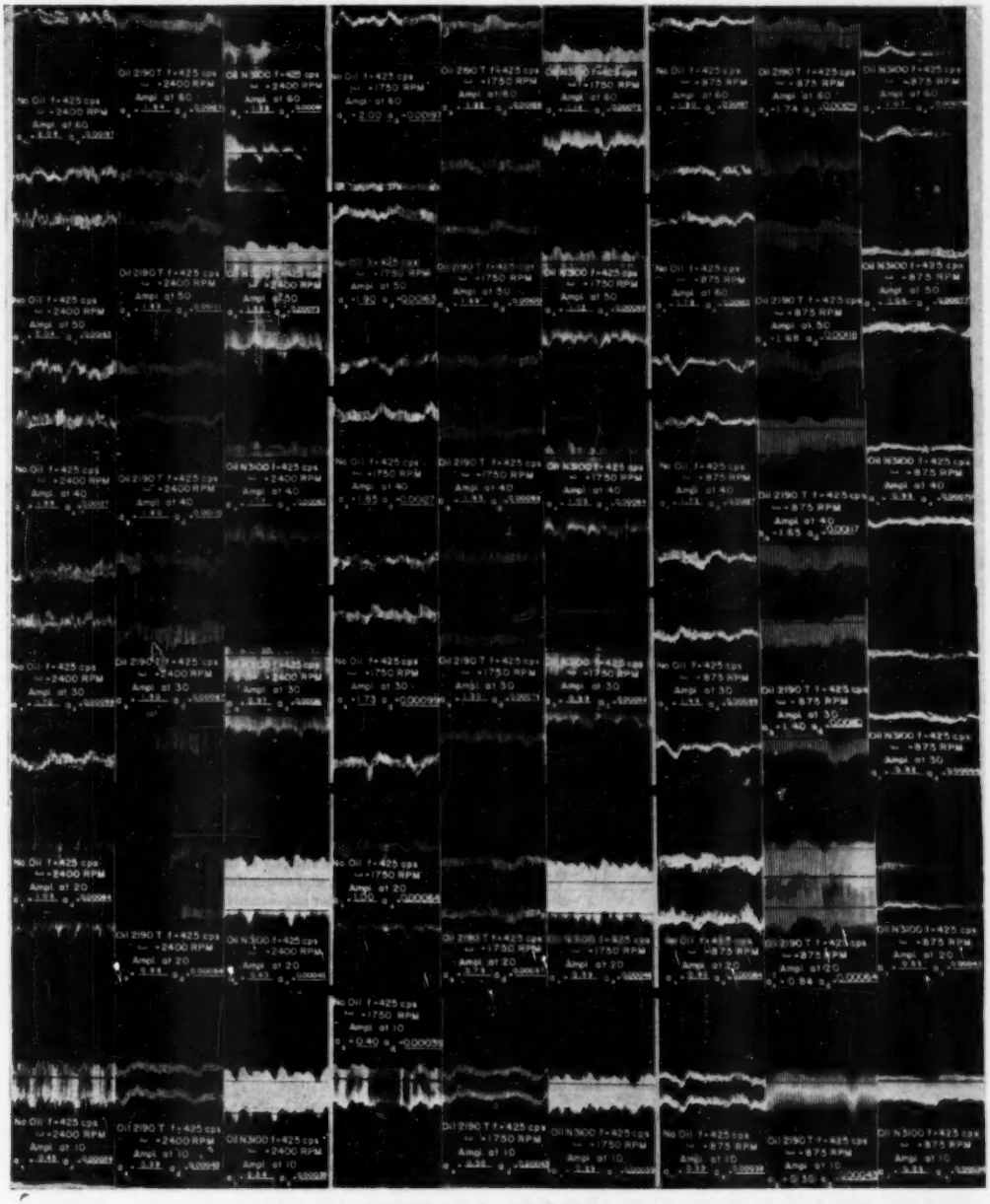

FIG. 7 PICTURES OF SCOPE WAVE FORMS

width of the supporting band of contact x_b, then the average pressure within the film will be

$$P_{av} = \frac{F_0}{A} = \frac{81.0}{0.5 \times 0.0344} = 4710 \text{ psi} \quad [62]$$

One may count on the maximum pressure being approximately seven times the average. This would give a maximum pressure of

$$p_{max} = 33{,}000 \text{ psi} \quad [63]$$

It will be of considerable interest now to compute the load which this same minimum-thickness oil-film wedge will support on the basis of steady-state conditions. Equation [39] or Equation [48] may be used to obtain this result. In Equation [48]

$$G = \frac{12\, u_a\, U \sqrt{2\, r\, h_0}}{h_0^3} \quad [64]$$

$\mu_a = 1.29 \times 10^{-4}$ reyns (N3100, 70 F)
$U = 378$ in. per sec (2400 rpm, 3-in-diam disk)
$h_0 = 0.00197$
$G = 8130$ psi

Thus

$$P = \frac{G}{6} \sqrt{2\, r\, h_0}$$

$$= \frac{8130}{6} \times 0.054 = 73.3 \text{ lb per in. of face width or}$$

$P = 36.6$ lb per half inch of face width.

This is the load which the oil wedge could be expected to carry on the basis of steady-state conditions. It is observed that the nonsteady-state solution indicates that this same wedge can carry 81 lb. The nonsteady-state solution then shows that the wedge can carry 2.22 times as much load as the steady-state solution indicates. From Fig. 10 it will be observed further that

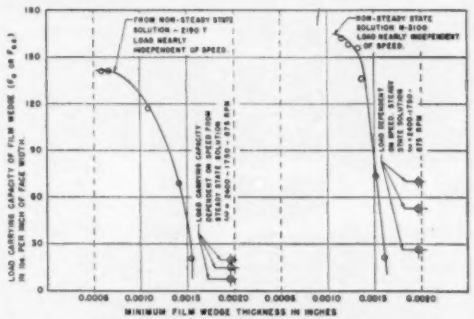

FIG. 10 LOAD-CARRYING CAPACITY OF FILM WEDGE VERSUS MINIMUM FILM WEDGE THICKNESS

the ratio of the largest value of F_0 to the smallest value of F_{ss} is $\frac{62}{27} = 6$. This means that the load-supporting action of the film, resulting from the approach motion of the metal bounding surfaces, can be six times as large as that resulting from the rotational effects of the disks. In other words, the nonsteady-state solution gives values which are six times as large as those of the steady state. This is a factor which we may no longer omit in predictions of the load-carrying capacity of films. It is no wonder that we have not been able to account for the large loads which bearings and gears actually carry. The theory is based on steady-state conditions.

The preceding point is the prominent part of this whole research project. The oil-film wedge in bearings and gears supports loads because they operate under nonsteady-state conditions.

INFORMATION ON USE OF STRAIN GAGES

The amplitude of the motor output force was determined through the use of strain gages. Two A-7 strain gages were used on the flat section of the drive rod. A third temperature-compensating gage was employed. The strain indication was received on a cathode-ray oscillograph, through the employment of a Baldwin Southwark strain calibration and amplifier instrument. Two gages were used so that bending of the drive rod could be detected. It was determined that a strain of 120 micro-inches per inch corresponded to an amplitude ordinate height of 0.7 in. on the cathode-ray oscillograph with the gain as used. The cross-sectional area of the steel drive rod was A = 0.0100 sq in.

INFORMATION ON OILS USED

N3100—Navy symbol: Specific gravity at 60/60 F = 0.903; API deg 25.2; viscosity, SUV, at 100 F, 1318 sec; viscosity, SUV at 130 F, 492 sec; viscosity, SUV at 210 F, 90.9 sec; viscosity index (Dean and Davis), 72 9.

2190T—Turbine oil: Specific gravity at 60/60 F, 0.8844; API deg 28.5; viscosity, SUV, at 100 F, 420 sec; viscosity SUV at 130 F, 193 sec; viscosity, SUV at 210 F, 50 sec. (Engineering Experiment Station Test No. 1 BDT031.)

ADDITIONAL REMARKS

During the operation of the test equipment, it was found that an optional method of measuring the value of h_0 gave a good check on those values already found through the use of leads. All these test results are reproducible.

In the test program to date the value selected for the neutral gap setting ($h_0 = 0.00197$ in.) was relatively large so that the beam would, in effect, vibrate about its static neutral equilibrium position, rather than about some displaced position. In future work, if small values of h_0 are used, it will be necessary to correct the film thickness to account for this fact. The material in the steel disks was SAE 1045 steel hardened to 45 RC. The surface roughness was 20 millionths of an inch.

The irregular frequency components of vibration present in the various wave forms shown in the photograph result from various causes such as nonconcentricity of the disks, nonuniformity of the rollers in the bearings, and nonuniform speed of the disks. These components do not alter appreciably the results of the test.

CONCLUSIONS

A prominent characteristic of the load-supporting capacity of fluid films has been uncovered in this research. It is definitely shown that thin fluid films strongly resist being squeezed out from between meta surfaces, especially if the bounding surfaces are approaching each other at high velocities. In other words, the nonsteady-state character of the motion of the bounding surfaces of fluid films is responsible for their ability to support relatively great loads.

The steady-state theory never has been able to account satisfactorily for the relatively large loads which bearings and gears carry every day. This theory indicates unreasonably thin film thicknesses for these members when used with heavy loads at low speeds; many times these thicknesses are much smaller than the surface roughness of the metal bounding surfaces. Neither can the theory account for the loads which are carried successfully in high-speed gearing such as in certain turbine gear units. In such

cases the period of mating is very short, and the whole lubrication phenomenon is nonsteady state, without question. It is highly probable that the prominent point uncovered in this work partly explains why such gears actually work.

Two external-type cylindrical disks, which formed the metal bounding surfaces of the fluid film under investigation, were chosen in this work in preference to actual bearings, because of their basic character is relation to gears as well as to bearings. The results of this work may be used in studies of gears as well as in internal and external bearings. For one of the cases examined in this work, the nonsteady-state figures collected from actual experimental tests indicated that the film under investigation carried a load *six* times as large as the steady-state solution would have indicated.

No attempt will be made at present to formulate a nonsteady-state theory to explain this nonsteady-state phenomenon. But it will not be difficult to do this once more test data are available to draw from in forming semiempirical theories. This work should be considered a simple beginning in the investigation of a most complex problem.

It has been the opinion of this author for some time that theory alone is an insufficient tool for completely explaining some of these complex lubrication phenomena. Thus, at the Naval Postgraduate School, the last three years have been spent in acquiring and testing accurate instruments for carrying out this mission. It cannot be overemphasized that actual operating conditions have been simulated and that actual steel disks with real lubricants were used. These disks are deformable: they have surface roughness; they have certain adhesive and cohesive properties. The lubricants act in their natural fashion. Above all we have worked with nonsteady-state conditions.

This problem should be pursued vigorously along these combined experimental and theoretical lines until enough data are gathered so that the proper semiempirical theories may be formulated to give important guidance to designers in the fields of bearings and gears as well as in other related fields.

Acknowledgment

The author is indebted to Lieutenant Commander A. Ahrens and to several colleagues in the mathematics, physics, and mechanical-engineering departments for their assistance. The machine shops of the U. S. Naval Postgraduate School, the Engineering Experiment Station, and the Naval Gun Factory cooperated fully.

Aircraft Turbosupercharger Bearings—Their History, Design, and Application Technique

By S. R. PUFFER,[1] WEST LYNN, MASS.

Introduction

IN 1917, during the latter part of World War I, the author's company was called upon to undertake the development of an aircraft-engine booster, or turbosupercharger, along the general lines of a similar device previously built by Professor Rateau in France. At this late date it is necessary to describe this booster only as being a small, light, high-speed centrifugal compressor driven by a turbine wheel from the exhaust gases of the piston engine. Its purpose is to maintain engine power at altitude by compressing the atmospheric air before it enters the cylinders.

The problems associated with this development, arising from operation at high speeds, high temperatures, and high altitudes, were legion, and many years of intensive effort were spent in obtaining satisfactory solutions. This paper deals primarily with the first of these, high speeds, and is restricted mainly to bearing problems, but of necessity will have to consider to some extent the contingent effect of both high temperatures and high altitudes.

The development of bearings and lubrication methods to solve these problems has benefited not only aviation, but industry in general.

From the small bearings operating at very high speeds, it has not been too great a step to the larger gas-turbine bearings operating at speeds of 8000 to 13,000 rpm. The same general principles apply.

This development has also been of service to the ball-bearing manufacturers, as from it they have learned much about the characteristics and operation of their own bearings. The quality of these bearings has been greatly improved, so that now industry can specify a high-speed bearing application with reasonable assurance that it will function successfully from the first.

In the past it was necessary to determine these bearing characteristics by running them for thousands of hours in very expensive and delicate equipment—the supercharger itself. Only a government agency, such as the Air Force, with its vast resources, could have financed a development of this nature. The tests were extremely costly to run, and a bearing failure invariably resulted not only in the loss of the bearing itself, but also the loss of an expensive supercharger, with frequent major damage to the test cell and equipment.

Prior to 1917 the principal and practically the only builder of small high-speed turbines was the De Laval Company in Sweden. Nikola Tesla had also built a few high-speed rotors—largely experimental. With the exception of this limited experience, and the relatively few hours of operation of the Rateau turbobooster, practically no information on high-speed bearings and their lubrication was available. To appreciate the magnitude of the problem, it is well to consider the requirements, not in the light of present knowledge, but on the basis of information available in 1917, thirty-three years ago.

The De Laval turbine operated at a constant speed somewhat higher than 20,000 rpm and at relatively normal steam and ambient temperatures. It was mounted on a solid base, where careful alignment could be obtained and maintained. Weight, or rather the elimination of it, was not a factor. Great as was the engineering accomplishment of De Laval, the problems he faced were simple compared to those involved in this new device, some of which are enumerated as follows:

1 Rated operating speed, 20,000 rpm—about the same as the De Laval turbine.

2 Unit had to be capable of operating at variable speed, from zero to maximum, with the possibility of prolonged operation within one or more critical-speed zones.

3 Operation might be with the shaft in any position—vertical, horizontal, or anywhere between. Bearings had to lubricate and drain during flight in any position.

4 One bearing, at the compressor inlet, was subjected to air ambient temperatures of —40 F (in later years temperatures as low as —90 F have been encountered), the other bearing to operate while surrounded by a hot gas collector or nozzle box, the temperatures of which were as high as 1400 F to 1500 F (now nozzle-box gas temperatures run as high as 1800 F).

5 In addition to the high temperature surrounding the bearing, it would have to operate immediately adjacent to the hot turbine wheel which was exposed to the engine exhaust gases.

6 Besides the normal operating loads on the bearings, additional loads of a gyroscopic nature would be imposed by maneuvers of the airplane.

7 Instead of having a firm base on which to mount the bearings and maintain them in alignment, the mounting in this case had to be light, rather flexible, and subject to vibrations from both plane and engine.

8 The extreme range of temperature mentioned would be encountered within the very short span of approximately 10 in., the distance between bearings.

Faced by these problems, it is small wonder that there were many doubts about the practicability of this device. Seldom, if ever, has there been a development where previous experience availed so little.

Early Designs—Sleeve Bearings

Fig. 1 is a diagram of the early turbosuperchargers built by the author's company—about 1919. In accordance with established practice, both elements of the rotor, the impeller, and turbine wheel, were mounted on the shaft between two bearings, one on either end. The bearings themselves consisted of tin-base babbitt-metal linings poured into aluminum bearing supports. Diameters of the bearings were made as small as possible consistent with the calculated loads in order to keep rubbing speeds low. Lubrication was supplied from the engine oiling system at a pressure of approximately 40 psi. Oil used at that time was equivalent to SAE 50 in the summer and SAE 30 to 40 in the winter.

Certain fundamentals were learned during the first few hours of operation which are just as true today as they were thirty years ago:

[1] Aircraft Gas Turbine Engineering Division, General Electric Company.

Contributed by the Machine Design and Aviation Divisions and presented at the Semi-Annual Meeting, Toronto, Ontario, Can., June 11–15, 1951, of The American Society of Mechanical Engineers.

Note: Statements and opinions advanced in papers are to be understood as individual expressions of their authors and not those of the Society. Manuscript received at ASME Headquarters, August 11, 1950. Paper No. 51—SA-12.

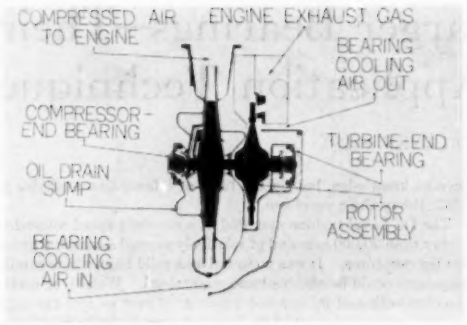

FIG. 1 EARLY TURBOSUPERCHARGER WITH SLEEVE BEARINGS

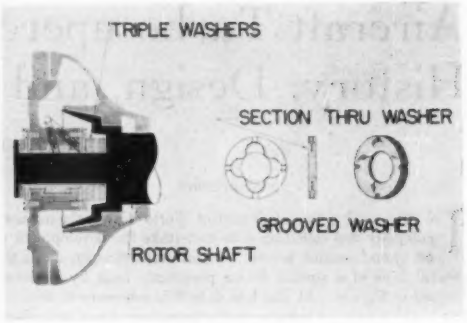

FIG. 2 TRIPLE-WASHER THRUST BEARING

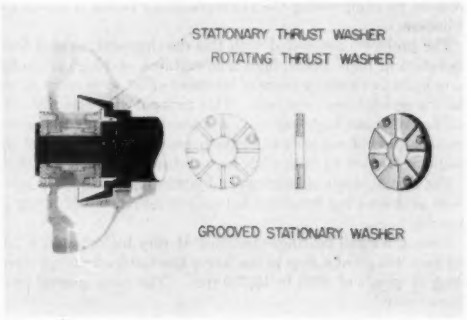

FIG. 3 TAPERED-LAND THRUST BEARING

1 Bearings must be in alignment.

2 Enough clearance must be allowed between bearing and journal to permit free circulation of the oil.

3 Oil grooves should have generous radii or be brought in tangent with the bearing surface in the direction of rotation, so that oil-film pressure may be built up. It was also desirable to vent the oil grooves axially through each end of the bearing lining so that any sediment could be washed out. Failure to do this frequently resulted in filling of the oil grooves and shutting off or restricting the flow of oil.

4 Rotor must be in both static and dynamic balance within very close limits. Particular attention must be given to balance, if operation within critical-speed zones is a requirement.

5 Lubricating oil must be clean. This is rather easy of attainment in these days of improved filters, but it was a major problem 30 years ago.

6 Oil drains dependent on gravity flow to clear the bearing housing must be many times larger than the feed line, especially for high-altitude operation. Oil which can be supplied easily at moderate pressures through a $^1/_{16}$-in. nozzle requires at least the equivalent of $^1/_2$-in. opening out of the bearing, and, if bends or any appreciable length of run are introduced, the oil-return pipe should be even larger. This is to take care of the increased volume caused by the natural tendency of the oil to foam, which is greatly aggravated at high altitudes.

7 A high-speed bearing acts as a centrifuge, so that any sediment or sludge is thrown to the outer periphery and lodges in depressions in the bearing surface. Grooves in both sleeve and thrust bearings must avoid dead-end pockets and allow for a free flow of oil, even at the expense of using a larger quantity.

8 Thrust-bearing surfaces must be flat and at right angles to the axis within very close limits. Failure to observe either of these precautions results in a concentrated loading at the high spot, which will cause failure of the bearing within a matter of minutes or even seconds.

In this early design it will be observed that an oil-drain sump completely surrounded the compressor-end bearing, so that oil could drain to it from any position. Although the idea was good it did not prove to be practical, because the low temperatures prevailing at the higher altitudes promptly congealed the oil in this chamber, so that it would not drain at all. It was further learned at this time that it was not necessary to provide drainage from the bearings in any position. For most of the normal plane maneuvers, centrifugal force takes the place of gravity. Conditions for which this does not apply are usually of only a few seconds' duration.

The first attempt at keeping the turbine end bearing cool was by means of a water jacket using water from the engine cooling system. This was only partially satisfactory as it did not prevent heat from reaching this bearing by conduction through the turbine wheel and along the shaft. To reduce the amount of this conduction as much as possible, air from the propeller slip stream was scooped into a duct at the outer diameter of the supercharger casing, conducted around the bearing, and discharged against the turbine wheel. By this means the bearing was cooled and some cooling of the turbine wheel was achieved.

In this early design, calculated thrust was about 60 lb, not much in the light of present experience, but of appreciable magnitude when the size and speed of the bearings were considered. This thrust was absorbed by a triple-washer combination at the compressor end, as shown in Fig. 2. Originally a grooved phosphor-bronze thrust washer between hardened-steel washers did not prove adequate for the service, so that three hardened-steel washers were finally used. These gave satisfactory service after some familiarity was acquired with the operating characteristics of high-speed bearings in general, and with this combination in particular.

The three-washer thrust arrangement, while effective under favorable conditions, was not too practical from a manufacturing and servicing standpoint. The washers were delicate, had to be accurately made, and as they were made from hardened steel, they had a tendency to crack, often with disastrous results. A better design was essential, and this was obtained through a gradual process of development which resulted in the bearing

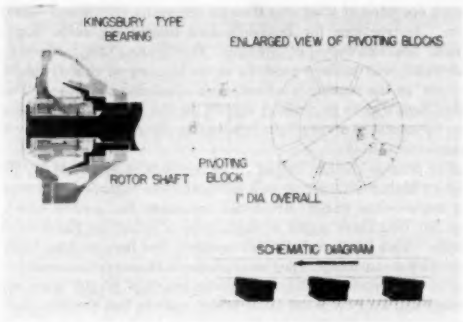

FIG. 4 KINGSBURY-TYPE THRUST BEARING

FIG. 5 LEPERE BIPLANE WITH TURBOSUPERCHARGER

shown in Fig. 3. Here the thrust was taken between one stationary and one moving thrust surface, both made from hardened steel. This construction was simpler, more economical to manufacture, and much more rugged. It was used with a high degree of success in several hundred of the earlier turbosuperchargers.

In the early 1920's a contract was placed by the Air Corps covering the development of a supercharger to maintain engine power at an altitude of 35,000 ft as contrasted with 20,000 ft for the initial developments. This was to operate at the even more fantastic speed of 30,000 rpm, and the thrust load was increased to approximately 150 lb. As the journal bearings were still kept small, rubbing speeds were not even now considered excessive. Thrust, however, was another matter. The load was increased, the speed was increased, but the bearing surface over which it might be distributed was still very small.

To meet this problem, a small Michell or Kingsbury-type thrust bearing was used. This bearing, shown in Fig. 4, was built with a number of individual tilting blocks—in the best approved manner—and was probably the smallest bearing of this type ever built. The outside diameter of the thrust faces was 1 in. A real jeweler's job to produce, this type required even finer workmanship than previous thrust bearings. During factory tests, where extra precautions could be taken to insure clean oil, this bearing operated perfectly, carrying a thrust higher than the design value at full rated speed. However, when tested in service with oil provided from the engine lubrication system, the essential cleanliness

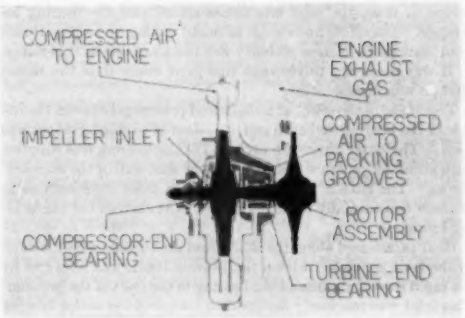

FIG. 6 TURBO WITH SLEEVE BEARINGS AND OVERHUNG TURBINE

could not be obtained, with the state of the art as then developed, and results were not encouraging.

The first few hundred superchargers were built to this same general arrangement. The unit was installed on the front of the engine, directly behind the propeller, as shown in Fig. 5. It soon became apparent that this was not the best possible location. The supercharger occupied the space normally taken by the engine radiator, which meant that the radiator had to be mounted on the top of the upper wing or suspended below the fuselage, thereby greatly increasing the drag of the plane. Also, long lengths of water and oil piping were required, which were liable to fatigue and cracking, depriving the engine of either coolant, oil, or both. As flight experience was gained, it became evident that even better cooling of the turbine wheel was essential. All of these problems could be solved by mounting the supercharger on the side of the plane with the turbine wheel flush with the fuselage, but this move introduced new problems in the design of the supercharger. For example, the turbine wheel, weighing about 15 lb, would have to be overhung from its bearing, and this would require a larger bearing, with attendant higher rubbing speeds.

Up to this time a certain amount of oil leakage had been tolerated as being incidental to the development. As the art progressed this leakage was looked upon with increasing disfavor, and with these new modifications the additional stipulation was made that oil leakage must be eliminated. The resulting design is shown in Fig. 6. In keeping with past practice the larger overhung bearing also consisted of a babbitt lining poured into the aluminum casing.

It will be observed that the problem of sealing against oil leakage at this bearing was quite difficult, for the following reasons:

1 The bearing was split along the horizontal center line. To maintain the desired running clearance, no gasket of any kind could be used in this joint.

2 The eye or inlet to the impeller, closely adjacent to one end of this bearing, created an area of reduced pressure right at the point where oil would be likely to leak out.

3 The centrifugal effect of the turbine wheel, closely adjacent to the other end of the bearing, created another but unequal low-pressure area at this point.

4 The journal diameter was larger than that of the journals used previously, so that the heat conducted from the turbine wheel to the bearing was greater than before.

By careful attention to the following details these difficulties were largely overcome:

The horizontal bearing joints were scraped together carefully. Then, after the supercharger was operated at full speed for a

period of time, the unit was disassembled and the bearing rescraped. Complete knowledge of heat-treating and aging aluminum castings to acquire stability was not available as it is today, so it was necessary to rescrape this joint every time the supercharger was disassembled.

To eliminate the effect of unbalanced pressures between the inside of the bearing and each end, a system of packing grooves was used. The outer groove on each end of the bearing was supplied with air under pressure from a tap in the side wall of the impeller casing. The sizes of the drilled air bleed holes were such as to produce substantially balanced pressures at each end of the bearing lining.

Heat transferred along the shaft from the turbine wheel, as well as the heat generated within the bearing itself, was removed by the rapid flow of air around the bearing to the inlet of the impeller. This inlet was purposely designed to surround the entire bearing for this reason.

A number of superchargers to this design were built and installed as shown in Fig. 7. They represented a definite advance,

FIG. 7 DE HAVILLAND BIPLANE WITH TURBOSUPERCHARGER

both in the unit itself and in the installation, over the previous models mounted on the front of the engine.

Throughout the early years of this development, three fundamental objections to the use of sleeve bearings were raised:

1 It was impossible to use oil from the engine lubricating system and maintain the necessary degree of cleanliness. This resulted in rapid deterioration of both journal and thrust bearings.

2 Regardless of the precautions taken, the oil-return line from the supercharger would freeze when flights to high altitudes were made. This frequently meant that the engine oil supply was pumped directly into the cylinders through the supercharger, or overboard onto the outside of the plane.

3 On a cold morning, or after a long glide at high altitude, the bearings and lubricant would become thoroughly chilled. The rotor would start only with difficulty, and would operate sluggishly for some minutes until the system warmed up. Since a supercharger with a stationary rotor, or a rotor which is turning too slowly, definitely restricts the volume of air flowing to the cylinders, this in turn caused a serious loss of engine power which could not be tolerated.

ANTIFRICTION BEARINGS, GREASE LUBRICATION

The solution to these problems appeared to lie in one direction —antifriction bearings and a self-contained lubrication system. For reasons of simplicity and saving in weight, grease instead of oil was considered advisable.

At about that time the ball-bearing manufacturers were quite elated because a number of installations had been made recently which operated at what was then an unusually high speed—3600 rpm. Instructions for installing and lubricating such "high-speed" bearings were quite specific. One bearing race, preferably the outer, was to be a push fit in its housing so that it might "creep" as the bearing revolved, thus equalizing the wear. The inner race was to be pressed tightly on the shaft. Lubrication was by means of a very light lubricating oil, supplied either by a dropper or a wick.

The proposal to run ball or roller bearings at speeds of 20,000 rpm or higher with grease as a lubricant was regarded as purest nonsense. One manufacturer did not share the general belief, and felt that there might be some hope of achieving the desired result. This company's British associate had been making bearings with a much higher degree of precision than was then customary in this country. None of these bearings in the sizes required had ever operated at such high speeds, but the manufacturer expressed a willingness to co-operate in the development of this project.

The British-made bearings, on their first trial, gave a good account of themselves, and demonstrated that the problem could be solved. Many modifications of the bearings themselves, the method of mounting, and their lubrication were necessary before practical operation was obtained.

The first such design made use of one ball and one roller bearing. The roller bearing, next to the turbine wheel, was used to carry the greater load and to take any expansion in the shaft. The ball bearing at the compressor end carried the thrust and some radial load.

The following rules for high-speed antifriction bearings and their installation were gradually evolved:

Bearings. Even with the high degree of accuracy maintained in these bearings, still closer tolerances were required. Much detailed attention was necessary not only to the balls and races but to all other dimensions of the bearing as well.

(*a*) Both the inner and outer races must be closely concentric, and the assembled bearing must maintain concentricity within very close limits.

(*b*) The bearing-race grooves must not only be accurately and smoothly finished but must be parallel with both faces of the inner and outer races.

(*c*) The bore and outer diameter must be *round* and held to very close tolerances to insure the proper fit of each member.

(*d*) A definite clearance must be maintained between balls and races. Too small a clearance will cause excessive loading—too large a clearance will permit rattling, resulting in vibration and rapid wear.

(*e*) The usual type of pressed-steel ball retainer is usually inadequate. The so-called "land-riding retainer" is generally employed, and usually runs with a closely regulated clearance on the inner race. For ball bearings a plastic retainer is most generally used; for roller bearings—bronze. Within the last year and a half it has been found that silver plating of the retainer results in much greater reliability and life.

This progressive advance first produced what was known as a "precision-type" bearing. Later it became a "superprecision" bearing, and finally a "carefully selected superprecision bearing." Limits of accuracy and inspection tolerances which have been developed for these bearings as necessary for successful high-speed operation are shown in detail in Table 1.

Mounting. Given a bearing of the required accuracy, the proper mounting of such a bearing requires the utmost attention to detail. A list of such detailed requirements was developed, which resulted then and has continued to result in the use of antifriction bearings for ever increasing speeds. Owing to the improved stability of present materials, and better manufacturing processes,

TABLE 1 HIGH-SPEED BALL-BEARING INSPECTION LIMITS

1 High-grade superprecision bearings suitable for operation up to 30,000 rpm and 300 F temperature of the bearing parts.
2 Thrust capacity. Rated thrust load, against either face of the outer race, must equal 125 per cent of the rated radial load.
3 Limits of accuracy. All bearing dimensions must be within the limits given in the following and diameters must be round:
(a) Bearings must feel smooth by the hand-spinning test
(b) Inner-race faces must be parallel within 0.00015 in. maximum. Allowable variation from this limit, due to localized depressions, must not exceed a total of 90 deg of the race circle. Localized depressions 0.005 maximum.
(c) Outer-race faces must be parallel within 0.0002 in. maximum. Allowable variation from this limit, due to localized depressions, must not exceed a total of 90 deg of the race circle. Localized depressions 0.005 maximum.
(d) Outer-race radial play, inner race held rigid, 0.0002 minimum to 0.0007 in. maximum (clearance with no load). Gage readings to be corrected for load used in gaging.
(e) Inner-race eccentricity, outer race held rigid, 0.0002 in. maximum.
(f) Outer-race eccentricity, inner race held rigid, 0.0002 in. maximum.
(g) Inner-race faces must be square with bore within 0.0002 in. maximum.
(h) Outer-race faces must be square with OD within 0.0003 in. maximum.
(j) Axial play 0.007 in. maximum.
(k) Outer-race faces runout, inner race held rigid, 0.0005 in. maximum.
4 Maximum difference between widths of inner and outer races, of any one bearing, must not exceed 0.002 in. at any point.
5 Retainer to be made from tubular plastic stock cured for dimensional stability.
6 All bearings must be etched with a serial number, on one face of the outer race, for identification purposes.
7 Protection of bearings by the vendor. All bearings must be:
(a) Thoroughly cleaned.
(b) Coated lightly with an AAF approved rust preventative.
(c) Wrapped separately in waxed or oiled paper.
(d) Packed in individual cartons.

some of these precautions possibly may be omitted without undue hazard, but in the early days of this development attention to each of the details enumerated in the following was of the utmost importance:

1 When mounted in an aluminum or magnesium casing, a steel ring or bearing housing was necessary between this alloy casing and the outer race of the bearing. This steel bearing housing was made heavy enough so that it would retain its shape, regardless of thermal or stress distortions occurring in the casing itself. It was important that this steel member be precision-ground or lapped so that the inside was smooth and round to within 0.0003 in. Also, its dimensions had to be such that the bearing outer race would fit snugly, without shake, but without the necessity of a heavy press or shrink fit.

2 It was discovered early in the development that if this race were left free to creep, in accordance with the practice then recommended, it would invariably gallop or spin, or it would develop what is now known as fretting corrosion of the housing. To eliminate these possibilities the outer race was firmly clamped axially.

3 The inner race was also made a push or light tapping fit on the shaft, which had to be round within 0.0002 in. A tighter fit would cause the inner race to expand and take up the clearance in the balls or rollers. Furthermore, a tight fit invariably resulted in galling or cold-welding of the bearing to the shaft, so that removal after a period of operation was impossible. As in the case of the outer race, the inner race was clamped axially to prevent rotation on the shaft.

4 Alignment of both bearings was an obvious requirement. Not only was it necessary for the races to be aligned accurately, but the shoulders against which these races were clamped had to be accurately square with the shaft. This was a must, so that the bearings would track properly, and in the case of the ball bearing taking the thrust, divide the load evenly.

Balance and Accuracy of Shaft. At this point it becomes necessary to depart briefly from the consideration of bearings and lubrication to consider two other factors extremely vital to the successful operation of any high-speed rotor. Without proper attention to them, no high-speed bearing system can be expected to operate, even for short periods.

The first of these is balance. Any high-speed rotor must be in static and dynamic balance. To balance a rotor at its actual operating speed is highly impractical, so this is always accomplished at a much lower speed. When done carefully, this suffices for operation at the higher speeds. One important precaution must be observed. Elements of high-speed rotors are subjected to easily measurable expansion due to stresses at the higher speeds. They must be so mounted or attached to the shaft that when any tendency toward looseness on the shaft occurs, the element remains accurately centered, otherwise no balancing operation can ever be effective.

Accuracy of the shaft is essential. For years it was believed that accurate dynamic balance of a rotor could be maintained only if the various elements were assembled on the shaft permanently. With the advent of ball and roller bearings such a procedure was obviously impossible. On the other hand, a balance, once obtained, must be maintained while the rotor is being disassembled and reassembled in the supercharger. This was accomplished by building the shafts to a degree of precision previously found only in gages.

The following precautions were required; when carefully followed, good results were usually assured:

1 The shaft, when rolled in vee blocks at the bearing supports, must run true throughout its length within 0.0001 in.

2 All shoulders on the shaft against which bearings seat must be flat and square with the axis within 0.0002 in. maximum.

3 All holding sleeves must fit without shake on the shaft, and the ends of these sleeves must be flat and square within 0.0002 in. maximum.

4 Sleeves of any appreciable length should fit the shaft for only a short distance at each end. Longer fits may interfere with the natural inclination of the shaft to deflect, thereby causing a whip or other serious vibration.

5 All sleeves, bearings, gear worms, and other members strung on the shaft must be marked for alignment in their position when the rotor is balanced. After a subsequent disassembly of the rotor, they must be reassembled with these reference marks in line.

6 All such sleeves and bearings must be selected so that accumulated errors in squareness are minute to avoid cramping and bowing of the shaft.

Lubrication. The decision to use grease as a lubricant was arrived at because it had several favorable features to recommend it:

The supply of lubricant would be self-contained within the bearing.

No oil, oil tank, pumps, or piping were required, hence a saving of several pounds in weight would be realized by omitting these items.

Danger from frozen lubricant lines would be eliminated.

Grease guns and their fittings were common garage and hangar appliances, hence easily obtainable. The system would thus be simple to operate and service.

It was originally expected that lubricant could be supplied from any army garage or aircraft service shop. As will be explained, this did not prove feasible.

The problem of selecting a grease was complicated by the fact that service operations required the use of only one grease, and this must suffice for both the subzero temperatures at the compressor end bearing and temperatures in excess of 200 F at the turbine end. The use of a pressure-type grease gun on the different joints of an automobile is entirely practical, the approved practice being to apply pressure until grease visibly oozes out of the joints. It was immediately learned that this practice would not suffice for a ball bearing in a turbosupercharger. A grease gun can exert a pressure of several hundred or even thousands of pounds per square inch, much too high for a high-speed bearing chamber. Furthermore, grease that oozed out through the seals and around the shaft went directly into the supercharger, thence

to the carburetor, and from there to the engine cylinders. The first attempts at lubricating these bearings with a grease gun resulted in bearings tightly packed with grease, and, as previously mentioned, the only escape was around the shaft into the supercharger.

All greases expand in the presence of heat, and all greases contain a certain amount of moisture, air, or both, which increases the expansion materially. The result of trying to operate a tightly packed housing with a high-speed bearing may easily be imagined. As heat is developed, the grease tries to expand. There is no adequate vent, so the temperature increases, thus aggravating the tendency to expand. This process continues until the grease becomes nearly fluid, and still higher pressures are built up within the housing. The result then becomes decidedly visible and discouraging as the bearing starts to get seasick. Once this starts, the bearing continues to empty itself until all of the grease is gone.

When this program first started, there were no greases on the market for either extremely high or extremely low temperatures. To find one grease which would answer the widely differing requirements of both bearings was a major development in itself. All of the major oil and grease companies were tried without success. At last a small company, manufacturing high-quality, but not widely advertised, greases, came forward with a grease which it felt sure would work. By this time, as the leaders in the industry had been contacted, there was a tendency to be skeptical, but their product was given a try. It was a pleasant surprise to find that it did a creditable job on both bearings. This grease met the following specifications: Penetration 270–290, made from soda-lime-base soap and 300 SUS paraffinic oil. Needless to say, the problem of procuring satisfactory greases no longer exists. Many companies now make greases suitable for this kind of service.

While the development of a proper grease was continuing, modifications in the housing and means for applying the grease to the bearing were being developed. The design as finally arrived at is shown in Fig. 8. In this design each bearing was supplied with a vent pipe of ample proportions, so that as grease was added with the gun it could escape through this vent, without building up extreme pressures. This left a bearing still full of grease under moderate pressures, but the grease was able to expand and any excess could escape easily. The technique finally worked out was to fill the bearing until grease started to come out the vent, operate the supercharger slowly for some minutes until an appreciable amount of grease had been vented, and then cap the vent pipes. This process sounds unduly complicated, but the venting period of the bearing was made to coincide with the warm-up period of the engine. Strange as it may seem, this lubrication system finally turned out to be both reliable and practical.

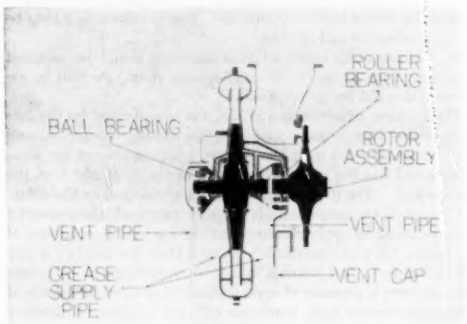

FIG. 8 TURBO WITH GREASE-LUBRICATED ANTIFRICTION BEARINGS

The first complete squadron of planes to be equipped with turbosuperchargers—Consolidated PB-2A's—used this grease-lubricated ball bearing. This installation is shown in Fig. 9. Thousands of flying hours were logged under all kinds of conditions, with remarkably little trouble. The only drawback experienced was that once about every fifteen to twenty hours it was necessary to recharge the bearings.

The development of grease lubrication has left a definite impression on industry, as evidenced by the fact that it was the forerunner of many applications that today are considered commonplace. For example, electric motors, with grease-lubricated bearings, are now being manufactured by the hundreds of thousands, and high-speed, grease-lubricated ball bearings have wide industrial acceptance.

FIG. 9 CONSOLIDATED PB-2A AIRPLANE WITH TURBOSUPERCHARGER

The principles developed in this program led to the adaptation of ball and roller bearings to various electric-railway locomotives, and these successful applications have led to the widespread use by the railroads of grease-lubricated antifriction bearings in freight and passenger cars.

Some basic principles governing the use of grease in high-speed ball and roller bearing applications are outlined in the following:

1 "Grease-packed" ball bearings, in which the space around the balls is filled with grease, are not satisfactory for high-speed applications. However, prefilling bearings of this type with prescribed amount of grease, so that at least one half the available volume is left free for expansion, tends to improve their suitability.

2 Where grease is to be added manually, the bearing housing should not be filled more than half full.

3 If grease is added by a grease gun a vent must be provided for pressure relief. After each filling the bearing should be run a while to get initial venting, and then allowed to cool down.

4 Where external vents are objectionable, an outer pocket surrounding the bearing chamber is sometimes used for the excess grease to vent into. This can be made so it is easily cleaned even with the bearing in operation. This was not a problem with the aircraft turbosupercharger.

5 Grease suitable for the specific application should be used. Most of the reputable oil and grease companies are now prepared to recommend greases for a wide range of conditions, and should be consulted before the grease is specified.

As the science of aviation advanced, the Air Force planners began to foresee the day when a single flight might last more than the 15 or 20-hr interval that this system of lubrication would permit. Recharging of the bearings in flight appeared to impose major obstacles. From then on, attention was directed to the development of a separate oil-lubrication system for the super-

chargers, using built-in lube and scavenge pumps so as not to jeopardize the engine system and to insure clean oil for the supercharger bearings.

Antifriction Bearings, Oil Lubrication

The Boeing B-17 "Flying Fortress" bomber was the first of a series of long-range planes, both bombers and fighters, that introduced another new set of problems:

1 Flights of long duration which for some years had been contemplated were now a reality. As was expected, this made obsolete the system of grease lubrication.

2 Higher altitudes, with correspondingly higher rotative speeds of the supercharger, were called for. Whereas altitudes of 20,000 to 25,000 ft had been the order of the day, the latest requirements called for operation at altitudes of 30,000, 35,000, and even 40,000 ft. This meant an increase in shaft speeds from 20,000 rpm to approximately 26,000 rpm.

3 Engine power output, spurred on by combat requirements, increased at an astonishing rate. Starting with the 1000 hp already established, it rose rapidly until by the end of World War II it had reached 2400 hp. Superchargers also became larger and heavier, requiring stronger rotors and higher thrust loadings. These factors meant larger bearings.

4 Along with the changes mentioned came higher peripheral speeds of both turbine wheel and impeller. The resulting higher stresses caused greater stretch of the rotor members at high speed, with attendant difficulties of keeping them centered properly to maintain balance.

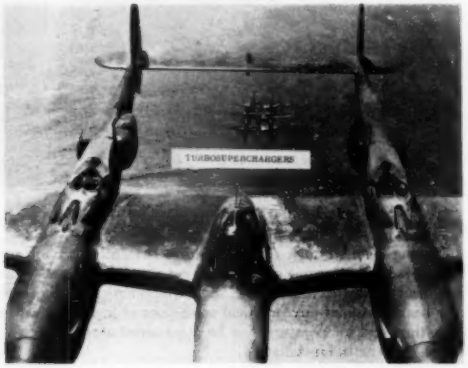

Fig. 10 Lockheed P-38 Airplane With Turbosuperchargers

Fig. 11 Boeing B-17 Airplane With Turbosuperchargers

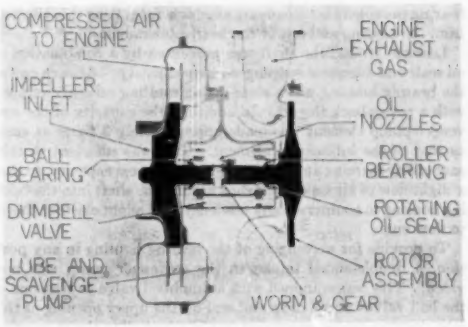

Fig. 12 Turbo With Oil-Lubricated Antifriction Bearings

5 For reasons of efficiency and ease of installation, it was decided that a single-inlet impeller would be used in place of the double-inlet design used up to this time. For the same reasons it was decided that both impeller and turbine wheel would be overhung. This arrangement was completely novel and untried, but the benefits to be obtained made it highly desirable.

6 From the beginning of this whole development, it had been a requirement that the supercharger be capable of operating in any position during flight, but the normal installation had always been with the shaft horizontal. It was now required that the unit be adapted to installation with the shaft in any position. In some planes, like the Lockheed P-38, Fig. 10, the turbine wheel was on top. In others, like the Boeing B-17, Fig. 11, the turbine wheel was on the bottom.

7 The high altitude for which the B-17 was designed, together with the large crew, meant that any oxygen systems carried would be heavy and complicated. A pressurized cabin appeared to be the ideal solution. Of several methods for accomplishing this result, that of bleeding air from the supercharger itself appeared to be the most promising. This decision introduced one very particular requirement. The air delivered from the supercharger had to be "free from oil," as even the slightest trace of oil vapor in the cabin would cause sickness and discomfort to the crew. With the specifications as written, the answer was obviously a separate oil system, with the necessary pressure and scavenging pumps incorporated within the supercharger itself.

The development of such a separate system brought its own problems. In order to save space and weight, the allowable oil supply for each supercharger could not exceed 1, or at the most 2 gal, and since this must suffice for long flights, the total oil consumption due to leakage and evaporation had to be reduced to a minimum. In addition, the scavenging pump must keep the bearing housing clear of oil in any position and at any altitude. The design shown in Fig. 12 successfully met the conditions specified, as evidenced by the fact that several hundred thousand were built and flown in all theaters of operation during World War II. The oiling problem as such was taken care of by a small, compact, two-element combined lubrication and scavenging pump, with both elements mounted on a single shaft. This was driven by a worm on the main supercharger shaft.

In order to cool the bearings, especially the roller bearing at the turbine end, a supply of oil appreciably greater than required for lubrication alone, was provided. This was in direct violation of the principle that high-speed bearings should be lubricated by a wick or dropper. Operation was entirely successful and established another principle, namely, that there is practically no limit to the amount of oil that can be supplied to an antifriction

bearing provided that means are available for getting this oil away from the bearing and out of the bearing chamber.

Leakage around the shaft was prevented by a combination of oil seals and adequate scavenger-pump capacity. At each end of the bearing housing was a close-fitting rotating oil seal equipped with a pump-back thread. In addition, the capacity of the scavenger-pump element was made approximately 3 times as great as that of the lubricating element. This was sufficient to take care of any foaming and also provide some excess capacity, so that a slight flow of air was established around the shaft into the bearing housing to counteract any tendency that might exist for the oil to flow out.

To provide for scavenging of the bearing housing in any position, a double-ended intake to the scavenger pump was provided. This was equipped with a dumbbell valve so that one of the ball valves would drop and seal off the upper opening of this inlet, leaving the lower opening free to admit oil to the scavenging line. In principle, this arrangement was excellent. In practice, the ball valve often bounced and chattered on its seat, destroying the air-tight fit. To overcome this tendency, the double scavenger intake was maintained, but in the normal installation, the upper opening was plugged. As a means of preventing oil leakage into the compressor chamber, a complete separation was provided between the bearing housing and the compressor casing.

Again, one of the most interesting problems did not concern bearings or lubrication directly, but did have a vital influence on the operation of the unit. In some later designs, in which impeller-tip speeds in excess of 1600 fps were required, the stresses were actually approaching the proportional limit of the material. No matter how tightly the impeller was pressed onto its hub bushings, a permanent set would result whenever the unit was run to its full rated speed. This would leave the impeller loose on the shaft and destroy the balance so that operation was impossible. To overcome this condition, the impeller was first assembled on hub bushings with a bore diameter smaller than finally required, then overspeeded so that a definite set occurred in the material. The bore was then machined out to its final size and fitted with its final bushings before final assembly of the unit.

Conclusion

This completes the historical outline of the development of aircraft turbosupercharger bearings.

Today, many well-known military aircraft such as the Convair B-36, Fig. 13, are equipped with turbos built by the author's company. Turbos have been applied to commercial aircraft, also. Boeing's "Stratocruiser," Fig. 14, now in service with about a half-dozen airlines, has turbosupercharged engines.

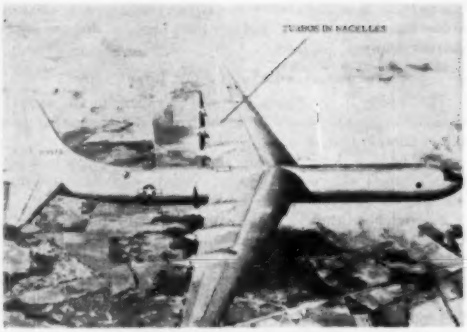

Fig. 13 Convair B-36 Airplane

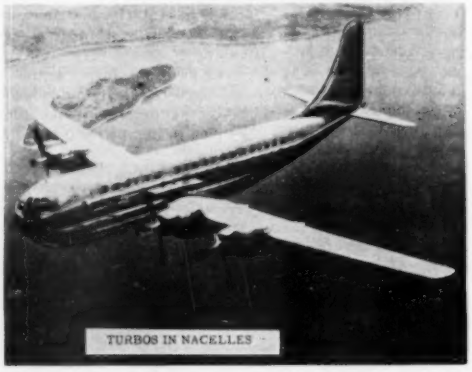

Fig. 14 Boeing "Stratocruiser" Airplane

Having been through this experience, the author's company, and, it is believed, some others, have set up complete and elaborate bearing test centers, where the characteristics of practically any bearing, under any practical conditions of load, lubrication, vibration, and temperature, can be determined accurately in advance of its actual installation.

The Fatigue Strength of Threaded Connections[1]

By R. C. A. THURSTON,[2] OTTAWA, ONTARIO, CANADA

Published information on the strength of threaded connections subjected to dynamic loading has been surveyed and summarized, with particular reference to high-duty applications. After a consideration of the load distribution and the concentration of stress at the thread roots, the subject is discussed from the following viewpoints: Effect of thread form; effect of method of manufacture; effect of degree of tightness; methods for improving performance; special modifications in design. In general, the basic principles to be followed in the design of high-strength bolt and stud assemblies are outlined, the reasons underlying them explained, and evidence in their support given when possible.

Introduction

IT is seldom that the design of machines and machine components does not involve the use of threaded connections—bolts, screws, or studs. The strength of these connections under dynamic loads is a matter of considerable importance, particularly in view of the increasing demand for greater output which generally necessitates higher stresses and operating speeds. In order to obviate the possible occurrence of premature fatigue failures, causing damage to machines and, perhaps, injury to personnel under such conditions, it is essential that the designer be kept well informed as to the numerous factors which affect the fatigue strength of threaded parts, and the various methods which are now available to produce the desired increase in strength.

A considerable amount of technical literature on the subject has been published during the past 25 years, but no systematic study of the effect of thread form was carried out until the proposals for a unified thread form initiated joint researches in England, the United States, and Canada, the results of which have not yet been published. Many investigators have devoted their efforts to an examination of the load and stress distribution, which in consequence is now fairly well established. Others have studied the effect of the method of processing the thread, the effect of the tightening torque, and the different techniques for introducing favorable stresses into the threaded surface. The present paper is an attempt to co-ordinate the more important facts which have emerged from these researches, to outline the basic principles which should be followed for the most efficient design of threaded connection, and to draw attention to those aspects of the problem on which further information is required. A short bibliography will be found at the conclusion of the paper, but those wishing to pursue the subject further are referred to an excellent article by Arnold (1),[3] which contains an extensive bibliography of some 160 references.

Distribution of Load and Stress

It has been recognized for many years that the distribution of load in the threads of a screwed joint is far from uniform. Assuming the threads of a bolt and nut to be a perfect fit at no load, the bolt would tend to stretch under load while the nut would contract, hence there no longer could be complete contact along the threads. Actually, there is a concentration of load toward the base of the nut, and the difference arising from the simple consideration of stretching and contracting is largely accounted for by bending of the threads. This problem has been attacked theoretically and experimentally by several investigators, notably J. N. Goodier (2), J. P. Den Hartog (3), Earle Buckingham, M. Hetenyi (4), and D. G. Sopwith (5).

Den Hartog (3), from purely theoretical considerations, developed a simple exponential formula for the stress distribution in bolt threads, and showed that the peak stress, assuming no yielding took place, could be as much as 9 times the nominal or average stress, the first two threads taking about one half the load. This condition, of course, is somewhat improved if yielding takes place and the load is redistributed.

Den Hartog's analysis was based on the extension of the bolt core and axial contraction of the nut wall, and on the bending of the two threads as cantilevers, but he did not allow for the circumferential stretch of the nut wall. This was done later by Goodier (2), who actually measured the bending of the nut wall and the thread recession due to the radial pressure between the bolt and the nut, and he showed that they were of the same order of magnitude as the simple axial strain and the bending of the threads.

Both Buckingham, and Sopwith (5) approached the problem mathematically, giving due consideration to all the factors concerned, and their results were substantially in agreement with those just mentioned. Sopwith developed a formula for the load-concentration factor, defined as the maximum value of the thread loading in terms of the mean, and showed that it depended on the proportions of the thread (pitch/diameter ratio, length/diameter ratio, relative size of nut), the form of the thread (semi-angle and depth factor), and the degree of lubrication. Typical theoretical curves for the load distribution along a standard American $1^1/_4$-in. bolt and nut under a 25,000 lb load are given in Fig. 1, together with the experimental values as determined by Goodier. In view of the necessary assumptions made in the analysis, the agreement is reasonably good. In addition, Sopwith showed that in the normal bolt and nut the maximum intensity of loading occurs at the bearing face of the nut, and may be from 2 to 4 times the mean. Another interesting point which emerged was that there is little to be gained by increasing the length of the engaged thread beyond a certain point, in so far as the maximum intensity of loading is concerned.

Several investigators have applied photoelastic methods successfully to the analysis of the stress distribution in threaded connections. Solakian (6) used two-dimensional models with only one

---

[1] Presented by permission of the Director-General of Scientific Services, Department of Mines and Technical Surveys, Ottawa.

[2] Metallurgical Engineer, Physical Metallurgy Division, Mines Branch. Mem. ASME.

Contributed by the Machine Design and Aviation Divisions and presented at the Semi-Annual Meeting, Toronto, Ont., Can., June 11–15, 1951, of The American Society of Mechanical Engineers.

Note: Statments and opinions advanced in papers are to be understood as individual expressions of their authors and not those of the Society. Manuscript received at ASME Headquarters, March 23, 1951. Paper No. 51—SA-11.

[3] Numbers in parentheses refer to the Bibliography at the end of the paper.

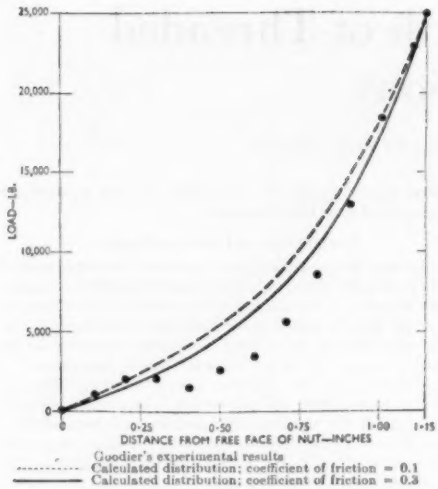

FIG. 1 DISTRIBUTION OF LOAD ALONG THREAD; FROM SOPWITH

thread in contact, and determined the stress-concentration factors. For the American standard thread he reported a factor of 3.8, and for the Whitworth thread with its rounded roots, a factor of 2.9. Later, Hetenyi (4) made a valuable contribution to the subject when he employed the three-dimensional "stress-freezing" technique in a careful study of several nut designs. With a conventional nut on a 1-in. Whitworth bolt, he obtained a maximum stress-concentration factor of 3.85 at the root of the bolt thread just inside the nut, the stress then falling off fairly rapidly toward the other end of the nut.

In general, the fatigue failure of a bolt will occur at the first or second thread inside the nut, which is in accordance with the theoretical and experimental findings, but the actual magnitude of the stress-concentration factor in a specific case is a function of the load distribution and the stress-raising effect of the thread, regarded as a geometric notch. The actual reduction in fatigue strength produced by this stress concentration is then dependent upon the notch sensitivity of the material concerned, so it is evident that designing a threaded connection for an application which involves cyclic loading is still a matter which calls for experience and the intelligent application of well-defined principles.

EFFECT OF THREAD FORM

The deleterious effect of a single circumferential groove on the fatigue strength was observed by some of the earliest investigators in this field, and it was soon found that the effect of a series of grooves or a screw thread was less severe, owing to the beneficial stress interference of the threads with each other. This was clearly shown by R. R. Moore (7) in rotating-beam tests on a hardened and tempered chrome-vanadium steel with two different sizes of American standard thread. The steel was heat-treated to 140,000 psi tensile strength; the results are given in Table 1.

No load was transmitted through the threads in these tests, but subsequently the same investigator carried out comparison rotating-beam tests on ANC and special aero threads in which stud specimens were fitted into threaded plugs held in the machine. The aero thread has a shallow spiral groove on the bolt with a coarse vee thread in the nut, and a stainless-steel or bronze spring-

TABLE 1 EFFECT OF THREAD FORMS ON ENDURANCE LIMIT

		¼ in. 28 TPI		⅜ in. 24 TPI	
	Plain	Single groove	Thread	Single groove	Thread
Endurance limit, psi	51000	12000	43000	21000	37000
Strength-reduction factor[a]	...	4.25	1.19	2.43	1.38

[a] Strength-reduction factor = endurance limit (plain)/endurance limit (notched).

wire insert in the form of a helix. For the 5/16-in. 18 TPI thread employed in these tests on SAE 3140 steel, the results showed a strength-reduction factor of 2.7 for the ANC form, and 1.85 for the aero thread with the larger root radius.

However, since screw threads are more commonly used under repeated tension loading, the data presented by H. F. Moore and P. E. Henwood (9) are of interest. They compared the effect of the American standard and the Whitworth thread forms on 3/4-in. 16 TPI threaded studs under cyclic loading (applied through nuts) from zero to a maximum in tension. Their results are given in Table 2, and indicate that under this condition of stressing the Whitworth form has a marked superiority over the American standard form on a medium-carbon steel, but less on a higher-strength alloy steel.

TABLE 2 COMPARISON OF WHITWORTH AND AMERICAN STANDARD THREADS UNDER REPEATED TENSION

Material	Tensile strength, psi	Thread form	Endurance limit, psi	Strength-reduction factor	Stress-concentration factor[a]
0.3 C steel	57400	None	37000	...	...
		Whitworth	21000	1.76	3.86
		U. S. Standard	13000	2.84	5.62
SAE 2320	109000	None	73000	...	...
		Whitworth	22000	3.32	3.86
		U. S. Standard	19000	3.85	5.62

[a] Obtained by photoelastic methods.

The greater notch sensitivity of the higher-strength alloy steel can be clearly seen, altho igh the magnitude of the strength-reduction factor for the Whitworth thread (3.32) is somewhat surprising. On the basis of their results, the investigators suggested that for design purposes, involving repeated tension, a safe estimate of the stress at the thread root would be $3P/A$ for ordinary steel, and $4P/A$ for heat-treated alloy steel, A being the core area, and P the load.

A more extensive series of tests was conducted by R. Cazaud (10) on the effect of thread form alone under rotating bending. Three types of thread form were used: (*a*) 60-deg angle with very sharp root, (*b*) 60-deg angle with rounded root, (*c*) half round with no straight portion, as used on the French railways. The tests were made on three steels—a mild steel (A), a nickel-chrome steel as-quenched (B), a nickel-chrome steel tempered at 200 F (C), and the same steel tempered at 650 F (D). The results are given in Table 3.

TABLE 3 RESULTS OF ROTATING-BENDING TESTS ON VARIOUS THREAD FORMS

Form of test piece	Strength-reduction factor			
	A	B	C	D
Plain	0	0	0	0
With sharp 60-deg threads	1.35	9.30	4.23	2.00
With rounded 60-deg threads	1.28	4.23	2.74	1.75
With half-round threads	1.24	2.91	2.33	1.62

The effect of increasing the root radius of the thread is quite evident, and is most marked in the case of the quenched alloy steel as would be expected. These results were substantiated by more recent data reported by A. Schwartz, Jr. (11) of the Bethlehem Steel Company, who compared the strengths of the American National form, coarse and fine, and the Whitworth form, with a special high-fatigue-resistant (HFR) form developed by the com-

pany. The new thread is coarser and has a flat top with a large root radius, details of which were not given. Rotating-beam fatigue tests were made on $^5/_{16}$-in-diam samples of medium-carbon steel with the various thread forms superimposed, the major diameter being kept constant in one series, and the minor diameter in a second series. The results are summarized in Table 4.

TABLE 4 EFFECT OF WHITWORTH, AMERICAN NATIONAL, AND HFR THREADS ON FATIGUE STRENGTH

Thread form	—Strength-reduction factor[a]— Major diam const	Minor diam const
$^5/_{16}$ in. 12 HFR	1.40	1.53
$^5/_{16}$ in. 18 ANC	2.19	2.31
$^5/_{16}$ in. 24 ANF	1.93	
$^5/_{16}$ in. 18 BSW	1.93	2.08

[a] Endurance limit of plain samples = ± 40,500 psi.

The lower notch effect of the Whitworth form as compared to the American National form has been demonstrated earlier, but the marked superiority of the HFR thread from the point of view of fatigue strength should be a definite advantage in high-duty applications. It is understood that subsequent service tests over long periods confirmed the improvement predicted in the laboratory.

Some unpublished work by the author was carried out on an aluminum alloy under repeated tension loading with a preload. The tests were made on plain, threaded, and jointed samples with a Whitworth thread form and in different sizes. Although there was a significant decrease in strength in the larger sizes, the strength-reduction factor due to the thread was sensibly constant at about 1.3, while the load-concentration factor due to the application of load through the threads was about 4.5. The design factor, therefore, or the ratio of the endurance limit of plain polished test pieces to the design stress, was about 6.

Effect of Method of Processing

Three principal screw-thread production methods are in general use at the present time, namely, cutting (or milling), grinding, and rolling. Ground and cut threads are produced from stock of the same diameter as the major thread diameter, whereas the diameter of stock for roll-threading is always less than the major thread diameter, and depends upon the thread pitch and the bolting material. The rolled-thread process is considerably faster than the other methods, wastes no stock, gives a smoother finish with a compressive stress in the roots, and can be held to very close tolerances. Fig. 2 is a comparison of the grain structures in machined and rolled threads, and shows the flow pattern at the root and crest of the latter. The cleavage noticeable at the crest of the rolled thread is due to the upward displacement of the material during rolling, and occurs particularly in the first and last threads where axial flow of the material is possible.

The effect of the method of manufacture on the fatigue strength of bolts was investigated by A. M. Smith (12) for three processes; (*a*) cut threading, (*b*) roll threading on single extruded wire, (*c*) roll threading on double-extruded wire. In method (*b*) wire of the required outside diameter of the thread is first extruded to the pitch diameter and then roll-threaded. In method (*c*) wire larger than the desired outside diameter of the thread is first extruded to this diameter, then extruded to the pitch diameter, and finally roll-threaded. The tests were carried out under rotating bending using special samples, threaded $^5/_8$-in. 24 ANF, of two low-carbon steels. The results showed that the cut threads had an endurance limit/tensile strength ratio of 0.30, while the others had a ratio of 0.33, the tensile strength being that for a threaded test piece and calculated on the mean area. The ratios based on the strength of the original wire were 0.30, 0.37, and 0.43, respectively. It is interesting to note that the majority of

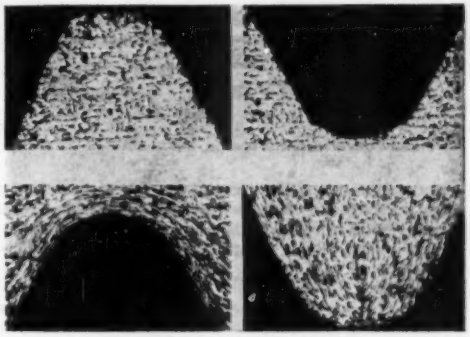

Top left, crest of machined thread
Top right, root of machined thread
Bottom left, root of rolled thread
Bottom right, crest of rolled thread

Fig. 2 Grain Structure of Threads; From Dinner and Felix

failures of the single and double-extruded specimens occurred in the collets, so that the actual endurance limits for threads made by these two processes were probably somewhat higher. The endurance-limit ratio for the cut threads is higher than that obtained by R. R. Moore (rotating-beam) or by H. F. Moore and P. E. Henwood (repeated tension), but this is almost certainly due to the fact that the threads in this investigation were made with a radius at the roots, rather than the theoretical flat.

Further work on the properties of the double-extruded bolt, as compared to its more expensive quenched and tempered counterpart, has been reported recently by A. S. Jameson, J. A. Halgren, and S. A. Sheridan (13). Fatigue tests under repeated tension loading (zero to maximum) were made on $^1/_2$-in. 13 TPI hexagon-head bolts, with and without the underside of the bolt head machined to improve the axiality of loading. No static strength data were given, but it is understood that the extruded bolts were to SAE Grade 3 which demands a minimum tensile strength of 100,000 psi, while the heat-treated bolts were to SAE Grade 5 with a corresponding value of 125,000 psi. The conditions of test and the results obtained are given in Table 5.

TABLE 5 ENDURANCE LIMITS OF HEXAGON-HEAD BOLTS

Condition of bolts	$^1/_2$ in. 13 × $1^1/_4$ in. bolts Not machined under head, psi	$^1/_2$ in. 13 × $1^1/_2$ in. bolts— Not machined under head, psi	Machined under head, psi
Cold-worked	23000	19000	27000
Cold-worked, aged at 700 F	13000	18000	22000
Quenched and tempered at 875 F	9000	10000	10000
Quenched and tempered at 1100 F	10000	...	18000

Although subsidiary tests showed that the quenched and tempered bolts possessed greater plasticity than the cold-worked bolts, the superior endurance properties of the latter are clearly evident. This was confirmed by additional fatigue tests with a prestress of 50,000 psi tension.

One of the most complete investigations of the effect of the manufacturing process was carried out by H. Dinner and W. Felix (14). Threaded samples, 1 in. diam, of open-hearth bolting materials were prepared by rolling, lathe-cutting, grinding, and milling, and tested under repeated tension. Tests were made with and without thread loading through a nut, and the results are summarized in Table 6.

TABLE 6 EFFECT OF THREADING PROCESS ON ENDURANCE LIMIT

Threading process	Endurance limit,* psi: Without thread loading	With thread loading
Rolling	41500	28500
Cutting	24500	17100
Grinding	26300	
Milling	27300	17100

* Ultimate tensile strength of material, 68,000 psi.

Cutting, grinding, and milling are shown to have about the same effect, while rolling is much less harmful, the rolled threads being over 50 per cent stronger than the others. When loading is applied through a nut, a further strength reduction of some 30 to 40 per cent takes place.

N. B. Green (15) also examined the effect of processing on bolt strength by means of endurance tests under a constant range of tension loading. He found that the best performance was given by bolts roll-threaded after heat-treatment, and that cut threads were slightly superior to ground threads.

From a consideration of the data referred to in this section, it is clear that the roll-threading process gives the best fatigue properties. If the bolt material requires heat-treatment, this preferably should be carried out before processing. With regard to the other methods, cutting, milling, and grinding, the small amount of evidence available suggests that there is little to choose between them. Grinding is normally used for the higher-strength studs and bolts, while milling or cutting is used for those of lower strength. The former process is often abused, with the consequent development of high surface tensile stresses and incipient cracks which will lower the fatigue resistance. However, with careful grinding, laboratory tests (16) have shown no adverse effect on the fatigue strength at hardness levels up to Rockwell C 59.

Effect of Tightening

The importance of adequate tightening when assembling threaded connections has been generally appreciated only during the last 10 years. J. O. Almen (17) has estimated that the relative responsibility for the durability of highly stressed, dynamically loaded bolts is about 82 per cent for "the man with the wrench," and 6 per cent each for the designer, the metallurgist, and processing. A properly tightened nut is defined as one that applies a tension preload to the bolt or stud that is equal to or greater than the maximum operating load. Under this condition, and assuming reasonably rigid bolted assemblies, the bolt will be subjected to negligible cyclic stress regardless of the fluctuations of the service load, and, therefore, will not fail by fatigue. This fact was demonstrated by Almen in a series of fatigue tests on $^3/_8$-in. 24 ANF bolts under various initial tensions. The external load applied to the bolted members alternated from zero to 9215 lb, and the results are given in Table 7.

TABLE 7 FATIGUE-TEST DATA FOR BOLTED ASSEMBLIES

Initial tension, lb	External applied load, lb	Approximate load change, lb	Stress range*	Number of tests	Average life, cycles
1420	0 to 9215	8000	0.85	17	5960
5920	0 to 9215	3300	0.36	16	35900
7220	0 to 9215	2000	0.215	15	214500
8420	0 to 9215	800	0.087	2	5000000+

* Stress range, $R = 1 - \frac{\text{minimum stress}}{\text{maximum stress}}$

The increase in endurance of the bolts as the initial tension is increased is very marked in these tests. Theoretically, therefore, it would appear that the maximum cyclic load a bolt could withstand should approach its static strength, assuming the initial tension to be equal to the operating load, and the bolted members to be rigid.

Unfortunately, in practice such is not the case; there is always a certain amount of elasticity present in the bolted members which results in a change of stress in the bolt at each application of load, irrespective of the magnitude of the initial tension. The stress change will be proportional to the rigidity of the bolt, and inversely proportional to the rigidity of the bolted members. An immediate deduction from this conclusion is that a properly tightened bolt will be weaker when used with aluminum abutments than when used with steel abutments of similar dimensions because of the lower elastic modulus of the aluminum. Furthermore, the number of parts in a bolted assembly will affect the bolt strength because of the additional deformation due to imperfect fitting and surface roughness.

Various methods are available for improving the efficiency of a bolted assembly, particularly with regard to increasing the elasticity of the bolt. For high-duty applications the bolt should be as long as possible and "waisted" or provided with reduced-diameter sections in the shank (e.g., connecting-rod bolts). A spring washer of the Belleville type under the nut will increase the effective bolt elasticity and assist in maintaining the initial tension. This latter point is also of obvious importance, although it is considered in some quarters that friction is sufficient to keep in place a nut that is properly tightened.

The rigidity of the abutments or bolted members is often a factor over which little control can be exercised by the designer, but where possible it should be maintained at a high level. If gaskets are necessary, their elasticity should be kept to the minimum which will still serve the purpose.

Other factors which will affect the degree to which the initial tension is maintained during service are wear, corrosion, embedding, the displacement of material such as soft plating, or the use of materials that may yield at elevated operating temperatures. These factors will be increasingly detrimental as the length of the bolt or stud is reduced.

Since the correct tightening of the bolt is of such importance from the point of view of bolt strength, it is desirable to consider the various means by which the required initial tension can be obtained. The three principal methods (30) are as follows:

1 By measuring the bolt elongation.
2 By the use of a torque wrench.
3 By measuring the angular twist of the nut.

Method 1 is the most accurate, but practicable only when both ends of the bolt are accessible. The length of the bolt is measured with a micrometer or special indicator gage before and after tightening. Assuming a modulus of elasticity of 30×10^6 psi, a strain of 0.001 in. per in. in a steel bolt will correspond to a stress of 30,000 psi. This practice has been followed by aircraft-engine manufacturers with satisfactory results.

Method 2, i.e., the use of the torque wrench, is probably the most popular and assumes a constant ratio between the torque and the induced bolt tension. Unfortunately, this is not always true, since the ratio depends upon the friction between the nut and the abutment, and the friction between the threads of the nut and bolt. These in turn depend upon a wide variety of factors such as surface finish, degree of lubrication, materials, plating, dirt, burrs, washers, and the like. Nevertheless, a considerable amount of data have now been accumulated regarding the effect of these variables (see reference 18), and it is possible under reasonably standardized conditions to obtain consistent results. Whether the torque wrench is as reliable as the experienced mechanic who has developed wrench "feel" is still a matter for argument.

Method 3 is more recent and makes use of the nut as a rough

micrometer. The nut is first tightened to seat firmly the contacting surfaces, then released and retightened "fingertight," this being the zero position. From this setting the nut is turned through a specified angle to give the required initial bolt tension. Although the technique is rather involved and time-consuming, it is more accurate than the torque-wrench method and gives greater assurance of tightness.

The extent to which individual bolts or studs should be tightened, from the point of view of their strength characteristics, will depend upon their application, but it is preferable to stress them above the yield point of the material than to risk lack of tightness in the assembly. For example, if cotters are being used with castle nuts, it is better to advance the nut beyond the required tightness to admit the cotter than to slacken it.

Methods for Improving Performance

A number of methods have been suggested for improving the strength of threaded connections by reducing the load-concentration effect. By using nut material with a lower modulus of elasticity than that of the bolt, the nut will conform more readily to the bolt-thread deformation and give a more uniform load distribution. Sopwith has calculated that replacing the steel nut on a steel bolt in a specific case by a duralumin nut will reduce the load-concentration factor from 3.38 to 2.54. On the practical side, Wiegand (19) has shown the superiority of cast-iron and aluminum-alloy nuts over steel nuts on steel bolts in direct stress-fatigue tests. Kaufmann and Jäniche (20) made pulsating-tension tests with steel and magnesium-alloy nuts on three different bolt steels and found increases in the endurance limits of 35 to 60 per cent.

Another method is to taper the screw threads in the nut; this produces its optimum effect at the load at which the lower threads just make contact. The use of a smaller pitch in the bolt than in the nut will also improve the load distribution. Initially, the threads will be in contact only at the free face of the nut, but as the load increases so will the degree of contact, until the whole length of thread is in contact. According to Sopwith, for a 1-in. Whitworth nut and bolt the required change in pitch would amount to less than 0.001 in. per in. of pitch. Other methods involving design changes are discussed in the next section.

Probably the most efficient method for increasing the strength in any specific case is the application of rolling to the thread roots as shown in Fig. 3, reference (31). The superior properties of completely rolled threads have already been mentioned in a previous section of this paper, but it was subsequently discovered that further improvements could be obtained by rolling the roots of the threads. As an example of this, Wedemeyer (21) has reported an improvement of 10 per cent. The radius of the rollers should be somewhat less than the root radius of the thread, and the flank angle should be about 5 deg less than the included thread angle. Three rollers are generally used and the roll pressure obtained by means of a calibrated compression spring. The intensity of pressure must be sufficient to produce some permanent deformation of the thread root, but the optimum pressure must be determined for each individual case.

The beneficial effects of this process are due to the residual compressive stresses induced in the surface layers at the weakest points, the removal of surface imperfections, and the increase in strength through cold-working. The best results are obtained when the rolling is carried out after heat-treating and threading. All the steels investigated have not responded to this treatment, particularly the low-yield-point steels, but no data have been found for high-strength steels which did not show an improvement.

Wedemeyer also reported an average increase of 25 to 27 per cent in endurance limit when the process was applied to ground threads, and 12 to 20 per cent for cut threads, though in one case the increase amounted to 40 per cent. Bertram (22) and Staedel (23) have shown similar increases; in the former case the improvement being retained up to temperatures in the region of 1000 F, though to a lesser degree. It should be mentioned here that the improvement will be less marked in the presence of a decarburized surface layer.

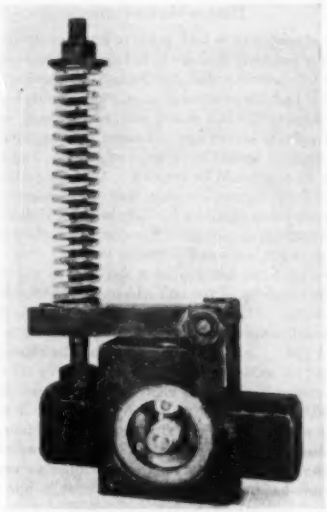

Fig. 3 Method of Rolling the Root Radius of Screw Threads on Bolts; From Horger (31)

Since the beneficial effect of rolling the thread roots is largely due to the residual surface compressive stresses induced thereby, it seems reasonable to expect that other processes producing a similar state of stress also might increase the strength of threaded members. Carburizing, cyaniding, and nitriding have been proved to develop compressive stresses in the surface layers and to improve the fatigue resistance in many cases, but little evidence is available regarding their application to bolts or studs. Schwartz (11) has stated that cyanide hardening effected an increase in the endurance limit for all types of threads (Whitworth, ANC, ANF, and HFR previously discussed) in laboratory tests. Furthermore, the cyanide-hardened bolts showed less breakages in service trials than similar bolts without the surface-hardening treatment.

On the other hand, Ritchie (24) has reported an example of rear-axle drive-shaft studs on trucks where those with a partially decarburized skin proved more satisfactory in service than those with a slightly carburized surface (0.004 in. deep). He considers that the lack of plasticity and the notch sensitivity of the hard skin is more detrimental than the lowered endurance limit resulting from decarburization, but emphasizes that his conclusion applies only to this specific case.

Generally, however, decarburization should be kept to a minimum particularly for high-duty bolts. For automotive bolts Jameson (25) gives limits of 0.008 in. for complete decarburization, and 0.015 in. for complete and partial decarburization. These limits seem to be fairly generous and would not be applica-

ble to highly stressed engine bolts where decarburization should preferably be completely eliminated. This may be done by centerless grinding or by recarburizing in a special controlled-atmosphere furnace.

Design Modifications

Various attempts have been made to improve the design of the bolt and nut assembly in order to reduce the stress-concentration effect and to render the load distribution more uniform. One of the points of high stress concentration which should be mentioned is the junction of the bolt shank and the underside of the head. From our general knowledge of fatigue it is apparent that the radius of the fillet should be as large as possible, and that rough-machining marks should be avoided. According to Staedel (23) the radius should be not less than 0.08 times diameter for small bolts, and 0.1 times diameter for bolts of $^3/_4$ in. in diam and over. This is particularly important in the case of the more notch-sensitive high-strength steels and eccentric loading.

Considerable attention has been devoted to methods for increasing the elasticity of the bolt which was shown earlier to be a desirable feature. Classical work in this direction was carried out by Staedel, some of whose results are illustrated in Fig. 4 (26) and Fig. 5 (26). In Fig. 4 the effect on the repeated impact fatigue limit of reducing the shank diameter in relation to the thread diameter is clearly demonstrated for three plain-carbon steels of 80,000 to 100,000 psi tensile strength. A marked improvement was obtained by reducing the shank diameter below the root diameter of the thread, though the increase in fillet radius under the head may have contributed to some extent. This principle has been incorporated successfully into the manufacture of connecting-rod bolts for many years. It is claimed that a similar improvement can be obtained by drilling a hole down the center of the bolt as far as the commencement of the thread.

Similar tests were used to show the effect of the length of free thread between the head of the bolt and the nut. In a particular example, increasing the length of free threads from $^9/_{64}$ in. to $2^3/_{32}$ in. doubled the fatigue resistance. This effect was confirmed subsequently by direct stress-fatigue tests, though the increase was not so marked. On the basis of these tests it was recommended that the free thread length should be at least equal to the bolt diameter. Thum (1) has shown that the endurance limit for a bolt threaded for only the thickness of the nut is about one third of that for a bolt with a free thread length of twice the thickness of the nut.

Other factors affecting the fatigue strength of the bolt and shown diagrammatically in Fig. 5, are the run-out angle of the thread, and the use of stress-relieving circumferential grooves. Staedel recommended that for optimum performance the former should not exceed 15 deg. The latter may be used under the head of the bolt (29) for special applications, and between the shank and the commencement of the thread, particularly where bending stresses are involved and where a completely "waisted" bolt is not practicable. The minimum diameter of the groove in the second case should be slightly less than the core diameter, and the length of the reduced section should be at least 0.5 times thread diameter with a good fillet (radius = 0.2 times thread diameter) at each end. For bolts used in centering and locating members, reduced sections may be provided between the fitted guide portions of the bolts as indicated in sketch F (Fig. 5).

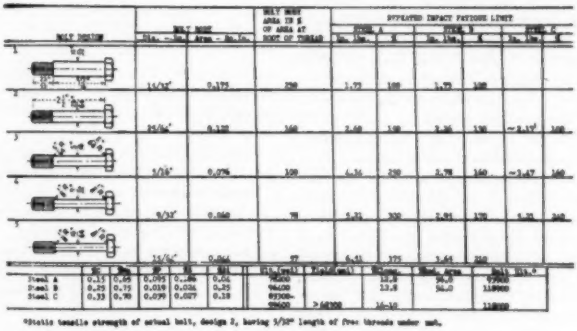

Fig. 4 Effect of Shank Diameter on Repeated Impact Fatigue Strength of Bolts; From Staedel

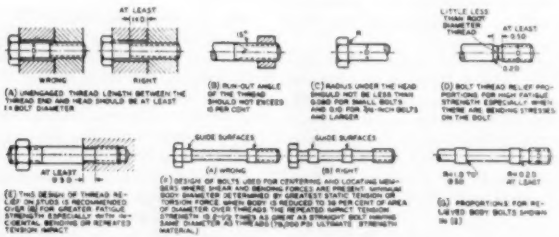

Fig. 5 Recommendations for Design of High-Duty Bolts; From Staedel

Similar remarks to those just made also apply in the case of studs. A typical stud design for high-strength purposes is illustrated in Fig. 6 (27). The shoulder enables the stud to be prestressed on assembly, and the provision of the reduced section above the thread for stress-relieving is consistent with good practice. The damping collar shown is to prevent the stud from vibrating, and should not be placed at $^1/_2$ or $^1/_4$ the distance from the nut to the joint surface, since it is claimed that these points may be nodes when vibration occurs.

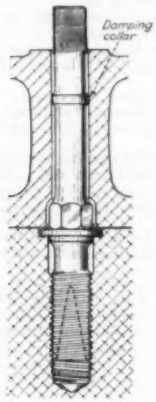

FIG. 6 RECOMMENDED STUD DESIGN

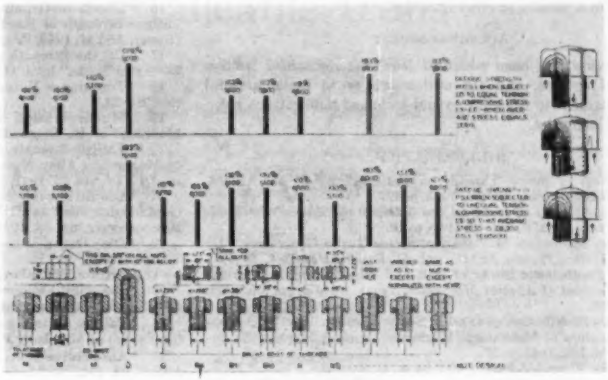

FIG. 7 FATIGUE STRENGTH OF VARIOUS THREADED JOINTS; FROM WIEGAND

In the particular case of a steel stud in an aluminum member, it was found experimentally that the stress in the aluminum increased steadily to a maximum adjacent to the bottom thread of the stud. Fatigue failures were also observed at this location. One method for improving the load distribution in this region is the use of hollow studs as shown in Fig. 6. This has the additional effect of making the stress distribution in the stud more uniform and thereby increasing its fatigue resistance. Another method proposed involves the use of a counterbored hole, the depth of which should be equal to the pitch diameter.

A considerable amount of study has been devoted to the improvement of the design of the nut, Wiegand (28) being particularly prominent in this respect. A summary of some of his work is shown diagrammatically in Fig. 7. One of the designs embodied an annular groove in the base of the nut, and the depth of this groove was found to be important. The maximum increase obtained in the endurance limit was 30 per cent, which confirms the results of photoelastic experiments.

The use of 10-deg thread relief alone gave an increase of 10 per cent, the fatigue tests being carried out under direct stress. In the same diagram can be seen the marked improvement produced by changing to a nut material of lower modulus of elasticity such as cast iron. It is interesting to note that by packing a material such as hemp in the thread, a considerable improvement in strength is also obtained.

Hetenyi (4) was able to reduce the stress concentration at the root of the bolt thread near the base of the nut by two changes in design, the first incorporating a tapered thread and the other a tapered lip; the latter design is sometimes known as the tension nut (Fig. 8). His technique was that of three-dimensional photoelasticity, and the stress-concentration factors reported were 3.85 for a conventional nut, 3.10 for a nut with tapered thread, and 3.00 for a nut with tapered lip. Theoretically, the tapered-thread nut will give its best performance at a particular value of the bolt load, whereas the effectiveness of the second design will be about the same at any value of the load. The only problem in the latter case is that of providing proper support for the nut under the flanges.

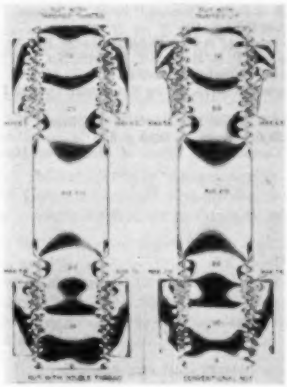

FIG. 8 PHOTOELASTIC STUDY OF NUTS WITH TAPERED THREAD AND LIP; FROM HETENYI

On theoretical grounds it has been suggested by Goodier (2) that rounding the base of the nut would improve the load distribution by permitting more radial expansion. Also, that making axial cuts into the wall of the nut from the outside would have the same effect, due to the increase in bending flexibility. No practical evidence, however, is available on these points.

With regard to the optimum thickness of the nut, the consensus of opinion seems to be in favor of a value equal to 0.7 to 0.8 times bolt diameter.

CONCLUSION

The primary purpose of this paper is to provide adequate, up-to-date information for the machine designer with respect to high-duty threaded connections under repeated loading. It will

be realized that many factors are involved, some metallurgical, some geometrical, some in the manufacturing procedure, and some in the assembly. Probably the most important individual factor is the necessity for insuring and maintaining sufficient tightness, but the neglect of any one factor may be responsible for a fatigue failure. Provided due attention is paid to the basic principles brought out in the text, little difficulty should be experienced in obtaining an efficient design.

ACKNOWLEDGMENT

This review has been compiled from data obtained from a variety of sources, and the author wishes to make grateful acknowledgment to the authors and technical publications given in the Bibliography.

BIBLIOGRAPHY

1 "Effect of Screw Threads on Fatigue," by S. M. Arnold, *Mechanical Engineering*, vol. 65, 1943, p. 497.

2 "Distribution of Load on the Threads of Screws," by J. N. Goodier, Trans. ASME, vol. 62, 1940, p. 10.

3 "The Mechanics of Plate Rotors for Turbo Generators," by J. P. Den Hartog, Trans. ASME, vol. 51, Paper APM-51-1, 1929.

4 "A Photoelastic Study of Bolt and Nut Fastenings," by M. Hetenyi, *Journal of Applied Mechanics*, Trans. ASME, vol. 65, 1943, pp. A-93–100.

5 "The Distribution of Load in Screw Threads," by D. G. Sopwith, Institution of Mechanical Engineers, Applied Mechanics Proceedings, vol. 159, 1948, p. 373.

6 "Why Threaded Parts Fail," by A. G. Solakian, *Product Engineering*, July, 1933, p. 261.

7 "Effect of Grooves, Threads, and Corrosion Upon the Fatigue of Metals," by R. R. Moore, Proceedings of the ASTM, 1926, part 2, p. 255.

8 "Strength of Screw Threads," by R. R. Moore, *Product Engineering*, November 1939, p. 475.

9 "The Strength of Screw Threads Under Repeated Tension," by H. F. Moore and P. E. Henwood, Bulletin No. 264, University of Illinois Engineering Experiment Station.

10 "La Fatigue des Métaux," by R. Cazaud, Dunod, Paris, France, 1948, p. 165.

11 "New Thread Form Reduces Bolt Breakage," by A. Schwartz, Jr., *Steel*, vol. 127, September 4, 1950, p. 86.

12 "Screw Threads—the Effect of Method of Manufacture on Fatigue Strength," by A. M. Smith, *Iron Age*, vol. 156, August 22, 1940, p. 23.

13 "Tests Prove Worth of Cold Extruded Bolts," by A. S. Jameson, J. A. Halgren, and S. A. Sheridan, *Iron Age*, vol. 166, June 22, 1950, p. 81, and June 29, 1950, p. 72.

14 "Rolling of Screw Threads," by H. Dinner and W. Felix, Technische Rundschau Sulzer, No. 1, 1945, p. 131.

15 "How Processing Affects Bolt Fatigue Strength," by N. B. Green, *Machine Design*, December, 1947, p. 138.

16 "Effects of Grinding and Other Finishing Processes on the Fatigue Strength of Hardened Steel," by L. P. Tarasov and H. J. Grover, ASTM, 1950, Preprint No. 18.

17 "On the Strength of Highly Stressed, Dynamically Loaded Bolts and Studs," by J. O. Almen, *SAE Journal*, April, 1944.

18 "Torquing of Nuts in Aircraft Engines," SAE Special Publication, SP-23.

19 "Mutterwerkstoff und Dauerhaltbarkeit der Schraubenverbindung," by H. Wiegand, *Zeitschrift VDI*, vol. 83, 1939, p. 64.

20 "Fatigue Strength of Steel Bolts and Studs Fitted With Steel or Magnesium Alloy Nuts," by F. Kaufmann and W. Jäniche, *Zeitschrift VDI*, vol. 85, 1941, p. 504.

21 "Die Steigerung der Dauerhaltbarkeit von Schrauben durch Gewinde drücken," by E. Wedemeyer, *Mitteilungen des Wöhler-Inst.*, Braunschweig, no. 33, 1938, p. 3.

22 "Die Dauerhaltbarkeit von Gewinden bei verschiedenen Temperaturen und ihre Beeinflussung durch Oberflachendrücken," by W. Bertram, *Mitteilungen des Wöhler-Institute*, no. 37, 1940, p. 3.

23 "Dauerfestigkeit von Schrauben," by W. Staedel, *Mitteilungen der Materialprüfungsanstalt*, Darmstadt, Germany, vol. 4, 1933.

24 "Fatigue of Bolts and Studs," by J. G. Ritchie, Symposium on the Failure of Metals by Fatigue, Melbourne, Australia, 1946, p. 260.

25 "Automotive Bolts," by A. S. Jameson, *Iron Age*, vol. 161, August 23, 1945, p. 64.

26 "Photoelasticity as Applied to Design Problems," by O. J. Horger and T. V. Buckwalter, *Iron Age*, vol. 156, May 23, 1940, p. 42.

27 "Design of Highly Stressed Studs to Improve Their Fatigue Strength," *Product Engineering*, May, 1943, p. 288.

28 "Über die Dauerfestigkeit von Schraubenwerkstoffen und Schraubenverbindungen," by H. Wiegand, Bauer and Schaurte A.G., Neuss, Germany, 1934.

29 "Improving Bolt Performance," by A. R. Anderson, *Product Engineering*, May, 1949, p. 109.

30 "Engineering Aspects of Bolt Variables," by V. E. Hillman, *Iron Age*, vol. 163, November 20, 1947, p. 62.

31 "Stressing Axles by Cold Rolling," by O. J. Horger, Surface Stressing of Metals, ASM, 1947.

Comparative Surface-Hardening Characteristics of Commercial Pearlitic Malleable Irons

By S. H. BUSH,[1] W. P. WOOD,[2] and F. B. ROTE,[3] ANN ARBOR, MICH.

Nine pearlitic malleable irons, produced by commercial foundries and exhibiting wide differences in chemical composition, production practices, and microstructures have been investigated to determine the hardness and effective case depth with different surface-hardening heat-treatments. Flame- and induction- (3000, 9600, and 300,000 to 347,000 cycle) heating, followed by oil, water, or spray quenches have been used for the surface-hardening treatments. Case hardness and depth were determined by superficial Rockwell or Rockwell C measurements and metallographic examination of etched specimens. Of the structures investigated, one, a dense pattern of extremely small spheroids of cementite, was most responsive to all types of treatment. However, it was found in surface-hardening that at all frequencies an optimum power input existed which minimized the influence of microstructure to a pronounced degree.

Introduction

An examination of the literature reveals that no systematic investigation has been made of the effect of heating cycle and microstructure on the hardness and case depth of pearlitic malleable irons. The effect of these variables, when surface-hardening with high or low-frequency induction or flame-hardening equipment, is of importance due to the increased use of pearlitic malleable iron in automobile camshafts, refrigerator crankshafts, or other pieces of equipment where a hard surface and a tough case are necessary.

Nine irons manufactured to conform to ASTM specification A220-48T were selected for the investigation. The entire range of microstructure, chemical composition, and malleabilizing cycle normally experienced in pearlitic malleable irons were represented in these nine irons. Their properties are shown in Fig. 1 and in Table 1.

Several variables were examined to determine their effect on the hardness and depth of case obtained. These variables included the type of heat-treatment (i.e., flame and induction-hardening at high or low frequency), rate of power input, time of heating, surface temperature, and type of quench. These variables cover the normal industrial conditions encountered in the surface-hardening of pearlitic malleable irons. From these data it is possible to select the most favorable conditions for surface-hardening as well as the optimum microstructure for such hardening.

The Research Committee of the Malleable Division of the American Foundrymen's Society, who initiated and sponsored this research project, considered that these variables covered the factors of commercial importance.

Materials

Nine irons were supplied by the following foundries:

1 Belle City Malleable Iron Company.
2 Central Foundry Division, General Motors Corporation.
3 Chain Belt Company.
4 Deere and Company.
5 Link Belt Company.
6 National Malleable and Steel Castings Company.

These irons were the standard products of the participating foundries.

The nine irons, coded A, B, D, E, H, K, M_1, M_2, and Y could be divided into four broad microstructural classifications. These four general classifications are as follows:

1 A finely spheroidized cementite structure (iron Y).
2 A fine to medium pearlite partially decomposed to spheroidized cementite (irons A, B, D; iron E approximates this structure).
3 A coarse pearlite partially decomposed to spheroidized cementite with a pronounced bull's-eye pattern (irons H, M_2).
4 A coarsely spheroidized structure (irons K, M_1).

Typical microstructures are shown in Fig. 2 at 1000 diam for irons Y, A, K, and M_2.

Prior to heat-treatment the bars were machined to 1 in. diam from an as-cast diameter of $1^1/_8$ to $1^3/_8$ in. This gave a uniform smooth, machined surface for the heat-treatment. The bars were 8 in. in length after machining.

Equipment and Procedures

3000-Cycle Induction-Heating. Tests at 3000 cycles were run in a 150-kw unit at the Tocco Division of the Ohio Crankshaft Company. A single-turn coil capable of heating a zone about 1 in. in width was coupled to the generator. A perforated plate was an integral portion of the coil, allowing the samples to be spray-quenched with no delay, at the end of the heating cycle. Three tests were run on each bar, permitting a better comparison of response to hardening, since the differences from bar to bar were eliminated. Test bars were heated as follows:

25 kw for 7 sec
50 kw for 3.5 and 4.0 sec
75 kw for 2.25 sec
100 kw for 1.5 and 2.0 sec

9600-Cycle Induction Heating. A 150-kw experimental motor-generator unit was used for tests at 9600 cycles. The same single-turn coil used at 3000 cycles was also used at 9600 cycles. Sam-

[1] Research Fellow, Department of Chemical and Metallurgical Engineering, University of Michigan.
[2] Professor of Metallurgical Engineering, University of Michigan.
[3] Associate Professor of Metallurgical Engineering and Metal Processing, University of Michigan.

Contributed by the Metals Engineering Division and presented at the Annual Meeting, New York, N. Y., November 26–December 1, 1950, of The American Society of Mechanical Engineers.
Note: Statements and opinions advanced in papers are to be understood as individual expressions of their authors and not those of the Society. Manuscript received at ASME Headquarters, May 4, 1951.

TABLE 1 PROPERTIES OF THE AS-RECEIVED PEARLITIC MALLEABLE-IRON BARS

Type	Typical analysis C	Si	Mn	P	S	Cr	Melting procedure	Malleabilization cycle	Microstructure	Average Brinell hardness	Range of Brinell hardness	ASTM Classification[a]
A	2.60	1.40	0.42	0.06	0.12	0.025	Duplex (cupola electric)	12 hr at 1750 F; air quench; draw at 1225 F	Bull's-eye 50% fine-medium pearlite 50% spheroidized cementite	208	199–219	48005
B	2.42	1.47	0.48	0.09	0.15	0.03	Duplex (cupola air)	16 hr at 1750 F; still air from 1600 F; draw 1240 F for 6 hr	Bull's-eye 70% medium pearlite 30% spheroidized cementite Some massive cementite	211	193–232	48005 or 60003
D	2.20	0.90	0.78	0.15	0.122	0.017	Air furnace	50 hr to 1600 F, 45 hr at 1600 F, cool to 1320 F in 32 hr; hold between 1270 F–1320 F for 24 hr; cool from 1270 F–1200 F in 8 hr	No bull's-eye 75% spheroidized cementite Small islands of medium pearlite	196	182–204	48005
E	2.35	1.00	0.30	0.16	0.06	...	Air furnace	Completely malleabilized, followed by heat to 1475 F 15 min, and oil quenching; draw—1200 F	No bull's-eye Spheroidized or chainlike structure of carbide at ferrite grain boundaries	187	179–206	43010
H	2.35	1.05	1.05	0.12	0.15	...	Triplex (cupola air-electric)	1st stage 1800 F; oven 187–206 cooled to 1400 F, 4 deg per hr, 1400–1300 F; total time, 100–140 hr	Bull's-eye Medium pearlite surrounded by ferrite. Some spheroidized cementite. Many inclusions	198	187–206	48005
K	2.41	0.94	0.70	0.16	0.10	0.015	Air furnace	50 hr to 1600 F; 45 hr at 1600 F; cool to 1320 F in 32 hr; hold between 1270 F–1320 F for 24 hr; cool from 1270 F–1200 F in 8 hr	No bull's-eye 80–90% spheroidized cementite a few scattered lamellae	183	170–192	43010
M_1	2.50	1.05	0.50	0.135	0.175	0.030	Duplex (cupola-air)	1800 F maximum, 30 hr above 1500 F oil quench; draw 2½ hr at 1280 F	Completely spheroidized. Very irregular graphite	188	183–192	43010
M_2	2.50	1.05	0.75	0.135	0.175	0.030	Duplex (cupola-air)	1700 F maximum; 65 hr above 1500 F; furnace cool	Large bull's-eyes Pearlite; coarse and largely decomposed. Mainly spheroidized cementite	191	183–204	43010
Y	2.69	1.40	0.43	0.06	0.12	0.025	Duplex (cupola electric)	12 hr at 1750 F; air-quenched from 1650 F; reheat to 1550 F; hold 45 min; oil-quenched; draw 3 hr at 1230 F	No bull's-eye Dense pattern of finely spheroidized cementite	234	223–248	60003

[a] ASTM Specification A220-48T—Classification based upon Brinell hardness of the irons.

ples were spray-quenched, as in the case of the 3000-cycle unit. Three tests were run on each bar, permitting a better comparison. Test bars were heated at a power input as follows:

32 kw for 3, 4, and 5 sec
50 kw for 2 sec
75 kw for 1.5 and 2 sec

High-Frequency Induction-Heating. High-frequency induction heating tests were conducted at the Westinghouse Corporation, Baltimore, Md. A unit operating at 300,000 to 347,000 cycles at a rating of 100 kva was used for the tests. A single-turn copper coil was used in conjunction with a spindle for rotating the piece, and a perforated plate was coupled to the coil for spray-quenching. A zone of about 1 in. in width was heated so three tests could be made on each bar.

Test bars were heated as follows:

60.1 kva, 300 kc, for 3.0 and 3.5 sec
35.5 kva, 347 kc, for 5.0 and 5.7 sec
51.5 kva, 347 kc, for 3.5, 4.0, 4.5, and 5.0 sec
91.8 kva, 347 kc, for 1.5, 1.75, and 2.0 sec

Flame Heating. Flame-hardening tests were carried out on Flamatic units of the Cincinnati Milling Machine Company. These units were equipped with a pyrometer to control electronically the length of the heating cycle and the maximum surface temperature. Temperatures given in the report were those indicated by the pyrometer. The bars were rotated between the torches during heating and quenched immediately into still oil, agitated oil at 125 F (51 C), or agitated water. The rate of heating was controlled by the spacing between tips and piece. Tests were made at indicated temperatures of 1450 F (788 C), 1500 F (815 C), and 1600 F (870 C).

Test Procedures

A longitudinal hardness survey was made on the heat-treated sections to locate the point of maximum surface hardness. The bars were sectioned transversely at this point for a transverse hardness survey and macroetching. The samples were etched with 15 per cent nitric acid to determine the case depth which was compared with the results obtained from a superficial Rockwell and a Rockwell C survey. Two or three series of hardness tests were run in the form of skew curves extending from the surface to the interior beyond the edge of the hardness zone denoted by the macroetch.

The Rockwell C hardness values were plotted versus the radial distances of the penetrations from the surface. Hardness of bars from the same foundry heat, when heat-treated in the same fashion, were plotted together. The hardness-depth data fell within a band 2 to 6 points Rockwell C in width and similar in shape to a hardenability band. The median lines of these bands, as well as the width of the hardness band at 50 Rockwell C, and the range of Rockwell C hardness at 0.060 in., were used as a means of comparing the irons; these irons were surface-hardened

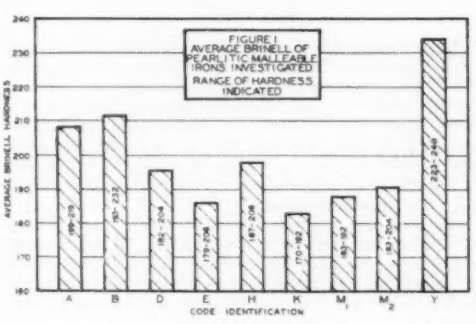

FIG. 1

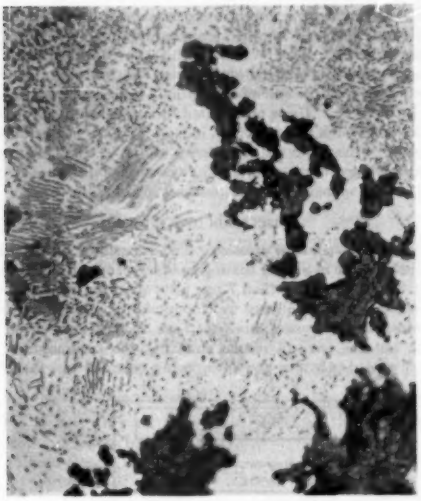

(a) Code A Iron

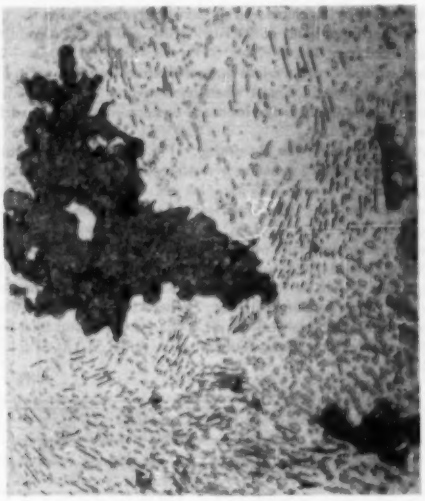

(b) Code K Iron

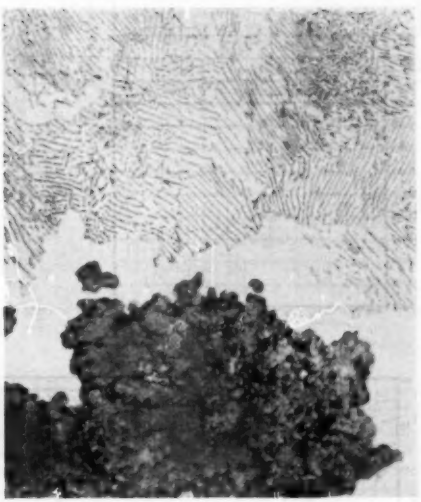

(c) Code M_3 Iron

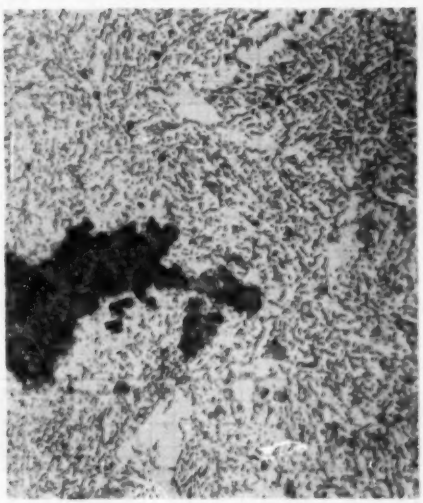

(d) Code Y Iron

FIG. 2 TYPICAL MATRIX MICROSTRUCTURES OF PEARLITIC MALLEABLE IRONS INVESTIGATED; PICRAL ETCH; ×1000

in the same fashion to compare the effect of different heating cycles.

RESULTS

Criterion. Arbitrary limits of 50 Rockwell C at a depth of 0.060 in. were selected as a standard for purposes of comparing the response of the various irons to the power inputs, heating times, and quenching media investigated.

On this basis the most favorable case would be one measuring 50 Rockwell C at 0.060 in. and dropping rapidly to the hardness of the untreated bar. In some bars, cases were less than 0.060 in., and in several instances the total case depth was very pronounced.

3000-Cycle Induction Hardening. The results of three of the series of experiments are given in Fig. 3. The range of hardness at 0.060 in., that is, the width of the hardness band at 0.060, as

determined by the hardness surveys, is given as well as the width of the hardness band at 50 Rockwell C. The three conditions considered were 25 kw—7 sec, 50 kw—3.5 sec, and 100 kw—2 sec. The hardness-depth median lines of the four irons shown in Fig. 2 are also plotted in Fig. 4 when hardened at 50 kw for 3.5 sec. These results indicate the influence of microstructure on surface-hardening.

9600-Cycle Induction Hardening. Fig. 5 shows results obtained under three of the conditions investigated. These were 32 kw—4 sec, 50 kw—2 sec, and 75 kw—1.5 sec. The effect of increased power is obvious. A comparison is again made in Fig. 6 between the four irons (Y, A, K, M_2) at 50 kw—2 sec to denote the effect of microstructure on the response to hardening.

300,000 to 347,000-Cycle Induction Heating. The effect of slight increases in the length of the heating cycle, as well as changing the power is shown in Fig. 7 where the conditions investigated were 51.5 kva—4.0 sec, 51.5 kva—4.5 sec, and 91.8 kva—2.0 sec. Fig. 8 compares four irons (Y, A, K, M_2) at 51.5 kva—4.0 sec.

Flame Hardening. Initial tests were made to determine the optimum indicated surface temperature for hardening. The most satisfactory was found to be 1500 F (815 C). Tests were made, using still oil, agitated heated oil, and agitated water quenches. Neither still oil nor agitated heated oil were found to be satisfactory. Using an agitated water quench, two runs were made with torch settings of $^9/_{16}$ in. and $^3/_4$ in. from tips to piece. Results of these two tests are shown in Fig. 9. The influence of microstructure is shown in Fig. 10 where the four irons (Y, A, K, M_2) are compared at a tip to piece setting of $^3/_4$ in.

Discussion of Results

3000-Cycle Induction Heating. The importance of attaining a proper balance in time of heating and power input is illustrated in Fig. 3. At times less than 7 sec, tests at 25 kw were uniformly unsatisfactory. The cases were nonuniform both with respect to hardness and microstructure. At 7 sec, the criteria set were met with but the over-all results were not too satisfactory. The total case depth was excessive, being over 0.2 in. At higher

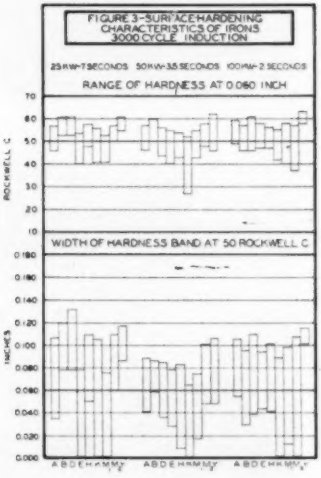
FIGURE 3-SURFACE HARDENING CHARACTERISTICS OF IRONS 3000 CYCLE INDUCTION
25 KW-7 SECONDS 50 KW-3.5 SECONDS 100 KW-2 SECONDS
RANGE OF HARDNESS AT 0.060 INCH
ROCKWELL C
WIDTH OF HARDNESS BAND AT 50 ROCKWELL C
INCHES
A B D E H K M M Y

Fig. 3

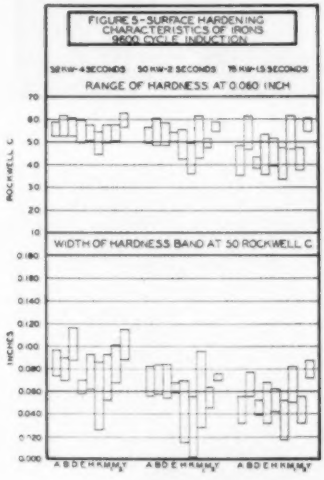
FIGURE 5-SURFACE HARDENING CHARACTERISTICS OF IRONS 9600 CYCLE INDUCTION
32 KW-4 SECONDS 50 KW-2 SECONDS 75 KW-1.5 SECONDS
RANGE OF HARDNESS AT 0.060 INCH
ROCKWELL C
WIDTH OF HARDNESS BAND AT 50 ROCKWELL C
INCHES
A B D E H K M M Y

Fig. 5

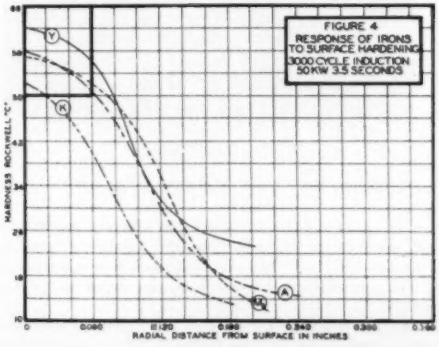

Fig. 4

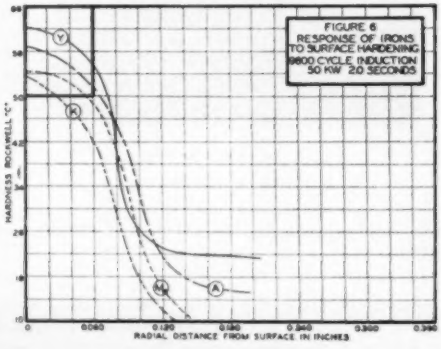

Fig. 6

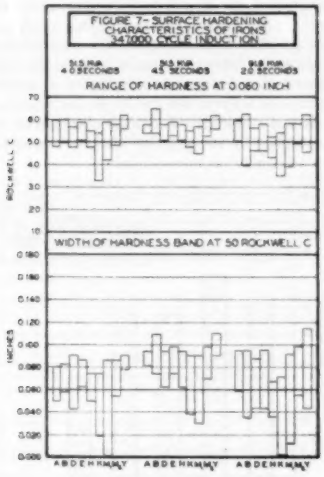
FIGURE 7- SURFACE HARDENING CHARACTERISTICS OF IRONS 347000 CYCLE INDUCTION
5.5 KVA 4.0 SECONDS
5.5 KVA 4.5 SECONDS
9.8 KVA 2.0 SECONDS
RANGE OF HARDNESS AT 0.060 INCH
ROCKWELL C
WIDTH OF HARDNESS BAND AT 50 ROCKWELL C
INCHES
A B D E H K M M Y

FIG. 7

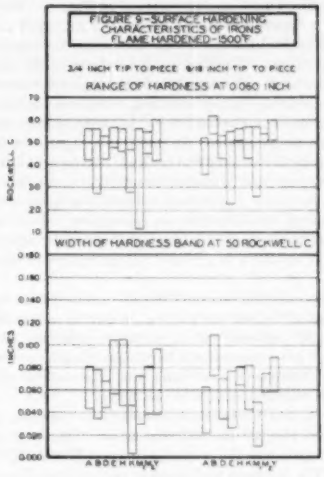
FIGURE 9- SURFACE HARDENING CHARACTERISTICS OF IRONS FLAME HARDENED-1500°F
3/4 INCH TIP TO PIECE 9/8 INCH TIP TO PIECE
RANGE OF HARDNESS AT 0.060 INCH
ROCKWELL C
WIDTH OF HARDNESS BAND AT 50 ROCKWELL C
INCHES
A B D E H K M M Y

FIG. 9

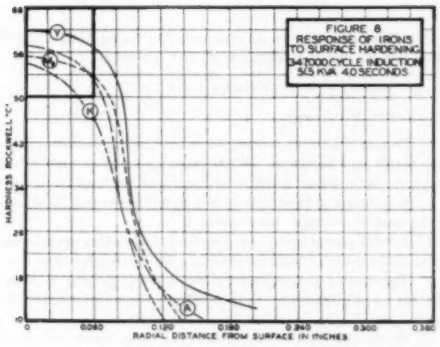
FIGURE 8 RESPONSE OF IRONS TO SURFACE HARDENING 347000 CYCLE INDUCTION 5.5 KVA 4.0 SECONDS
HARDNESS ROCKWELL "C"
RADIAL DISTANCE FROM SURFACE IN INCHES

FIG. 8

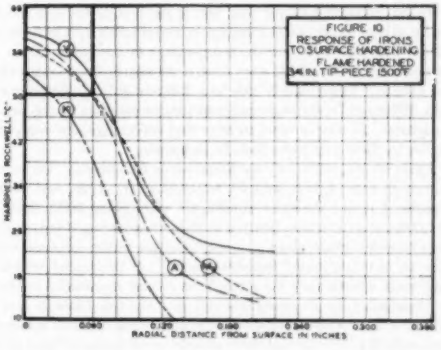
FIGURE 10 RESPONSE OF IRONS TO SURFACE HARDENING FLAME HARDENED 3/4 IN TIP-PIECE 1500°F
HARDNESS ROCKWELL "C"
RADIAL DISTANCE FROM SURFACE IN INCHES

FIG. 10

power inputs total case depth was not as excessive as was the case at 25 kw, but it was necessary to control the heating time to keep the case depth within limits. In general, the spread of the hardness data was quite pronounced. Since this occurred in all tests at 3000 cycles, it is believed that it is a characteristic of this frequency: At very high power input it is necessary to control the time closely to prevent sweating of the bars.

9600-Cycle Induction Heating. As in the case with tests at 3000 cycles, the heating time at low power input, e.g., 32 kw, must be of fairly long duration, if a hardness of 50 Rockwell C at 0.060 in. is to be obtained. In meeting this specification the case depth again becomes excessive.

At 50 kw—2 sec, conditions were generally satisfactory. The criteria were satisfied, the total case depth was not excessive, and the irons, with the exception of K, proved to be satisfactory. At higher power inputs the heating time becomes more critical, and it becomes more difficult to harden the majority of the irons satisfactorily, based upon the criteria established. A variation in heating time of 0.5 sec at 75 kw is sufficient to alter conditions so that six out of nine irons were unsatisfactory at the shorter time (1.5 sec), while all exceed the specification at 2.0 sec, and the case depth is not excessive. No difficulty was experienced with sweating or exfoliation in tests at 9600 cycles.

300,000 to 347,000-Cycle Induction-Heating. At lower power inputs the variation in hardness and depth from iron to iron is excessive. When heating times are long enough to satisfy the criteria of 50 Rockwell C at 0.060 in., the over-all case depth is excessive. Increasing the power cuts down on the time and there appears to be an optimum operating power at about 50 kva where the cases are most satisfactory on the basis of uniformity, hardness, over-all depth, and partial elimination of microstructure as a variable. At higher power inputs the variation in response from iron to iron under the same conditions again becomes excessive, and heating time is critical, since it is extremely easy to overheat and badly burn the bars. In some cases, at very high power input the bars sweated badly, and the surface was actually porous, evidently due to burning out the graphite.

Flame Hardening. Results of experiments conducted at the

Cincinnati Milling Machine Company appear in Fig. 9. Tests were conducted on a flame-hardening machine using oxygen and acetylene, and equipped with a ray-o-tube pyrometer for control of the surface temperature. The depth and hardness of the case were fixed by the distance separating the test bar and the torch heads. The flame used was slightly oxidizing. Since the pyrometer controlled the torches electronically, all tests supposedly were run at the same temperature. An initial investigation indicated that the temperature setting was critical. Tests made at a setting of 1600 F were uniformly unsatisfactory, due to overheating, which caused incipient fusion and converted a large area adjacent to the surface to white iron on quenching. Tests at 1450 F were likewise unsatisfactory because the irons were still in the two-phase region, resulting in a mixed microstructure of nonuniform hardness.

Tests made to determine the practicability of various quenching media indicated that a violent quench, e.g., water, is necessary. Quenching in still oil, agitated oil at room temperature, and agitated oil at 125 F gave nonuniform hardness owing to a mixture of pearlite and martensite, indicating that the cooling rate was not fast enough to miss the nose of the S-curve.

Both tests at $^3/_4$ in. and $^9/_{16}$ in. show considerable variation in the response to hardening of the different irons. One item of interest was noted; that was the response of irons H and M_2 to flame-hardening. The hardness and depth of case of irons H and M_2 were much higher as compared to the other irons than occurred in the induction-hardening experiments. This is believed to be due to three factors; the first of these is inherent in the flamatic unit. Since the heating cycle is controlled by a pyrometer, the heating time to attain the temperature desired may vary. In this case irons H and M_2 were heated for nearly 2 sec longer than the others. This could be due to a different surface emissivity or to a difference in chemical composition, or possibly to the microstructure. It is of interest to note that the manganese content is higher in these two irons than in the others.

Effect of Microstructure on Response to Hardening. On examination of Figs. 4, 6, 8, and 10, where irons Y, A, K, and M_2 are compared under the same conditions when using 3000, 9600, or 347,000-cycle induction heating or flame hardening, it is apparent that microstructure plays an important role in the response of an iron to any particular heat-treatment. A treatment which is uniformly satisfactory for irons Y or A may invariably prove to be unsatisfactory for irons M_2 and K. On this basis it can be said that irons with a microstructure consisting of finely spheroidized carbides (Y) respond most readily to all forms of heat-treatment; a microstructure consisting of medium to fine pearlite plus some spheroidized carbides responds quite readily to the various forms of heat-treatment (irons A, B, D, E). In general, these irons proved to be more sensitive to differences in power or frequency, showing considerable variation from one condition to another.

Irons H and M_2, characterized by a microstructure made up of coarse pearlite together with pronounced bull's-eyes, are much less responsive to the various forms of induction heat-treatment; they respond satisfactorily to flame-hardening.

Irons K and M_1 were least satisfactory. In general, the response of these irons, whose microstructure consisted of a ferritic matrix containing coarsely spheroidized carbides, was very sluggish.

A comparison of the response of the different irons is given in Fig. 11. The values were obtained from a system of weighted averages based on two criteria, the media hardness of the band at a depth of 0.060 in. from the surface and the median depth of the hardness band at a hardness of 50 Rockwell C. The iron having the greatest hardness at 0.060 in. was given the value 1, and succeeding irons were given the values 2, 3, 4, 5, 6, 7, 8, and 9, where 9 represented the iron with the lowest hardness at 0.060 in. In like fashion, the iron having a value of 50 Rockwell C at the greatest depth was given the value 1; the least depth would then be 9. Since 27 conditions were investigated, the best possible total value would be 54, the worst possible value 486. The difference between 486 and 54 divided into the difference between 486 and the weighted average obtained for each iron, and then multiplied by 100 gave the per cent response of each iron, based on all conditions investigated.

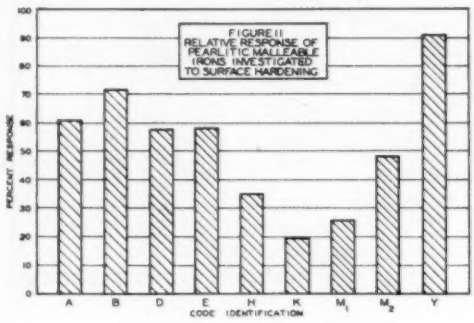

FIG. 11

Iron Y was superior to all others with a rating of 91.3 per cent while iron K was least effective at 19.8 per cent.

CONCLUSIONS

Induction Hardening:

1 Proper time and powers were controlling factors in fixing case depth and hardness. When time and power were selected properly, satisfactory results were obtained with all irons tested.

2 A sufficiently hard case at low power input can be obtained at the cost of excessive case depth.

3 At high power inputs the length of the heating cycle must be controlled closely to prevent sweating due to overheating.

4 The spread in hardness values is much greater at 3000 or 300,000 to 347,000 cycles than at 9600 cycles under most of the conditions investigated.

5 By the proper selection of the operating power, it is possible to minimize the effect of microstructure on response to hardening.

6 An increase in heating time or in power input produced higher case hardnesses, deeper cases, and a more homogeneous microstructure.

7 Chemical composition within the limits investigated had no noticeable effect on the response of the iron to hardening.

8 A microstructure consisting of a dense pattern of finely spheroidized cementite consistently yielded the highest hardnesses at 0.060 in. and maximum depth of case at a value of 50 Rockwell C over the range of power and time investigated at frequencies of 3000, 9600, and 300,000 to 347,000 cycles.

9 A microstructure consisting of a matrix of ferrite and coarsely spheroidized cementite proved to be least satisfactory over the range of power and time investigated at frequencies of 3000, 9600, and 300,000 to 347,000 cycles.

Flame Hardening:

1 Temperature control is critical because of the necessity for adequate homogenization of the austenite which requires a certain minimum temperature, and the danger of fusion which establishes a maximum possible temperature.

2 An increase in heating time produces a more uniform and deeper-hardened case.

3 To meet the specifications of 50 Rockwell C at 0.060 in., a water quench is necessary. A still oil quench and a violently agitated heated oil quench were both unsatisfactory for the irons investigated.

4 All irons were hardened satisfactorily under selected conditions. Variations from these conditions produced variations among the irons.

5 In flame-hardening apparatus in which the maximum temperature is electronically controlled, a variation in heating time was noted from iron to iron under similar conditions. Irons containing a higher percentage of manganese and having a coarse lamellar structure came to temperature more slowly, resulting in deeper, harder, more uniform cases.

6 A microstructure consisting of a dense pattern of finely spheroidized cementite proved to be consistently most satisfactory under all conditions investigated.

7 A microstructure made up principally or completely of coarse spheroids of cementite proved least satisfactory under the conditions investigated.

Acknowledgments

The authors express their appreciation to the following persons:

The members of the American Foundrymen's Society Malleable Iron Research Committee for their advice and assistance in preparing the report. They are: C. F. Joseph, chairman; W. D. McMillan, vice-chairman; H. Bornstein, W. A. Kennedy, C. F. Lauenstein, R. Schneidewind, and M. Tilley.

Milton Garvin of the Flamatic Division, Cincinnati Milling Machine Company, for assistance and advice concerning flame-hardening.

J. T. Sabol and W. E. Benninghoff, Tocco Division of the Ohio Crankshaft Company, for the assistance and advice in 3000 and 9600-cycle induction-hardening.

John Edwards and T. P. Kinn, of the Westinghouse Corporation, for their assistance and advice in high-frequency induction-hardening.

Belle City Malleable Company, Central Foundry Division, General Motors Corporation, Chair Belt Company, Deere and Company, Link-Belt Company, and National Malleable and Steel Castings Company, for contributing the pearlitic malleable iron bars for the investigation.

J. Bates, J. Betts, R. Bush, B. Davidson, R. Eichbauer, K. Packer, C. Perry, C. Rudy, G. Sloane, L. Stair, and W. Steupker, engineering students of the University of Michigan, who assisted in making mechanical tests and photomicrographs.

Dynamic Force Reactions in Double-Ported Control Valves

By C. F. KING[1] and G. F. BROCKETT,[2] MARSHALLTOWN, IOWA

Torsional force reactions on V-port inner valves, and vertical force reactions on plug-type inner valves in double-ported control-valve bodies are of sufficient magnitude to cause concern if pressure drop is high. These forces are proportional to the mass velocity of the flowing fluid. It is possible to design inner valves so that these forces will be reduced to a point where they are not objectionable.

A CONTROL valve is normally the final control element in an automatic controller, and its function is to control continuously the rate of flow of a fluid in accordance with the dictates of a controlling instrument. The control valve accomplishes this by positioning an inner valve or plunger, which varies the area through which the fluid or control agent must pass.

The double-ported or semibalanced valve body is the type of control-valve construction that will be considered in this paper. Because of the balancing action of the two inner valve disks, the double-ported valve body is capable of handling relatively high pressure drops; hence its use has become widespread. The net unbalanced force that is transmitted to the valve stem of the double-ported semibalanced control valve when closed is easily calculated, and is vertical in direction. However, when the inner valve is open, the vertical forces that are imposed upon the inner valve by the flowing fluid, and transmitted to the valve stem, are not easy to predict and may be of such magnitude as seriously to affect the ability of the conventional operator to position the inner valve correctly. Also the impingement of the flowing fluid against certain types of inner valves will create pulsating torsional forces that oftentimes are great enough to cause mechanical failure of the valve structure.

It is possible to overcome these forces by the utilization of powerful operators and heavy valve components, but it appears that a more satisfactory and economical approach to the problem would be to minimize, or eliminate the objectionable force reactions within the valve body itself. With this in mind, a research program was instituted in which a study of these forces resulted in solutions which successfully minimized the force reactions caused by a dynamic fluid flow through a double-ported control-valve body. The results of the research program are presented in this paper.

The measurement of the vertical and rotational forces acting on the inner valve stem was accomplished by the use of Baldwin Southwark SR4 wire-resistance-type strain gages and a Hathaway galvanometer-type recording oscillograph. The strain gages and oscillograph are standard laboratory equipment, and will require no further comment, but a word of explanation on the measuring elements to which the strain gages were adapted is in order.

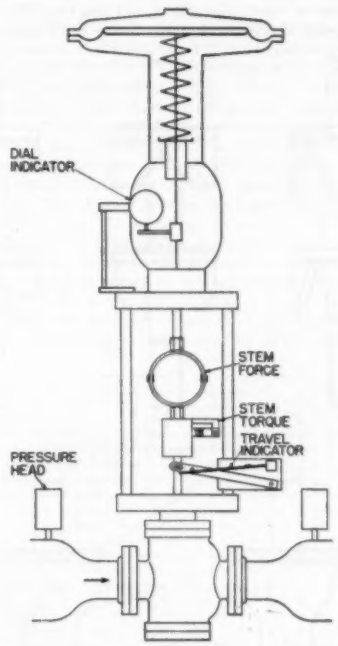

FIG. 1 DIAGRAMMATIC SKETCH OF FORCE-MEASURING EQUIPMENT

The assembled measuring equipment mounted on a valve body is illustrated diagrammatically in Fig. 1.

Pressures were measured by the use of pressure heads, each consisting of a diaphragm acting upon a proving ring, to which four strain gages were cemented. Torsional forces on the valve stem were measured by a torsion meter consisting of strain gages attached to a cantilever-beam arrangement. Stem travel was measured by a cantilever beam, and vertical stem forces were measured by means of a proving ring with attached strain gages. A rotation indicator, consisting of a cantilever beam deflected by a cam rotating with the stem, was used in some tests, and this is not shown in Fig. 1. With this equipment it was possible to record simultaneously all pertinent data when the control-valve body was subjected to various conditions of fluid flow.

Before each test, calibration runs were made by statically loading each measuring element to predetermined values. This made it possible to evaluate quantitatively the deflections of the recorded signal traces.

Force-analysis tests were made with the various sizes of control-valve bodies installed in either a 4 or an 8-in. metering line.

---

[1] Director of Research, Fisher Governor Company. Jun. ASME.

[2] Chief Engineer, Fisher Governor Company.

Contributed by the Industrial Instruments and Regulators Division and presented at the Semi-Annual Meeting, Toronto, Ont., Canada, June 11–15, 1951, of THE AMERICAN SOCIETY OF MECHANICAL ENGINEERS.

NOTE: Statements and opinions advanced in papers are to be understood as individual expressions of their authors and not those of the Society. Manuscript received at ASME Headquarters, January 2, 1951. Paper No. 51—SA-1.

Air and water at a maximum pressure of 400 psig were used as flowing mediums. Available storage capacity made it possible to obtain for short periods of time, flows of approximately 2,000,000 cfh of standard air, or 3000 gpm of water.

Valve-body assemblies made by three different manufacturers, and in sizes from 1 through 8 in., were used in the tests. However, most of the test work was done on 4-in. bodies, since this is a popular size, and was found to have large force reactions.

The most commonly used types of inner valves may be classified as skirt or V-port type, Fig. 2, and plug type, Fig. 3. Early tests showed that vertical thrust forces on V-port-type inner

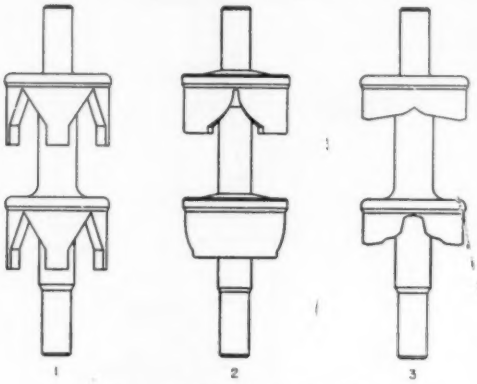

FIG. 2 V-PORT-STYLE INNER VALVES

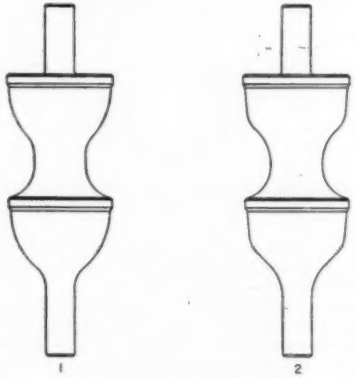

FIG. 3 PLUG-STYLE INNER VALVES

valves are not of such magnitude as to cause serious concern, but that the torsional reaction of this type of inner valve is high enough to merit further study. On the other hand, as would be expected from their smooth contour, the torsional reactions on plug valves are not large, but the vertical forces are even greater than might be anticipated. As a result of these preliminary tests it was decided to confine further studies to torsional reactions on V-port inner valves, and to vertical reactions on plug-style valves.

TORSIONAL FORCE REACTIONS—V-PORT INNER VALVES

Fig. 4 shows an oscillogram of torsional forces transmitted to the valve stem of a 4-in. control valve with a double-ported straight-sided V-port inner valve with four V's in each skirt as shown in Fig. 5. The flowing medium was water with a pressure drop of 170 psi, and a maximum stem travel of $1^1/_2$ in. Valve action was push down to close. Note that the maximum torque on the valve was 20 ft-lb when the valve was wide open, and that this torsional force was pulsating between 8 and 20 ft-lb at a frequency of approximately 30 cycles per second (cps). The pulsating nature of this force makes it particularly damaging to the valve parts. Similar tests were run using air as the flowing medium, with similar results, except that the magnitude of the

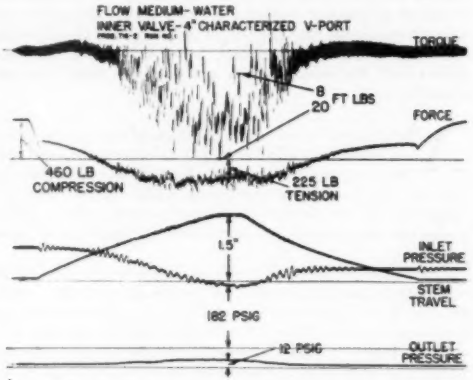

FIG. 4 OSCILLOGRAM SHOWING TORSIONAL FORCES ON 4-IN. V-PORT INNER VALVE

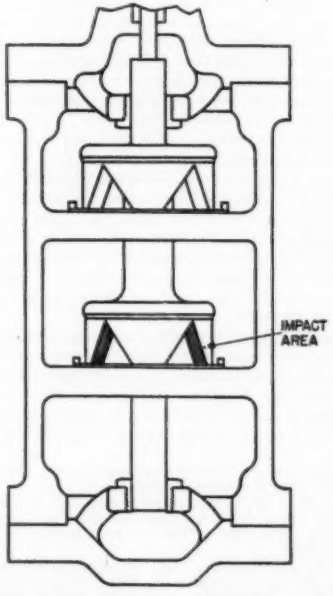

FIG. 5 CROSS SECTION OF VALVE BODY WITH V-PORT INNER VALVE

torsional forces was not quite as great for the same pressure drops.

The next series of tests were performed by locking the inner valve at a constant lift and observing the magnitude and direction of the torque reactions as the inner valve was rotated by hand with a crank on the upper end of the stem. Fig. 6 is an oscillogram recording of one of these tests run on a 4-in. straight-sided, V-port valve with air as the flowing medium at approximately 220 psig inlet and 50 psig outlet pressure. This valve construction was the same as illustrated in Fig. 5. The four peak torque values occurred when two of the openings in each skirt were 15 deg from parallel and two were 15 deg from perpendicular to the pipe axis of the valve body. It will be noted that the torque approaches zero at a point approximately 45 deg from the maximum. This suggests the possibility of positioning the openings

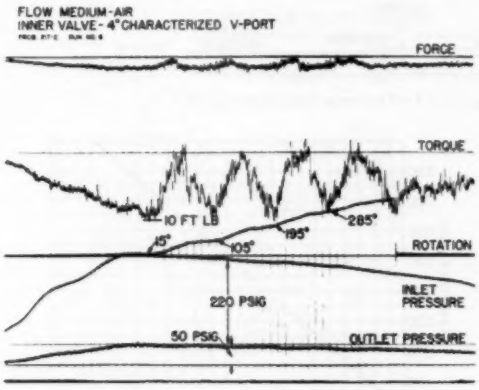

FIG. 6 OSCILLOGRAM SHOWING RESULTANT TORSIONAL FORCES AS V-PORT INNER VALVE IS ROTATED IN VALVE BODY

correctly with respect to the valve body so that the torque would be eliminated. This solution was not considered practical inasmuch as it is mechanically difficult and expensive to position the inner valve rotationally with respect to the valve body, and, also, this zero-torque zone did not appear at exactly the same location on all the bodies tested.

A special inner valve was constructed for the 4-in. double-ported body with removable and interchangeable skirts. One skirt was a plain piston with no openings, and the other skirt had the conventional straight sided V's; thus all of the flow could be directed through either the top or the bottom port. Tests on this valve, assembled so that all the flow passed through the top port, indicated that the torque reaction was negligible. However, with the valve assembled so that all of the flow passed through the bottom port, the torque reaction was nearly as great as that found in a standard double-ported valve. This indicated that the bottom skirt was causing most of the torque reaction.

It was concluded that most of the torque reaction was a result of an impulse reaction on the bottom skirt, caused by the impingement of the incoming fluid against the projected area of the edges of the V-notches. This is the shaded area on the lower skirt in Fig. 5. The top skirt had little of this reaction because the fluid that passes through its ports had its impinging force absorbed by the body walls.

It was then deduced that the torque reaction which might be expected from a skirt or V-port-type inner valve is proportional to the following: The momentum or mass velocity of the incoming fluid at the valve body inlet, the impingement area presented by the lower skirt, and to the port diameters. Tests indicated that the number of V's in the lower skirt was also a contributing factor. This leads to the conclusion that, for a given valve body with fixed dimensions, torque reactions will be proportional to mass velocity only. This supposition was verified when air and water of equal mass velocities were allowed to pass through a valve-body assembly, resulting in identical torque reactions for both.

The authors were unsuccessful in predicting mathematically the torque reaction that would result from a given mass-velocity flow through a specific valve. This relationship was easily determined by test and is illustrated in Fig. 7 for three styles of 4-in. skirt-type valves. Valve A was a percentage characteristic V-port with four V's in each skirt and with supporting webs between the skirts and valve post directly in the line of flow. Valve B was a straight-sided V-port with four V's in each skirt. Valve C was a percentage characteristic V-port designed especially to reduce torque, as explained later in this paper, with two V's in each skirt and a short bottom skirt. Hence, by establishing the amount of torque reaction the component parts of a control-valve assembly can safely handle, a manufacturer can limit the application of skirted valves to pressure-drop and flow conditions that will result in trouble-free service.

Thus it had been established that the torque reaction for a given mass velocity was a function of the length of skirt, the

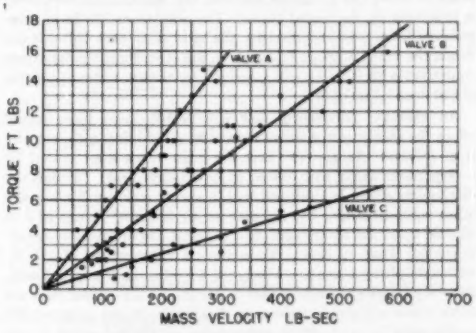

FIG. 7 MASS VELOCITY-TORQUE CURVES

thickness of skirt, and the number of ports in each skirt, and that the greater portion of the reaction comes from the lower port. Using this supposition as a basis, a line of percentage characteristic V-port inner valves was designed, holding these factors to a minimum by the use of two V's in each skirt instead of four, and by the use of short bottom skirts that lifted entirely out of the seat rings. This design proved very successful in reducing the torque effect, reducing it by a factor of about 2.5, without sacrificing capacity or characteristic or increasing its cost.

VERTICAL FORCE REACTIONS—PLUG-TYPE INNER VALVES

Vertical unbalanced forces resulting from a high-velocity fluid flow through double-ported valve bodies equipped with parabolic or throttle-plug inner valves probably cause more unsatisfactory control-valve operation than do the torsional forces on V-port valves. Fig. 8 shows an oscillograph of unbalanced vertical forces acting on the valve stem of a 4-in. control valve with a double-ported throttle-plug inner valve. Note that the inlet pressure was 160 psig and that the outlet pressure was 12 psig

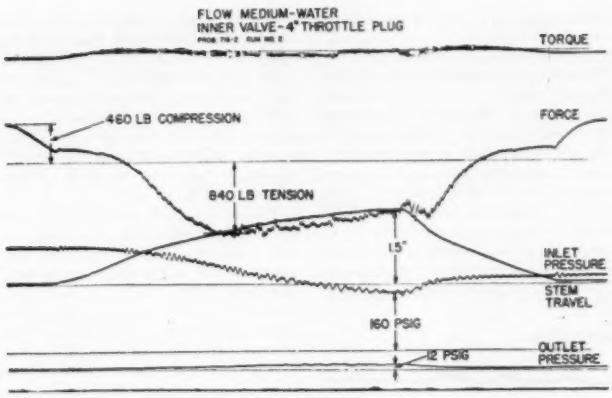

FIG. 8 OSCILLOGRAM SHOWING VERTICAL FORCES ON 4-IN. THROTTLE-PLUG INNER VALVE

when the valve was wide open at $1^1/_2$ in. travel. At the start of this test there was a compressive force on the stem of 460 lb. At the point where the stem started movement, a compressive force of 231 lb being exerted on the stem by the 300-psi differential pressure times the difference between top and bottom port areas is indicated by the signal trace. The additional 229 lb of compressive force was absorbed by the seat rings and valve body. When the valve is about $^1/_2$ in. open, the stem force changes from compression to tension, and reaches a maximum value in tension of 840 lb at 1.1 in. of lift.

An example illustrating how this 840-lb stem force would affect the ability of the valve to control a fluid flow satisfactorily is as follows: Assume (1) that the inner valve is motivated by a diaphragm motor with 100 sq in. of effective area; (2) that the diaphragm motor is equipped with a spring which will allow the inner valve to stroke $1^1/_2$ in. with an air pressure change of 3 to 15 psig upon the diaphragm, and (3) that the inner-valve action is pushed down to close. To achieve a valve stroke of $1^1/_2$ in. with a diaphragm pressure change of 3 to 15 psig, the spring must have a compression rate of 800 lb per in., and in order that the inner valve will start stroking at 3 psig diaphragm pressure, the spring must have an initial compression of 300 lb force or $^3/_8$ in. Referring to the previous paragraph, it was noted that when the inner valve was 1.1 in. from the seat there was an 840-lb closing force. At this point the spring would have an additional compression of 320 lb or 0.4 in., which, added to the initial compression of 300 lb, would result in an available opening force of 620 lb. Thus it can be seen that the inner valve would come to equilibrium at some point less the 1.1 in., inasmuch as there is an 840-lb force tending to close the valve, and only 620 lb of spring force available to open the valve. The addition of a valve positioner in this case would be of no help inasmuch as the upward movement of the valve would be entirely dependent upon the available spring force. The only solution would be the installation of a larger more costly diaphragm motor with a heavier spring.

Early experiments indicated that vertical unbalanced forces on plug valves were dependent upon the mass velocity of the fluid at the valve-body entrance. Air and water flows of equal mass velocities always resulted in identical stem forces. The curve in Fig. 9 illustrates the relationship between stem force and mass velocity. The points on the curve represent data for both water and air flow, and for valve sizes ranging from 1 to 8 in. The data

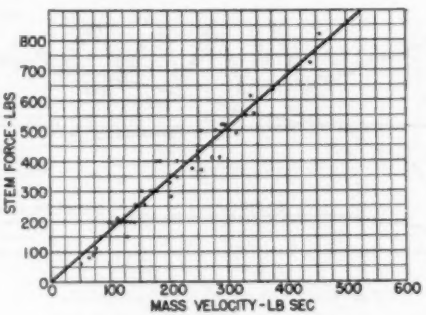

FIG. 9 MASS VELOCITY-STEM FORCE CURVE

plotted represent the point of maximum unbalanced force for each of the various sizes of valves. This usually occurs when the valve is approximately 70 per cent open. From the slope of this line drawn through the data points, it is concluded that the vertical stem force is equal to 1.7 times the mass velocity of the fluid at the valve-body inlet.

Mass velocities determined mathematically may be multiplied by this factor of 1.7 to arrive at the actual unbalanced forces acting on the conventional parabolic or throttle-plug valves wherein the top and bottom plugs are symmetrical.

In an attempt to determine which of the ports was responsible for this excessive vertical stem force, identical tests were made on two single-seated 4-in. throttle-plug valves assembled as follows: (1) With push down to close, flow opens valve action; and (2) with push down to close, flow closes valve action. The first assembly, which simulated conditions in the top port of a double-ported body resulted in practically no vertical thrust when in the wide-open position, regardless of pressure drop.

The second assembly, which simulated conditions in the lower port of a double-ported valve, indicated 325-lb tensile force on the stem with 95 psi differential at wide-open position.

From these tests it was concluded that vertical force reactions on a double-ported plug valve are principally due to dynamic force reactions at the lower port.

A series of tests were then made using a 4-in. valve-body as-

sembly with pressure registrations drilled at locations as shown in Fig. 10. Several holes were actually drilled around the valve body at the elevations shown, and connected together with collecting rings. Note that pressure registrations were located so that static pressure readings could be acquired simultaneously on the top and bottom of each of the plugs. These data were acquired for several valve lifts, and for both air and water flow. A calculated net unbalanced force was then determined by multiplying the static differential pressures times the respective plug areas, and totaling the results. Fig. 10 illustrates the results obtained with water flowing at $1^1/_4$ in. lift. Note that the differential pressure across the top port was only 10 psi, but that the differential pressure across the bottom port was 90 psi. This resulted in a calculated unbalance of 935 lb tending to close the valve. An actual unbalanced force of 700 lb was measured

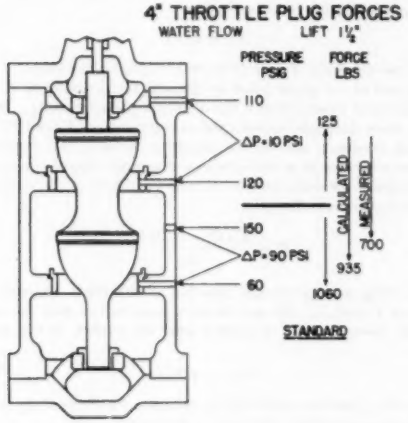

FIG. 10 CONVENTIONAL THROTTLE-PLUG FORCE CHART

by the force ring during the test run. The discrepancy between the calculated and the test results was probably due to inability to choose the exact projected port area upon which the differential pressures were acting. Tests at 1 in. and $^1/_2$ in. lift, and with both air and water flowing, gave similar results.

The reason for the greater differential across the bottom port was probably because the fluid flowing through this restriction had its velocity greatly increased with resultant reduction in static pressure. This region of reduced pressure was directly beneath the bottom plug, and a downward force resulted. The top port also had a region of increased velocity and lower static pressure, but this region was located away from the inner valve out in the valve-body chamber. By the time the turbulent fluid had reached the top of the upper plug, it had lost most of its velocity head and regained its static pressure. Also, the volume taken up by the top plug in the upper valve-body chamber probably caused enough restriction to account for some of the pressure build-up in this region.

As a result of these tests the theory was advanced that if the flow through the top port were restricted, a greater differential could be built up across the top plug to help balance the lower plug. It was also predicted that if the bottom port area were increased, its differential would decrease, which would also aid in balancing the inner valve.

After much calculation and several test samples, a plug-valve design with contours similar to those shown in Fig. 11, was completed. This inner valve had the same capacity, and the same flow characteristic as the conventional symmetrical throttle plugs previously tested. Flow tests with this inner valve assembled in the 4-in. test body resulted in static pressure readings and unbalanced force reactions as indicated in Fig. 11 Note that the unbalanced force has been reduced to 10 per cent of its previous value.

Fig. 12 is a reproduction of an oscillogram obtained from the balanced throttle plug, and further demonstrates the effectiveness of the proper design of plug contours in eliminating excessive vertical stem forces.

The area relationship between the top and bottom plug that proved successful in the case of the 4-in. inner valve was then tried successively on 3, 6, and 8-in. valve sizes, but with disappointing results. Finally, it was concluded that this was due to lack of exact similarity between all the component parts of different valve-body sizes. However, it was possible, by a program combining test results with mathematical analysis for each valve size, to develop a complete line of throttle-plug valves

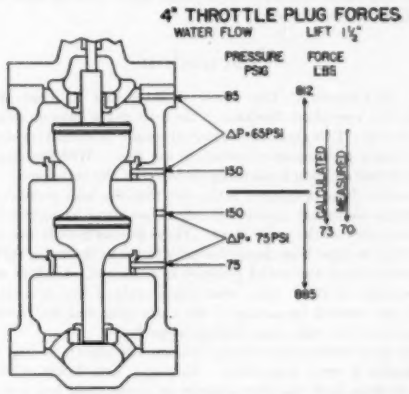

FIG. 11 BALANCED THROTTLE-PLUG FORCE CHART

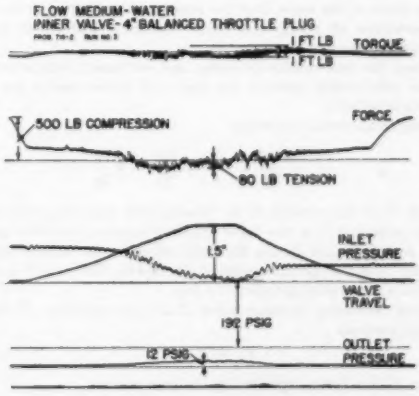

FIG. 12 OSCILLOGRAM SHOWING VERTICAL FORCES ON BALANCED 4-IN. THROTTLE-PLUG INNER VALVE

that were dynamically balanced to the extent that they could handle extremely high pressure drops with conventional operators.

Conclusion

With high fluid-flow rates through double-ported, semibalanced control-valve assemblies, V-port inner valves may be subjected to seriously high torsional forces, and plug-type inner valves of symmetrical design to vertical forces of great magnitude. These forces are proportional to the mass-velocity of the flowing fluid at the body inlet.

The proportionality constant for torsional forces on V-port inner valves must be determined by test for each valve size and design. However, after these factors have been determined, it is possible to predict the maximum pressure drops that can be handled successfully. It is also possible, by proper inner-valve design, to reduce these torsional forces by a substantial amount.

The mass velocity-vertical force proportionality factor for conventionally designed plug valves is approximately 1.7. It is possible by using different contours on the top and bottom plugs, to reduce this factor to a point where vertical force reaction is not of grave concern.

Discussion

M. D. Creech.[3] The writer is interested in what effect, if any, the very short duration of the tests might have on some of the results. This short time interval results in almost no steady state but a continuous variation in the flow. Will the authors express their opinion concerning the effect of the transients?

Another thing of interest is the fact that the inlet pressure has a definite oscillatory pressure of somewhat lower frequency than the frequency of the valve stem. These fluctuations in the pressure seem to have been damped out by the time the water reaches the point where the outlet pressure is measured. Is there some explanation for this? Also, what relationship, if any, is there between the natural frequency of the valve plug and the recorded frequency of the valve plug during the test?

The stem force-mass velocity relationship shown in Fig. 9 of the paper is very interesting. However, this linear relationship satisfies both the force-change of momentum law and the conservation of energy-continuity equations. The change of momentum probably will exert an upward force on the valve plug while at the same time the pressure drop derived from the conservation of energy-continuity equations will result in a downward force on the valve stem.

From the conservation of energy and continuity equations the linear relationship between the force and mass-velocity can be shown as follows:

From conservation of energy

$$\frac{P_1}{w} + \frac{V_1^2}{2g} = \frac{P_2}{w} + \frac{V_2^2}{2g} + f\frac{V_2^2}{2g}$$

where P_1 is the pressure in the flowing fluid upstream from the valve plug and P_2 is the lower pressure between the valve plug and seat; V_1 and V_2 are the fluid velocities at corresponding points; w is the specific weight of the flowing fluid, and f is the coefficient representing the friction loss.

Next, assuming incompressible fluid, the equation of continuity becomes

$$V_1 = K_1 V_2$$

where K_1 is a factor representing the area ratios.

These two equations can be combined, and it can be shown readily that

$$\Delta P = K_2 V_1^2$$

where K_2 is a constant. But the mass velocity is some constant multiplied by the velocity, and the force on the valve stem is some constant multiplied by ΔP; therefore

$$\text{Force on valve stem} = KMV$$

Likewise, for the change of momentum relationship, let V_1 be the velocity of the fluid at some point upstream from the plug. Also, let V_2 be the velocity at some point on the valve plug. The force due to this change of momentum will be

$$F = M(V_1 - V_2)$$

where M is the mass velocity flowing through the valve. If incompressible flow is assumed, then

$$V_1 = K_1 V_2$$

Also the direction of V_2 will be determined by the shape of the plug, and at any given point on the plug the direction of V_2 will remain fixed irrespective of the quantity of fluid flowing. However, since the angle between the velocity vectors V_2 and V_1 will remain constant, and, in the foregoing formula, the difference of the velocities is a vector whose direction depends upon the difference of the angle between V_1 and V_2, therefore the force due to this momentum change is

$$F = \frac{K_2(K_1 - 1)MV_1}{K_1}$$

K_2 being a trigonometric function of the angle between the vectors V_1 and V_2. To get the total force on the stem the component force must be integrated over the surface of the stem; thus

$$F_{\text{total}} = KMV_1$$

where K is a constant and will depend upon the shape of the valve plug, the areas in the valve body, and so forth.

It seems probable, therefore, that the force on the valve plug will be the sum of both of these effects. However, their relative magnitudes cannot of course be determined until further information is available.

In Fig. 9 of the paper, information for a variety of valves at different flows has apparently been plotted. However, if the points plotted could be identified with a particular valve, it would be expected that they would fall on a single straight line, but for different valves the value K would be different. For geometrically similar plugs the variation in K does not seem to be large. Can the points in Fig. 9 be represented by a series of lines with slightly different slopes, each line representing a particular valve body and plug?

In Fig. 7 only the change in momentum should affect the torque. The angular position of the valve plug, however, will be a factor upon which the slope of the torque-mass velocity curves will depend.

Authors' Closure

The authors are indebted to Professor Creech for his interesting analysis of the correlation between the linear relationship of the stem force and the momentum law and conservation of energy-continuity equations.

The short time interval was necessary for larger-sized valves because of limited storage and pumping capacity; however, these tests were also made on smaller-sized valves on which we were able to establish a steady-state condition, and the results were analogous with those described in this paper.

[3] Professor, Mechanics and Metallurgy, The University of Oklahoma, Norman, Okla. Mem. ASME.

The inlet-pressure oscillation would be present in some tests and completely absent in other tests. The oscillation was more apt to happen with water flows than with air flows. We attributed it to the matter of timing of opening the control valve and the natural frequency of the piping system. The over-all stem force results remained practically the same, however, whether or not the oscillations were present. There was also a 60-cycle oscillation of smaller magnitude present in the inlet-pressure signal trace which can be attributed either to the alternating-current amplifier or the impeller impulses of the centrifugal pump.

The oscillatory nature of the stem force and stem movement is a problem that the authors feel is just as important as the problem presented in this paper. It was assumed that factors that might contribute to this condition were the natural frequencies of the valve plug, the diaphragm motor spring, and the piping system, and also the turbulence inside the control-valve body. A study of the causes of the oscillations in these stem forces would be an interesting subject for another paper.

Although it is a logical thing to anticipate, the points in Fig. 9 cannot be represented by a series of straight lines with slightly different slopes, each line representing a particular valve body and plug. There was nearly as much "scatter" in plotting the points for one valve-body assembly as is present in the plotting of the composite curve.

Metastable Flow of Saturated Water[1]

By J. F. BAILEY,[2] KNOXVILLE, TENN.

This paper discusses the nature of the flow of saturated and nearly saturated water into regions where the pressure is less than the saturation pressure. It presents a method of computing the mass rate of flow through orifices and nozzles which is based on the rate of evaporation from a metastable liquid core into a surrounding ring of vapor. The flow rates for orifices are predicted accurately, and rates for nozzles are predicted to within 10 per cent. The analysis is based upon experimental investigations and is restricted to adiabatic flow conditions.

Introduction

THE flow of saturated or nearly saturated water through orifices, nozzles, and pipes has been the subject of study periodically since 1892. From these previous investigations come two concepts of the nature of the fluid stream passing through a nozzle or an orifice.

In all but one case it was assumed that the vapor bubbles formed throughout the stream cross section at that section where the saturation pressure is reached. This means that for initially saturated water, bubbles begin to form at the nozzle entrance, and that if the water is initially subcooled but only a few degrees below the saturation temperature, vapor begins to form at some section within the nozzle. It was further assumed that for the reversible and adiabatic flow process the fluid properties varied according to stable equilibrium conditions as indicated by steam-table data.

Calculations based on these assumptions yield mass flow rates which are considerably smaller than experimentally determined values, and so-called discharge coefficients of from 2.0 to 7.5 have been reported. It is explained generally that these unusually high values are due to the effects of surface tension retarding the formation of vapor bubbles.

The second concept is due to Silver and Mitchell (1).[3] They developed a theory based on the assumptions that vaporization occurs only from the liquid stream surface and that the rate of evaporation depends on the rate of heat transfer from a surface layer of this stream. This theory leads to calculated flow rates which are greater than measured rates but which more nearly represent the experimental values than do the calculations based on stable equilibrium conditions.

The purpose of the work presented in this paper is to determine the nature of saturated and nearly saturated water flowing through orifices and nozzles and to derive a means whereby mass flow rates can be computed or predicted.

The experimental work was carried out in three phases. The first was conducted primarily to observe the nature of the fluid stream. From the results of this phase and from information reported by previous investigators an equation (Equation [3]) is derived from which mass flow rates may be computed. In the second experimental phase, a value of the coefficient of evaporation was determined from the flow characteristics of short tubes. This coefficient is needed in Equation [2]. The flow characteristics of a $^1/_8$-in-diam nozzle and a $^1/_4$-in-diam orifice were obtained in the final phase. This permitted a comparison between computed and experimental values of flow rate.

Experimentation

The experimental work was conducted in the laboratories of the mechanical engineering department of Northwestern Technological Institute, Evanston, Ill. The equipment arrangement was essentially the same for all three phases of experimentation and is shown schematically in Fig. 1. The apparatus was designed to operate from atmospheric pressure into the vacuum region.

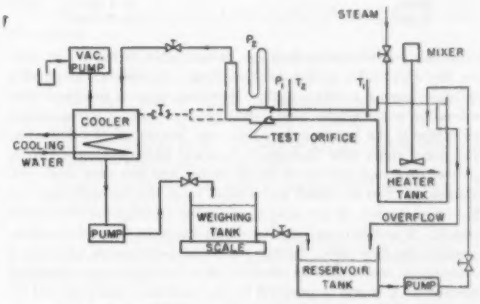

FIG. 1 FLOW DIAGRAM OF EXPERIMENTAL APPARATUS

Water was heated in an open-top tank shown at the right in Fig. 1. The heating was accomplished by bleeding steam from the laboratory high-pressure steam line (140 to 150 psia) into the bottom of the heater tank. Immediately above the steam-distribution pipe is a mixer which maintained uniform water temperature. The water passed from the top of the heater tank through a 2-in. pipe to the flow device (orifice, nozzle, or short tube) under test.

The water temperature was measured with two precision thermometers, one located near the heater tank T_1, and the other mounted near the orifice (or nozzle or tube) T_2. The water temperature entering the orifice was predicted from T_1 and T_2. The pressure before the orifice P_1, was measured with a piezometer. The discharge-region pressure P_2, was measured with a mercury manometer.

When the discharge pipe leading to the cooler was arranged as shown by the full lines, the discharge region was kept flooded. When the arrangement was as shown by the dashed lines, open-channel flow conditions prevailed in the discharge region.

Cooling water was supplied to the cooler in order to condense what vapor was formed and to cool the water to a temperature suitable for pumping. The noncondensables were removed and the vacuum was maintained by a rotary-type vacuum pump.

---

[1] Summary of a Doctoral Dissertation submitted to Lehigh University, October, 1949.

[2] Professor of Mechanical Engineering, The University of Tennessee. Jun. ASME.

[3] Numbers in parentheses refer to the Bibliography at the end of the paper.

Contributed by the Industrial Instruments and Regulators Division and presented at the Semi-Annual Meeting, Toronto, Ont., Can., June 11-15, 1951, of THE AMERICAN SOCIETY OF MECHANICAL ENGINEERS.

NOTE: Statements and opinions advanced in papers are to be understood as individual expressions of their authors and not those of the Society. Manuscript received at ASME Headquarters, May 22, 1951. Paper No. 51—SA-55.

This pump discharged into a container so any possible loss of water at this point could be checked.

The water was pumped from the cooler to the weighing tank and then flowed by gravity to a reservoir tank from which it was pumped to the heater tank. An overflow line, which discharged into the reservoir tank, kept a constant water level in the heater tank.

The test procedure was essentially the same for all phases. The temperature of the water, as measured by T_2, was held constant by manual operation of the steam-line valves. The discharge-region pressure was regulated by the valve in the line between the orifice under test and the cooler. A series of runs were made for each water temperature selected, and each run was made with a different discharge pressure. The length of run was determined by the time required to collect from 100 to 150 lb of water. Temperature and pressure readings were taken during each run. During any run the water temperature did not vary more than $^1/_2$ deg F above or below the selected temperature, and the initial pressure for all tests was 29.70 ± 0.30 in. Hg.

The accuracy of the measurements was estimated to be as follows:

Water temperature	0.2 deg F
Water piezometer, pressure	0.05 in. water
Mercury manometer, pressure	0.05 in. Hg
Mass	0.5 lbm
Time	0.01 min

At this point it seems desirable to define the terms orifice, nozzle, and short tube, as they are used here. An orifice is a cylindrical hole having a zero length. However, from a practical consideration some length must exist and, therefore, it is considered an orifice if the length is less than one quarter of the diameter. The term short tube includes cylindrical holes having a length greater than one quarter of the diameter, and less than thirty-six diameters. For an orifice and a short tube, the size and shape of the cross section of the hole is the same throughout the entire length. A nozzle is an opening which has been formed to aid or increase the flow rate. In this paper the term nozzle refers to a convergent nozzle having circular cross sections and a rounded entrance. A nozzle is specified by its minimum diameter and its over-all length, which includes the rounded entry.

In the first group of tests, which were conducted primarily to study bubble or vapor formation, an observation chamber was used. This is seen in Figs. 4, 5, and 6. Water flows vertically upward through a short tube 0.250 in. in diam and $^7/_{32}$ in. long. Tests were made with water temperatures of 79 F, 196.6 F, 201.8 F, 204.3 F, and 209.3 F. In addition to obtaining numerical data, the appearance of the stream was noted so that the nature of the fluid could be correlated with the flow characteristics.

In the second portion of the experimental work, the flow characteristics (flow rate versus pressure difference) were obtained for four short tubes. The tube sizes were as follows:

Tube	Diameter, in.	Length, in.
A	0.252	$1^1/_4$
B	0.252	$2^1/_2$
C	0.247	$2^1/_2$
D	0.247	5

A pressure tap was located $^1/_{16}$ in. from the exit end of tubes *C* and *D*. From the information obtained in this series of tests, a value for the coefficient of evaporation was computed. A fifth tube *E*, was a duplicate of tube A, but had pressure taps $^1/_8$ in. from the entrance and $^1/_{16}$ in. from the exit. This tube was used to determine pressure variations within the tube.

In the third part a 0.250-in-diam orifice and a 0.125-in-diam nozzle were investigated. The entry of the nozzle was rounded to a 0.275-in. diam, and the downstream section was cylindrical and $^1/_4$ in. long. The data obtained in this group of tests along with data from Danforth (2) are used to determine the ability of Equation [3] to predict the metastable flow of water.

Discussion and Interpretation of Data

Part 1. The data obtained in the first phase of experimentation were essentially qualitative in nature. They were, however, similar to data reported under Part 2.

Fig. 2 shows a flow rate versus pressure-difference curve which is typical of these data and is for an initial temperature of 209.3 F. The flow rate is given by *OADEF*. For lower temperatures, the shift from *OAB* to *CDEF* occurs at greater values of pressure difference.

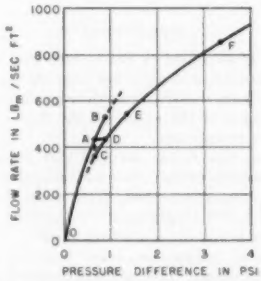

Fig. 2 Flow of Water Through a Short Tube (T = 209.3 F, D = 0.250 in., L = $^7/_{32}$ in.)

At point *D* the pressure difference is equal to the initial pressure minus the saturation pressure. The fact that the mass flow rate increases after the saturation pressure is reached indicates that part of the fluid is superheated liquid because computations, based on the existence of stable equilibrium conditions, show that the flow rate should decrease after the saturation pressure is reached.

The flow condition for that part of the curve from *O* to *A* is represented by Fig. 3(*a*); the tube is flowing full. When point *D* is reached the flow is as shown in Fig. 3(*b*). The stream has broken away from the tube wall, and the flow rate is the same as for an orifice of the same diameter.

For points between *A* and *D*, the condition within the tube is alternately that of Fig. 3(*a*), and that of Fig. 3(*b*), and the measured mass flow rates are statistical averages of the rates given by curve *AB* and curve *CD*.

The discontinuity in the flow curve at *A* occurs because the pressure at the vena contracta has reached the saturation pressure. This fact was verified in experiments with tube E. This tube had a pressure tap located $^1/_8$ diam from the entry. As the saturation pressure is reached, vapor begins to form, and the tube ceases to flow full, Fig. 3(*b*). The pressure at the vena contracta now is equal to the discharge-region pressure which is higher than the saturation pressure and so evaporation ceases. Since the tube discharges vertically upward, the water in the discharge region restores the full-flowing condition Fig. 3(*a*). The cycle of events is then ready to start again.

If the tube discharges into a region which is not flooded, there is no tendency to restore the full-flowing condition. In such cases the flow-rate curve is *OACDEF* being discontinuous from *A* to *C*.

Figs. 4, 5, and 6 are views taken under the conditions indicated

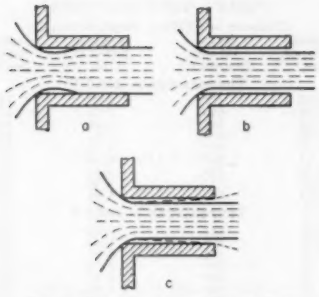

FIG. 3 FLOW THROUGH A SHORT TUBE
(*a*, Tube flowing full; *b*, tube not filled; *c*, vapor forming at stream surface.)

by points *A*, *D*, and *E*, Fig. 2, respectively. The illustrations are typical of what was observed at corresponding points for other temperatures.

In Fig. 4, which shows the conditions of *A*, Fig. 2, small bubbles are visible in the discharge region but, in general, bubbles could not be seen at the tube exit. Between *A* and *D* a faint stream of vapor became visible at the tube exit, and it was still only a faint stream when *D* was reached. Fig. 5 fails to show this stream, but shows the bubbles in the discharge region growing to large proportions. Fig. 6, which indicates the condition *E*, Fig. 2, is for a pressure about $^1/_2$ psi less than the saturation pressure and shows a definite vapor stream issuing from this tube. The vapor is discharged in an annular ring around a liquid core as shown in Fig. 3(*c*).

The information just discussed plus information presented by Danforth (2) and Dean (3) leads to the following concepts: Considering the reversible and adiabatic flow of saturated or nearly saturated water, there is ample evidence (3) to show that uncontaminated liquid water may be superheated many degrees under quiet conditions. Mechanical disturbances, however, cause the metastable liquid to revert to a stable state. Since a reversible process must exclude disturbances which would destroy the metastable state, it may be expected that the reversible flow of saturated water will be completely metastable, and the flow characteristics will be identical with those of an incompressible (or inexpansible) fluid. This probably is not true for initial states near the critical point.

The isentropic mass flow rate for negligible initial velocity is given by

$$G_s = \sqrt{2g_c(p_0 - p_e)/v} \quad \ldots\ldots\ldots\ldots\ldots\ldots [1]$$

where

G_s = isentropic mass velocity, lbm/sec sq ft
v = specific volume of liquid, cu ft/lbm
p_0 = initial pressure, psf
p_e = discharge-region pressure, psf
g_c = dimensional constant, 32.2 lbm ft/lbf sec^2

The derivation of Equation [1], or a comparable expression, may be found in any text on thermodynamics.

In actual flow the factors which promote ebullition will be present in varying degrees, and the mass flow rate will be correspondingly less than that given by Equation [1]. The following assumptions are made concerning actual flow:

1 That vapor begins to form when the saturation pressure is reached.

2 That the vapor forms at the interface between the fluid and the nozzle.

3 That the flowing fluid consists of a metastable liquid core surrounded by an annular ring of vapor.

4 That the mass of vapor discharging from the nozzle is negligible in comparison with the mass of liquid.

5 That the change in the temperature of the liquid core as it passes through the nozzle is negligible.

6 That the velocity and pressure are uniform throughout any cross section of the fluid stream.

Based on these assumptions, the following expression for the coefficient of contraction of the liquid core due to evaporation is derived in Appendix 1.

$$C_c = 1 - 17.2 \times 10^3 K (L/D)v^{-0.5} p_0^{-0.435} Z \quad \ldots [2]$$

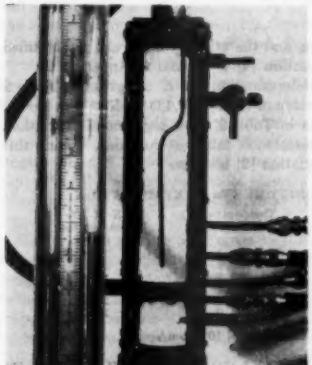

FIG. 4 FLOW THROUGH A SHORT TUBE
(Represents point *A* in Fig. 2; T = 209.3 F; p = 0.64 psi.)

FIG. 5 FLOW THROUGH A SHORT TUBE
(Represents point *D* in Fig. 2; T = 209.3 F; p = 0.88 psi.)

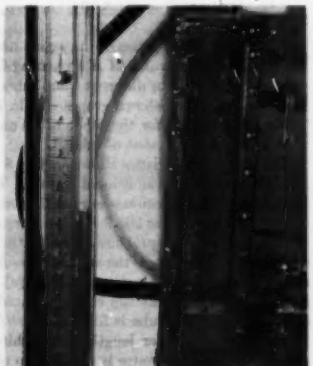

FIG. 6 FLOW THROUGH A SHORT TUBE
(Represents point *E* in Fig. 2; T = 209.3 F; p = 1.38 psi.)

where

K = coefficient of evaporation, lbm/lbf sec
L = length of nozzle or orifice, ft
D = diameter of nozzle or orifice, ft
v = specific volume of liquid core, cu ft/lbm
p_0 = initial pressure, psf
Z = function of p_0, saturation pressure p_s, and exit pressure p_x

Values of Z are given in Fig. 7, plotted against p_x' for various values of p_s'. The p_x' and p_s' are equal to p_x/p_0 and p_s/p_0, respectively.

The value of C_v, computed from Equation [2], is used with the usual coefficient of discharge C and Equation [1] to give the actual flow rate.

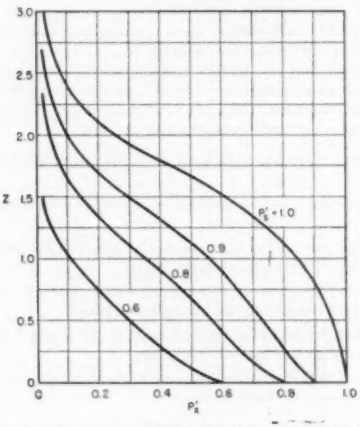

FIG. 7 VALUES OF FACTOR Z FOR USE IN EQUATION [5]
($p_x' = p_x/p_0$, and $p_s' = p_s/p_0$.)

$$G = C_v C \sqrt{2g_c (p_0 - p_x)/v} \quad \ldots\ldots\ldots\ldots [3]$$

Part 2. The next phase of the experimental work was devoted to determining the value of K appearing in Equation [2]. Data were obtained for four different short tubes (A, B, C, and D), and those for tube B are shown graphically in Fig. 8 and tabulated in Table 1. The data for the other tubes and for the tube used in Part 1 are similar to that of tube B.

The flow characteristics shown in Fig. 8 are similar to those in Fig. 2 but present an additional feature. The flow rate for water initially at 209.1 F becomes essentially constant at a pressure difference of 3.5 psi. For 206.9 F this occurs at a pressure difference of about 4 psi. The pressure at which the flow rate begins to be constant is referred to as the critical pressure. The flow condition at the critical pressure is shown in Fig. 3(*c*). The vapor is forming at such a rate that at the exit the annular space between the liquid core and the tube is filled completely with moving vapor. For a tube of shorter length, other things being the same, a greater pressure difference is required to obtain the critical-pressure condition; for a longer tube, a smaller pressure difference is required.

At this critical flow condition the pressure is constant throughout practically the entire length of the stream. This fact was verified with tube E which had pressure taps near the entrance and exit.

TABLE 1 DATA FOR TUBE B
(Diameter = 0.252 in.; length = 2 1/8 in.)

Pressure difference, psi	Mass velocity lbm/sec ft²	Pressure difference, psi	Mass velocity lbm/sec ft²
	TEMPERATURE = 206.9 F		
0.73	477	2.83	783
1.24	600	3.17	815
1.44	594	3.66	875
1.63	599	3.97	905
1.69	607	4.16	915
1.93	645	4.43	931
2.18	683	4.65	931
2.45	712	4.86	921
2.68	749	5.04	920
	TEMPERATURE = 209.1 F		
0.71	442	2.95	794
1.00	496	3.20	820
1.07	494	3.44	851
1.24	530	3.70	865
1.46	563	3.93	867
1.73	609	4.20	865
1.97	648	4.42	880
2.22	686	4.69	880
2.47	727	5.06	881
2.70	756	5.16	880

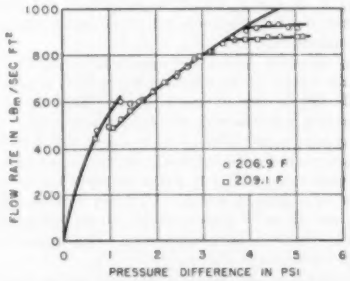

FIG. 8 DATA FROM A SHORT TUBE
(D = 0.252 in.; L = 2 1/8 in.)

The following expression is obtained by equating the amount of vapor passing out the tube through the annular space to the amount of vapor being evaporated. The amount being evaporated is expressed in terms of K, the coefficient of evaporation.

$$K = 3.52 \times 10^{-4} (D/L)\, p_c^{0.913} [(p_0 - p_s)p]^{1/2} / (p_s - p_x) \ldots [4]$$

where

P_c is critical pressure, and the other symbols are as identified for Equation [2]. Equation [4] is derived in Appendix 2.

Seven independent determinations of K are given in Table 2 and yield an average value of $(2.45 \pm 0.43) \times 10^{-4}$ lbm per lbf sec. Although the data in Table 2 show a systematic variation, the coefficient of evaporation is taken as constant. Using this average value of K Equation [2] becomes

TABLE 2 COEFFICIENTS OF EVAPORATION

Tube length, in.	Temperature, deg F	$K \times 10^4$ lbm/sec lbf
1 1/8	209.0	3.18
2 1/8	201.5	2.64
2 1/8	206.9	2.29
2 1/8	209.1	2.14
2 1/8	209.1	2.22
5	192.2	2.62
5	209.0	1.85

NOTE: Average $K = (2.45 \pm 0.43) \times 10^{-4}$ lbm/sec lbf.

$$C_v = 1 - 0.42(L/D)^{0.5}\, p_0^{-0.135}\, Z \ldots\ldots\ldots [5]$$

Part 3. In the final phase of the experimental work the flow characteristics of a nozzle and an orifice were obtained. These data are presented in Figs. 9 and 10 and in Tables 3 and 4.

TABLE 3 DATA FOR ORIFICE

(Diameter = 0.250 in.)

Pressure difference, psi	Mass velocity, lbm/sec ft²	Pressure difference, psi	Mass velocity, lbm/sec ft²
	Temperature = 196.9 F		
1.21	515	5.15	1052
1.99	647	5.68	1111
2.50	734	6.21	1161
3.48	857	6.56	1191
	Temperature = 209.1 F		
0.54	308	1.85	629
0.77	415	2.05	664
1.01	466	2.24	690
1.06	477	2.43	719
1.31	520	2.63	753
1.45	561	4.21	950
1.70	599	5.64	1102

TABLE 4 DATA FOR NOZZLE

(Diameter = 0.125 in.; length = 0.20 in.)

Pressure difference, psi	Mass velocity, lbm/sec ft²	Pressure difference, psi	Mass velocity lbm/sec ft²
	Temperature = 196.3 F		
4.52	1538	8.36	1825
5.35	1643	10.92	1940
6.88	1765		
	Temperature = 201.8 F		
3.19	1318	8.30	1782
4.71	1547	8.86	1840
5.30	1590	9.58	1858
6.24	1660	10.65	1880
7.32	1740	10.65	1890
7.51	1750		
	Temperature = 206.5 F		
5.25	1560		
9.39	1812		
10.65	1860		

In Fig. 9 are shown the data obtained with a 0.250-in-diam orifice for two different initial temperatures, 196.9 and 209.1 F. The solid line is the plot of Equation [3] in which $C_v = 1.0$ and $C = 0.63$. For an orifice $L = 0$ and Equation [5] gives $C_v = 1$. The value of C was determined by calibration with water at 70 F. It is evident from Fig. 9 that the flow through an orifice is given by Equation [3] and is the same as the flow of an incompressible fluid. These results are identical with those of earlier investigators (1, 4).

Fig. 10 shows the data from a 0.125-in-diam nozzle, the dimensions of which appear in Fig. 13(a). The data presented are for an initial temperature of 201.4 F. The solid line is the plot of Equation [3], where C_v is computed from Equation [5] and the dashed line is an extension of the incompressible flow curve.

From Fig. 10 it would appear that Equation [3] predicts accurately the flow rates through this nozzle. However, for an initial temperature of 196.3 F, Equation [3] gives results which are about 4 per cent high; for 206.5 F about 4 per cent low.

It will be recalled that K was taken as a constant, although Table 2 indicates a variation with both temperature and tube length. If the variation with temperature is accounted for, Equation [3] yields values within about 1 per cent for all initial temperatures. The data obtained from this nozzle are given in Table 4.

Danforth (2) gives data for a 0.125-in-diam nozzle the dimensions of which are shown in Fig. 13(b). These data cover initial pressures from 45 to 95 psia. Fig. 11 compares Danforth's data for an initial pressure of 45 psia and a saturation pressure of 35 psia with Equation [3] for the same conditions. The solid line up to a pressure difference of about 25 psi is the plot of Equation [3]. For pressure differences greater than 25 psi Equation [3] gives flow rates which decrease to zero as the exit pressure decreases to zero. Actually, at these greater pressure differences, the flow rate remains constant at the maximum value given by Equation [3]. A maximum discrepancy between measured and

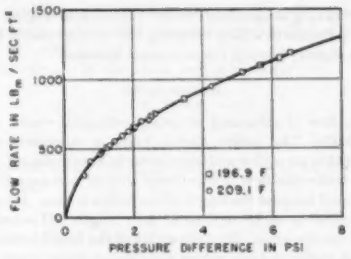

FIG. 9 DATA FROM A 0.250-IN-DIAM ORIFICE COMPARED WITH EQUATION [3]
(Equation [3] is shown by solid line. $C_v = 1.0$ and $C = 0.63$.)

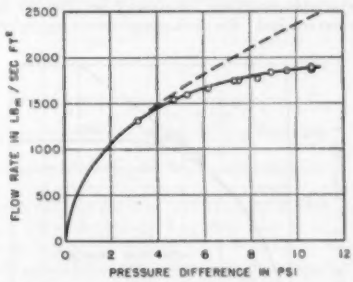

FIG. 10 DATA FROM A NOZZLE COMPARED WITH EQUATION [3]
(Equation [3] is shown by solid line. $D = 0.125$ in.; $L = 0.20$ in.; $p_0 = 14.7$ psia; $p_s = 11.9$ psia. The dashed line is an extension of the incompressible flow curve.)

computed values of about 10 per cent is indicated in this case. The dashed line indicates flow rates for an incompressible fluid.

A similar comparison is made in Fig. 12 for an initial pressure of 95 psia and a saturation pressure of 85 psia. In this case the agreement between values computed from Equation [3] and the experimental values is almost exact. Danforth's data are given in Tables 5 and 6.

TABLE 5 DATA FOR DANFORTH'S NOZZLE

(Diameter = 0.125 in.; length = 0.5 in.; initial pressure = 45 psia; saturation pressure = 35 psia)

Discharge pressure, psia	Mass velocity, lbm/sec ft²
33.0	2700
31.0	2740
30.0	2860
29.0	2920
28.0	2980
27.1	2935
25.3	3010
19.8	3210

TABLE 6 DATA FOR DANFORTH'S NOZZLE

(Diameter = 0.125 in.; length = 0.5 in; initial pressure = 95 psia; saturation pressure = 85 psia)

Discharge pressure, psia	Mass velocity, lbm/sec ft²
80.0	2880
79.0	2920
78.1	2980
76.2	3010
75.0	3130
72.0	3190
64.8	3480
52.7	3740

Figs. 11 and 12 indicate the magnitude of the error introduced by assuming that vapor forms when the saturation pressure is reached. Actually, in a well-shaped nozzle, a measurable degree

of superheating is obtained before evaporation begins. This is shown by Danforth's data following the incompressible fluid-flow curve to slightly beyond the saturation pressure.

Conclusions

In the flow of saturated or nearly saturated water, complete metastability (the entire stream being a superheated liquid) occurs within an orifice and may occur in a well-shaped nozzle.

In an orifice the flow is effectively that of a completely metastable liquid because the length of the orifice is zero. Actually, it is not practical to make orifices of zero length. However, if the length is not too great, the contraction of the liquid jet is sufficient to permit vapor to form within an orifice of finite length without restricting the flow. In the case of a well-designed nozzle the completely metastable state persists for only a relatively few degrees of superheat. Fig. 12 shows that Danforth obtained complete metastable conditions for about 7 psi after the saturation pressure was reached. For discharge pressures appreciably below the saturation pressure, complete metastability does not exist in a nozzle, and the fluid consists of a metastable liquid core surrounded by a ring of vapor.

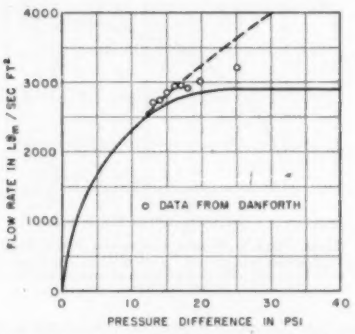

Fig. 11 Data From Danforth's Nozzle Compared With Equation [3]

(Equation [3] is shown by solid line. D = 0.125 in.; L = 0.5 in.; p_0 = 45 psia; p_s = 35 psia. The dashed line is an extension of the incompressible flow curve.)

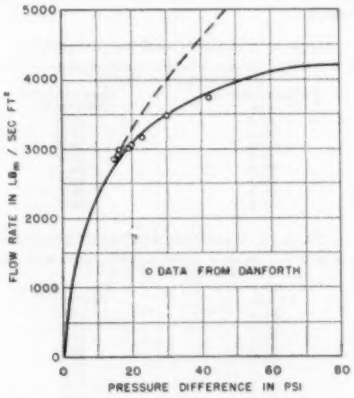

Fig. 12 Data From Danforth's Nozzle Compared With Equation [3]

(Equation [3] is shown by solid line. D = 0.125 in.; L = 0.5 in.; p_0 = 95 psia; p_s = 85 psia. The dashed line is an extension of the incompressible flow curve.)

A method of computing the mass flow rate of saturated or nearly saturated water through nozzles is given in the form of Equations [3] and [5]. This method is based on the rate of evaporation from the liquid core into the ring of vapor, and it gives results which agree rather well with existing experimental data.

For an orifice, Equation [5] gives C_v equal to 1, and mass flow rates may be computed accurately from Equation [3]. Equations [3] and [5] will also give flow rates through nozzles to within 10 per cent for initial pressure up to 100 psia. In Equation [5] the coefficient of evaporation K, is taken as a constant, although there is some evidence (Table 2) to the contrary. It is believed that a more complete knowledge of the relationship between K and other quantities would permit more accurate computations for flow rates through nozzles.

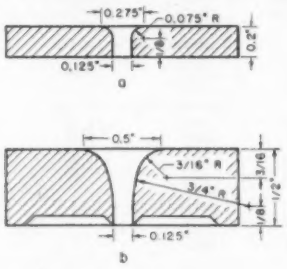

Fig. 13 Nozzle Dimensions

(a, Author's nozzle; b, Danforth's nozzle.)

As mentioned previously, Equations [3] and [5] give flow rates per unit area which increase with pressure difference up to a maximum value. With further increases in pressure difference, these equations yield decreasing values of flow rate. Actually, the flow rate remains constant after the maximum value is reached.

Appendix 1

Fig. 14 shows diagrammatically the flow of saturated water through a circular nozzle. The amount of liquid evaporated per unit time from the differential cylindrical area is

$$dm = K\pi D' dy(p_s - p) \quad \ldots\ldots\ldots\ldots\ldots\ldots [6]$$

where

m = mass per unit time
K = coefficient of evaporation
D' = liquid core diameter
dy = differential length of the fluid stream
p_s = saturation pressure
p = pressure at the section under consideration

It is assumed that the velocity of the entire fluid stream (liquid and vapor) is uniform at any cross section. Therefore, as the fluid moves through the nozzle, the increase in the amount of vapor will require an increase in the cross-sectional area for the vapor and bring about a corresponding decrease in the area for the liquid. The rate of change in cross-sectional area of the liquid core is given, with the aid of Equation [6], as

$$dA/dt = -v_g(dm/dy) = -K\pi D'(p_s - p)v_g$$

where

t = time
v_g = specific volume of vapor

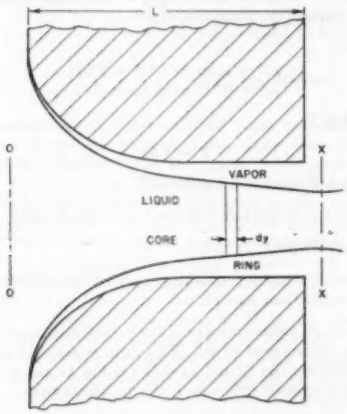

FIG. 14 FLOW OF SATURATED WATER THROUGH CIRCULAR NOZZLE

Since the velocity is given by

$$V = dy/dt$$

then

$$dA = -K\pi D'(p_s - p)v_g(dy/V)$$

and

$$\Delta A = -\int_0^L K\pi D'(p_s - p)(v_g/V)dy \quad \ldots\ldots\ldots [7]$$

where L is the length of the nozzle.

The coefficient of contraction due to evaporation is defined as the ratio of the cross-sectional area of the liquid core issuing from the nozzle to the cross-sectional area of the nozzle exit. In equation form

$$C_c = (A + \Delta A)/A = 1 + (\Delta A/A) = 1 + (4\Delta A/\pi D^2)$$

where

A = area of nozzle exit
ΔA = change in area of liquid core, a negative quantity
D = nozzle diameter

Combining the last two equations gives

$$C_c = 1 - (4/D^2)\int_0^L KD'(p_s - p)(v_g/V)dy \quad \ldots\ldots [8]$$

In order to integrate this expression certain simplifying assumptions are necessary as follows:

(*a*) The coefficient K is taken to be a constant.

(*b*) The core diameter D' is taken equal to the nozzle diameter D. Actually D' varies from a value greater than D to a value less than D.

(*c*) The specific volume of the vapor is expressed

$$v_g = 34{,}350\ p^{-0.935}$$

This relationship is derived from steam-table data by assuming that the specific volume of the vapor is equal to that of saturated vapor at the same pressure.

(*d*) The velocity of the liquid core is given by

$$V = \sqrt{2g_c v(p_0 - p)}$$

where

v = specific volume of liquid core and is assumed to be a constant

p_0 = initial pressure
g_c = dimensional constant

This expression comes from the energy equation for isentropic flow with negligible initial velocity.

(*e*) The variation of pressure p with distance through the nozzle y is approximated by the expression

$$p = p_s + \frac{p_s(p_0 - p_s)}{p_s + 3p_s}(1 - y/L) \quad \ldots\ldots\ldots [9]$$

Thus

$$dy = -\frac{L(p_s + 3p_s)}{p_s(p_0 - p_s)}dp$$

The variation of p with y is complex and changes as p_s changes. Equation [9] is obtained by assuming the pressure variation to be linear with y and that the slope of this straight line is a function of p_0 and p_s. This line is nearly horizontal when p_s equals p_0, and when p_s equals zero, the pressure varies from p_0 to p_s in length L. Substitution of these simplifications into Equation [8] results in

$$C_c = 1 + 17.2 \times 10^3 K\left(\frac{L}{D}\right)v^{-1/2}\frac{p_s + 3p_s}{p_s(p_0 - p_s)}\int_{p_0}^{p_s}\frac{(p_s - p)dp}{p^{0.935}(p_0 - p)^{1/2}} \quad [10]$$

The integral in Equation [10] must be evaluated for each set of conditions; but by setting

$$p_s' = p_s/p_0$$

and

$$p_s' = p_s/p_0$$

and by letting

$$Z = -\frac{p_s' + 3p_s'}{p_s'(1 - p_s')}\int_1^{p_s'}\frac{(p_s' - p')dp'}{(p')^{0.935}(1 - p')^{0.5}}$$

the expression for C_c becomes

$$C_c = 1 - 17.2 \times 10^3 K(L/D)v^{-0.5}p_0^{-0.435}Z \quad \ldots\ldots [2]$$

Since Z is dimensionless, one set of evaluations will suffice for all cases.

Appendix 2

When the discharge pressure is equal to the saturation pressure, a short tube does not flow full, and the flow rate is the same as for an orifice. As the exit pressure is reduced below the saturation pressure, the rate of flow continues to be identical with the orifice flow. Eventually, a critical pressure is reached such that further reductions in exit pressure produce no change in flow rate. When flowing with the discharge pressure equal to this critical value, the vapor formed within the tube is sufficient to fill

completely the annular space created by the contraction of the stream. At this flow condition, the pressure is constant throughout the length of the stream from the vena contracta to the end of the tube and is equal to the exit pressure.

Since p is constant for approximately the entire length of the tube, the D', v_g, and V are also constant. Equation [7], written to represent the increase in area needed for the passage of the vapor, is

$$\Delta A = K\pi D'(p_s - p)(v_g/V)L \quad \ldots\ldots\ldots\ldots [11]$$

At the critical condition

$$\Delta A = A(1 - C_c) = (\pi D^2/4)(1 - C_c)$$

and

$$D' = C_c^{0.5}D$$

where

A = cross-sectional area of tube
D = diameter of tube
C_c = contraction coefficient of tube = 0.63

Using these relationships and the expressions for v_g and V given in Appendix 1, and solving Equation [11] for K, yields

$$K = 3.52 \times 10^{-4}(D/L)P_c^{0.318}[(p_0 - p_c)g]^{1/2}/(p_s - p_c) \quad [4]$$

where p_c is the critical pressure. The critical pressure p_c is determined experimentally, and values of K are computed from Equation [4].

Appendix 3

In order to clarify the use of Equations [3] and [5], and Fig. 7, the following examples are given:

Example 1. Compute the mass rate of water flowing per unit area through a 0.125-in-diam nozzle which is 0.5 in. long. The initial pressure is 45 psia, the saturation pressure is 35 psia, and the exit pressure is 25 psia. The usual discharge coefficient is 0.99.

Solution:

$$p_s' = p_s/p_0 = 35/45 = 0.778$$
$$p_c' = p_c/p_0 = 25/45 = 0.555$$

From Fig. 7

$$Z = 0.45$$

From steam tables for saturated liquid at 35 psia

$$v = 0.01708 \text{ cu ft/lbm}$$

Equation [5] gives

$$C = 1 - 0.42(0.5/0.125)(0.01708)^{-0.5}(144 \times 45)^{-0.125}(0.45)$$
$$= 1 - 0.127 = 0.873$$

Equation [3] gives

$$G = (0.873)(0.99)\sqrt{2(32.2)(45 - 25)(144)/0.01708}$$
$$= 2850 \text{ lbm/sec sq ft}$$

The nozzle dimensions and the initial conditions in the foregoing example are the same as for the nozzle in Fig. 11. This example indicates a flow of 2850 lbm/sec ft^2 when the exit pressure in 25 psia (a pressure difference of 20 psi), giving one point on the flow curve.

Example 2. Compute the flow rate for the conditions of Example 1 but with an exit pressure of 5 psia.

Solution:

$$p_s' = p_s/p_0 = 5/45 = 0.111$$
$$p_c' = 0.778 \text{ as in Example 1}$$

From Fig. 7

$$Z = 1.52$$

Since only Z changes in Equation [5]

$$C_c = 1 - 0.127(1.52/0.45) = 1 - 0.428 = 0.572$$

Equation [3] gives

$$G = (0.572)(0.99)\sqrt{2(32.2)(45 - 5)(144)/0.01708}$$
$$= 2640 \text{ lbm/sec sq ft}$$

This example yields a computed flow rate of 2640 lbm/sec ft^2 for a pressure difference of 40 psi. This value is less than the maximum of 2900 lbm/sec ft^2 and, as shown in Fig. 11, the actual flow rate for this pressure difference is the maximum value.

BIBLIOGRAPHY

1 "The Discharge of Saturated Water Through Nozzles," by R. S. Silver and J. A. Mitchell, Transactions, North East Coast Institution of Engineers and Shipbuilders, vol. 62, 1945, p. 51.

2 "Flow of Hot Water Through a Rounded Orifice," by J. L. Danforth, Master of Science thesis, M.I.T., 1941.

3 "The Formation of Bubbles," by R. B. Dean, *Journal of Applied Physics*, vol. 15, 1944, p. 446.

4 "Flow of Saturated Water Through Throttling Orifices," by M. W. Benjamin and J. G. Miller, Trans. ASME, vol. 63, 1941, pp. 419–426.

5 "Écoulement de leau des Chaudiéres," by M. Sauvage and M. Pulin, *Annales des Mines*, ninth series, vol. 2, 1892, pp. 192–202.

6 "Experimental Researches on the Flow of Steam Through Nozzles and Orifices and the Flow of Hot Water," by A. Rateau, translated by H. B. Brydon, Constable, 1905.

7 "Discharge Capacity of Traps," by A. E. Kittredge and H. S. Dougherty, *Combustion*, vol. 6, September, 1934, pp. 14–19.

8 "Fluid Flow Through Two Orifices in Series," by M. C. Stuart and D. R. Yarnall, *Mechanical Engineering*, vol. 58, 1936, pp. 479–484.

9 "Flow of Boiling Water Through Orifices and Pipes," by W. T. Bottomley, Transactions, North East Coast Institute of Engineers and Shipbuilders, vol. 53, 1936–1937, pp. 65–100.

10 "The Flow of Hot Water Through a Nozzle," by B. Hodkinson, *Engineering*, vol. 143, 1937, pp. 629–630.

11 "The Flow of a Flashing Mixture of Water and Steam Through Pipes," by M. W. Benjamin and J. G. Miller, Trans. ASME, vol. 64, 1942, pp. 657–669.

12 "Fluid Flow Through Two Orifices in Series-II," by M. C. Stuart and D. R. Yarnall, Trans. ASME, vol. 66, 1944, pp. 387–397.

13 "Flow of Boiling Water Through Nozzles, Orifices, and Pipes," by J. G. Burnell, *Engineering*, vol. 164, 1947, p. 572.

14 "Temperature and Pressure Phenomena in the Flow of Saturated Liquids," by R. S. Silver, Proceedings of the Royal Society of London, series A, vol. 194, 1948, pp. 464–480.

15 "Theory of Heat," by J. C. Maxwell, Longmans, Green and Company, London, England, 1875.

Intermittent Heating for Aircraft Ice Protection With Application to Propellers and Jet Engines

By MYRON TRIBUS,[1] CINCINNATI, OHIO

The equations for intermittent heat transfer during icing conditions are presented and solved by means of an electrical analog. The results of the analog investigation are compared favorably with measured time-temperature data previously reported in the literature. The analysis shows that contrary to the experience with steadily heated ice-prevention systems, the energy requirements for ice prevention using intermittent heating decrease with increasing ice-accretion rate. Corroborative evidence is found in the literature. The thermal analyzer is used to demonstrate how the protection afforded for propeller deicing may be increased without an increase in the energy required from the electrical supply of the airplane and without major redesign of existing propeller heaters. In the case of jet-engine guide-vane deicing, for a typical installation, the indicated power requirements are 1 kw per engine. In each case the minimum energy requirements occur when large amounts of power are applied for very short intervals of time. Suggestions for further reductions in power are given.

Nomenclature

The following nomenclature is used in the paper:

- a = radius of droplet, ft
- A = surface area, sq ft
- b = dimensionless modulus, $\frac{R_w C_{pw}}{f_c}$
- B = barometric pressure, in. Hg
- C = chord length, ft
- C_p = unit heat capacity of air, Btu/lb deg F
- C_{pi} = unit heat capacity of ice, Btu/lb deg F
- C_{pw} = unit heat capacity of water, Btu/lb deg F
- E = fractional catch, local; dimensionless ratio of number of intercepted droplets to number of droplets directly ahead of surface
- E_M = fractional catch, total, dimensionless
- $\Delta E/E_M$ = dimensionless ratio of local water-catch rate for an element of area to catch rate of entire airfoil
- f_c = unit thermal conductance for heat transfer, Btu/hr sq ft deg F
- g_c = conversion constant 32.2 fps per sec
- J = conversion constant 778 ft-lb/Btu
- k = thermal conductivity Btu/hr sq ft (deg F/ft)
- L = heat of vaporization or sublimation, Btu per lb
- p = vapor pressure of water or ice, in. Hg
- p_s = vapor pressure of water or ice at surface, in. Hg
- p_∞ = vapor pressure of water in free stream, in. Hg
- q = heat flux, Btu per hr
- r = "recovery" factor, dimensionless
- Ru = Reynolds modulus, dimensionless

$$Ru = \frac{2U_\infty a\rho_a}{\mu}$$

- R_w = rate of water impingement, lb per hr per sq ft
- s = distance measured along surface of airfoil from stagnation point, ft
- t = temperature, deg F
- t_s = surface temperature, deg F
- T = temperature, deg R
- U_∞ = free-stream velocity, fps
- w = liquid water content, grams per cu m (or lb per cu ft)
- x = distance, ft
- γ = density of air, lb per cu ft
- θ = functions defined in Equations [3], [4], [5], [8], deg F
- τ_∞ = free-stream temperature, deg F
- ψ = scale modulus, dimensionless, $\psi = \frac{9C\rho_a}{a\rho_d}$
- ρ_a = mass density of air, slugs per cu ft
- ρ_d = mass density of droplet, slugs per cu ft
- μ = viscosity of air, lb sec/ft^2

Introduction

Extensive analytical methods have been devised for the design of ice-prevention equipment for surfaces utilizing continuous heating (1, 2, 3, 4.)[2] No similar analysis has been made for the case of intermittent heating. By experiments with propellers it has been found that the periodic application of heat to propeller blades provides better ice protection than the continuous application of heat and requires less energy.

A literature search revealed few reports of significance in this regard (5, 6, 7). Reference (5) treats the problem the most thoroughly, attempting to account for all the known factors. However, the analysis therein treats a propeller without regard for the heat-transfer processes occurring in the blade. References (5) and (6) suggest the melting of specified thicknesses of ice at the ice-blade interface as a criterion for successful ice prevention. This criterion is not considered justified, and the analysis which follows considers that the ice adhesion will be reduced to zero when the surface reaches the freezing point.

Considerable experimental data dealing with propellers have been reported, but little correlation has been attempted (8, 9, 10, 11, 12).

[1] Assistant Professor of Engineering, University of California, Los Angeles, Calif. On leave with General Electric Company, Cincinnati, Ohio. Jun. ASME.

Contributed by the Heat Transfer Division and presented at the Annual Meeting, New York, N. Y., November 26–December 1, 1950, of The American Society of Mechanical Engineers.

Note: Statements and opinions advanced in papers are to be understood as individual expressions of their authors and not those of the Society. Manuscript received at ASME Headquarters, September 1, 1950. Paper No. 50—A-55.

[2] Numbers in parentheses refer to the Bibliography at the end of the paper.

Equations for Energy Transfer at Ice Surface

The energy balance at a point on the surface of a streamlined body, where supercooled liquid water is impinging, is expressed in words as:

Heat transfer from beneath ice surface	Equals	Heat loss by convection
	Minus	Heat gain from frictional heating of air
	Plus	Energy loss by sublimation (or evaporation)
	Plus	Heat loss via sensible heating of water
	Minus	Gain from heat of fusion
	Minus	Gain from kinetic energy of droplets relative to surface

When the surface temperature is above the freezing point there will be no benefit from the heat of fusion of ice, and the fifth term on the right side of the foregoing equation will be absent.

In reference (13) the foregoing equation was applied to the prediction of the energy required to maintain a small cylinder at the freezing point during icing conditions. As demonstrated in the reference cited, the energy balance may be written

$$q = f_c A\,[t_s - \tau_\infty - r(U_\infty^2/2g_c JC_p)] + 2.90\, f_c\, LAB^{-1}(p_s - p_\infty) + R_\infty A\left[0.47\, t_s - \tau_\infty - 127 - \frac{U_\infty^2}{2g_c J}\right], \quad t_s < 32\text{ F} \quad \ldots [1]$$

For purposes of calculation it is convenient to define the following functions

$$b = \frac{R_\infty C_{p\infty}}{f_c} \quad \ldots [2]$$

$$\theta_1 = \theta_1(t_s, B, b) = t_s(1 + 0.47\, b) + 2.90\, LB^{-1} p_s \quad \ldots [3]$$

$$\theta_2 = \theta_2(\tau_\infty, B, b) = \tau_\infty(1 + b) + 2.90[LB^{-1} p_\infty + 127b] \quad \ldots [4]$$

$$\theta_3 = \theta_3(b, U_\infty) = \left(\frac{r}{C_{p\infty}} + b\right)(U_\infty^2/2g_c J) \quad \ldots [5]$$

The equation for the heat flow from the surface then is written

$$q = f_c A(\theta_1 - \theta_2 - \theta_3), \quad t_s < 32\text{ F} \quad \ldots [6]$$

When the surface temperature is above the freezing point, the term for the heat of fusion is absent, and the equation for the energy balance becomes

$$q = f_c A\left\{[t_s(1 + b) + 2.90\, LB^{-1} p_s] - [\tau_\infty(1 + b) + 2.90\, LB^{-1} p_\infty] - [r/C_{p\infty} + b]\left[\frac{U_\infty^2}{2g_c J}\right]\right\} \quad \ldots [7]$$

Defining the function

$$\theta_4 = \theta_4(t_s, B, b) = t_s(1 + b) + 2.90\, LB^{-1} p_s \quad \ldots [8]$$

the equation for the heat flow becomes

$$q = f_c A\,[\theta_4(t_s, B, b) - \theta_4(\tau_\infty, B, b) - \theta_3(b, U_\infty)] \quad \ldots [9]$$

The functions θ_1, θ_2, θ_3, and θ_4 are shown presented in Figs. 1(*a*), (*b*), (*c*), and (*d*) for B equal to atmospheric pressure.

Comparison of Equation [6] With Experimental Data

If the heat-flow term in Equation [6] is set equal to zero, the solution of the equation for the surface temperature yields a prediction which may be compared directly with experimental data. Reference (14) gives measurements of the temperature on a propeller heated intermittently while subjected to icing conditions. During the "heat-off" intervals, the propeller temperatures approached a steady-state temperature. These values may be used as a rather crude check upon Equation [6] since the heat-flow term was not equal to zero but was presumably very small. The data are not considered accurate to better than 5 deg F by the experimenters, and certain necessary measurements for the evaluation of the terms which enter into Equation [6] were not made. Nevertheless, Tables 1 and 2 show the experimental data, and the predictions are in fair agreement; all but a few of the cases showed agreement within the 5 deg F limit.

The data in Table 2 were obtained as follows:

(*a*) From the given radius and rpm the tangential velocity in the propeller disk was calculated for each measuring station.

(*b*) This velocity was added vectorially to the tunnel velocity which was reported as 120 mph for all tests, but which was not measured near the plane of the propeller during propeller operation.

(*c*) The resultant velocity, the blade-profile data of reference (14), the average droplet size of 50 microns (approximate value), the tunnel air density and temperature were all used to compute the dimensionless moduli Ru and Ψ; see nomenclature, also reference (15).

(*d*) Using the data of reference (16), a portion of which is reproduced in Figs. 2(*a*) and (*b*), the rate of ice accretion on each measuring station was computed. The liquid water content of the tunnel at each radius was determined using the measured values reported in reference (14), Fig. 8(*b*). (The spray devices did not produce uniform icing conditions in this portion of the tunnel.)

(*e*) From equations given in reference (17) for laminar flow over streamlined bodies, the unit thermal conductance for heat transfer was computed. (The laminar-flow values gave the best agreement.)

(*f*) From the foregoing values for f_c and R_∞ the modulus b was computed (see nomenclature).

(*g*) From the values of the resultant air velocity, free air temperature, barometric pressure and b, the functions θ_2 and θ_3 were computed using graphs similar to Figs. 1(*b*) and (*c*).

(*h*) Setting the heat flow equal to zero in Equation [6] the function θ_1 may be computed from

$$\theta_1 = \theta_2 + \theta_3$$

(*i*) Using this value of θ_1 and the value of b as given, the value of t_s was computed, using a figure similar to Fig. 1(*a*).

A second test for Equation [6] also may be made. Equation [6] predicts that the temperature of an unheated surface exposed to icing conditions should begin to rise when the ice begins to form. If the rate of icing is great enough, the surface should reach 32 F. Reference (18) reports data of this nature. Figs. 3 and 4 are taken from reference (18) and show time-temperature histories on the surface of propeller blades heated intermittently.[3] The interesting feature of these figures is that they show the temperature on the blade during the time the water sprays were turned on and before the heaters were energized. In Fig. 3 it can be seen that when the water sprays were turned on the temperature of the blade rose from 20 F to 32 F without the addition of heat from the heaters. This latter experiment was conducted with a relatively high liquid-water content in the tunnel. Note that the

[3] A more detailed analysis of the data of reference (18) is presented in this issue of the Transactions (pp. 1131–1137), by Mr. Frederick Weiner of the Engineering Department, University of California. Using the same methods as presented herein, excellent agreement between measured and predicted temperatures was obtained.

TABLE 1

Case	T_∞	w‡	radius	rpm	x **	Measured values of t_s	Figures in TN 1520
	°F	g/m³	ft		in	°F	
a	2	0.25	1.98	675	1.8	24	28a,29a
b	2	0.25	1.98	925	1.8	22,23,23	24a,24b,28b
c	11	0.46	1.98	675	1.8	27,24,34,34,33	25a,26a,27a, 30a,31a
d	11	0.46	1.98	925	1.8	32,32,33,34,31	25b,26b,27b, 30b,31b
e	2	0.20	3.02	675	1.2	25	29a
f	2	0.20	3.02	925	1.2	19,21,16	24a,24b,29b
g	11	0.40	3.02	675	1.2	24,24,27,29,26	25a,26a,27a, 30a,31a
h	11	0.40	3.02	9.25	1.2	25,32,33,32,28	25b,26b,27b, 30b,31b
i	2	0.15	4.22	675	1.3	22	29a*
j	2	0.15	4.22	925	1.3	25,27,29,27	24a,24b,28b,29b
k	11	0.30	4.22	675	1.3	28,30,32,33,32	25a,26a,27a, 30a,31a
l	11	0.30	4.22	925	1.3	30,35,36,36,34	25b,26b,27b, 30b,31b
n	2	0.30	1.15	925	1.2	28	28b
o	11	0.50	1.15	675	1.2	23,29,33,27	26a,27a,30a, 31a
p	11	0.50	1.15	925	1.2	28,30,32,28	28b,27b,30b,31b

TABLE 1 Temperature on propeller blades in icing conditions when the heat flow is very small. (Taken from figures 24 to 31 of NACA TN 1520.)

*This figure in TN 1520 must be in error. Points labeled Δ should be ▽ as a study of the other curves will indicate.

‡ Values of the liquid water content, w, were corrected for uneven distribution of water across the tunnel section using figure 8b of TN 1520.

** The distance, x, in column 6 is measured along the surface from the leading edge.

TABLE 2

Case	r/R	rpm	T_∞	U_∞	ψ	Re	E_M	LWC*	$\Delta E/E_M$	f_c	b	θ_2	θ_3	θ_1	t_s	t_{meas}
a	0.38	675	2	239	101	325	0.80	13.1	0.30	15.5	0.248	34.4	4.3	38.7	22	24
b	0.38	925	2	290	101	395	0.80	13.1	0.30	17.0	0.276	38.0	6.7	44.7	25	22 to 23
c	0.38	675	11	239	101	225	0.80	31.2	0.30	15.5	0.594	93.7	5.1	98.8	32	27 to 34
d	0.38	925	11	290	101	395	0.80	31.2	0.30	17.0	0.552	87.7	7.2	94.9	32	31 to 34
e	0.58	675	2	304	112	415	0.79	11.2	0.28	17.4	0.124	18.4	7.5	25.9	16	25
f	0.58	925	2	363	112	495	0.80	11.2	0.28	19.1	0.138	20.2	10.5	30.7	19	16 to 21
g	0.58	675	11	304	112	415	0.79	25.6	0.28	17.4	0.285	51.9	7.8	59.7	32	24 to 29
h	0.58	925	11	363	112	495	0.80	25.6	0.28	19.1	0.316	55.3	11.0	66.3	32	25 to 33
i	0.81	675	2	367	91	500	0.85	6.24	0.28	19.2	0.560	74.6	12.0	86.6	32	22
j	0.81	925	2	466	91	622	0.86	6.25	0.28	21.6	0.641	84.9	19.2	104.1	32	25 to 29
k	0.81	675	11	367	91	500	0.85	19.9	0.28	19.2	0.18	26.5	10.8	37.3	22	28 to 33
l	0.81	925	11	466	91	622	0.86	19.9	0.28	21.6	0.205	40.0	17.1	57.1	32	30 to 36
m	0.22	675	2	234	54	319	0.85	15.6	0.04	15.3	0.219	30.6	4.1	34.7	20	25
n	0.22	925	2	246	54	333	0.85	15.6	0.04	15.7	0.224	32.0	5.0	37.0	21.5	20 to 28
o	0.22	675	11	234	54	319	0.85	34.3	0.04	15.3	0.481	77.1	4.2	81.3	32	23 to 33
p	0.22	925	11	246	54	333	0.85	34.3	0.04	15.7	0.495	80.0	5.5	85.5	32	28 to 32
			F	ft/sec				*								

* $\frac{\text{BTU}}{\text{hr sq ft F}}$

TABLE 2 Comparison of measured and predicted temperatures on propeller blade during icing conditions.
*LWC denotes liquid water content in millionths of a pound of liquid water per cubic foot of air. The other columns are dimensionless or have their units given.

Additional data:

r/R	s/C	t/C	C
0.38	0.167	0.24	9"
0.58	0.150	0.12	10
0.81	0.186	0.10	8.1
0.22	0.10	0.75	4.8

R = 5.208 ft. $b = (R_w C_{p_w}) / (f_c)$

$$b = \frac{(3600)(\Delta E / E_M)(E_M)(1/C)(LWC)(U_\infty)}{(\Delta s/C)(f_c)}$$

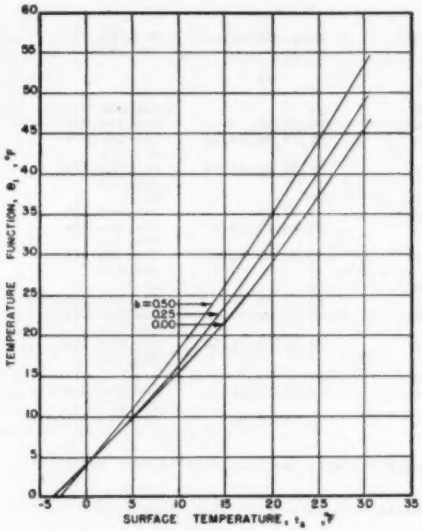

FIG. 1(a) GRAPH OF $\theta_1(t_s, B, b) = t_s(1 + 0.47b) + 2.90\,LB^{-1}p_s$ FOR THE CASE $B = 29.9$ IN. OF MERCURY, $L = 1218$ BTU PER LB
(p_s corresponds to saturation pressure over ice at temperature t_s.)

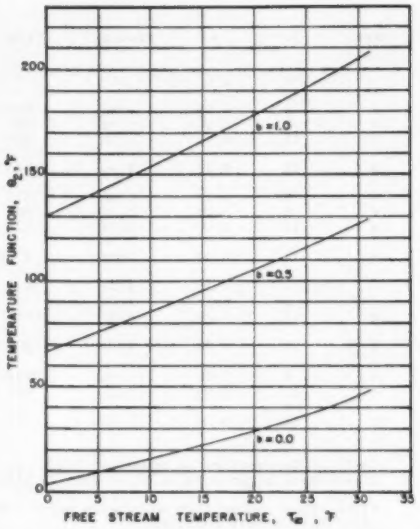

FIG. 1(b) GRAPH OF $\theta_2(\tau_\infty, B, b) = \tau_\infty(1 + b) + 127b + 2.90\,LB^{-1}p_\infty$ FOR THE CASE $B = 29.9$ IN. OF MERCURY, $L = 1218$ BTU PER LB
(p_∞ corresponds to vapor pressure of supercooled liquid water at temperature τ_∞.)

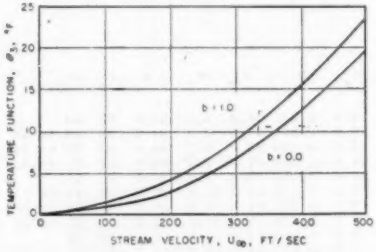

FIG. 1(c) GRAPH OF $\theta_3(b, U_\infty) = \left(\frac{\tau}{C_p} + b\right)(U^2_\infty/2g_cJ)$

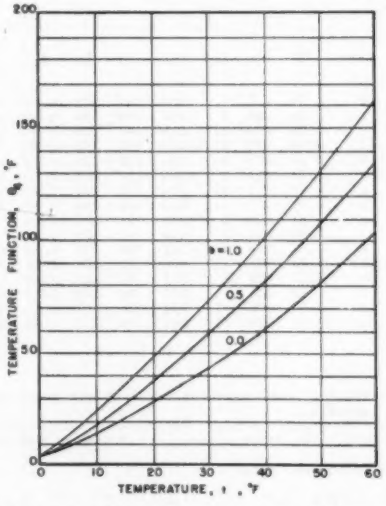

FIG. 1(d) GRAPH OF $\theta_4(t, B, b) = t(1 + b) + 2.90\,LB^{-1}p$ FOR THE CASE $B = 29.9$ IN. OF MERCURY, $L = 1070$ BTU PER LB
(p corresponds to vapor pressure of water at temperature t.)

temperature rise on the blade is larger than that produced by the electrical heaters. Fig. 4 demonstrates a similar effect, only this time the liquid-water content is much lower, and the temperature does not rise to the freezing point.

TEMPERATURE VARIATIONS ON A PROPELLER WITH INTERMITTENT HEATING

Although sufficient data were not available for a careful comparison between the predictions of the present analytical treatment and the temperature-time measurements of Lewis (14), a few cases were considered in order to check whether the analysis would predict results yielding the same order of magnitude.

Fig. 5 shows the type of heating system used by Lewis. The heating pads consisted of 0.048 in. of rubber cemented to the blades, nichrome heater wires, and 0.024 in. of rubber as an outer layer.

The heat-flow circuit was idealized as follows:

Consider a small section of the blade, as in Fig. 6(B), and note that the heat from the nichrome ribbons flows partially outward and partially inward toward the blade. The heat which flows inward flows along the steel blade to the cooler trailing edge. The heating is not steady, and a great deal of energy is used in heating up the rubber and steel. For the calculations, the heat flow was postulated as occurring normal to the rubber

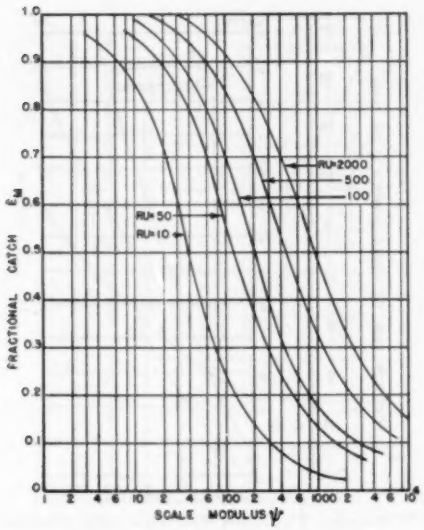

FIG. 2(a)

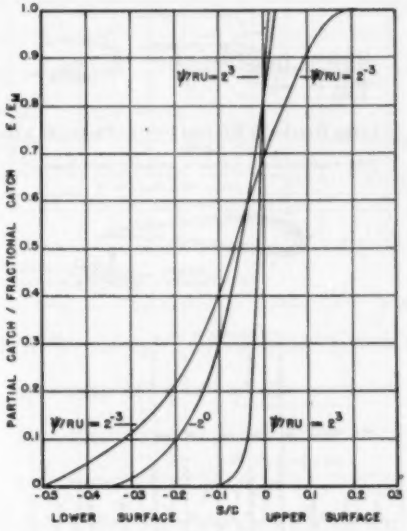

FIG. 2(b)

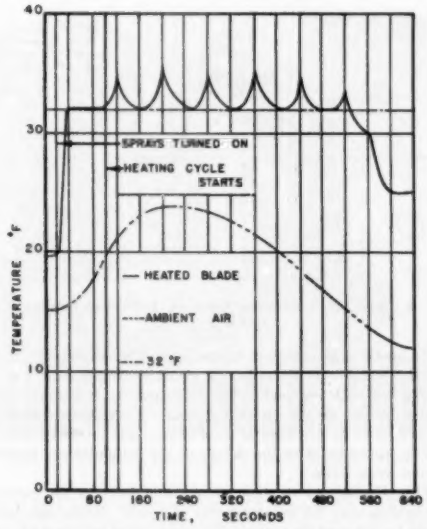

FIG. 3 MEASUREMENTS BY LEWIS FOR INTERNALLY HEATED BLADE
(Liquid-water content of air, 0.9 gram per cu m taken from fig. 10(a), reference 18.)

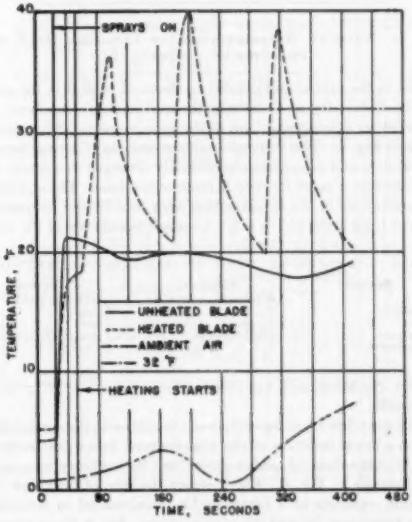

FIG. 4 MEASUREMENTS BY LEWIS FOR INTERNALLY HEATED BLADE
Liquid-water content of air, 0.3 gram per cu m taken from fig. 10(d), reference 18.)

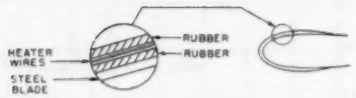

FIG. 5 LAYER DETAILS OF HEATERS USED IN PROPELLER TESTS BY LEWIS
(This construction is typical of presently used heaters.)

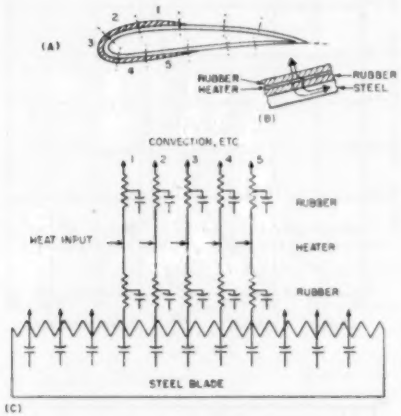

FIG. 6 NETWORK REPRESENTATIVE OF IDEALIZED HEAT FLOW INDICATED BY ARROWS IN (B)

layers in the rubber and parallel to the steel surface in the metal.

The University of California thermal analyzer has been constructed for solving problems of the type represented by the network in Fig. 6. The thermal analyzer consists of a large number of resistors and capacitors conveniently arranged in a frame with terminals on a panel for ease of interconnections. The equivalent networks used in this investigation were constructed according to the relations given in Table 3. A sample calculation of the values

TABLE 3 RELATIONS USED IN EQUIVALENT NETWORKS

Quantity	Electrical	Thermal
Flux	0.06 milliampere	3.413 Btu per hr (1 w)
Potential	4 volts	1 deg F
Time	1/4 sec	1 sec
Resistance	172 kilo-ohm	1 deg F/(Btu/hr)
Capacitance	5.2×10^3 microfarad	1 Btu/deg F

of the resistance and capacitance for one case is given in the appendix.

The heat flow from the surface of the rubber to the surroundings is not a linear function of the temperature, hence the linear elements of the thermal analyzer could not be combined to complete the network in Fig. 6. Fig. 7 shows the rate of heat flow from various segments of a propeller blade calculated in accordance with Equations [6] and [9] of this paper. Fig. 8 shows the nonlinear network constructed to produce current-voltage characteristics analogous to Fig. 7. Fig. 9 shows a comparison between the measured behavior of the analogous network and the thermal system. Constant current sources and a timer were constructed to provide an analogy to the intermittently operated constant-power heaters. Fig. 10 shows the thermal analyzer and the associated equipment.

The behavior of the nonlinear network was computed, using Equations [6] and [9] for each of the five segments of the propeller.

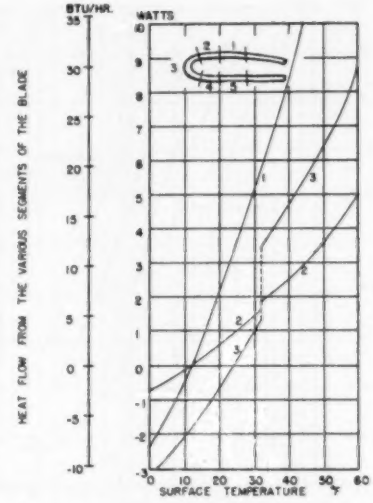

FIG. 7 COMPUTED VALUES FOR HEAT FLOW FROM SEGMENTS OF PROPELLER BLADE DURING ICING CONDITIONS
(925 rpm, free-stream temperature 2 F, radial station 3.02 ft, air velocity 120 mph, liquid-water content 0.20 gram per cu m.)

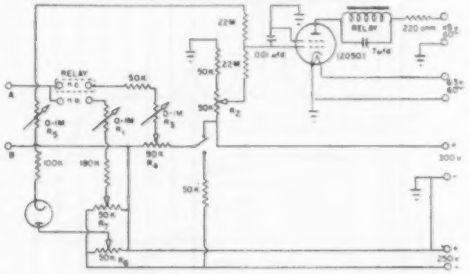

FIG. 8 NONLINEAR NETWORK USED TO REPRESENT ENERGY FLUX AT ICE SURFACE

Data for the segments were taken from drawings donated by the Curtiss-Wright Corporation. A separate computation was required for each segment. The heat-transfer resistance represented by the ice was omitted as small in comparison with the uncertainties in the thermal conductance due to convection.

The Appendix gives the details of the computations required for one calculation.

Figs. 11, 12, and 13 show comparisons between the analyzer predictions and the measurements of Lewis. Better agreement could be obtained by varying the value of the unit thermal conductance by 20 per cent or by comparing the measured values with predicted temperatures just beneath the rubber surface, as in the case of a thermocouple embedded in the rubber and partially insulated from the surface. Because of the many uncertainties mentioned before, no further analysis of these data was attempted.

The thermal analyzer permits easy measurement of some of the variables which are not determined readily in full-scale tests on a rapidly whirling propeller. For example, Fig. 14 shows the

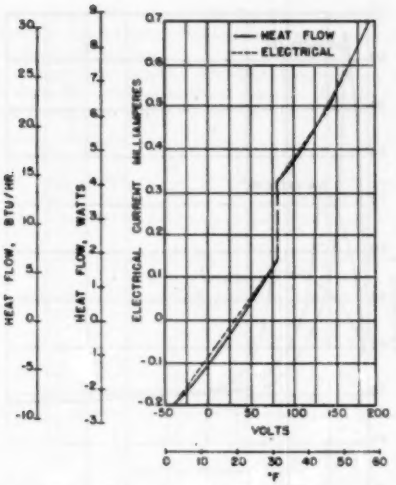

FIG. 9 BEHAVIOR OF NONLINEAR NETWORK SHOWN IN FIG. 8, WHEN PARAMETERS ARE ADJUSTED TO APPROXIMATE HEAT-TRANSFER CHARACTERISTICS OF SEGMENT 3 IN FIG. 7

(Straight dashed-line segments represent electrical-network current-voltage characteristics.)

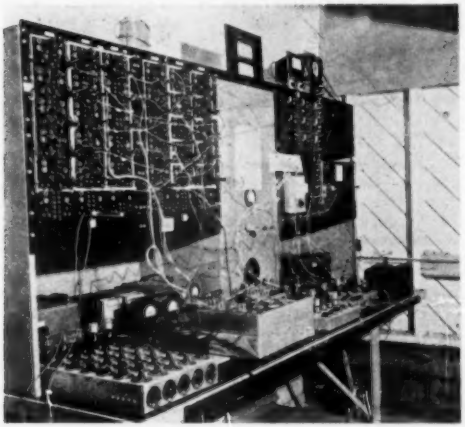

FIG. 10 THERMAL ANALYZER AND ASSOCIATED EQUIPMENT

rate of heat flow from the heating wires to the metal blade during one cycle. This figure is significant because it reveals that almost two thirds of the energy put into the heating elements flows to the blade rather than the ice.

Since so much of the energy goes to heating up the blade metal, the equilibrium temperature of the blade when there is no heating assumes considerable importance. A conclusion to be drawn from this fact is that less energy should be required for ice protection as the ice-accretion rate increases, all other conditions remaining the same. A search of the literature did not reveal corroborative evidence beyond the one experiment given later and

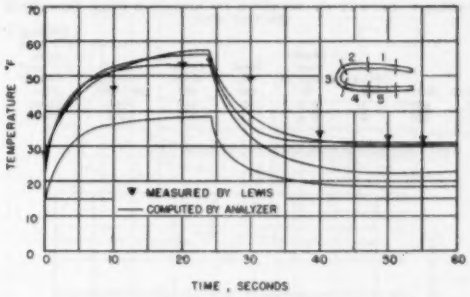

FIG. 11 COMPARISON BETWEEN DATA OF LEWIS AND THERMAL ANALYZER

(v_∞ = 2 F, 925 rpm, 9 w per sq in. at segment 3, 8 w per sq in. on 1, 2, 4, 5, r/R = 0.81. Points correspond to highest curve; see fig. 24, reference 14).

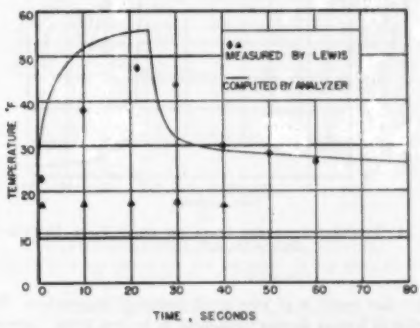

FIG. 12 TIME-TEMPERATURE HISTORY ON A PROPELLER BLADE

(Same conditions as Fig. 11, but with r/R = 0.58. Lower curve corresponds to afterbody of blade.)

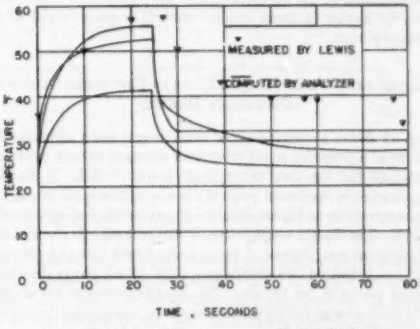

FIG. 13 TUNNEL TEMPERATURE 11 F, 925 RPM

(See fig. 30b of reference 14.)

taken from reference (18), since apparently this matter has not been considered important to other experimenters. Table 4 demonstrates that the change in liquid-water content in this test made a very great difference in the reported deicing effectiveness. Unfortunately, these two runs are the only ones available for comparison.

TABLE 4 EFFECT OF CHANGE IN LIQUID-WATER CONTENT ON DEICING

Run	Rpm	Air temp, deg F	Liquid water, grams/cu m	Heat on, sec	Cycle time, sec	Heater power, per blade	Deicing effectiveness, per cent de-iced area
T...	800	5	0.3	40	160	1000	20-20
U...	800	5	0.4	44	160	1000	60-70

NOTE: Reproduced from Table 2 of reference (18).

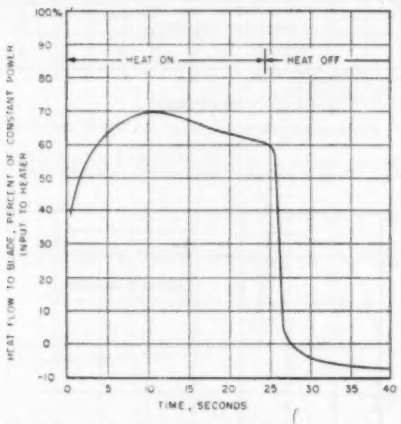

FIG. 14 THERMAL-ANALYZER DATA ON HEAT FLOW INWARD TO BLOCK DURING A CYCLE

This last result is of very great technical importance. The practice in testing deicing equipment is to test under "severe" conditions. For example, reference (14) reports that the rates of icing in the tunnel were less than those recommended by the NACA. However, the recommended values are high liquid-water contents in the air stream, and the equipment would have shown up better in these severe conditions than it did in the tests as reported.

IMPROVEMENTS WHICH MAY BE MADE IN PRESENTLY OPERATING PROPELLER DEICERS

Fig. 15 shows a comparison of time-temperature histories on a segment of a propeller blade wherein a constant energy input was maintained but the time of application was varied. If the time of application is decreased while the power is increased the surface temperatures rise to higher values. Considerable improvement in ice protection should result, then, if the propeller is divided into three sections and, instead of being heated with 10 watts per sq in. for 20 sec, is heated one section at a time with a power density of 30 watts per sq in. for 6.6 sec. The electric system of the airplane would have to supply the same amount of power, but the protection would be enhanced.

AN APPLICATION TO JET-ENGINE GUIDE-VANE DEICING

Figs. 16(*a*) and (*b*) show a jet-engine guide vane and the method of constructing the analogous electric circuit representing the heat-flow paths when electric heating is applied to the guide vane. The configuration chosen for detailed study on the analyzer was a guide vane with the heat applied uniformly to the

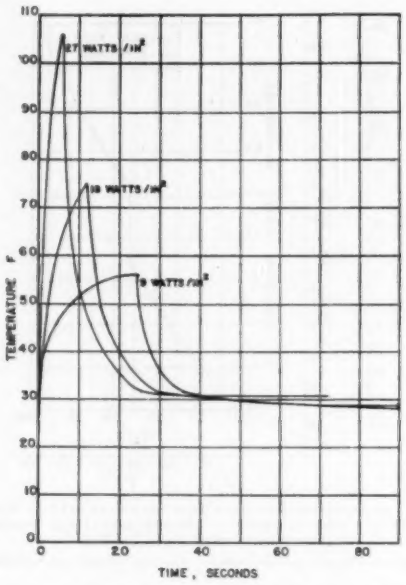

FIG. 15 EFFECT OF VARYING POWER DENSITY AT CONSTANT ENERGY

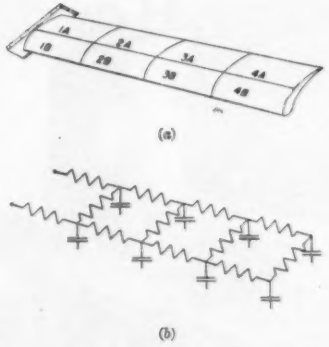

FIG. 16 TYPICAL GUIDE VANE (*a*) AND EQUIVALENT NETWORK (*b*)

TABLE 5 CASES CHOSEN FOR STUDY OF GUIDE-VANE DEICING*

Case	Air temp at blade, deg F	Icing rate, in. per min	Air velocity past blade, fps	Liquid-water content grams per cu m	Unit thermal conductance, Btu/hr sq ft deg F: Leading edge	Trailing edge
I.....	2	0.035	463	0.10	50	92
II.....	2	0.14	463	0.38	50	92
III.....	11	0.042	175	0.30	30	42
IV.....	11	0.14	175	1.00	30	42

* The peculiar mixture of units appearing in this table is the result of the present state of the art in ice prevention. The meteorologist reports data in the CGS system while the icing observers are habituated to measuring ice accretion in inches per minute.

NOTE: The surface area, both sides, for each segment, leading or trailing edge, was 7.63×10^{-4} sq ft.

leading edge only. (It turns out that this is not an efficient heat distribution.) Table 5 indicates the cases chosen for study of the guide-vane deicing problems.

Fig. 17 shows the computed heat-flow characteristics, while Fig. 18 shows the completed electrical network. Figs. 19(*a*) and (*b*), show typical data.

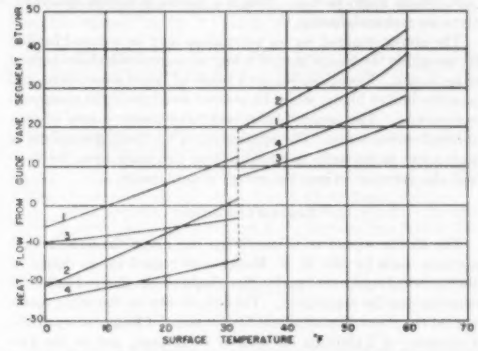

FIG. 17 HEAT FLOW FROM GUIDE-VANE LEADING-EDGE HALF FOR CONDITIONS GIVEN IN TABLE 5

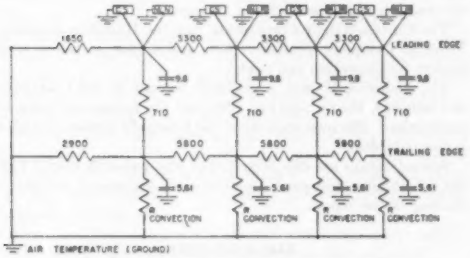

FIG. 18 COMPLETED NETWORK FOR GUIDE VANE
(Ice impingement was considered as occurring only over leading edge in calculations.)

CONCLUSIONS CONCERNING ENERGY REQUIREMENTS FOR JET-ENGINE GUIDE-VANE DEICING

The analysis of the data obtained from the thermal analyzer for the stainless-steel guide vane indicates that the spanwise heat conduction is not very large and that if the entire vane is subjected to icing conditions, the entire vane must be heated. The most economical heating system will be one which does not heat any portion of the blade hotter than the average temperature. Such a system yields a very simple type of thermal network, for the conduction of heat between the segments may then be put equal to zero. The circuit representation of Fig. 18 may then be simplified to the diagram, Fig. 20. A conservative design results if the nonlinear network is replaced by a linear element having an impedance equal to the lowest value occurring during the cycle. Fig. 21 then shows the conservative simplified circuit.

The lowest value of the impedance occurs when the highest temperature is attained across the nonlinear portion of the thermal network. In a good design the maximum surface temperature will be in the neighborhood of 32 F. Reference (2)[4] shows at this surface temperature that at sea level and low outside-air temperature the evaporative term accounts for 30 per cent as much heat transfer as the convective term in the energy flows at the surface of the ice. The benefits from the heat of fusion are zero at this temperature. Therefore the lowest resistance across the nonlinear portion of the network is taken equal to $(^1/_{1\text{-}3})$ $(^1/_{f_c A})$. The maximum energy requirements for ice prevention will occur at low temperatures and when the rate of ice accretion is very low. In arriving at the conservative design, then, the contributions from the heat of fusion will be put equal to zero.

The time-temperature variation in a circuit such as shown in Fig. 21 is given by

[4] Reference (2), p. 101.

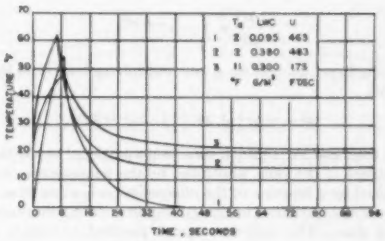

(*a*)

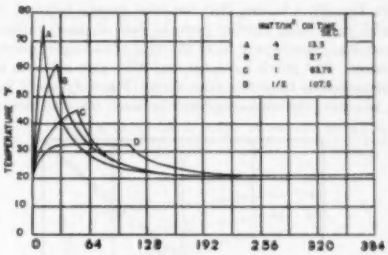

(*b*)

FIG. 19 TYPICAL DATA OBTAINED FROM ANALYZER
(In Fig. 19(*a*), power density was 4 w per sq in. In Fig. 19(*b*), τ_∞ = 11 F, U_∞ = 175 fps, w = 0.30g/m².)

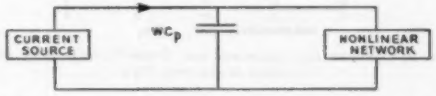

FIG. 20 SIMPLIFIED REPRESENTATION OF THERMAL CIRCUIT FOR EFFICIENTLY HEATED GUIDE VANE

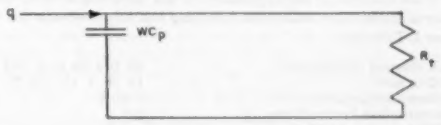

FIG. 21 CONSERVATIVE SIMPLIFIED NETWORK FOR EFFICIENTLY HEATED GUIDE VANE

$$\frac{\Delta t}{qR} = 1 - e^{-\theta/RC} \quad [10]$$

Solving Equation [10] for q, and multiplying both sides by time θ, yields

$$q\theta = C\Delta t\,[(\theta/RC)/(1 - e^{-\theta/RC})] \quad [11]$$

The total energy required, then, is proportional to the thermal capacitance of the vane, multiplied by the temperature rise, and multiplied by a function of the dimensionless heating time. Fig. 22 shows the variation in energy required versus dimensionless heating time. The minimum energy required, of course, is the energy required to heat the guide vane through the stipulated temperature rise.

From Fig. 22 it is seen that the total energy required diminishes with decreasing heating periods, that is, short intervals of high-power application are more effective than longer intervals at low powers. The graph indicates that little gain is had in taking the dimensionless time less than 0.10. For very short heating times, however, the correspondence between the distributed system behavior and the network approximation will be less close. The deviations will be such as to yield a conservative design.

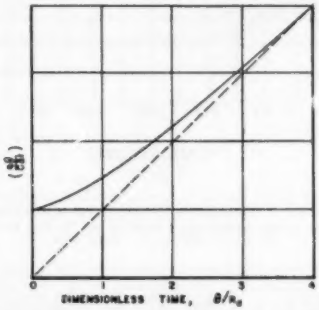

FIG. 22 ENERGY REQUIREMENTS FOR GUIDE-VANE DEICING AS A FUNCTION OF HEATING TIME

As an example of the application of the foregoing results, consider a guide vane where the following conditions obtain (as in Case I, Table 5):

Unit thermal conductance	66 Btu/hr sq ft deg F
Surface area	15.26×10^{-4} sq ft
Ambient temperature	−40 F
Dimensionless heating time (thus requiring 1.05 times the minimum energy)	0.1
Weight of guide vane	0.13 lb
Unit heat capacity of guide vane	0.1 Btu/lb deg F
Design temperature rise (to 35 F)	75 deg F

Therefore

$$q\theta = 1.05\,C\Delta t$$
$$= 1.05 \times 0.13 \times 0.1 \times 75$$
$$= 1.03 \text{ Btu/blade cycle}$$

$$\theta = 0.1\,RC$$
$$R = (1/1.3)\,(1/66)\,(1/15.26)\,10^3 \text{ deg F/(Btu/hr)}$$
$$C = 0.13 \times 0.1 \text{ Btu/deg F}$$

$$\theta = \frac{0.1 \times 0.13 \times 0.1}{1.3 \times 66 \times 15.2}\,10^3$$
$$= 1.02 \times 10^{-3} \text{ hr} = 3.6 \text{ sec}$$

$$q = \frac{1.03 \times 10^3}{1.02} = 1.01 \times 10^3 \text{ Btu/hr} = 296 \text{ watts}$$

If each guide vane is to be unheated (and, therefore, permitted to gather ice) for a maximum time of 1 min and there are 51 guide vanes per engine, they may be heated in groups of three with a continuous power required from the airplane of less than 1 kw. It may be found more economical from the point of view of saving weight to use a greater amount of power than seventeen separate connections might permit. This is a matter of special considerations for each installation.

The power required for ice prevention may be reduced further by designing the blades in such a way as to diminish their thermal capacitance. Fewer blades, each blade of larger dimensions and possibly hollow blades might be utilized to diminish the energy requirements. The larger blades will have lower values of unit thermal conductance. The application of the heating elements in such a way as partially to insulate them thermally from the vane will also serve to reduce the energy requirements.

ACKNOWLEDGMENTS

The author wishes to acknowledge the many timesaving suggestions made by Mr. H. R. Kaiser with regard to the design of the electrical equipment and to the efforts of Mr. James DuBois in constructing the equipment. Thanks are due to the other members of the research staff of the Department of Engineering of the University of California for loan of equipment, and to the Department of Engineering for sponsoring the project.

Prof. L. M. K. Boelter and other members of the author's Doctoral Committee are to be thanked for suggestions concerning the research and presentation of the results.

The Curtiss-Wright Corporation and the Hamilton Standard Propeller Company supplied reports and sample propellers with heaters for inspection and study.

Mr. Frederick Weiner, a graduate student at the University of California, kindly read and corrected the manuscript prior to publication. His own analysis of the internally heated propeller is now published.[9]

Special thanks are due Mrs. Tribus who patiently helped with the calculations, test runs, construction of equipment, and proofreading of the report.

BIBLIOGRAPHY

1 "Report on the Development and Application of Heated Wings," by M. Tribus, *SAE Journal*, vol. 54, June, 1946, pp. 261–269, 309.

2 "Report on the Development and Application of Heated Wings—Addendum I," by M. Tribus and J. Tessman, AAF TR 4972, 1946.

3 "General Results of NACA Flight Research in Natural Icing Conditions During the Winters of 1945 and 1946," by N. R. Bergrun, *Aeronautical Engineering Review*, vol. 7, January, 1948, pp. 20–27.

4 "The Calculation of the Heat Required for Wing Thermal Ice Prevention in Specified Icing Conditions," by C. B. Neel, et al, NACA TN 1472, December, 1947.

5 "Theory of Propeller De-Icing," by Franz Eder, AMC Translation F-TS-940-RE (from captured German document ZWB-FB-RE-11-5 S 123).

6 "Propeller Icing and Its Prevention," by E. Eck, AAF Translation 517, October 21, 1944.

7 "An Analytical Investigation of Thermal Electric Means of Preventing Ice Formation on a Propeller Blade," by Richard Scherrer, NACA ACR 4H31, 1944.

8 "Tests of Thermal Electric De-Icing Equipment for Propellers," by Richard Scherrer and L. A. Rodert, NACA ARR 4A20, 1944.

9 "C6338-A Propeller De-Icing Tests," by J. H. Sheets, Curtiss-Wright Corporation, Propeller Division, Caldwell, N. J.; company report C-1907, February 18, 1948.

10 "Outrigger Flight Tests to Determine the De-Icing Power Requirements of Several Propeller Heating Elements Having Chosen Heat Distributions and Operated Cyclically," by J. O. Schulze, AAF Technical Report 5445, March 22, 1946.

11 "Flight Tests of Hamilton Electrically Heated Propellers on

DC 6 Number NX-37051," by W. W. Reaser, Douglas Aircraft Company Report SM 12091, March 19, 1947.

12 "Flight Test of 50 Inch Blade Heaters (HSP 70101 on 23E50/-6491A-O Propeller)," by W. M. Alford, Hamilton Standard Propeller Company Report HSP 547, April 10, 1947.

13 "Analysis of Heat Transfer Over a Small Cylinder in Icing Conditions on Mount Washington," by Myron Tribus, et al, Trans. ASME, vol. 70, 1948, pp. 971–976.

14 "De-Icing Effectiveness of External Electric Heaters for Propeller Blades," by J. P. Lewis, NACA TN 1520, February, 1948.

15 "Limitations and Mathematical Basis for Predicting Aircraft Icing Characteristics From Scale-Model Studies," by M. Tribus, G. B. W. Young, and L. M. K. Boelter, Trans. ASME, vol. 70, 1948, pp. 977–982.

16 "Impingement of Waterdrops on Various Airfoils From Trajectories Obtained on Differential Analyzer," by A. G. Guibert, et al., NACA RM 9A05, February 16, 1949.

17 "An Investigation of Aircraft Heaters VIII A Simplified Method for the Calculation of the Unit Thermal Conductance Over Wings," by R. C. Martinelli, et al., NACA ARR March, 1943.

18 "Icing and De-Icing of a Propeller With Internal Electric Blade Heaters," by J. P. Lewis and H. C. Stevens, Jr., NACA TN 1691, August, 1948.

Appendix

Sample Calculation for Case Shown in Fig. 11

The following will serve to outline the calculations required to permit adjustment of the thermal analyzer to produce the data shown in this report:

Briefly, from the geometrical data given in reference (14), the blade characteristics may be determined. Since the exact blade construction was not specified, a blade, donated by the Curtiss Wright Propeller Division, was sectioned and measurements made directly. From these measurements and blueprints and the properties of steel and rubber, the thermal circuit representative of the blade and its heater was constructed.

From the given rpm, blade station, liquid-water content, tunnel temperature, and wind velocity, the heat and mass-transfer properties of the blades were determined. Knowledge of these heat and mass-transfer characteristics permitted adjustment of the nonlinear networks.

From the given data concerning the heat inputs to the various blade stations, the constant current sources were adjusted.

Fig. 23 shows the propeller section used for station $r/R = 0.58$.

The thermal capacity of segment 2 is obtained by measuring the cross-sectional area and multiplying by the depth to obtain the volume. This volume when multiplied by the density and heat capacity of steel yields the thermal capacity

$$C_t = (\text{volume}) \times (\text{density}) \times (\text{heat capacity}) \quad [12]$$

$$C_t = 8.09 \text{ Btu/°F (inch span)} \quad [13]$$

The analogous electrical resistor and capacitor are found to have values of

$$R_{\text{electrical}} = 805 \text{ K}\Omega \quad [14]$$

$$C_{\text{electrical}} = 36.2\ \mu fd \quad [15]$$

Table 6 shows the thermal properties used for the rubber and steel.

TABLE 6 THERMAL PROPERTIES OF RUBBER AND STEEL

	Rubber	Steel
Thermal conductivity, Btu/hr sq ft (deg F/ft)	0.147	14
Density, pcf	91	492
Unit heat capacity at constant pressure, Btu/lb deg F	0.406	0.12

The layer details of the rubber pads cemented to the blade are given in Fig. 5.

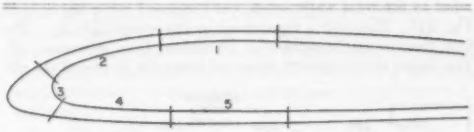

Fig. 23 Propeller Section for Station $r/R = 0.58$

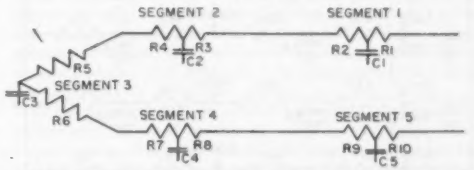

Fig. 24 "Equivalent" Ideal Lumped Thermal Circuit Representative of Propeller Section Shown in Fig. 23

[For example, the value of resistor R_4 of Fig. 24 was calculated as follows: The thickness of the metal blade at the center of segment 2 (d_2) and at the forward end (d_1) were measured. The length of the half segment was measured (X), Fig. 25.]

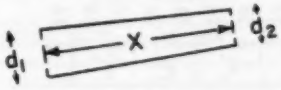

Fig. 25

[The resistance to heat transfer (per inch span) is given by

$$R = \frac{12X}{k^1/_2(d_1 + d_2)}$$

$$X = (0.80/12) \text{ ft}$$

$$\frac{(d_1 + d_2)}{2} = (0.15/12) \text{ ft}$$

$$k = 14 \text{ Btu/hr sq ft (deg F/ft)}$$

hence

$R_4 = 4.57$ deg F/(Btu/hr)]

The completed lumped circuit, including elements representing the rubber pads and the blade, but not the nonlinear networks, is shown in Fig. 26.

Using the data on the propeller rpm, radius, etc., from reference (14), the unit thermal conductance and the icing rate for each segment of the propeller-blade section were calculated. Table 7 summarizes the given data and the results of the calculations.

For each segmental area the ratio of water catch over that seg-

TABLE 7 PROPELLER DATA AND RESULTS OF CALCULATIONS

Given data:

Propeller radius, ft	5.208
Radius ratio (r/R)	0.58
Rpm	925
Free-stream temperature, deg F	2
Tunnel wind velocity, mph	120
Average droplet diam, microns	50
Barometric pressure, in. Hg	29.9
Chord length, in.	10.0
Thickness ratio	0.12
Local liquid-water content, pcf	11.2×10^{-6}

Computed data:

Relative velocity at this radius, fps	363
Scale modulus (ψ)	112
Reynolds modulus of droplet	495
Fractional catch for airfoil, E_M	0.80

Segment	$\Delta S/C$	$\Delta E/E_M$	f_a	b
1	0.15	0.99	98	0.00
2	0.16	0.93	19	0.014
3	0.12	0.56	41	0.159
4	0.16	0.29	19	0.133
5	0.15	0.12	86	0.017

ment to the total water catch was computed using the data in Fig. 2(*b*). This ratio is represented by the symbol $\Delta E/E_M$. The unit thermal conductance was determined from reference (17). The length of the segment measured along the surface of the air-

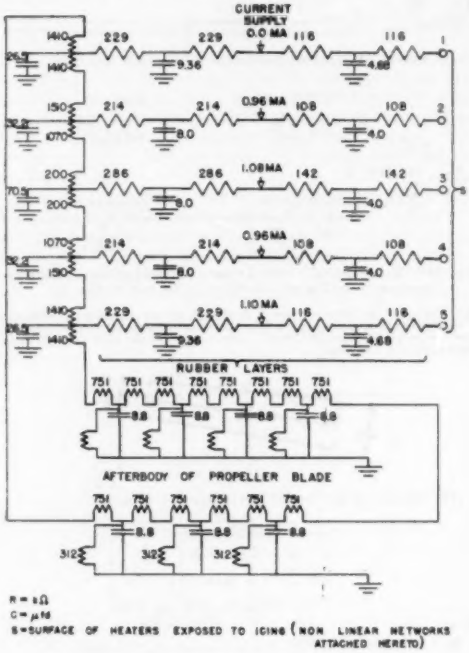

FIG. 26

foil, expressed as fraction of chord length is given by the symbol $\Delta S/C$. The value of b was calculated from the equation

$$b = \frac{E_M\,(\text{thickness/chord})\,U_\infty\,(3600)\,(\text{liquid-water content})\,(\Delta E/E_M)}{(\Delta S/C)_s}$$

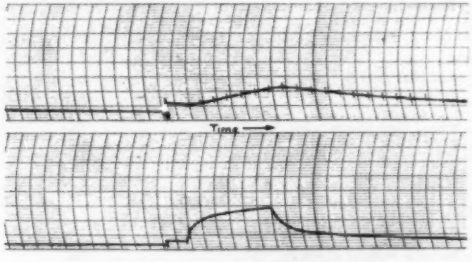

FIG. 27 TYPICAL RECORD OBTAINED FROM BRUSH RECORDER
(Lower curve represents variation in surface temperature on rubber pad, while upper curve represents variation in blade temperature under rubber heating pad. Scale is 2 deg F per division vertically, and 4 sec per division horizontally. Accuracy of recording equipment is estimated as one whole division or 2 deg F. Lowest line on recording tape corresponds to 18 deg F, which is sum of tunnel temperature, 2 deg F, and contribution of aerodynamic heating at this station, 16 deg F.)

Laminar flow was taken for segments 2, 3, 4. Turbulent flow was taken for segments 1 and 5.

The variation in heat flow with surface temperature was plotted as shown in Fig. 7, using Equations [6] and [9]. A separate calculation was required for each segment of the blade. Each of the five nonlinear networks was then adjusted to match the calculated heat-flow versus temperature curves as shown in Fig. 9. The equipment was allowed to cycle ten or more times under the control of an automatic timer adjusted to give 6 sec on and 18 sec off. The current inputs to each of the five segments were as shown in Table 8.

TABLE 8 CURRENT INPUTS TO SEGMENTS

Segment	Current, milliamp
1	0.00
2	0.96
3	1.08
4	0.96
5	1.10

These current inputs correspond to the heat inputs in Fig. 14(*b*) in reference (14). Fig. 27, herewith, shows a set of typical data obtained in this fashion.

Discussion

VICTOR HUDSON.[5] The field of aircraft ice prevention has been lacking a rational analytical method of predicting the performance of intermittent-type thermal ice-protective systems. The author's contribution toward gratifying this need is very praiseworthy.

Two major benefits of any analytical method of aircraft component design are good predictive accuracy of desired performance and a rapid as well as economic method of arriving at the quantitative values expressing such performance. The latter requirement the author's thesis fulfills extremely well by the method of transposition to analogous electrical circuits and adapting these for solution by the thermal analyzer. The former requirement is not always possible of complete isolation by analytical means. This is not to be construed as a weakness of the analytical approach but rather that in certain realms of application a degree of empiricism is unavoidable.

The writer believes that neglecting the thermal resistance of the ice layer is a serious omission from the analytical point of view. This omission appears reasonable as the theoretical method is evolved during the initial phases of formulation, however; as computed results are obtained and the predictive quality of the theory is correlated with experimental results, the conclusions drawn from these results become important from the standpoint of ice-layer resistivity. Thus it becomes possible to conclude that since ice resistivity was omitted and yet the results of theoretical computations lead to the conclusion that ice resistivity plays an important role in performance prediction, the analytical method begins to appear as unduly omniscient. As a corollary to such perusal, one may equally well conclude that the correlations are perhaps fortuitous. As an example, the deviation of the computed from the measured results, as depicted in Fig. 13 of the paper, during the heat-off cycle, may be attributed in a large part to ice-layer resistivity rather than completely to the heat of fusion.

The transposition of the thermal circuit into an analogous electrical circuit is clearly presented but for one troublesome omission. In the event of alternating-current application, aside from resistance and capacitance losses, induction losses also would take place. The question that arises is twofold, i.e., are the in-

[5] Senior Thermodynamics Engineer, Consolidated Vultee Aircraft Corporation, San Diego, Calif.

duction losses negligible or are they neglected because induction losses have no equivalent counterpart in the thermal circuit?

The criterion that the attainment of a +32 F blade-ice interface temperature is sufficient for adequate performance and should result in an economic system is intuitive in nature and is not a direct consequence of the theory itself. This hypothesis appears to be completely reasonable for propeller application in that the mechanism of shedding is accomplished by the radial inertial loads imposed on the ice accretions. Extending this concept to the protection of other (nonrotating) components in the aircraft merely in the interest of heater-source economy may not serve the attainment of adequate performance, i.e., from an over-all point of view. The latter argument well may apply to propellers also. In general, airframe designers consider any type of intermittent system (chemical, mechanical, or thermoelectric) as less desirable than a steady-state type. The extent to which over-all performance compromise is willingly made may be guided by the amount of armor plating necessary to shield the fuselage skin in the region of ice-fragment impingement. Thus longer "heat-off periods" and greater "sectionalizing" of heater surface may result in an undesirable weight penalty. Moreover, the loss due to propeller efficiency as affecting range and single-engine operation, during an emergency, may well outweigh the gains in heater-source decrease.

The writer is aware that the author's thesis is concerned primarily with propeller and jet-engine guide-vane application. However, since the methods are generic in nature and may be applied to the design of protective systems for other airframe components, some of the limitations of the analytical approach are offered as comments.

Jet-Engine Guide-Vane Deicing. While it is highly desirable to effect good economy with respect to heater source via the intermittent system, penalties attendant with its use also must be considered. The designer must be willing to accept loss in propulsive efficiency due to the decrease in the net air flow area resulting from ice accretions during the heat-off cycle. During development tests of protective systems, jet engines have been damaged by ice ingestion. Granted that in this instance damage would not be caused by impact of ice fragments, however, at present it is conceded by many test development engineers that an ice accretion "sliding off" the inlet guide vane may lodge in such a manner, between the guide vane and rotor blade, as to damage the rotor blade which in turn may, by "cascade" failure, damage the entire compressor section. It also has been observed that in the absence of radial inertia loads small airfoil sections do not always shed the accretion from the leading edge at every cycle. In jet engines this may lead to "bridging" the gaps between inlet guide vanes.

Wing and Empennage Leading-Edge Deicing. The following items are particularly true of large, long-range multiengine airframes (60,000 to 150,000 lb gross weight):

(*a*) The extent of surface area to be protected is such that even with the economies afforded by intermittent heating, electric generator capacities are excessive. This is particularly true of military types which impose large demands on electrical sources for use with armament, communication, and radar units.

(*b*) In design for the currently accepted "continuous icing" condition specifications, the intermittent system increased drag would affect range materially.

(*c*) The tenacity with which an ice cap persist in staying on the leading edge proper, even after several heat-on cycles, enables this accretion to build up to considerable proportions. Thus, when shedding finally does occur, the possibility of damaging empennage surfaces becomes high. Two interesting observations result from this phenomenon in the field of commercial aircraft. Airline operators have expressed a belief that they may be subject to litigation procedures in the event accretions are shed from low altitudes over inhabited areas, resulting in injury to persons on the ground. Objectionable psychological effects occur to passengers when they observe sheets of ice leaving the leading edge, followed by an impact noise as the accretions strike the tail surfaces.

J. L. Orr.[6] Interest in thermal deicing by intermittent heating is increasing due to energysaving over anti-icing by continuous heating. Canadian studies, concentrated on physical aspects and flight-test results in natural icing, have demonstrated the economy of ice removal using higher heating rates for shorter periods. This conforms with conclusions from thermodynamic study by the author.

However, we question the physical basis of his calculations and, particularly, supposed benefits of latent heat of fusion. Icing tunnel tests at Ottawa showed surface temperatures approaching the freezing point which did not change when water contents varied from $^1/_4$ to 3 grams per cu m.

Mr. Tribus is to be congratulated upon presenting such a powerful tool for solving difficult transient thermodynamic problems associated with the development of electrothermal deicing for wings, propellers, and jet engines.

V. Paschkis.[7] The author states that he disregards the thermal resistance of the ice layer as being small in comparison with the boundary resistance. This statement, together with the rather poor check of the experimental work with the predictions of Lewis as shown in Figs. 11, 12, and 13 (particularly the latter), makes it seem desirable to analyze systematically the influence of each variable independently. This should include the one omitted without proof by the author (thermal resistance of the ice). Such procedure is accepted standard in the writer's laboratory,[8] and, in way of example, reference is made to a systematic study of the influence of different variables on solidification of steel.[9]

W. M. S. Richards.[10] In Fig. 7 of the paper, why is the heat flow from section 3, the leading edge, less than from section 1 which is just aft of the maximum thickness? From the writer's recollection, this is contrary to most previous literature.

The idea of intermittent release of sizable chunks of ice from moving propeller blades or into the blades of an axial compressor rather amazes the writer. It was discussed at some length following presentation of the paper, but surely the cycling intervals must be made fairly short so as to hold down the propeller unbalance, or to avoid damage to the blading of an axial compressor.

On the whole this paper promises to bring the deicing problem back into the realm of practical possibility for turbojets and turboprops.

Frederick Weiner.[11] The author has made an excellent presentation on the use of an experimental analogous system to solve a complex heat-transfer problem. It is encouraging to find that

[6] National Research Council, Ottawa, Can.

[7] Technical Director, Heat and Mass Flow Laboratory, Department of Mechanical Engineering, Columbia University, New York, N. Y. Mem. ASME.

[8] "A Method for Determining Unsteady-State Heat Transfer by Means of an Electrical Analogy," by V. Paschkis and H. D. Baker, Trans. ASME, vol. 64, 1942, p. 105.

[9] "Influence of Properties on Solidification of Metals," by V. Paschkis, Trans. AFA, vol. 55, 1947, p. 54.

[10] Experimental Engineering Section, NEPA Division, Fairchild Engine & Airplane Corporation, Oak Ridge, Tenn. Mem. ASME.

[11] Research Assistant, Department of Engineering, University of California, Los Angeles, Calif. Jun. ASME.

the correlation with other published data is comparatively good. This paper will be a useful tool for those concerned with this problem.

The normal route of progress calls for emphasis being placed upon the design and testing of more efficient methods of deicing. Design engineers have had, and will continue to have, problems where a considerable amount of judgment is required in determining the best power cycle to satisfy the conditions of a given problem.

The data and methods submitted in this paper should be helpful in future studies in offering the user a means of investigating rapidly and economically a range of thermodynamic and aerodynamic parameters without recourse to the prohibitive expense of an icing wind tunnel.

The need for an investigation based on the intermittent method of heating a propeller blade became evident soon after the publication of test data on both the externally and internally heated propeller blade by Lewis and Stevens of NACA.[12] Accordingly, using the scheme proposed by the author, the writer has recently completed a deicing analysis on an internally heated propeller blade. Good agreement between measured and predicted temperatures was obtained. Typical results are published as Figs. 5 and 6 of a paper by the writer, published elsewhere in this issue of the Transaction.[2] These results are based upon the omission of the heat-transfer resistance represented by the growing layers of ice, as postulated by the author.

A check was made similar to data in the author's paper, with the following results:

Measured temperature, deg F	Predicted temperature, deg F
32	32
20	23
23	23
33	32

It is seen that all four comparisons came within the limits of accuracy of 3 deg F stated by the experimenters in their tests.

The author points out the increased efficiency obtained by using higher power densities. Fig. 8 of a paper by the writer[2] shows experimental results obtained by him in a test on an internally heated blade, showing similar tendencies as pointed out by the author in Fig. 15. Such a comparison with what are now considered established design conditions will serve as a valuable guide for analyzing the benefits to be derived from these higher current densities, and offers a challenge to designers to develop equipment to meet these advanced conditions.

Considered relevant to this discussion is the matter of power-density configurations. Owing to the contribution of the heat of fusion, it appears evident that the regions of greater water catch require less heat supply than do the portions of blade surface farther away from the stagnation point. Fig. 13 of a paper by the writer[2] shows a typical test result obtained by him, and is compared to a test using a power-density configuration tested by NACA which had earlier proved practical for a steady-state anti-icing system. It is evident that the power-density configuration used for a steady-state system will not apply to an intermittent system.

The solution to the intermittently heated deicing problem, as approximately solved with the aid of the electrical analogy has opened up a new field for experimentation. Refinements to existing treatments are suggested, one of which is a solution accounting for the ice resistance; the need for investigations of intermittent air systems and analyses of intermittent wing systems by this method logically follows.

[12] Author's Bibliography, references (14) and (18).

Author's Closure[13]

Messrs. Hudson and Paschkis raise the question of the neglect of the resistance to heat transfer offered by the ice layer. In a system of high thermal capacitance such as analyzed in this paper and the following one by Weiner[2], the error is not large. However, in systems of smaller capacitance, where the energy flux is not primarily into the structure, the added resistance and capacitance must be considered. Equipment for taking these terms into account is more complex than the devices used in this paper; however, such equipment is now under construction at the University of California, Los Angeles, and will be used to study thermal systems which bear a closer approximation to the actual deicing apparatus. The lack of agreement between the Lewis data and the analyzer results leads only to the conclusion that a simpler system should be chosen for analysis and experiment if the equations are to be checked.

Mr. Hudson comments upon the omission of a thermal inductance. The second law of thermodynamics indicates that if one follows the electrical-thermal correspondences in Table 3, an inductance cannot occur in a macroscopic thermal system, i.e., no passive element can spontaneously raise a thermal flux from a low to a higher thermal potential.

Mr. Hudson and Mr. Richards comment upon damage from shedding ice. In a well-designed intermittent system the ice should be shed in relatively small pieces. The allowable sizes of ice which may be safely shed limits the "off" period in the design. Axial compressors have been operated with pieces of ice shed into the inlet. Although the engine does not make a good "disposal," small pieces of ice have been ingested without damage.

Mr. Orr questions the role of the heat of fusion. Figs. 3 and 4 of the paper serve to demonstrate how the heat of fusion warms the airfoil. The author has inspected the data mentioned by Orr and finds nothing in them to dispute the equations advanced herein.

Mr. Richards asks why in Fig. 7 the heat flow from section 3 is less than from section 1. If the heat flux were reported per unit of area, the curves would be the other way round in relative magnitude.

Space does not permit complete comments upon the many issues raised by Messrs Hudson, Orr, Paschkis, Richards, and Weiner. Their comments have been greatly appreciated.

[13] See discussion on pages 1136 and 1137 of paper by Weiner[2] for comment on constants in Equations [1], [3], [4], [7], [8], and in captions of Fig. 1(*a*), (*b*), and (*d*).

Further Remarks on Intermittent Heating for Aircraft Ice Protection

By FREDERICK WEINER,[1] LOS ANGELES, CALIF.

An electrical analog technique is used to solve the equations for intermittent heat transfer during icing conditions. The results of the analog investigation applied to an internally heated propeller show good agreement with measured time-temperature data previously reported in the literature. The greater effectiveness obtained by using larger amounts of power for shorter time intervals is demonstrated. The power-density requirements over the heated area are shown to be different for the case of intermittent heating as compared to steadily heated ice-prevention systems. A more effective heater design, utilizing a conductive coating on the blade surface, would diminish the energy requirements considerably.

Nomenclature

The following nomenclature is used in the paper:

A = surface area, sq ft
b = dimensionless modulus, $R_w C_{pw}/f_c$
B = barometric pressure, in. Hg
C_p = unit heat capacity of air, Btu/lb deg F
C_{pw} = unit heat capacity of water, Btu/lb deg F
f_c = unit thermal conductance for heat transfer, Btu/hr sq ft deg F
g = conversion constant, 32.2 ft per sec^2
J = conversion constant, 778 ft-lb/Btu
k = thermal conductivity, Btu/hr sq ft (deg F/ft)
L = heat of vaporization or sublimation, Btu per lb
(LWC) = liquid water content, grams per cu m, or lb per cu ft
p_s = vapor pressure of water or ice at surface, in. Hg
p_∞ = vapor pressure of water in free stream at ambient temperature τ_∞, in. Hg
q = heat flux, Btu per hr
r = "recovery" factor, dimensionless
R_w = rate of water impingement, lb per hr per sq ft
t_s = surface temperature, deg F
U_∞ = free stream velocity, fps
θ = functions defined in Equations [4], [5], [6], [7], [8], deg F
τ_∞ = free steam temperature, deg F

The symbol $\triangleq$ means "equals by definition"

Introduction

An analysis has been devised for the design of ice-prevention equipment utilizing intermittent heating (1).[2] This reference compares results obtained by means of an electrical analog solution with measurements made by Lewis (2) on an externally heated propeller blade.

This paper is concerned with an extension of the application of the methods described in reference (1), and on new conclusions which have been reached.

Heat-Transfer Equations at Ice Surface

The energy balance at a point on the surface of a streamlined body where supercooled liquid water is impinging may be expressed as[3]

$$q = f_c A\,[t_s - \tau_\infty - r(U^2_\infty/2gJC_p)] + 2.90 f_c LAB^{-1}(p_s - p_\infty) + R_w A\,[0.47t_s - \tau_\infty - 127 - (U^2_\infty/2gJ)] \quad [1]$$

when $t_s < 32$F

$$q = f_c A\,\{[t_s(1+b) + 2.90LB^{-1}p_s] - [\tau_\infty(1+b) + 2.90LB^{-1}p_\infty] - [(r/C_p + b)(U^2_\infty/2gJ)]\} \quad [2]$$

when $t_s > 32$F

The following functions are defined

$$b \triangleq \frac{R_w C_{pw}}{f_c}\ \text{(dimensionless)} \quad [3]$$

$$\theta_1 \triangleq \theta_1(t_s, B, b) \triangleq t_s(1 + 0.47b) + 2.90LB^{-1}p_s \quad [4]$$

$$\theta_2 \triangleq \theta_2(\tau_\infty, B, b) \triangleq \tau_\infty(1 + b) + 2.90\,LB^{-1}p_\infty + 127b \quad [5]$$

$$\theta_3 \triangleq \theta_3(b, U_\infty) \triangleq (r/C_p + b)(U^2_\infty/2gJ) \quad [6]$$

$$\theta_{ts} \triangleq \theta_1(t_s, B, b) \triangleq t_s(1 + b) + 2.90\,LB^{-1}p_s \quad [7]$$

$$\theta_{t\infty} \triangleq \theta_1(\tau_\infty, B, b) \triangleq \tau_\infty(1 + b) + 2.90\,LB^{-1}p_\infty \quad [8]$$

The equations for the heat flow from the surface then are written

$$q = f_c A(\theta_1 - \theta_2 - \theta_3) \quad [9]$$

when $t_s < 32$ F

$$q = f_c A(\theta_{ts} - \theta_{t\infty} - \theta_3) \quad [10]$$

when $t_s > 32$ F

The functions θ_1, θ_2, θ_3, θ_4, are presented in Figs. 1(*a*), (*b*), (*c*), (*d*) of reference (1), for B equal to atmospheric pressure.

Comparison of Equation [9] With Experimental Data

A prediction from the solution of Equation [9] can be made and compared directly with experimental data, by setting the heat-flow term in Equation [9] equal to zero. Reference (4) gives measurements of the temperature at the start of the heating cycle on the leading edge of an internally heated propeller blade, heated intermittently while subjected to icing conditions; typical figures are shown in Figs. 3 and 4 of reference (1) and also in Fig. 1 of this paper. Table 1 shows the comparison with experi-

[1] Department of Engineering, University of California. Now Thermodynamics Engineer, Consolidated Vultee Aircraft Corporation, San Diego, Calif. Jun. ASME.

[2] Numbers in parentheses refer to the Bibliography at the end of the paper.

Contributed by the Heat Transfer Division and presented at the Semi-Annual Meeting, Toronto, Can., June 11–15, 1951, of The American Society of Mechanical Engineers.

Note: Statements and opinions advanced in papers are to be understood as individual expressions of their authors and not those of the Society. Manuscript received at ASME Headquarters, April 12, 1951. Paper No. 51—SA-38.

[3] The energy transfers are illustrated in reference (3).

mental results. The accuracy claimed for the surface-temperature data measured by the experimenters is ±5 deg F.

TABLE 1 COMPARISON OF EQUATION [9] WITH EXPERIMENTAL RESULTS

Figs. in reference (4)	Measured temperature, deg F	Predicted temperature, deg F
Fig. 10(*a*)	32	32
Fig. 10(*d*)	20	23
Fig. 10(*f*)	23	23
Fig. 10(*i*)	33	33

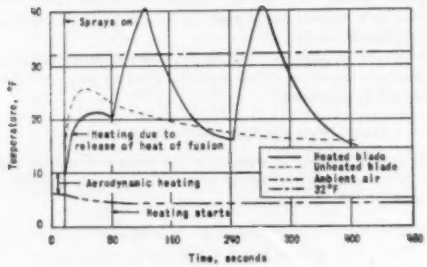

FIG. 1 MEASUREMENTS BY LEWIS FOR INTERNALLY HEATED BLADE (From fig. 10*f*, ref. 4.)

TEMPERATURE VARIATIONS ON A PROPELLER WITH INTERMITTENT HEATING

Fig. 2 shows the details of the heating system employed in the internally heated propeller blade tested by Lewis and Stevens (4).

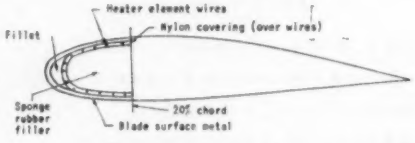

FIG. 2 DETAILS OF HEATER CONSTRUCTION USED IN REFERENCE (4)

Fig. 3(*b*) shows the idealized heat-transfer system employed for any one cross section.

The following conditions are postulated:

1 All of the heat flow caused by the heater wires occurs normal to the blade surface in the nylon, sponge filler, and ice.

2 All of the heat flow is chordwise in the steel. (The thermal conductivity for steel is quite high; the metal is relatively thin, and the temperature across the steel thickness is approximately uniform.)

The idealized thermal field problem is represented by a thermal-electric network shown in Fig. 3(*c*). The University of California thermal analyzer, used previously (1), was again used to solve this network problem. Detailed design and operational data of the analyzer have been reported elsewhere (5, 6). The equivalent networks used in this investigation were constructed in accordance with the relations given in Table 2.

TABLE 2 RELATIONS USED FOR EQUIVALENT NETWORKS

Quantity	Electrical	Thermal
Capacitance	5.56×10^3 μf	1 Btu per deg F
Resistance	64.8 kilo-ohm	1 deg F/(Btu/hr)
Potential	4 volts	1 deg F
Flux	0.0618 ma	1 Btu per hr
Time	1/10 sec	1 sec

The nonlinear network, necessary to produce the required characteristics of current versus voltage (analogous to heat flow versus blade-surface temperature), the constant-current source (used to simulate the flow of heat from the heaters), and an automatic timer were used again in this investigation. The behavior

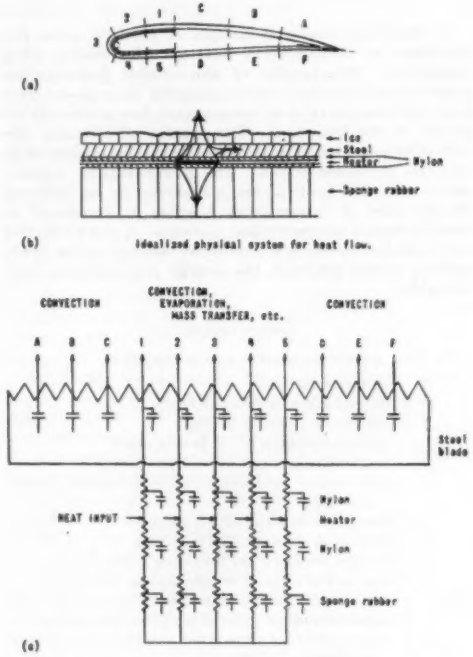

FIG. 3 REDUCTION OF IDEALIZED THERMAL FIELD TO A THERMAL ELECTRIC NETWORK

of the nonlinear network was computed using Equations [9] and [10] for each of the five segments of the heated front 20 per cent chord. The resistance to heat transfer represented by the ice was omitted as small compared to the other resistances and to the uncertainties in the thermal conductance due to convection. Fig. 4 shows the electric circuit set into the thermal analyzer.

Figs. 5, 6, and 7 show the good agreement between the measurements of Lewis and Stevens and the analyzer predictions.

IMPROVEMENTS IN EFFECTIVENESS OF PROPELLER DEICERS

Reference (1) points out that, for the same consumption of total energy, shorter bursts of power at high intensities provide greater effectiveness and, consequently, greater ice protection than low power spread over a longer interval.

A typical result of several tests on an internally heated propeller blade is shown in Fig. 8 where the total energy and total cycle time remained constant but the "power-on" cycles were doubled and tripled in power, while the "on" times were reduced correspondingly. In each case a higher temperature is achieved with no increase in power requirements from the electric system of the airplane.

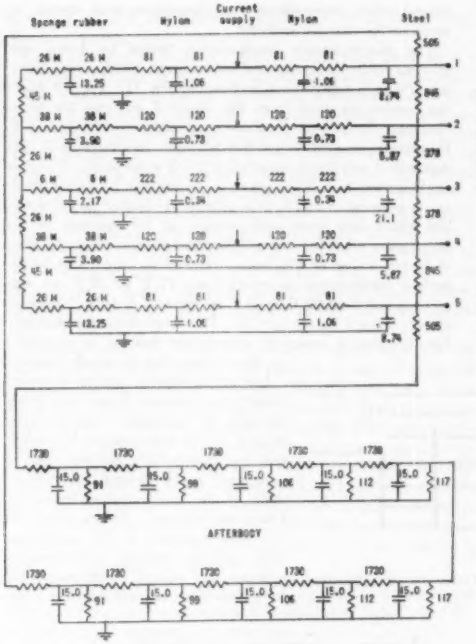

FIG. 4 ANALOGOUS ELECTRICAL NETWORK FOR AN INTERNALLY HEATED BLADE

(Numbers 1 to 5 are connected to the nonlinear network. R = Ω, C = μfd.)

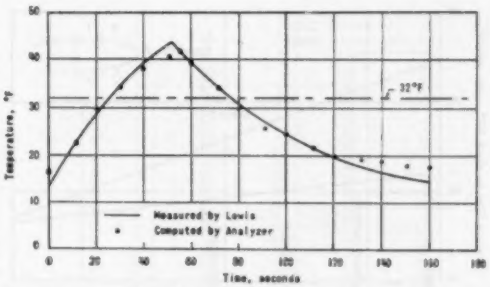

FIG. 5 TYPICAL DATA OBTAINED FROM THERMAL ANALYZER SHOWING TIME-TEMPERATURE VARIATIONS ON LEADING EDGE OF HEATED PROPELLER BLADE WITH COMPARISON TO DATA OF LEWIS

(Tunnel temperature 4 F, propeller rpm 800, r/R 0.33. Data taken from fig. 10g, ref. 4.)

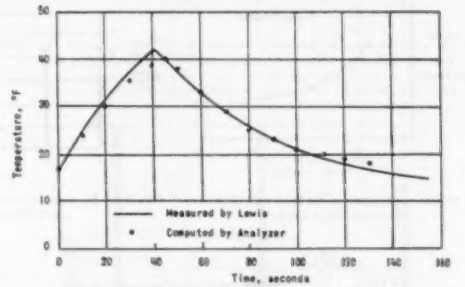

FIG. 6 COMPARISON BETWEEN DATA OF LEWIS AND THERMAL ANALYZER FOR LEADING EDGE

(Tunnel temperature 5 F, propeller rpm 800, r/R 0.33. Data taken from fig. 10f, ref. 4.)

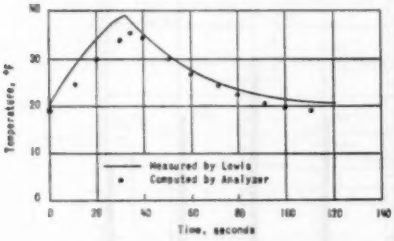

FIG. 7 COMPARISON BETWEEN DATA OF LEWIS AND THERMAL ANALYZER

(Tunnel temperature 5 F, propeller rpm 800, r/R 0.33. Data taken from fig. 10d, ref. 4.)

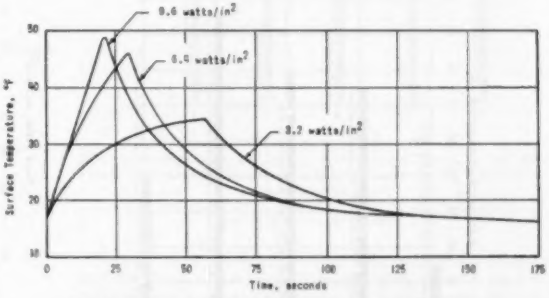

FIG. 8 EFFECT OF VARYING POWER DENSITY AT CONSTANT ENERGY

It has been suggested[4] that the greater effectiveness obtained from short bursts of power at high intensities be shown more clearly in a "power" versus "power × time for blade surface to reach 32 F" curve. A typical result is shown in Fig. 9. This curve shows the decrease in total energy required when higher power densities are used.

Equipment limitations prevented the investigation into the higher power region beyond 16 w per sq in. Fig. 10 shows an idealized sketch of a predicted extrapolation of the power-time curve. The limiting power might occur sooner than 40 w per sq in. because the heating elements might reach unsafe temperatures. In the present investigation the optimum power had not been reached.

REDISTRIBUTION OF POWER IN ACCORDANCE WITH NEEDS

Owing to the contribution of the heat of fusion occurring during

[4] Suggested by Bernard L. Messinger at an ASME Heat Transfer Seminar held at the University of California, Los Angeles, Calif., June, 1950.

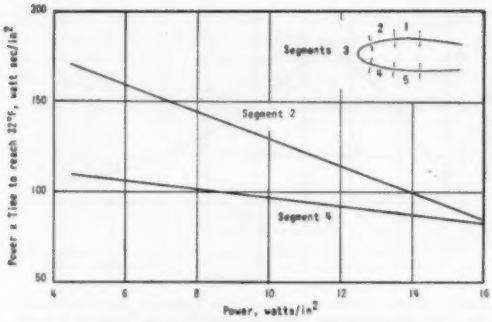

FIG. 9 INCREASE IN DEICING EFFECTIVENESS OF AN INTERNALLY HEATED PROPELLER WITH INCREASE IN HEATER POWER

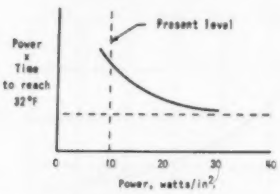

FIG. 10 PREDICTED EXTRAPOLATION OF POWER-TIME CURVE

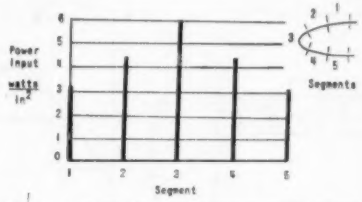

FIG. 11 POWER-DENSITY CONFIGURATION TESTED ON THERMAL ANALYZER

several other power-density configurations were tested by means of the thermal analyzer.

The power-density configuration tested by Lewis and Stevens for both steady and intermittent heating was averaged for each segment and is shown in Fig. 11. Fig. 12 shows the results obtained from the thermal analyzer by interchanging the power densities over segments 1, 3, and 5. Previously, segment 3 had 6 w per sq in. impressed on it, and segments 1 and 5 were supplied with 3.2 w per sq in. The new configuration used 3.2 w per sq in. on segment 3 and 6 w per sq in. on segments 1 and 5, thus putting the higher power densities where they were most needed, at the outskirts of the boundaries where less contribution was obtained from the heat of fusion owing to the lower water-catch rate. The blade-surface temperature increased from 17 F to 25 F on segment 1, and from 22 F to 29 F on segment 5, with a decrease of only 2 deg F on segment 3. The large deviations indicate the alteration in design for intermittent heating, as compared to the configuration for steady heating.

Fig. 13 indicates the predicted power-density requirements if one were flying through an assumed "severe icing hazard" of low temperature, low speed, and low liquid-water content, and is compared to the thermal-analyzer results of the configuration tested by Lewis and Stevens. Tribus points out (1) that, contrary to the experience with steadily heated ice-prevention systems, the energy requirements for ice prevention, using intermittent heating, decrease with increasing ice accretion; the rate of ice accretion is directly proportional to the liquid-water content. Thus a low liquid-water content provides a more severe test.

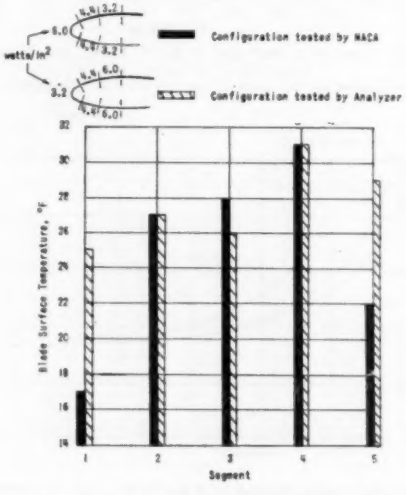

FIG. 12 COMPARISON OF PROPELLER-BLADE SURFACE TEMPERATURES OBTAINED FOR TWO TYPES OF POWER INPUTS TO AN INTERNAL ANTI-ICING HEATER

(t_∞ = 3 F, 800 rpm, LWC = 0.26 gram per cu m, droplet size 55 microns, cycle 20 sec on, 60 sec off.)

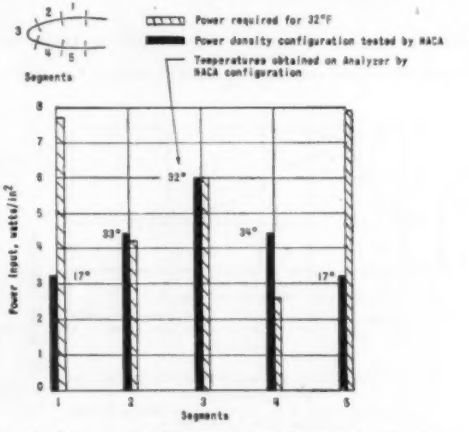

FIG. 13 COMPARISON BETWEEN A POWER-DENSITY CONFIGURATION TESTED BY NACA AND A POWER DENSITY TO GIVE 32 F BLADE-SURFACE TEMPERATURE

(t_∞ = 0 F, 800 rpm, LWC = 0.1 gram per cu m, drop diam 10 microns cycle 20 sec on, 60 sec off.)

intermittent heating, it might appear that the regions of greater water catch require less heat supply than do the portions of blade surface farther away from the stagnation point. Accordingly,

A MORE EFFECTIVE HEATER DESIGN

A more effective propeller heater design than is used in present-day airplanes would involve a system in which the heat would be

applied directly at the surface without being diminished by various heat-resisting media en route.

Experiments were made on a heater configuration made up of a conductive coating such as conducting graphite or conductive rubber placed on a propeller surface and insulated from it by a layer of glass cloth $^1/_{32}$ in. thick. Fig. 14(*a*) shows this arrangement, and the idealized system for heat flow; Fig. 14(*b*) presents the analogous electric circuit for this system. The results, as predicted by the thermal analyzer, are presented in Figs. 15 and 16. Fig. 15 illustrates the large improvement in temperature rise for each of the five segments of the propeller blade, using the same current densities as employed previously in the internal heater. Not included in this ideal system is any cement film necessary to bond the glass cloth to the steel surface. Fig. 16 shows the lower required power, compared to the internal heater, necessary to raise the airfoil heated surfaces from the ambient temperature to 32 deg F.

A configuration involving an abrasion-resistant film over the heater was also investigated. The thermal conductivity for the abrasion film was chosen to be 0.15 Btu/hr sq ft (deg F/ft), simulating a thin film of rubber sprayed on the surface. A typical result of tests on the system is shown in Fig. 17. This figure compares the blade-surface temperatures for all three heater configurations (including the internal heater) tested with the same power input, and shows that the abrasion film has only a minor effect in lowering the surface temperature of the external heater.

Fig. 18 shows the transient values of the blade-surface temperatures of segment 2 for all three heater configurations. From this graph the following facts are derived:

1 The temperature lag of the propeller surface, caused by the capacity for heat absorption and the resistance to heat flow of the steel and nylon covering, is clearly evident.

2 Both the power and the "power-on" time could be decreased until a minimum power or a minimum "on" cycle was found.

Fig. 14(*a*) Ideal Heat-Flow System for Proposed Heater Configuration

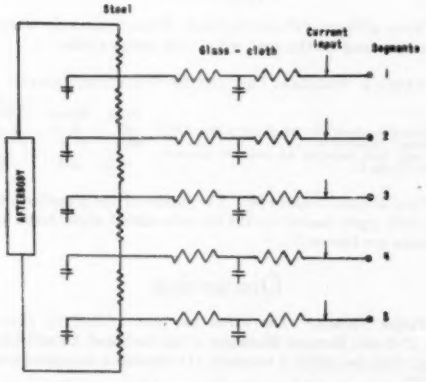

Fig. 14(*b*) Analogous Electric Network

Afterbody is same as Fig. 4. Capacitors are all grounded. Numbers 1, 2, 3, 4, 5 are connected to nonlinear network.)

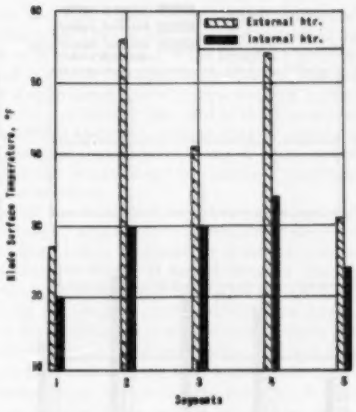

Fig. 15 Comparison of Surface Temperatures of Two Configurations for a Propeller Anti-Icing Heater

(Maximum temperature shown. r_m = 3 F, 800 rpm, LWC = 0.26 gram per cu m, drop diam 55 microns, cycle 10 sec on, 50 sec off.)

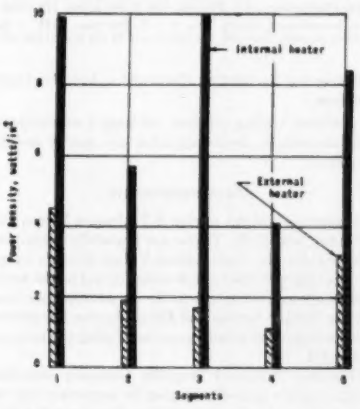

Fig. 16 Comparison of Current Densities Required on Two Propeller Anti-Icing Heater Configurations to Bring Surfaces to 32 F

(r_m = 3 F, 800 rpm, LWC = 0.26 gram per cu m, drop diam 55 microns, cycle 20 sec on, 60 sec off.)

Since this system is highly idealized, the practical case will show that the effects of the thermal capacity of the ice and the noninstantaneous heating of the heater will tend to make the temperature rise less steep.

Conclusions

The following conclusions may be presented:

1 The time-temperature histories of a typical internally heated propeller have been predicted very accurately.

2 The energy requirements for ice prevention can be greatly diminished by:

(*a*) Shortening the time of application of a given amount of energy.

(*b*) Redistributing the power in accordance with the needs.

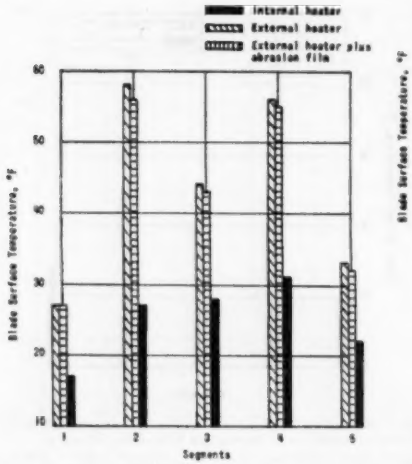

FIG. 17 COMPARISON OF SURFACE TEMPERATURES OF THREE CONFIGURATIONS FOR A PROPELLER ANTI-ICING HEATER
(Maximum temperature shown. T_∞ = 3 F, 800 rpm, LWC = 0.26 gram per cu m, drop diam 35 microns, cycle 20 sec on, 60 sec off.)

(*c*) Redesigning the heating elements to place the heaters near the ice surface.

3 A practical heating element, utilizing a conductive coating on the blade surface, would diminish the energy requirements considerably.

ACKNOWLEDGMENTS

The suggestions and the advice of Professors Myron Tribus, L. M. K. Boelter, and E. H. Taylor are gratefully acknowledged.

Thanks are due the Consolidated-Vultee Aircraft Corporation whose Fellowship provided ample financial aid to the author during the development of this research. In addition, the funds provided by the Hyman Levine and Emma Levine Foundation for a Research Assistantship aided the author during the preparation of the manuscript.

The Hamilton Standard Propeller Company supplied blueprints and a sample propeller section for inspection and study.

The stimulus to examine the problem of ice accretion on aircraft was provided by Messrs. Vic Hudson and H. T. Brooks of Consolidated-Vultee Aircraft Corporation.

BIBLIOGRAPHY

1 "Intermittent Heating for Aircraft Ice Protection With Application to Propellers and Jet Engines," by Myron Tribus, appearing in this issue of the Transactions, pp. 1117–1130.

2 "De-Icing Effectiveness of External Electric Heaters for Propeller Blades," by J. P. Lewis, NACA TN 1520, February, 1948.

3 "An Investigation of Intermittent Heating for Aircraft Ice Protection," by Frederick Weiner, MS thesis, University of California, Los Angeles, Calif., December, 1950.

4 "Icing and De-Icing of a Propeller With Internal Blade Heaters," by J. P. Lewis and H. C. Stevens, Jr., NACA TN 1691, August, 1948.

5 "Theory and Development of a Thermal Analyzer," by Robert Bromberg and William Martin, University of California, Los Angeles, Calif., August, 1947.

6 "The Thermal Analyzer," by Frederick Weiner, *California Engineer*, University of California, Berkeley, Calif., February, 1950.

7 "Impingement of Waterdrops on Various Airfoils From Trajectories Obtained on the Differential Analyzer, Addendum I," by A. G. Guibert, Engineering Waterdrop Trajectory Research, University of California, Los Angeles, Calif., April, 1949 (recently published in NACA TN 2476, by N. R. Bergrun, September, 1951).

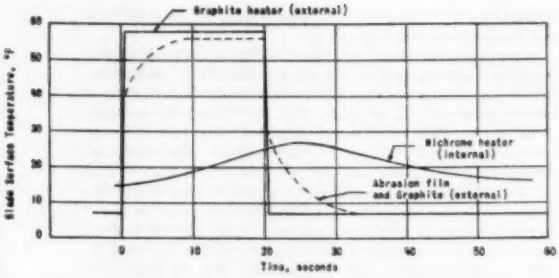

FIG. 18 COMPARISON OF PROPELLER-BLADE SURFACE TEMPERATURES FOR THREE HEATER CONFIGURATIONS
(Segment 2, T_∞ = 3 F, power input 4.4 w per sq in.)

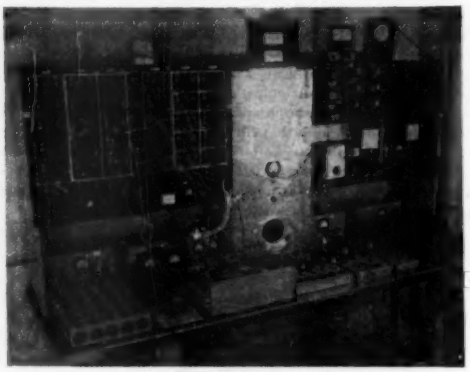

FIG. 19 VIEW OF THERMAL ANALYZER AND ASSOCIATED EQUIPMENT

Appendix

Values of Thermal Properties Used. Table 3 shows the thermal properties used for the steel, nylon, and sponge rubber.

TABLE 3 THERMAL PROPERTIES OF MATERIALS USED

	Steel	Nylon	Sponge rubber
k, thermal conductivity, Btu/hr sq ft (deg F/ft)	26	0.12	0.03
γ, density, lb per cu ft	490	67.3	16
C_p, unit heat capacity at constant pressure, Btu/lb deg F	0.12	0.5	0.35

Water-Droplet Trajectories. The profile of the propeller blade was best approximated by the 65 series airfoil whose water trajectories are known (7).

Discussion

MYRON TRIBUS.[8] The writer has been advised by Messrs. Ben Rich and Bernard Messinger of the Lockheed Aircraft Company, that the author's reference (1) contains a numerical error.

[8] Aircraft Nuclear Propulsion Project, Apparatus Department, Aircraft Gas Turbine Division, General Electric Co., Cincinnati, Ohio. Jun. ASME.

This error has been repeated in the present paper. Equations [1] and [2] of this paper contain the numerical factor 2.29 which should be 2.90 everywhere it occurs in these equations. The change in magnitude of the θ functions is not large until the temperature exceeds 50 F at which time the evaporation terms in the heat balance are more significant.

The effect upon the results given in this paper and in reference (1) is not large, since the major portion of the energy in the energy balance is in the heat-capacity terms. Thus it may be safely said that if the correct values of the θ functions had been used, the analog results would be negligibly different.

The results given in Fig. 18 of the present paper should be treated with caution. While the neglect of the resistance of the ice layer should not cause a large error in the types of systems studied by Weiner and in reference (1), a system of very low capacitance would still not produce the square wave of temperature indicated in Fig. 18, since the thermal capacitance of the ice would not then be negligible.

The agreement between the computed and experimental temperatures as well as the agreement in the heat fluxes gives added confidence in the equations developed in reference (1).

Author's Closure

The material in reference (1) originally appeared as a PhD thesis at the University of California, and subsequently in ASME Preprint No. 50—A-55. Both papers contained an error wherein the numerical factor 2.29 was used instead of the correct number, 2.90. This error was continued in the equations given in reference (3) and in ASME Preprint No. 51—SA-38. The detection of the error is appreciated, and it has been corrected in this paper.

Reference (1), contained in this issue of the Transactions, originally appeared in December, 1950, as ASME Preprint No. 50—A-55, and contained typographical errors in Equations [1], [4], and [7]. This fact is pointed out for the benefit of anyone desiring to use the equations.

Reference (1) and this paper have shown good agreement between experimental temperature measurements reported by the NACA and temperatures computed by a thermal analyzer, for both internally and externally heated propeller blades. The ease with which the thermal analyzer can predict optimum power designs affords the designer a valuable technique, for once the network has been established, a large variety of heater constructions, heating intensities, blade constructions, and heat on-and-off times may be investigated rapidly and economically.

An interesting paper has recently appeared which contains a discussion on the equilibrium surface temperature of an icing surface at 32 F, and presents the θ curves for 20,000 ft altitude. Reference is here made to "Equilibrium Temperature of an Unheated Icing Surface as a Function of Airspeed," by Bernard L. Messinger, IAS Preprint No. 342, June, 1951.

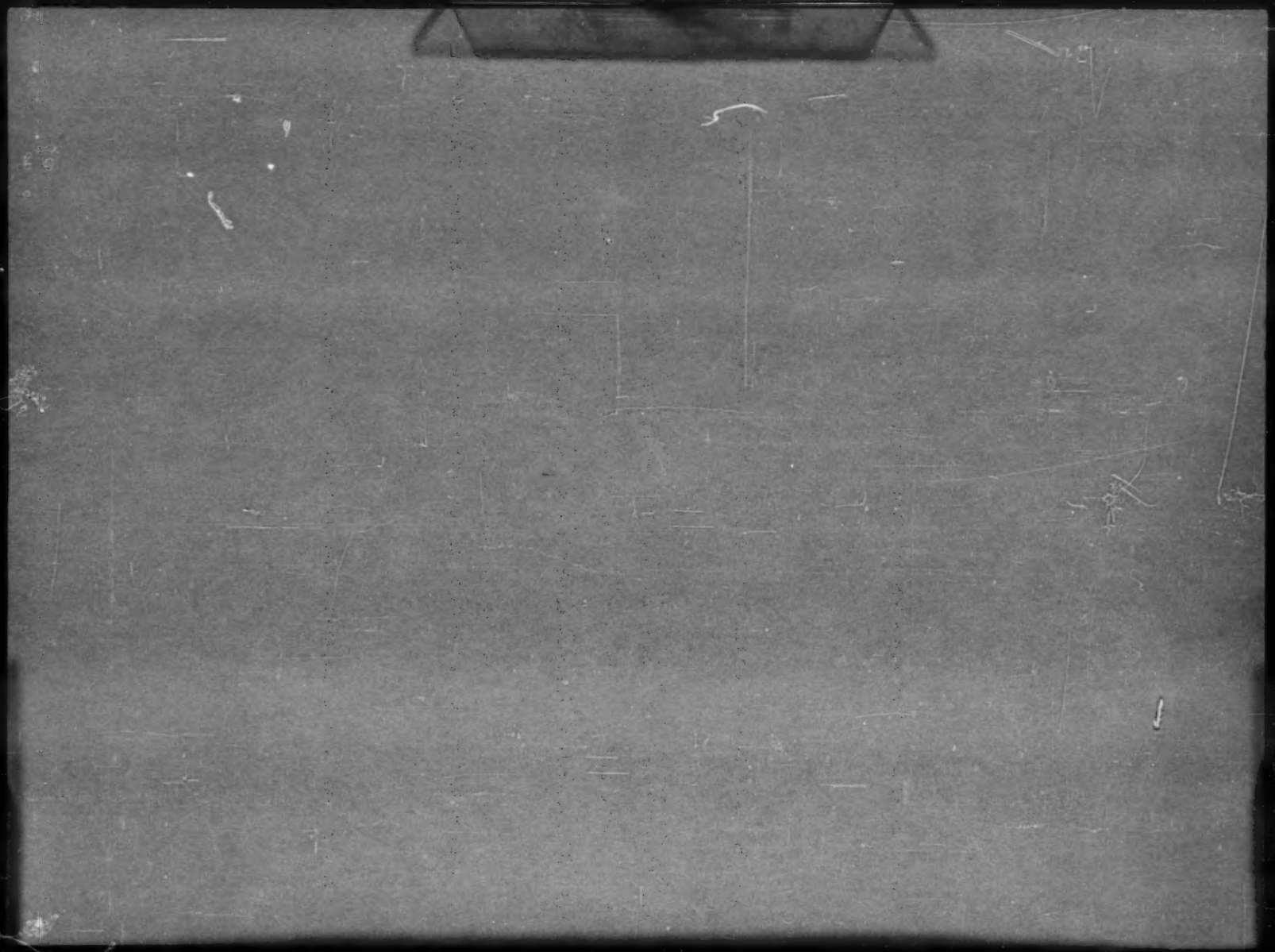

AN ASME PAPER

Its Preparation, Submission and Publication, and Presentation

To a large degree the pape
ASME sponsorship are evid
and leadership are judged.
for ASME sponsorship, a
subject matter, but it must
nized standards of good En

The pamphlet on "AN ASM
in meeting these requirem
of the Society relating to
manuscripts and accompa
suggestions for the presenta

PREPARATION OF A PA

General Information—Sc
Approvals and Clearances.

Contents of the Paper—T
Appendixes, Acknowledgm
graphs, Other Illustration

Writing the Paper—Outli
Computation, Drawings, M
ing, Lantern Slides, Motio

SUBMISSION AND PUBLI

Intention to Submit Pape
Dates for Manuscript, Dis
rance Copies and Reprin
Others.

PRESENTATION OF A PA

Time Limit, Addressing Y
Slides.

REFERENCES—

References on Writing and

Price 35¢. No discount all
all orders for $2.00 or less.

THE AMERICAN SOCIETY O
29 West 39th Street,

apers prepared and presented under the
idence by which its professional standing
ed. It follows, therefore, that to qualify
a paper must not only present suitable
ust be well written and conform to recog-
English and literary style.

SME PAPER" is designed to aid authors
ements and to acquaint them with rules
to the preparation and submission of
panying illustrations. It also includes
ntation of papers before Society meetings.

CONTENTS

PAPER—

-Style, Preferred Spelling, Length Limitations,
ces.

—Title, Author's Name, Abstract, Body of Paper,
gments, Bibliographies, Tables, Captions, Photo-
ions.

rtime, Tabulations, Tables, Graphs, Charts for
s, Mathematics, Accuracy, Headings and Number-
otion Pictures, Typing, Number of Copies.

BLICATION OF A PAPER—

Paper Required in Advance, Meeting Dates, Due
Discussers, Review and Acceptance, Proofs, Ad-
prints, Discussion and Closure, Publication by

PAPER—

g Your Audience, Public Address Systems, Use of

and Speaking, Engineering Standards.

allowed. *A remittance must accompany*
ss. U. S. Postage Stamps are acceptable.

OF MECHANICAL ENGINEERS
et, New York 18, N. Y.